

Bangor University

DOCTOR OF PHILOSOPHY

Thiophene substituted tetrathiafulvalenes and tetrathiafulvalene substituted polythiophenes

Roberts-Bleming, Susan Janet

Award date:
2001

Awarding institution:
Bangor University

[Link to publication](#)

General rights

Copyright and moral rights for the publications made accessible in the public portal are retained by the authors and/or other copyright owners and it is a condition of accessing publications that users recognise and abide by the legal requirements associated with these rights.

- Users may download and print one copy of any publication from the public portal for the purpose of private study or research.
- You may not further distribute the material or use it for any profit-making activity or commercial gain
- You may freely distribute the URL identifying the publication in the public portal ?

Take down policy

If you believe that this document breaches copyright please contact us providing details, and we will remove access to the work immediately and investigate your claim.

Thiophene Substituted Tetrathiafulvalenes
and
Tetrathiafulvalene Substituted Polythiophenes.

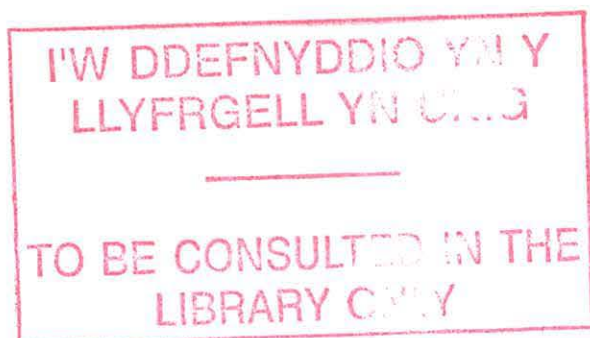
By

Susan Janet Roberts-Bleming BSc (Hons)

*A thesis submitted in accordance with the requirements for the degree of
Doctor of Philosophy*

Department of Chemistry
University of Wales, Bangor

2001.



For Dabe and Bob.

Declaration.

The research described in Chapter six, was performed initially by Susan Roberts-Bleming at the Department of Chemistry, University of Wales, Bangor. Professors Donato Donati and Fabio Ponticelli at the University of Siena, Italy performed the structure elucidation and further experiments comprising the main body of the text.

ABSTRACT

Doctor of Philosophy

Department of Chemistry

University of Wales, Bangor

*Thiophene Substituted Tetrathiafulvalenes
And Tetrathiafulvalene Substituted Polythiophenes.*

By **Susan Janet Roberts-Bleming** BSc (Hons)

The research comprised in the thesis covers three topics:

An investigation of the mode of polymerisation and charge-transfer mechanism of the polymerised form of *bis*-(3-thienyl)-1,3-dithiole-2-one. This was achieved in the preparation of 1,2-*bis*-(2-methyl-thiophen-3-yl) 2-hydroxyethyl-ethanone and 1,2-*bis*-(2,5-dimethyl-thiophen-3-yl) 2-hydroxyethyl-ethanone and by investigating the electrochemical and spectroelectrochemical properties of 1,2-dithienylethylene. The results showed that *bis*-(3-thienyl)-1,3-dithiole-2-one undergoes an intramolecular cyclisation during the polymerisation process, adopting a quinoidal structure with charge-transfer properties similar to that of polyacetylene. In all cases X-ray crystallographic data was obtained.

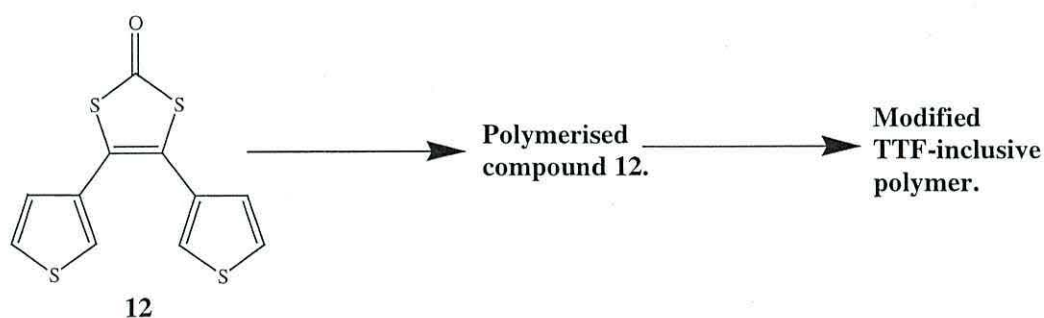
An *in-situ* chemical modification of the polymerised *bis*-(3-thienyl)-1,3-dithiole-2-one was performed resulting in the preparation of a TTF derivatised polythiophene. This provided further evidence in regard to the elucidation of mode of polymerisation and charge-transfer when spectroelectrochemical and electrochemical studies were carried out. The monomeric unit 2-(4,5-di-thiophen-3-

yl-[1,3] dithiol-2-ylidine)-benzo[1,3]dithiole was produced allowing a comparative study to be performed with its X-ray crystal structure being obtained.

A further aim of the research was the attempted preparation of 1,3,6,7-tetrathia-trinden-2-one in an effort to provide further evidence of the polymerisation mechanism of *bis*-(3-thienyl)-1,3-dithiole-2-one. The synthesis was found to be unsuccessful.

Finally, the photochemical transformation of *bis*-(3-thienyl)-1,3-dithiole-2-one in an effort to prepare 1,3,6,7-tetrathia-trinden-2-one was attempted. This resulted in the formation of thieno[3,4-*c*]dithiine, the first example of a transformation of this type.

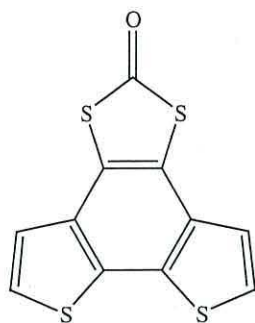
Once understood, TTF derivatised polythiophenes based on **12** would be prepared and polymerised. Within this rationale there are several approaches to take; direct electropolymerisation, and *in situ* polymer modification as shown in scheme 2.0.1.



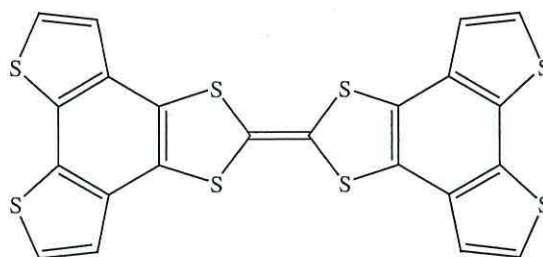
Scheme 2.0.1 Strategy for *in situ* polymer modification.

A further aim of the research was to prepare benzobithiophenes based on the unit **13** (figure 2.0.1), in which the two thiophene rings have been fused together, in order that we might investigate the possibility of allowing direct polymerisation of

TTF derivatives based on **14**. This was attempted using synthetic and photochemical methodologies.



13



14

Figure 2.0.1

Acknowledgements.

Firstly I would like to express my gratitude to my supervisors Dr. Maher Kalaji and Dr. Patrick J. Ikeepmyteethinajarbesidethebed Murphy for their support and kindness throughout the course of my Ph.D. It would also be prudent to thank Paddy for telling me so many pointless facts about life, the universe and road safety that all seem to commit themselves so easily to memory. I would like to think that as a small present in return, turning Paddy into departmental gossip was one of my greatest achievements to date!

The University must also be thanked; for funding the project, providing all of the technicians that helped me, and for introducing me to the secretaries Barbara, Caroline and Jenny-those photocopy room chats will be dearly missed!

I would also like to thank group 103 members past and present, the names are too many to mention. Though, to Dafs, so cruelly made to write up in the prime of his life whom never fully recovered from the experimental section, I will miss our experimental afternoons advancing the 'cutting edge' of chemistry and providing the true meaning of the term cowboy.

I would also like to thank Miss Teresa Parsons, so cruelly taken from us at such a crucial time in her formative years!., for providing me with much gossip and for being one of the few people I would like to call a best friend.

Mo thankyou for brightening up my life with the endless sagas and Ellena finally someone understands my sense of humour.

To my parents, the main reason for my somewhat muddled existence on this planet, thank you for everything. You are an inspiration to me and I love you both.

And finally to Dave 'the cat' Brassington. Your football skills may be somewhat limited, you may not know how to cook, but you know the true meaning of perseverance (– you're marrying me!!) and I hope that all whom mocked are eating the old proverbial now. I love you and one lifetime still is not enough.

To everyone else that I have not mentioned, you know who you are, thank you for everything.

P.S. Emma and Nigel thanks for the fridge.

Abbreviations.

MeCN	Acetonitrile
Ar	Aromatic
BEDT-TTF	<i>Bis</i> -(ethylenedithio)tetrathiafulavlene.
NBS	<i>N</i> -Bromosuccinamide
BuLi	Butyl Lithium
δ	Chemical Shift
J	Coupling Constant
CV	Cyclic Voltammogram
$^{\circ}\text{C}$	Degrees Celcius
$^{\circ}$	Degrees
DMIT	4,5-Dimercapto-1,3-dithiole-2-thione
d	Doublet
d.d.	Doublet of Doublets
Et ₂ O	Diethyl Ether
FTIR	Fourier Transform Infra-Red
ν	Frequency
Hz	Hertz
h	Hour
HOMO	Highest Occupied Molecular Orbital
IR	Infra-Red
IRAV	Infra-Red Active Vibration
LUMO	Lowest Occupied Molecular Orbital
MHz	Mega Hertz
mVs ⁻¹	Milli Volts Per Second
min	Minute
mol	Moles
M	Molar
m	Multiplet

n	Normal
nOe	Nuclear Overhauser Effect
NMR	Nuclear Magnetic Resonance
ppm	Parts Per Million
dm^{-3}	Per Decimeter Cubed
PA	Polyacetylene
PANI	Polyaniline
pDDT	Polydithieno [3,4-b:3'4'-d]thiophene
PPy	Polypyrrole
PT	Polythiophene
+I	Positive Inductive Effect
PCB	Printed Circuit Board
R.T.	Room Temperature
s	Singlet
SCE	Saturated Calomel Electrode
SNIFTIRS	Subtractively Normalised Interfacial Fourier Transform Spectroscopy
TBATFB	Tetrabutylammonium Tetrafluoroborate
THF	Tetrahydrofuran
TCNQ	Tetracyano- <i>p</i> -quinodimethane
TMTST-DMTCNQ	Tetramethyltetraselenofulvalene-tetracyano- <i>p</i> -quinodimethane
TSF-TCNQ	Tetraselenofulvalene-tetracyano- <i>p</i> -quinodimethane
TTF	Tetrathiafulvalene
t	Triplet
vs.	Versus
V	Volts
λ	Wavelength
cm^{-1}	Wavenumbers

Chapter One: Review of the Literature.

1.1.0 General Introduction.

This chapter comprises a generalised review of conducting polymers. The main aim of this review is to introduce the design, synthesis and modification of conducting polymers in general, though concentrating on polythiophene as this will comprise the main body of the text. The concept of 'charge-transfer' chemistry is introduced and a brief section about tetrathiafulvalene is given.

1.1.1 Background.

Synthetic chemists strive to create compounds that have novel properties and applications. Conducting polymers were found to exhibit such novel properties, but could be made to mimic the particular characteristics found in metallic/conducting materials. This was displayed with the discovery that an essentially non-conducting polymer; polyacetylene, could be doped with iodine resulting in one of the first conducting organic polymers. [1] This represented the birth of conducting organic polymers.

Conducting polymers, whilst mimicking metallic behaviour, would show advantages over metallic conductors in that they have a high resistance to corrosion, they are lightweight, processable, and, perhaps more importantly are relatively easy to produce. They have potential applications in electrochromic displays [2-4], artificial muscles [5,6], batteries [7-10] and fuel cell technology. [11-15] The application technology for conducting polymers although still in its infancy is already worth millions of pounds worldwide. For example the plating process for 'through-hole' copper deposition on printed circuit boards (PCBs), revolutionised by the use of polypyrrole (PPy), is now worth over \$10⁶ per annum. [16]

Perhaps one of the most exciting developments over the past three years has come from post-polymerisation functionalisation of electropolymers. The functionalisation or, modification of electropolymers that can: (i) specifically interact with for example, biological molecules [17], small peptides [18] or enzymes [19], (ii) allow the *de novo* building of structures on conducting surfaces [20], (iii) provide chiral interfaces [21], and (iv) provide redox control of the binding/release of bioactive molecules, are gaining widespread interest as potential advanced materials. Such modifications enable the production of electropolymers that are essentially 'tailor-made', combining electronic properties of an electropolymer with the specific properties of the incorporated functionality.

The applications and potential uses include sensor applications [22], microelectronic devices [23] and electrocatalysts. [24]

1.2.0 Review of Conducting Organic Polymers.

The idea of a conducting polymer was first proposed by Huckel, stating that, based on theoretical calculations of the electronic states of sp^2 carbon; polyacetylene (PA) should exhibit metallic behaviour. [25] It was not until 1977 though that the first report of polyacetylene with metallic properties was made by Heeger and MacDiarmid. [26] The study of PA prompted further research into organic conducting polymers, resulting in the creation of many new organic polymeric materials based on heteroatoms, for example polyaniline (PANI), polypyrrole (PPy), and polythiophene (PT). It is important to note that PA may only be made by chemical synthesis but PANI, PPy and PT are of interest to electrochemists because of their dual polymerisatability, being produced either chemically or electrochemically. [27]

Electrochemical polymerisation occurs, (in most cases, notably PANI being an exception) by the oxidation of the respective monomer in solution. This occurs *via* radical cation intermediates, and it is for this reason that the solvent and electrolyte are of great importance. There must be no co-interaction of the radicals

with the solvent and electrolyte, thus the solvents need to be aprotic in nature therefore reducing the possibility of nucleophilic interaction so, for example acetonitrile would be a good choice. The electrolytes need to be soluble in such solvents and have a high degree of dissociation; the most commonly used electrolytes are the tetraalkylammonium salts. Halide anions may be used though poor films are produced due to their high nucleophilicity.

Once polymerised such 'conducting' polymers can exhibit 3 different states: p- doped state, neutral state and n- doped state. The term doping used is analogous to that found in semi-conducting materials, though the levels found are higher but unlike semi-conductors, the process is reversible and controllable. In the p- doped state, the dopant is generally electron withdrawing; producing positively charged oxidised polymeric species (polycation) that is highly conducting, with formation of a monovalent anion also. The dopant acts to remove neutral solitons and converts them to positively charged solitons. In this case the conduction involves positive charge carriers. The second state in which the polymer can exist is the neutral undoped state. This is the insulating non-conductive state, although semi-conduction can occur if the p- doped polymer has not been fully de-doped. The third, n- doped state is rare, with only the 5-membered heterocycles (mainly polythiophenes) exhibiting it. The n- doped state is the reduced, negatively charged polymeric species. Electron transfer from the electron donating dopant occurs producing a stable polyanion and monovalent cation. In this instance, the neutral soliton gains electrons from the dopant to form negatively charged solitons. Like the p- doped state, the n- doped state is highly conducting but rare. A few polymers can undergo n- doping: PA *via* chemical means only and polythiophenes. During chemical doping, the polymer chain itself becomes oxidised or reduced as charge transfer between dopant and polymer chain occurs. Electrochemical doping is preferable to other methods as it is reversible and allows doping levels to be controlled. So the sample is allowed to return to its original neutral (if applicable) state. During this process electroneutrality must be maintained, this is achieved by incorporation of the appropriate ionic species within the electrolyte solution.

Name	Structure
Polythiophene	
Polypyrrole	
Polyaniline	

Figure 1.0.1 The main conducting polymers.

For a polymer to achieve a doped conducting state there must be a sufficiently small enough ‘band-gap’ to allow the passage of electrons between orbitals. Perhaps the best model for the explanation of ‘band-gap’ is band theory. For any sort of conduction in any material electrons contained within the HOMO or, valence band must be able to move easily into the LUMO or the conduction band. To move between the orbitals the distance between the two orbitals must be sufficiently small. In the case of metals there must be partial occupancy of the LUMO. This will occur by the promotion of HOMO electrons, though generally there is little or no band-gap due to there being orbital overlap (figure 1.0.2).

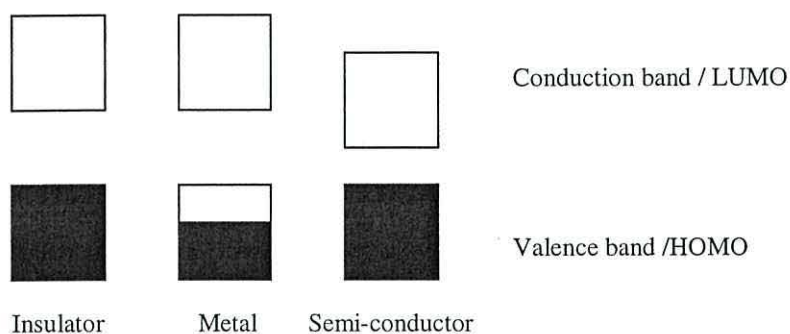


Figure 1.0.2 Band theory for metal, insulator and semi-conductor.

In the case of semi-conductors, the gap between the orbitals is slightly larger, although small enough to allow some electron promotion. Insulators, as the name would suggest, permit no excitation, as the orbital gap is large.

To fully explain the mode of conduction in conducting polymers the accepted band theory must be expanded. When a conducting polymer is doped, an electron is removed from the valence band. This results in the formation of a positive hole. This produces a structural deformation over several monomeric units in the polymeric structure. This deformation acts to alter the bond length thereby producing new energy levels in the band gap. The new energy level is found midway in the band gap and is given the term soliton. The soliton is a neutral defect that leads to semi-conducting properties only. The soliton level may accommodate 0, 1, or 2 electrons and so can be made positively or negatively charged. Doping enhances conductivity, and thus when doped with an acceptor; oxidation or p- doping, the soliton is positively charged. When doped with a donor; n- doping, the soliton is doubly occupied and the soliton is reduced and negatively charged. Solitons are mobile and can move along the chain (figure 1.0.3).

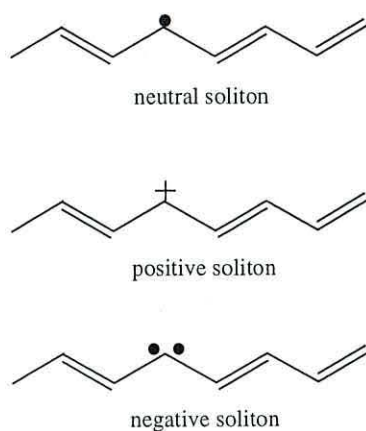


Figure 1.0.3 Schematic representation of soliton structures in polyacetylene.

With polymers that are aromatic in character it is found that the soliton states are not stable (the change in bond order dictating that radical cation formation is preferable). Radical cations essentially consist of a pairing of a neutral soliton and charged soliton. This pairing produces polarons – radical cations. The generation of polarons acts to produce 2 new energy states in the band gap that are placed around the soliton midgap level. If the doping (oxidation) continues there are two possible consequences;

- i) an independent polaron is produced, or
- ii) polarons will begin to pair resulting in bipolarons.

This pairing of the polarons leads to bipolaronic states that can combine to lower the ground state, which produces a quasi-metallic structure (figure 1.0.4). Both polarons and bipolarons act as mobile charge carriers – as a consequence of the rearrangement of the single and double bonds they move along the polymer. Because of this they are considered to be responsible for electrical conductivity in conjugated polymers.

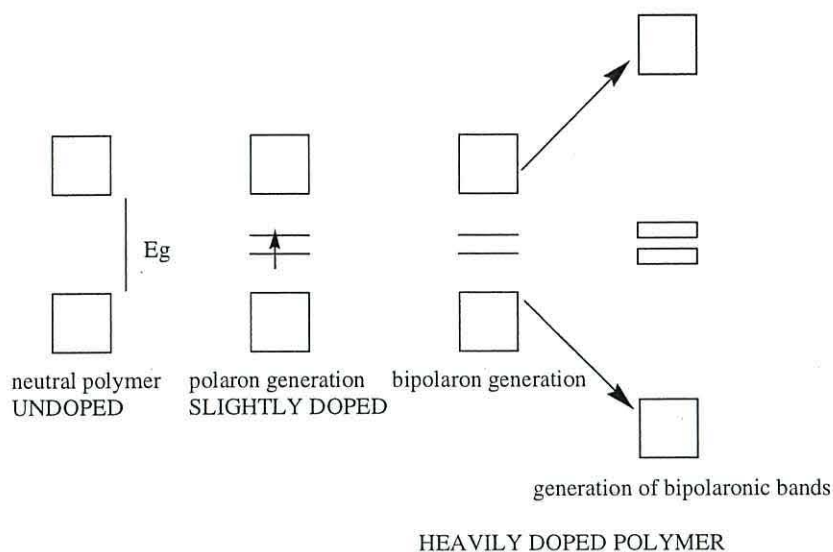


Figure 1.0.4 The formation of bipolaronic states.

Most conducting polymers have a non-degenerate ground state, which results in the instantaneous pairing of solitons. The exception being polyacetylene that has a degenerate ground state and thus shows the formation of the soliton, polaron and bipolaronic states.

Similar models have been proposed for the polyheterocycles, with most attention being given to polythiophene, which is the basis of the work reported in this thesis.

However it must be mentioned that in respect to bulk conductivity in polymers other factors need to be considered; conductivity is not only a matter of charge transfer along the chain but there is also an amount of interchain electron hopping.

1.3.0 Polythiophene (PT).

Polythiophene is a member of the polyheterocycle family. It can be produced synthetically or electrochemically, and compared to other polymeric materials, exhibit air and moisture stability in both the doped and un-doped states.

Several publications regarding the electrochemical properties and synthesis of these materials can be found in literature [29-32];

i) The chemical synthesis of polythiophene.

The chemical synthesis of PT or derivative is performed by the catalytic coupling of the Grignard reagent of brominated thiophene by nickel salts. [33] The resultant polymer is obtained in its neutral state and may be doped by chemical or electrochemical means.

ii) The electrochemical synthesis of polythiophene.

Reliable methods of preparation of extensively conjugated, highly conducting polymers or oligomers with defined structures are best performed by electrochemical polymerisation.

Polythiophene can be electrochemically obtained *via* the oxidative electropolymerisation of the monomer, but can also be obtained *via* a cathodic route involving the electroreduction of a thienyl complex. [34] The latter method however produces the polymer in its neutral insulating form.

It should be noted however that electropolymerisation has distinct advantages over other methods of polymerisation in that it uses no catalyst, enables direct deposition of polymer film onto the electrode surface and allows ease of control of polymer film thickness. Electropolymerisation can be carried out potentiodynamically, galvanostatically or by using potential step techniques. Thiophene monomers have a typical oxidation potential of 1.65 V (*vs.* SCE), and the resultant polymer oxidises around 1.1 V (*vs.* SCE). [35,36] Galvanostatic methodologies may also be used to produce PT; (generally current densities of around 1 mAcm⁻² are used), allowing control of the amount of film being deposited. In any of the above techniques for growing electrochemically PT, the mechanism of polymerisation is *via* a radical cation intermediate coupling reaction that is discussed further in chapter three.

1.4.0 Modification of Polythiophenes.

Along with doping PT (or other conducting polymers) the substitution of functionalities to the monomers not only has a large effect on the conductivity, there will also be a large effect on the physical polymeric properties. Substitution is widely investigated due to the ease with which modifications can be performed. [37,38] For example, poly-3,4-disubstituted thiophenes substituted in the ring with a methyl group, produce polymers that have decreased oxidation potentials (caused by the inductive effect of the methyl group) increased conjugation and conductivity.

The two main approaches used to improve conductivity are to:

- i) Precisely define the polymer structure by rigidifying the π -conjugated backbone, which can be achieved by bridging the thiophene rings. In doing this, considerable changes can be observed in the electrochemical properties of the polymer.
- ii) Modify the monomer structure by introducing functionalities. There are a large number of publications detailing the modification of PT to contain the 1,3-dithiole group. The introduction of 1,3-dithiolene induces large intermolecular interactions (e.g. tetrathiafulvalene) and reduces the band-gap by increasing the π -conjugation.

Polymer modification the 1,3-dithiole units used to modify PT can be used themselves as a potential source of new polymeric materials. As mentioned above tetrathiafulvalene (TTF), consisting of two 1,3-dithiolene units fused together, induces large intermolecular interactions. Such moieties could be incorporated into 'charge-transfer' compounds thus opening up a new avenue of organic metal research.

1.5.0 Tetrathiafulvalene (TTF).

Wudl et al. reported Tetrathiafulvalene in 1970. [39] TTF is electron rich and contains a 'Hückel driving force', producing low electronegativity and providing a potentially aromatic sextet. TTF readily loses electrons to form a radical cation and dication. Both species are aromatic in the Hückel sense and are very stable (figure 1.0.5).

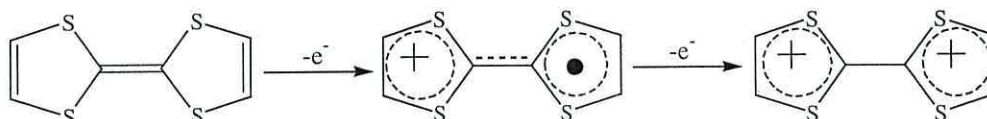


Figure 1.0.5

Salts of TTF, for example the chloride salt, were found to have high conductivities. The idea of forming a 'complex' between the donor TTF with the known acceptor TCNQ [40,41] was reported in 1973 (figure 1.0.6).

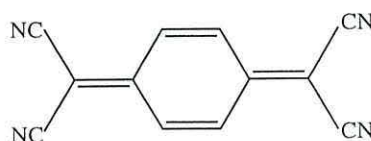


Figure 1.0.6

Since the discovery of TTF-TCNQ a lot of interest has been created in the design, synthesis and the properties of charge transfer complexes; TTF-TCNQ still remains amongst those with highest conductivity. This was the first reported organic metal, the crystal structure of which revealed the presence of TTF and TCNQ molecules in interlocking segregated stacks. [42] Both the TTF and TCNQ are planar with extended π -delocalisation through the molecule. The maximum conductivity was observed along the stack direction, in which short intermolecular, intra-stack S---S interactions of 3.47Å were present. [43] The formation of a

partially filled band gave rise to the high conductivity in this material. [44] It was envisaged that the intrastack interactions could be increased by the introduction of polarisable heteroatoms (Se, Te) into the organic donor molecules framework. This would result in the creation of materials showing increased electrical conductivity. [45] Indeed when TSF-TCNQ, TMTSF-DMTCNQ and BEDT-TTF (figures 1.0.7 a-c) were prepared, they were found to show higher conductivity and had enhanced inter-stack interactions compared to TTF-TCNQ.

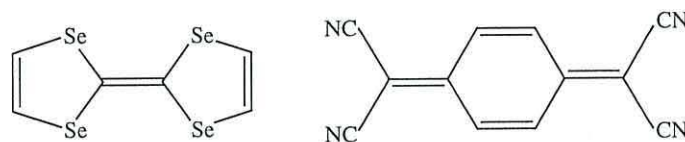


Figure 1.0.7a TSF – TCNQ.

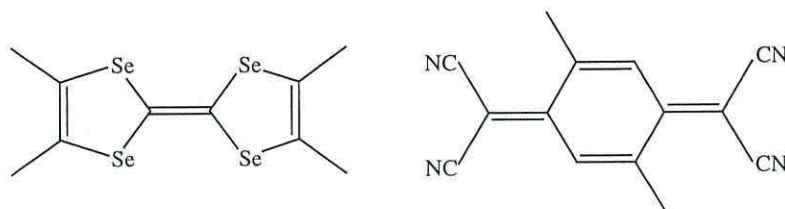


Figure 1.0.7b TMTSF – DMTCNQ.

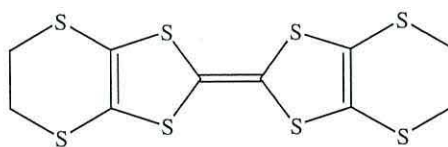


Figure 1.0.7c BEDT – TTF.

The derivatives of tetrathiafulvalene cover a wide spectrum. The previously described derivatives all have the TTF unit central to the compound. However hybrid TTF analogues have been prepared. [46] They consist of hybrid linearly

extended π -conjugated systems end-capped with 1,3-dithiol-2-ylidene groups (figure 1.0.8).

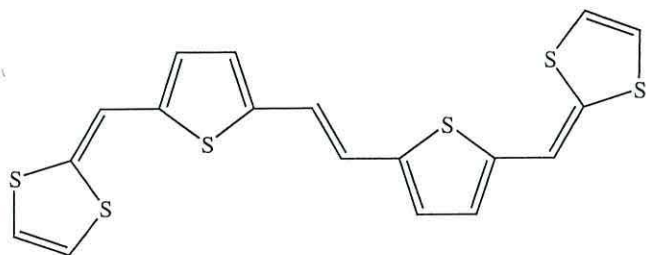


Figure 1.0.8

Another group of derivatives to emerge are the TTF vinylogues. [47] These involve ethanediylidene units between the two 1,3-dithiole units (figure 1.0.9) the synthesis of which is based mainly on a Wittig reaction of a (1,3-dithiole) phosphonium salt with appropriate aldehyde. [48]

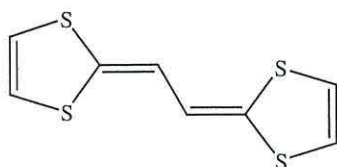


Figure 1.0.9.

Much effort has been put into variations on the structure of TTF leading to changes in the symmetry, size and electrochemistry of the donors. Present studies are concentrated on TTF derivatives containing the 1,3-dithiole units. [49] These derivatives are such that they undergo multi-stage redox reactions at relatively low potentials, with the extended conjugation stabilising the dication state found in TTFs, by a reduction in the intramolecular repulsion energy. [50]

1.5.1 The Synthesis of TTF compounds.

The synthetic methods employed in previous years have led to isomeric mixtures that proved difficult to purify. [51-53] However, developments in modern synthetic chemistry have led to selective synthesis, producing specific 'tailor-made' [52,54-56] compounds. The report, as can be seen, is restricted to TTF compounds only, although selenium and tellurium analogues of this type have been produced. [57-59] Once precursor synthesis has been accomplished (that can occur through a wide variety of mechanisms, dependant on the precursor in question), the final step of the synthesis for the TTF compound can be classified into 3 main categories;

- i) Synthesis involving the formation of the tetrathiosubstituted bond in the final step figure 1.1.0.

These methods involve π -bond formation *via* an elimination reaction using;
a) two protons, b) one proton or c) one or two heteroatoms.

In the case of (a) synthesis involving the oxidation of dihydrotetrathiafulvalene (2 proton loss), there is at present, only one route available for the oxidative dimerisation of 1,3-dithiole unit; electrochemical methodologies. [60] This happens only for 1,3-dithiole compounds containing an aryl group substituted in the 4' position. The yields found are low at ~ 30 %, and the reaction is synthetically restrictive.

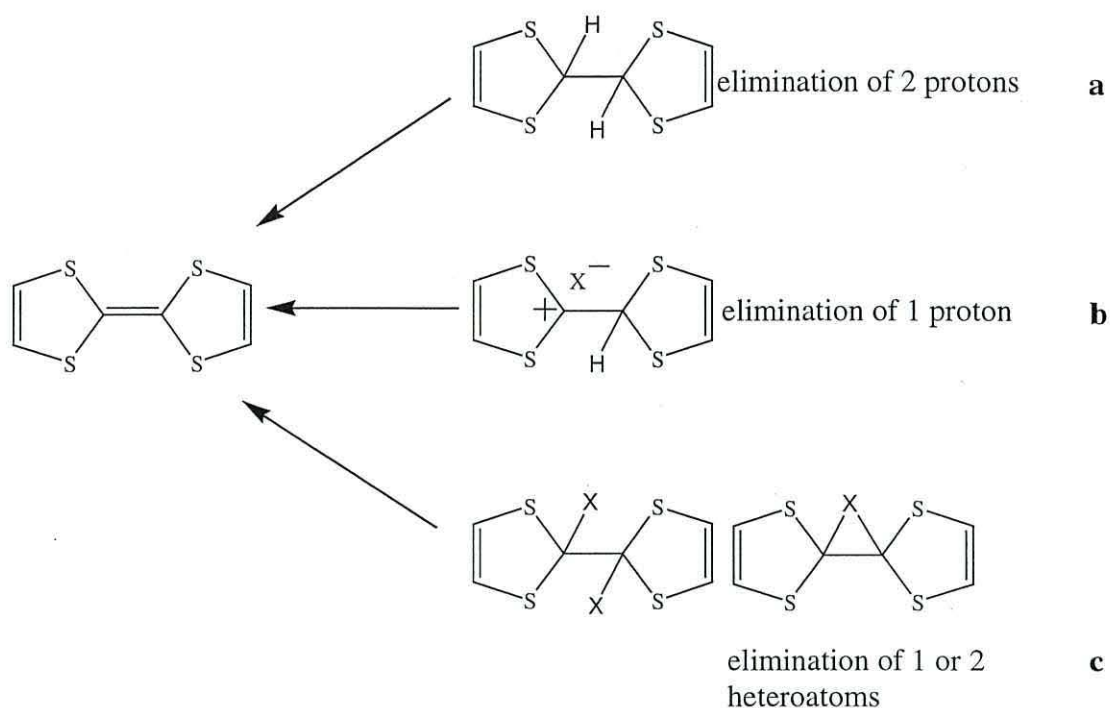


Figure 1.1.0

When the synthesis involving the elimination of one proton in the final step is considered (b), the general mechanism of this reaction involves the reaction of carbene on a 1,3- dithiole unit, or, phosphorous ylid on a 1,3- dithiole unit. The adduct produced is transformed to TTF by an amine that acts as a base.

An example of this type of synthesis can be found later on in the report in the production of a chemically modified TTF derivative. A number of further examples can be found in literature [61-67]; a generalised scheme is shown below (figure 1.1.1).

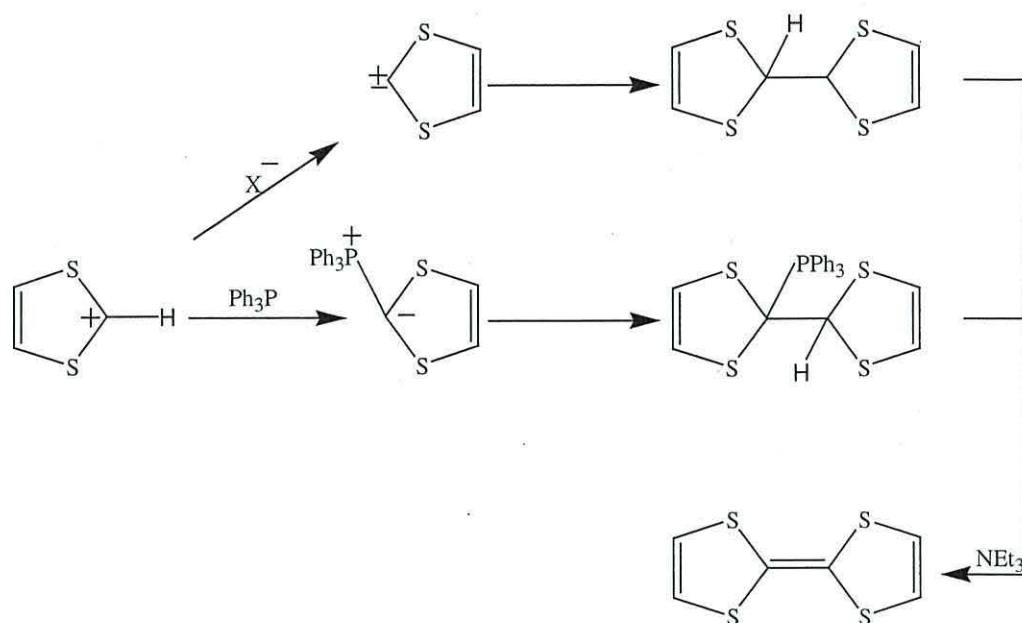


Figure 1.1.1

The synthesis through elimination of two heteroatoms (c) involves trivalent derivatives of phosphorus reacting with 2-thioxo 1,3-dithioles [68-72] to give the corresponding TTFs in varying yields (figure 1.1.2).

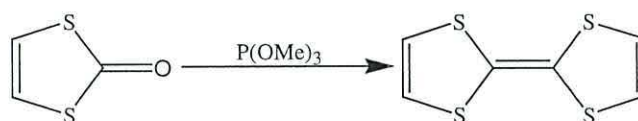


Figure 1.1.2

The above method is attractive as it allows access to large numbers of TTF derivatives. The synthesis is short, involving only 3 steps, with TTFs being produced from the 2-thioxo-1,3-dithioles in one step.

ii). Synthesis of tetrathiafulvalene from tetrachloroethylene.

In 1926, Hurtley and Smiles [73] noted that sodium *o*-benzene dithiolate reacts with tetrachloroethylene to produce dibenzotetrathiafulvalene [74]

(figure 1.1.3). This was the first unintentional report of the synthesis of TTF. The reaction is simple in that no preliminary synthesis of heterocycles is needed, so short step synthesis can be created. The yields however are poor.

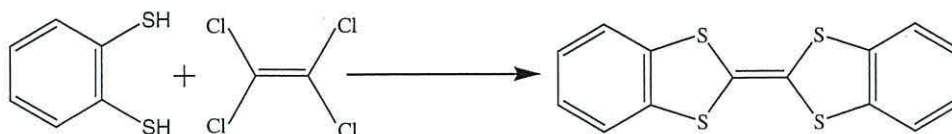
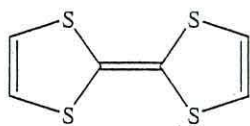


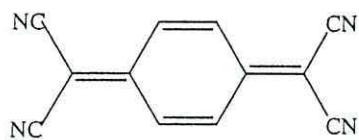
Figure 1.1.3.

iii) Synthesis of Tetrathiafulvalene *via* side chain modification.

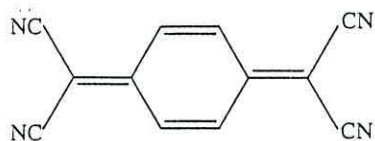
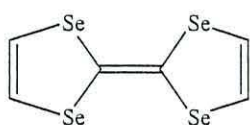
Modification of one or several functional groups on the starting TTF compound leads to TTF production. For example the hydrolysis or decarboxylation of esters [69,75,76], and hydrolysis of 2-thione-1, 3-dithiole [77] are commonly used procedures. This technique is little used due to molecule size limitations and reaction expense.



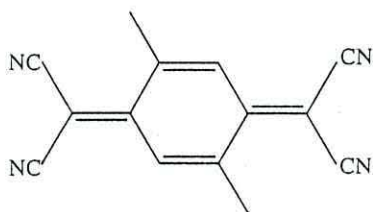
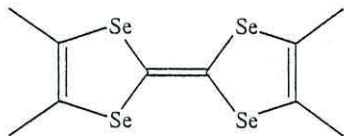
TTF



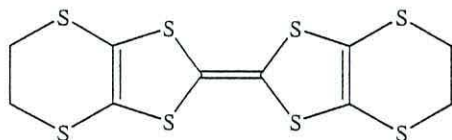
TCNQ



TSF-TCNQ



TMTSF



BEDT-TTF

1.6.0 References.

- 1) C. K. Chiang, M. A. Druy, S. C. Gau, A. J. Heeger, E. J. Louis, A. G. MacDiarmid, Y. W. Park and H. Shirakawa; *J. Am. Chem. Soc.*, (1978) 1013.
- 2) S. Takeda, K. Kaneto and K. Yoshimo; *Synth. Met.*, **18** (1987) 741.
- 3) J. P. Ferraris, C. Henderson, D. Meeker and D. Torres; *Synth. Met.*, **72** (1995) 147.
- 4) A. Corradini, S. Gracobbé, A. M. Mariangeli and M. Mastragostino; *Synth. Met.*, **28** (1989) 501.
- 5) K. Kaneto, M. Kaneto, Y. Min and A. G. MacDiarmid; *Synth. Met.*, **71** (1995) 221.
- 6) R. H. Baughman; *Synth. Met.*, **78** (1996) 339.
- 7) R. Hatami, T. R. Jow, M. Maxfield and L. W. Shacklette; *Synth. Met.*, **26** (1989) 665.
- 8) C. Arbizzani and M. Mastragostino; *Electrochimica Acta.*, **35** (1990) 251.
- 9) M. Biserni, M. Mariangel and M. Mastragostino; *J. Electrochem. Soc.*, **132** (1994) 1597.
- 10) B. A. Lopez de Mishima, H. T. Mishima and M. I. Sanchez de Pinto; *J. Appl. Electrochem.*, **27** (1997) 831.
- 11) M. C. Lefebure, Z. Qi and P. G. Pickup; *J. Electrochem. Soc.*, **146** (1999) 2054.
- 12) S. D. Thompson, L. R. Jordan and M. Forsyth; *Electrochimica Acta.*, **46** (2001) 1657.
- 13) M. Neergat, A. K. Shulka and K. S. Ghandi; *J. Appl. Electrochem.*, **31** (2001) 373.
- 14) F. Lufrano, G. Squadrito, A. Patti and E. Passalacqua; *J. Appl. Polym. Sci.*, **77** (2000) 1250.
- 15) P. Futertio and I.-M. Hsing; *Electrochimica Acta.*, **45** (2000) 1741.
- 16) J. S. Miller; *Adv. Mater.*, **5** (1993) 587.
- 17) T. Le Gall, M. S. Passos, S. K. Ibrahim, S. Morlat-Therias, C. Sudbrake, S. A. Fairhurst, M. A. Queiros and C. J. Pickett; *J. Chem. Soc. Perkin Trans. 1.*, (1999) 1657.
- 18) F. Garnier, H. Korri-Yousoufi, P. Srivastava and A. Yassar; *J. Am. Chem. Soc.*, **116** (1994) 8813.
- 19) P. N. Bartlett and J. M. Cooper; *J. Electroanal. Chem.*, **362** (1993) 1.

- 20) S. J. Higgins, C. L. Jones and S. M. Francis; *Synth. Met.*, **98** (1999) 211.
- 21) L. Pu; *Acta. Polym.*, **48** (1997) 116.
- 22) M. C. Pirrung; *Chem. Rev.*, **97** (1997) 473.
- 23) C. P. Howitz, N. Y. Suhu and G. C. Dailey; *J. Electroanal. Chem.*, **324** (1992) 79.
- 24) S. Morlat-Therias, M. S. Passos, S. K. Ibrahim, T. Le Gall, M. A. Queiros and C. J. Pickett; *J. Chem. Soc. Chem. Commun.*, (1998) 1175.
- 25) E. Huckel; *Z. Phys.*, **70** (1931) 201.
- 26) C. K. Chiang, C. R. Fincher, S. C. Gau, A. J. Heeger, E. J. Lousi, A. G. MacDiarmid, Y. W. Park and H. Shirakawa; *Phys. Rev. Lett.*, **39** (1977) 1098.
- 27) T. A. Skotheim (Ed.), *Handbook of conducting polymers*, Marcel Dekker, New York, (1986).
- 28) G. Tourillon and F. Garnier; *J. Electroanal. Chem.*, **135** (1982) 173.
- 29) V. L. Afanas'ev, I. B. Nazarova and M. L. Khidekel; *Izv.Akad.Nauk SSSR Ser.Khim.*, (1980) 1687.
- 30) K. Kaneto, K. Yoshimo and Y. Inuishi; *Jpn. J. Appl. Phys.*, **21:L** (1982) 152.
- 31) H. Hotta, T. Hoska and W. Shimotsuma; *J. Chem. Phys.*, **80** (1983) 154.
- 32) T. Yamamoto, K. Sanechika and A. Yamamoto; *J. Polym. Sci. Polym. Lett. Ed.*, **18** (1980) 9.
- 33) H. Hotta, T. Hoska and W. Shimotsuma; *Synth. Met.*, **6** (1983) 317.
- 34) G. Tourillon and F. Garnier; *J. Electroanal. Chem.*, **161** (1984) 51.
- 35) R. J. Waltman, J. Bargon and A. F. Diaz; *J. Phys. Chem.*, **87** (1983) 1459.
- 36) T. A. Skotheim; (Ed.) *Handbook of Conducting Polymers.*, Marcel Decker, N.Y, (1986).
- 37) J. Roncali; *Chem. Rev.*, **92** (1992) 711.
- 38) F. Wudl, G. M. Smith and E. J. Hufnagel; *J. Chem. Soc. Chem. Commun.*, (1970) 1453.
- 39) D. S. Acker and W. R. Hertler; *J. Am. Chem. Soc.*, **84** (1962) 3370.
- 40) L. R. Melby; *J. Am. Chem. Soc.*, **84** (1962) 3374.
- 41) T. E. Phillips, T. J. Kistenmacher, J. P. Ferraris and D. O. Cowan; *J. Chem. Soc. Chem. Commun.*, (1973) 1532.
- 42) J. P. Ferraris, C. Henderson, D. Meeker and D. Torres; *Synth. Met.*, **72** (1995) 147.

- 43) S. Takeda, K. Kaneto and Y. Yoshino; *Synth. Met.*, **18** (1987) 741.
- 44) F. Wudl, E. Aharon-Shalom; *J. Am. Chem. Soc.*, **104** (1982) 1154.
- 45) H. Brisset, S. L. Moustarder, P. Blanchard, B. Illien, A. Riou, J. Orduna, J. Garin and J. Roncali; *J. Mater. Chem.*, **7** (1997) 2027.
- 46) D. Lorey, P. Le Magueres, C. Rimbaud, L. Ouahab, P. Dehaes, R. Carlier, A. Tallec and A. Robert; *Synth. Met.*, **86** (1997) 1831.
- 47) T. Sugimoto, H. Awaji, I. Sugimoto, T. Kawase, S. Yoneda and Z. Yoshida; *J. Mater. Chem.*, **1** (1989) 535.
- 48) M. R. Bryce and A. J. Moore; *J. Chem. Soc. Perkin. Trans. I.*, (1991) 157.
- 49) M. Sato, M. V. Lakshmikantham, M. P. Cava and A. F. Garito; *J. Org. Chem.*, **43** (1978) 2084.
- 50) J. M. Fabre, E. Torreilles, J. P. Gibert, M. Chanaa and L. Giral; *Tet. Lett.*, 4033 (1977).
- 51) J. M. Fabre, C. Galaine, L. Giral and D. Chasseau; *Tet. Lett.*, (1982) 1813.
- 52) J. M. Fabre, C. Galaine and L. Giral; *J. Phys. Colloq.*, **44** (1983) 1153.
- 53) C. M. Lindsay, K. Smith, C. A. Brown and K. Betterto-Cruz; *Tet. Lett.*, (1984) 995.
- 54) C. A. Brown, R. D. Miller, C. M. Lindsay and K. Smith; *Tet. Lett.*, (1984) 991.
- 55) N. C. Gonella and M. P. Cava; *J. Org. Chem.*, **43** (1978) 369.
- 56) K. A. Lerstrup, D. Talham, A. Bloch, T. O. Poehler and D. O. Cowan; *J. Chem. Soc. Chem. Commun.*, (1982) 336.
- 57) F. Wudl and E. Aharon-Shalom; *J. Am. Chem. Soc.*, **104** (1982) 1154.
- 58) K. A. Lerstrup and D. O. Cowan; *J. Phys. Colloq.*, **44** (1983) C3. 1247.
- 59) F. D. Saeva, B. P. Morgan, M. W. Fichner and N. F. Haley; *J. Org. Chem.*, **49** (1984) 390.
- 60) C. M. Lindsay, K. Smith, C. A. Brown and K. Betterto-Cruz; *Tet. Lett.*, (1984) 995.
- 61) C. A. Brown, R. D. Miller, C. M. Lindsay and K. Smith; *Tet. Lett.* (1984) 991.
- 62) K. A. Lerstrup and D. O. Cowan; *J. Phys. Colloq.*, **44** (1983) C3. 1247.
- 63) F. Wudl, G. M. Smith, E. J. Hufnagel; *J. Chem. Soc. Chem. Commun.*, (1970) 1453.
- 64) F. Wudl, M. L. Kaplan, E. J. Hufnagel and E. W. Southwick; *J. Org. Chem.*, **39** (1974) 3608.
- 65) J. P. Ferraris, T. O. Poehler, A. N. Bloch and D. O. Cowan; *Tet. Lett.*, (1973) 2253.

- 66) E. M. Engler, V. V. Patel, J. R. Andersen, R. Schumaker and A. A. Fukushima; *J. Am. Chem. Soc.*, **100** (1978) 3769.
- 67) C.U. Pittman, M. Narita and Y. F. Liang; *J. Org. Chem.*, **41** (1976) 2855.
- 68) M. G. Miles, J. D. Wilson, D. J. Dahn and J. H. Wagenknecht; *J. Chem. Soc. Chem. Commun.*, (1974) 751.
- 69) M. G. Miles, J. S. Wagner, J. D. Wilson and A. R. Siedle; *J. Org. Chem.*, **40** (1975) 2577.
- 70) H. D. Hartzler; *J. Am. Chem. Soc.*, **95** (1973) 4379.
- 71) H. D. Hartzler; *J. Am. Chem. Soc.*, **92** (1970) 1412.
- 72) W. R. H. Hurtley and S. Smiles; *J. Chem. Soc.*, (1926) 2263.
- 73) M. V. Lakshmikantham, M. P. Cava and A. F. Garito; *J. Chem. Soc. Chem. Commun.*, (1975) 383.
- 74) D. L. Coffen, J. Q. Chambers, D. R. Willaims, P. E. Garret and N. D. Cranfield; *J. Am. Chem. Soc.*, **93** (1971) 2258.
- 75) M. V. Lakshmikantham and M. P. Cava; *J. Org. Chem.*, **41** (1976) 882.
- 76) M. V. Lakshmikantham, M. P. Cava and A. F. Garito; *J. Chem. Soc. Chem. Commun.*, (1975) 383.
- 77) R. R. Schumaker and E. M. Engler; *J. Am. Chem. Soc.*, **99** (1977) 5521.

Chapter Two: Aims of the research.

2.1.0 Introduction to Polymeric TTF systems.

Recently there has been a surge of papers detailing organic conjugated polymers containing the TTF unit. [1-7] These studies were prompted by the prospect of the novel conductivities anticipated from the increased dimensionality of the single axis TTF conduction. Such TTF derivatised polymers have been prepared by incorporating TTF moieties into the polymer backbone. Unfortunately the polymers were of 'spacer strategy' in design, in which the polymer and the TTF were not directly attached, merely coupled *via* linkages, and, as a consequence resulted in poor conjugation thus producing low conductivity.

2.2.0 A review of polymeric TTF systems containing polythiophene.

Polythiophene (PT), a highly conducting polymer in the doped state [8] has the ability to form other conducting polymer composites and undergo numerous synthetic functionalisations. This makes the thiophene monomer attractive to further studies. With this in mind the possibility of incorporating the redox active, electron donor tetrathiafulvalene (TTF) into PTs has become an exciting proposition, because of the enhanced electrical conductivities expected in the resultant polymer.

There are however, few reports of the synthesis of polymeric TTF systems that provide the possibility to produce processable, conducting materials. TTF moieties have been incorporated into the backbone of polymers for example methylacrylate [9] but the polymers produced were either insoluble or poorly conducting. More recent publications have shown the synthesis of main chain and side chain polymers [10] though these were also found to have poor conjugation and thus low conductivity. Bryce and co workers [11] reported the formation of a polymer solution of a thiophene unit linked to the TTF redox active centre *via* an

ester group linkage **1** (figure 2.0.1). This was followed by Thobie–Gautier *et al.* [12] reporting the electropolymerisation studies of a TTF-derivatised polythiophene (compound **2**, Figure 2.0.1), in which the monomeric electroactive units were separated by linear oxadecyl spacers. In both cases the resultant polymers were found to be poorly conducting arising from a lack of effective conjugation in the polymers.

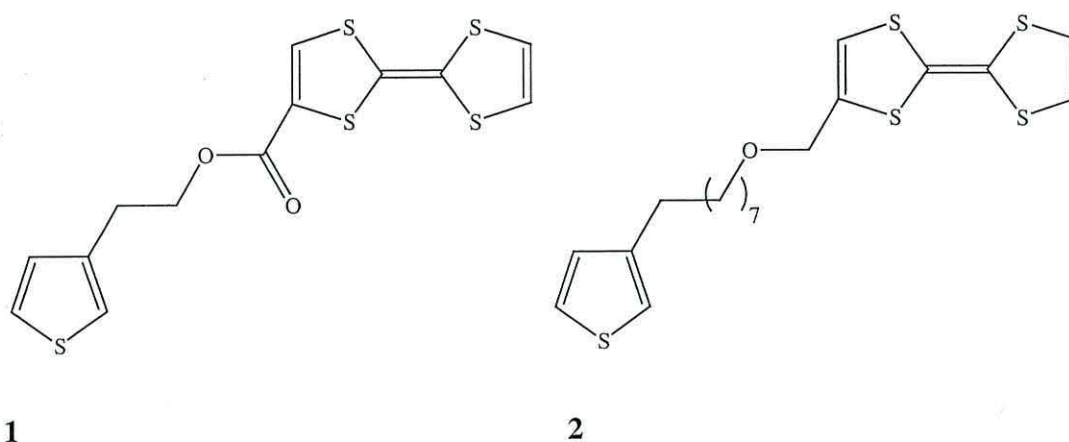


Figure 2.0.1 TTF-derivatised polythiophenes.

More recently, Skabara and co workers [13] reported electropolymerisable TTF-thiophene fused monomeric compounds, **3** and **4** (figure 2.0.2), based on terthiophene analogues. Such monomers show increased tendency to electropolymerise due to the higher donating abilities of the thiophene functionalities. Again as in previous reports, the resultant polymers produced did not contain the TTF moieties in the polymeric backbone.

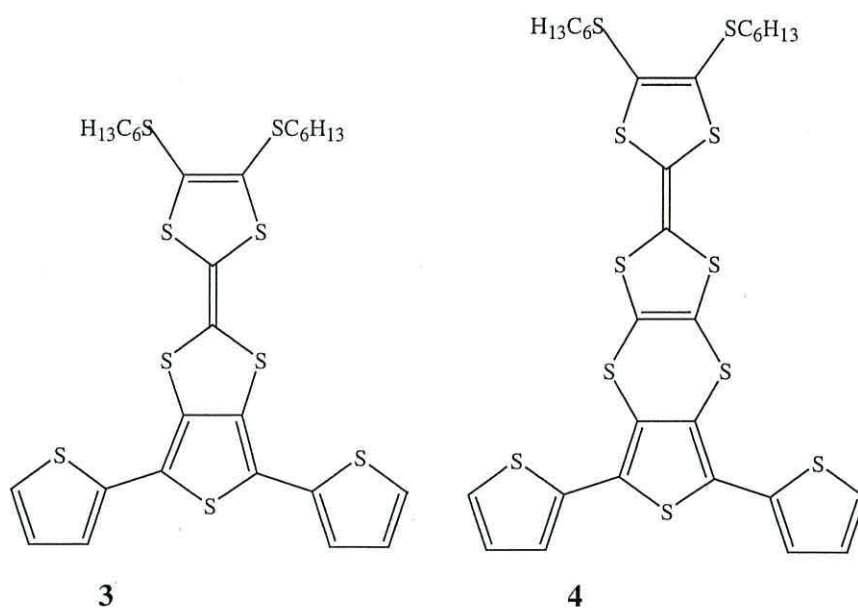


Figure 2.0.2 Terthiophene Analogues, TTF derivatised polythiophene.

Lately research tended to be concerned with increasing TTF concentration in polymers rather than producing an electropolymerisable TTF monomer. To this end Skabara and co-workers synthesised the compounds **5** and **6** (figure 2.0.3). [14]

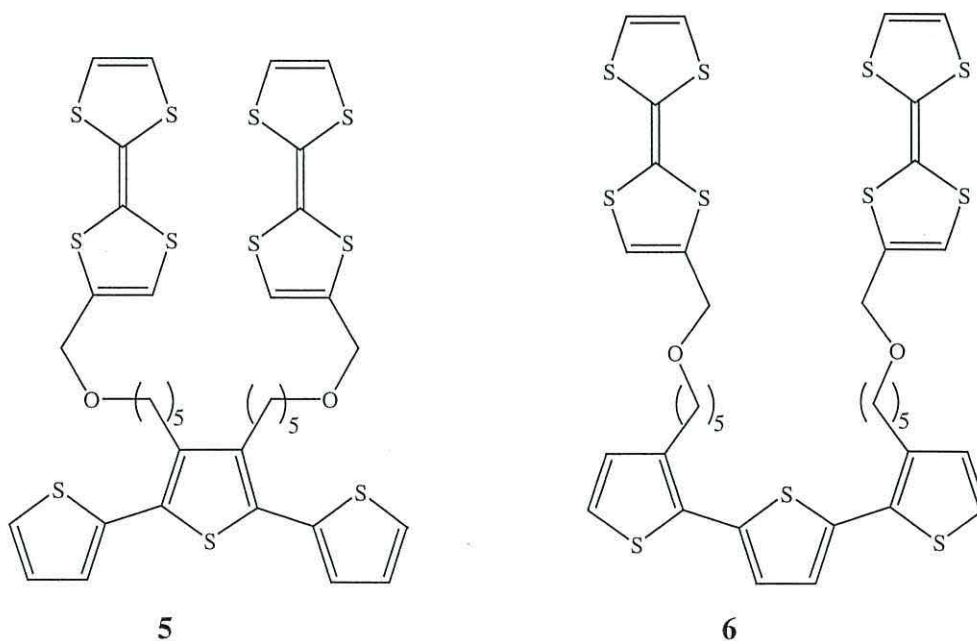


Figure 2.0.3 TTF-polymers.

It was noted that although homoelectropolymerisation attempts were failures, mixed valence interactions were observed in the cyclic voltammogram of the copolymers with bithiophene. This would suggest mixed valence interactions involve a significant contribution of intramolecular interactions [10], providing incitements for further studies to work towards the development of organic materials with hybrid electronic conduction.

2.3.0 Previous Research.

The initial research carried out by Charlton *et al.* concentrated on 2-thienyl TTF derivatives **7-9** derived from *bis*-4,5-(2-thienyl)-1,3-dithiole-2-one **10** (figures 2.0.4 a, b). [15,16] The TTF derivatives were designed in order to prepare novel polymers incorporating the TTF core and thiophene units. By substituting electron-withdrawing thiophene groups in the TTF unit it was predicted that polymerisation would be favourable. However it was found that electropolymerisation was not possible. This was attributed to complexities arising from the TTF core. During polymerisation the TTF core is sequentially oxidised TTF^+ and TTF^{2+} species, prior to the oxidation of the thiophene units. The generation of the dicationic TTF species results in the formation of an 'aromatic TTF core'. Any further oxidation to electropolymerise the monomer units would involve conjugation through the aromatic nucleus. Unfortunately this is energetically unfavourable making electropolymerisation unlikely.

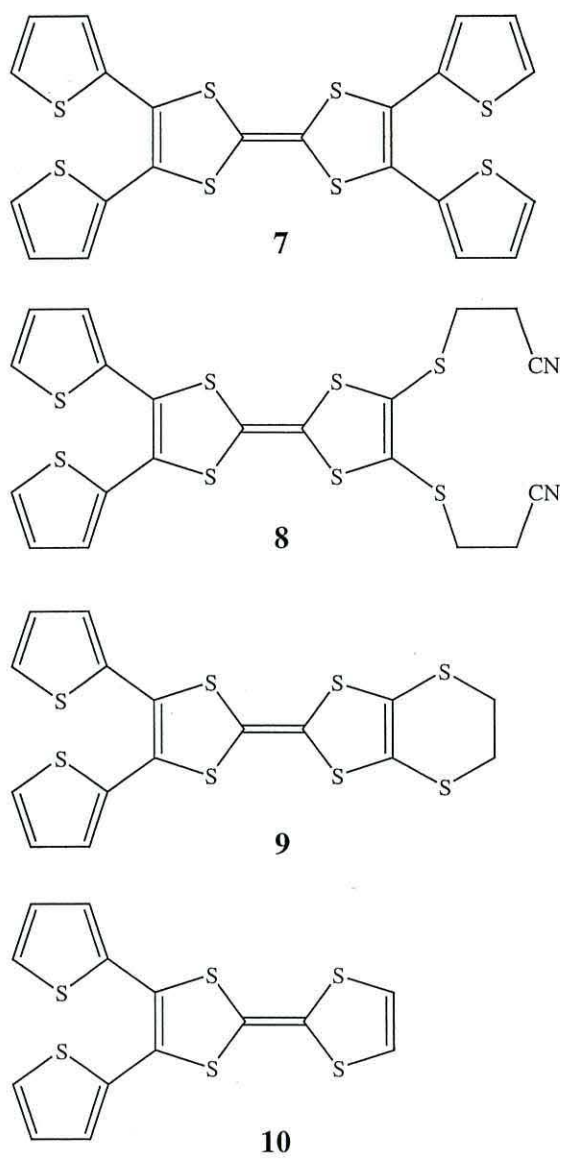
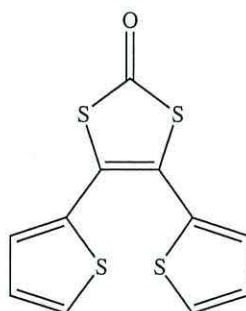


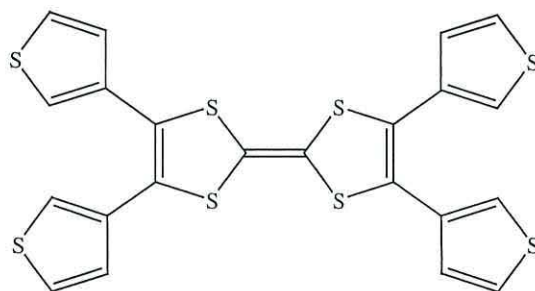
Figure 2.0.4a 2-thienyl TTF derivatives 7-9.



10

Figure 2.0.4b *Bis*-4,5-(2-thienyl)-1,3-dithiole-2-one **10**.

By introducing thiophene moieties in the 3-position, it was envisaged that electropolymerisation may be possible (figure 2.0.5). Substitution in the 3-position would result in more effective conjugation in the system, increasing the electron withdrawing tendencies of the thiophene moieties making electropolymerisation more likely.



11

Figure 2.0.5 4,4',5,5'-Tetra-thiophen-3-yl-[2,2']bi[[1,3]dithiolylidene] **11**.

Unfortunately, as in the case of the 2-thienyl TTF compounds, the 3-thienyl TTFs did not electropolymerise. [17] Again the lack of electropolymerisation was attributed to the aromatic TTF^{2+} core formed upon oxidation, the polymerisation of which may be energetically unfavourable. To test this assumption polymerisation of the 3-thienyl-TTF precursor, *bis*-(3-thienyl)-1,3-dithiole-2-one, **12** was attempted (figure 2.0.6).

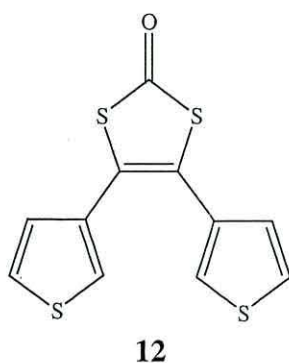


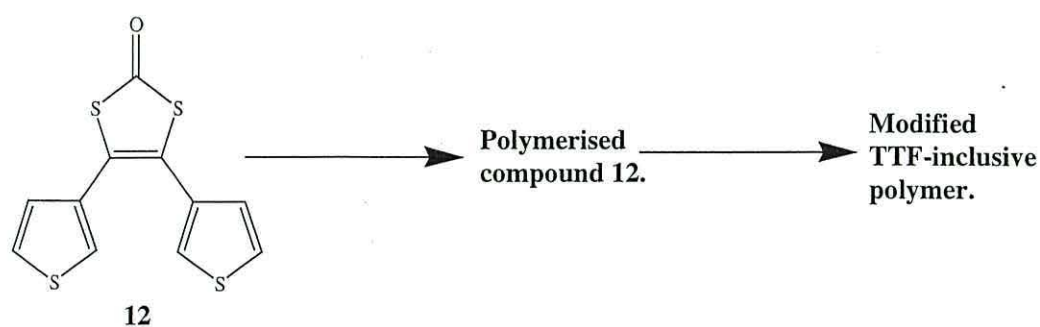
Figure 2.0.6 *Bis*-(3-thienyl)-1,3-dithiole-2-one **12**.

Polymerisation of **12** was found to be successful, resulting in the formation of a redox switching polymer. With the knowledge of the inability of the TTF derivatives **7-11** to undergo electropolymerisation, a new strategy was required in the preparation of the TTF inclusive polymers.

2.4.0 Aims of the research.

The main aim of the research comprised in this thesis was the investigation of the mode of polymerisation of compound **12** in comparison to the known non-polymerisable TTF derivative **11**.

Once understood, TTF derivatised polythiophenes based on **12** would be prepared and polymerised. Within this rationale there are several approaches to take; direct electropolymerisation, and *in situ* polymer modification as shown in scheme 2.0.1.



Scheme 2.0.1 Strategy for *in situ* polymer modification.

A further aim of the research was to prepare benzobithiophenes based on the unit **13** (figure 2.0.7), in which the two thiophene rings have been fused together, in order that we might investigate the possibility of allowing direct polymerisation of TTF derivatives based on **14**. This was attempted using synthetic and photochemical methodologies.

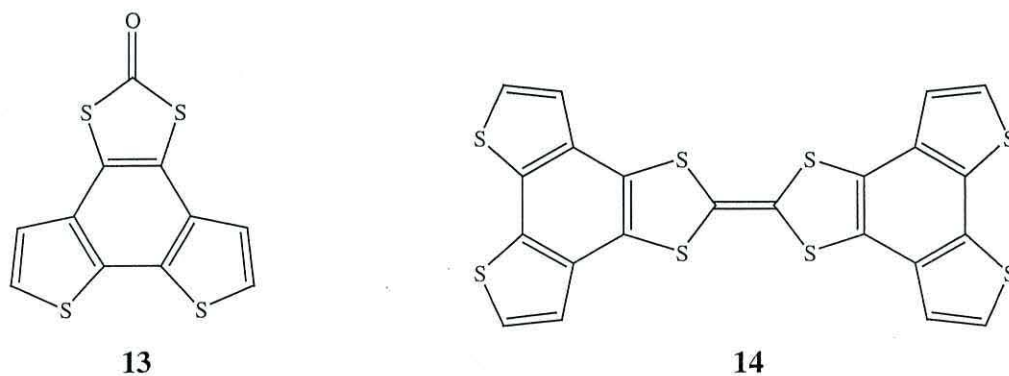
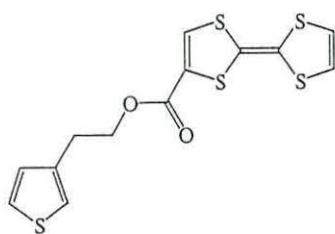
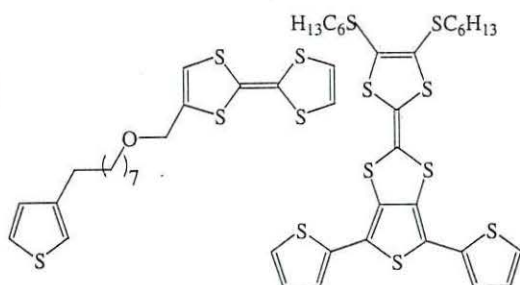


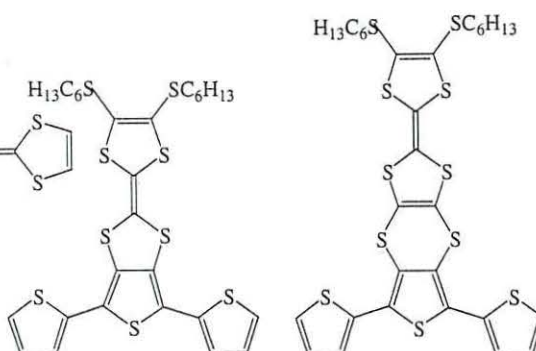
Figure 2.0.7 Compounds **13** and **14**.



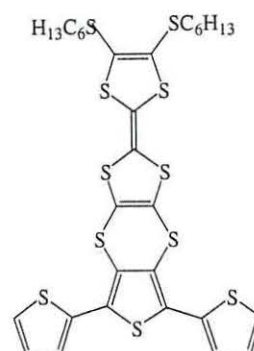
1



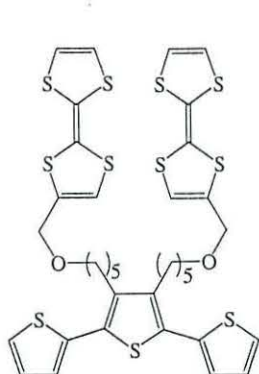
2



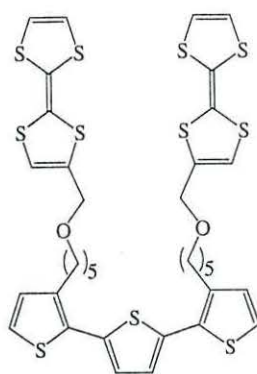
3



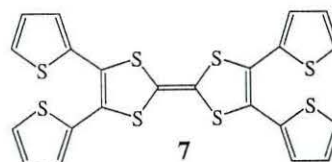
4



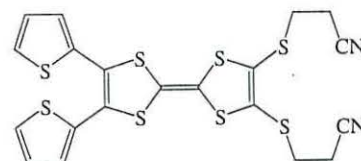
5



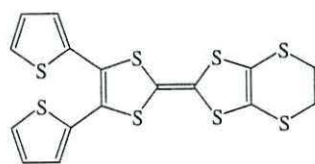
6



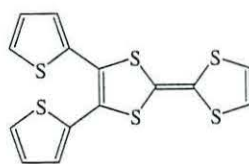
7



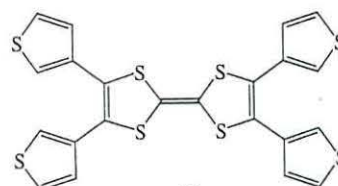
8



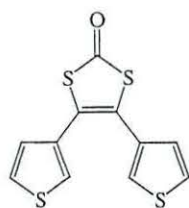
9



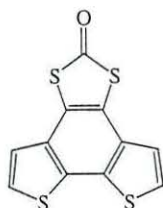
10



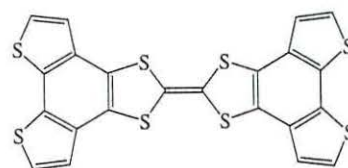
11



12



13



14

2.5.0 References.

- 1) M. L. Kaplan, R. C. Haddon, F. Wudl and E. D. Feit; *J. Org. Chem.*, **43** (1978) 4642.
- 2) M. Iyoda, N. Ueno and M. Oda; *J. Chem. Soc. Chem. Commun.*, (1992) 158.
- 3) M. Adam, A. Bohnen, V. Enkleman and K. Mullen; *Adv. Mater.*, **3** (1991) 1600.
- 4) F. B. Kaufman, A. H. Schroeder, E. M. Engler, S. R. Kramer and J. Q. Chambers; *J. Am. Chem. Soc.*, **102** (1990) 483.
- 5) V. Y. Khodorkovsky, J. Y. Becher, C. Wang, A. Ellern, L. Shapiro and J. Bernstein; *Adv. Mater.*, **6** (1994) 656.
- 6) J. Roncali; *Chem. Rev.*, **92** (1992) 711.
- 7) C. U. Pittman, M. Ueda and Y. F. Liang; *J. Org. Chem.*, **44** (1979) 3639.
- 8) J. Roncali; *J. Mater. Chem.*, **9** (1999) 1875.
- 9) M. R. Bryce, A. D. Chissel, J. Gopal, P. Kathirgamanathan and D. Parker; *Synth. Met.*, **39** (1991) 397.
- 10) C. Thobie-Gautier, A. Gorgues, M. Jubault and J. Roncali; *Macromolecules.*, **6** (1993) 4094.
- 11) P. J. Skabara, D. M. Roberts, I. M. Serebryakov and C. Pozo-Gonzalo; *J. Chem. Soc. Chem. Commun.*, (2000) 1005.
- 12) P. J. Skabara, I. M. Serebryakov, D. M. Roberts, I. F. Perepichka, S. J. Coles and M. B. Hursthouse; *J. Org. Chem.*, **64** (1999) 6418.
- 13) A. Charlton, A. E. Underhill, M. Kalaji, P. J. Murphy, D. E. Hibbs, M. B. Hursthouse and K. M. Malik; *J. Chem. Soc. Chem. Commun.*, (1996) 2423.
- 14) A. Charlton, A. E. Underhill, G. Williams, M. Kalaji, P. J. Murphy, K. M. Abdul Malik and M. B. Hursthouse; *J. Org. Chem.*, **62** (1997) 3098.
- 15) A. Charlton, M. Kalaji, P. J. Murphy, S. Salmaso, A. E. Underhill, G. Williams, M. B. Hursthouse and K. M. Malik; *Synth. Met.*, **95** (1998) 75.

Chapter Three: The Synthesis and Polymerisation of 2-(4,5-di-thiophen-3-yl-[1,3]dithiol-2-ylidine)-benzo[1,3]dithiole 15.

3.1.0 Aims.

One of the aims of the research comprising this chapter was to investigate the possibility of performing an *in situ* chemical modification of the polymerised compound **12** to obtain a thiophene based TTF polymer, in which the TTF moiety is directly attached to the polymer backbone (figure 3.0.1).

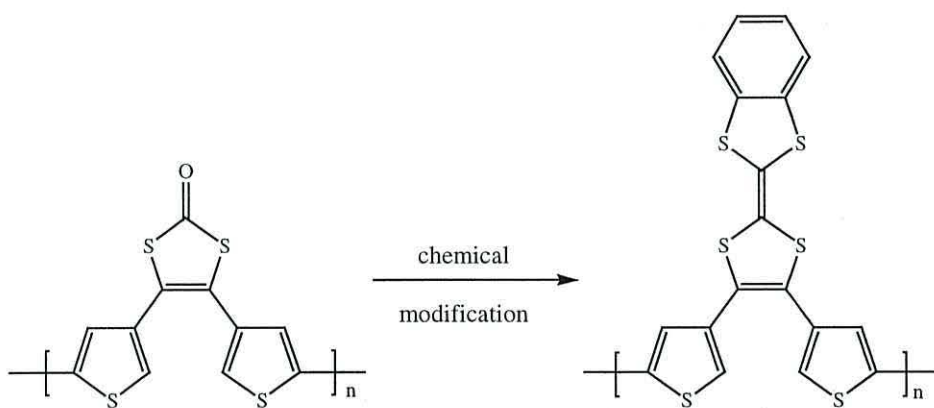
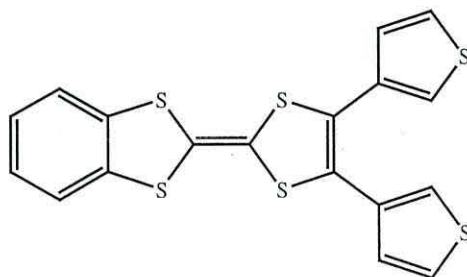


Figure 3.0.1 *In situ* modification of the polymerised **12**.

A further aim of the research was to synthesise compound **15** (figure 3.0.2), 2-(4,5-di-thiophen-3-yl-[1,3]dithiol-2-ylidine)-benzo[1,3]dithiole and investigate its electrochemical properties for comparative reasons.



15

Figure 3.0.2 2-(4,5-Di-thiophen-3-yl-[1,3]dithiol-2-ylidine)-benzo[1,3]dithiole **15**.

The final aim was to investigate the polymer structures in the unmodified polymerised form of **12** and the chemically modified polymer. This was carried out using Subtractively Normalised Interfacial Fourier Transform Infra-Red Spectroscopy (SNIFTIRS), which was also used as a tool to confirm polymer modification.

3.2.0 Previous research.

As mentioned in chapter two, previous work by Charlton *et al.* was carried out on a series of 2/3-thienyl substitute TTF derivatives (**7-9**), [1,2] as part of an investigation into the production of PT-TTFs (figure 3.0.3).

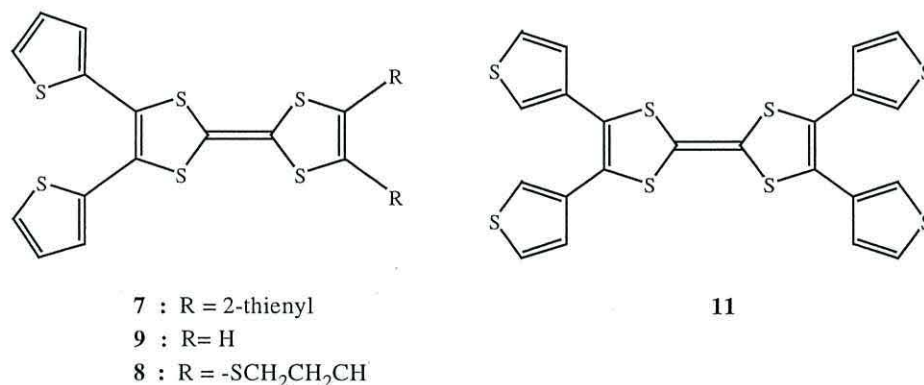


Figure 3.0.3 TTF compounds previously prepared by Charlton *et al.*

There was very limited success when electropolymerisation was attempted; a result that was attributable to the differences in oxidation potential of the TTF and thiophene described previously. The accepted theory for overcoming the oxidation potential difference is that if, somehow, the polymerisation of the thiophene could occur before the sequential oxidations of the TTF core to the pseudo aromatic TTF²⁺ species, PT-TTFs would be easily obtained. All reported literature noted the limited success found from the electropolymerisation of thiophene-TTF monomers, so it was thought that modification of a functionalised PT would be an interesting avenue of research to pursue.

3.2.1 Introduction to polymer functionalisation.

Electrochemical polymerisation has been the most accepted and accessible route for the synthesis of some of the most important classes of conjugated polymers, including PPy, PT and PANI. These polymers have been the focus of much attention over the past 20 years owing to not only their potential use in technological applications, but also the fundamental problems posed by their structure and electronic properties. Perhaps the most attractive feature of electropolymerisation is that it is the basis for functionalisation of modified electrodes in which the inherent electrochemical and/or optical properties of the conjugated polymer backbone are associated with specific properties afforded by covalently bound functional groups.

Tailored electropolymers possessing functional groups that react/interact to specific requirements (for example: to interact with biological molecules such as redox cofactors and to provide chiral interfaces) are attracting wide-spread interest as advanced materials. [3,4] The process of the modification of such functionalised polymers to provide polymers of differing properties has been well documented in literature. [5,6] However, the reports of solid-state conjugated polymer modification are providing the most promising approach for gaining access to polymers thought otherwise unattainable via electropolymerisation of the corresponding monomer. [7,8] This would allow the possibility of producing conducting polymers that are essentially 'tailor-made', having the particular electronic properties needed but also with the incorporation of specific properties of the functional group. This combination results in new possibilities for materials in sensor applications, [9] microelectronic devices [10] and electrocatalysis. [11]

However, despite an apparent simplicity, the realisation of this concept poses a number of complex problems related to direct/indirect electronic and steric parameters of the attached functional group. These include 1) the electronic properties of the resultant conjugated polymer 2) the electropolymerisation process itself and 3) the electronic effects the substituents (functional groups) have when directly connected to the conducting polymer. [12] Examples that have been reported in the literature were generally found to have a large number of chemical reactions for which

the conditions are difficult to control leading to little derivatisation of the polymers, or prove post-modification to increase oxidation potentials to values incompatible with solvent stability limits and electrolytes used in electrochemistry. Also, reports of the functionalised monomers with easily oxidisable groups have been found to scavenge cation radicals in the polymerisation process, therefore interfering or inhibiting completely the electropolymerisation process. Or from a different viewpoint, a monomer containing a functional group of inferior oxidation potential may be irreversibly degraded upon electropolymerisation.

The derivatisation of polythiophenes by covalent attachment of TTF has been the focus of much interest. This is because the expected resultant polymers would show an increase in the polymers' long-range order (due to the high propensity of TTF to form regular π -stacks). This would result in a new class of organic conducting materials in which the overall conductivity could be ensured in parallel by the intra-stack aromaticity transfer associated with mixed-valence interactions in TTF π -stacks and the polaron/bipolaron conduction in the π -conjugated chain. Whilst potential precursors of such conducting polymers have been synthesised by several groups, most of the attempts to electropolymerise these precursors have remained unsuccessful. [13]

The first reported electrosynthesis of an extensively conjugated PT-TTF compound (figure 3.0.4) was reported by Thobie-Gautier *et al.*, [14] in which the TTF group was linked *via* an oxadecyl spacer in order to minimise steric interactions. Electropolymerisation was difficult with little conductivity being observed.

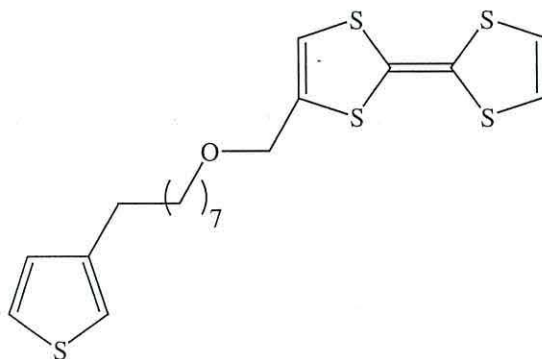


Figure 3.0.4 PT-TTF separated by oxadecyl spacer.

The problem posed by electrosynthesis of PT-TTFs is found in the considerable difference between the oxidation potential of the TTF and that of the thiophene. Thus at the potential required to form the PT backbone, the oxidised TTF aromatic core is now consuming the bulk of the current, with the possibility of TTF to act as a thiophene cation radical scavenger further impeding any attempt at polymerisation. More recently Skabara and co-workers [15,16] reported electropolymerisable TTF-thiophene fused monomers (figure 3.0.5) based on terthiophene analogues, the premise being that such monomers show increased tendency to electropolymerise due to the higher donating abilities of the thiophene functionalities. Again as in previous reports the resultant polymers exhibited poor conductivity and did not indicate the presence of TTF moieties directly attached to the polymeric backbone.

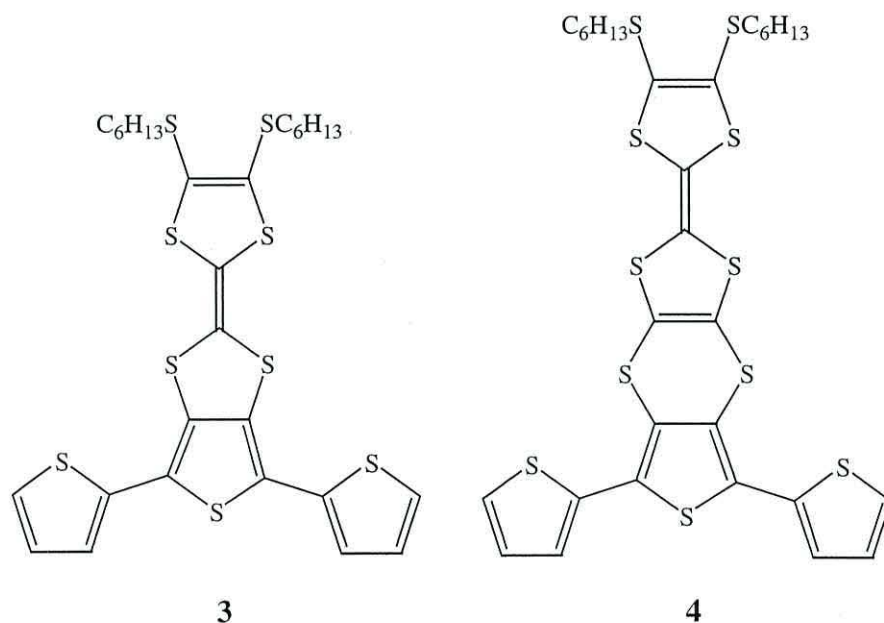


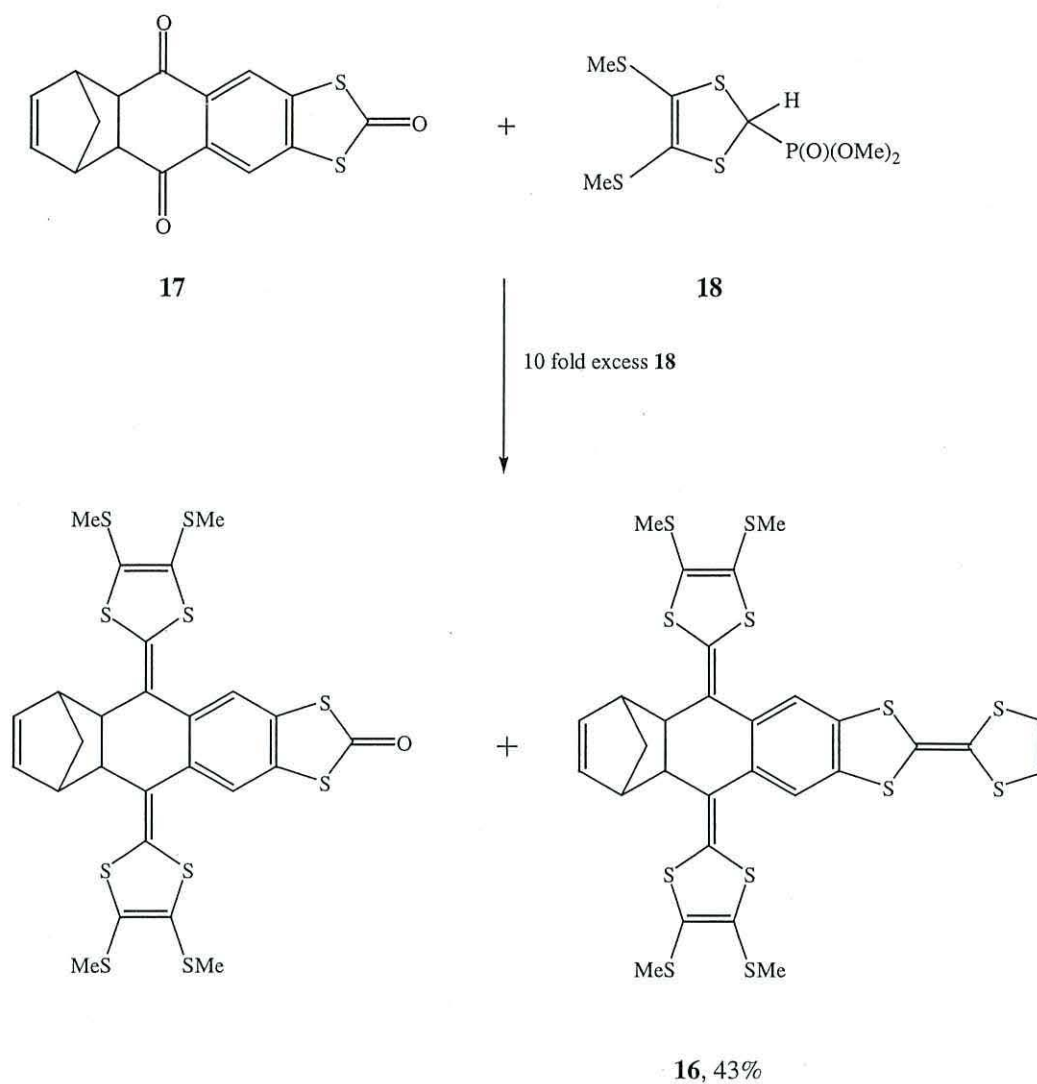
Figure 3.0.5 Terthiophene TTF analogues studied by Skabara and co-workers. [13,14]

3.3.0 Synthetic Strategy.

The synthesis of **12** is described in detail in chapter four, and will not be discussed in this chapter.

3.3.1 The synthesis of 2-(4,5-di-thiophen-3-yl-[1,3]dithiol-2-ylidene) - benzo[1,3]dithiole, **15**.

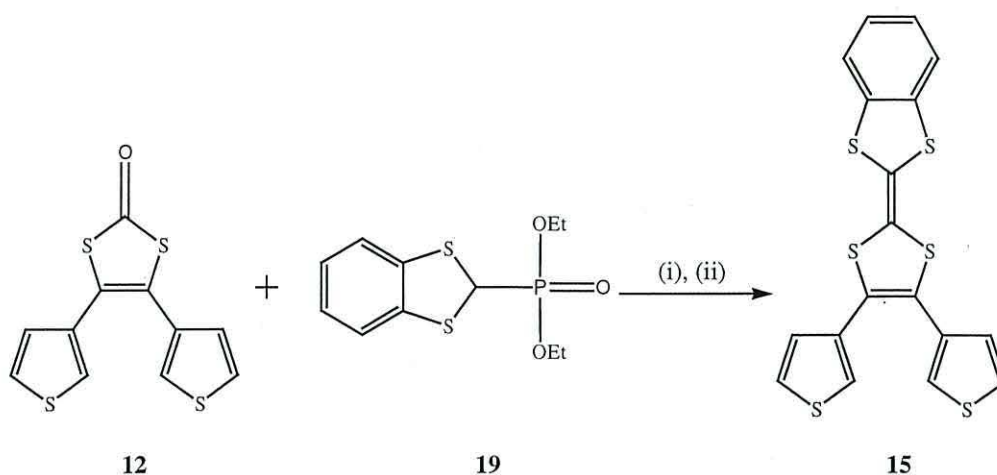
At the onset of this work Hudhome *et al.* [17] reported the preparation of an extended TTF derivative **16** in 43% yield by the treatment of **17** with a ten-fold excess of the anion generated from the phosphonate ester **18** (figure 3.0.6). This previously unprecedented Horner-Wadsworth-Emmons reaction was precisely what was required to effect on our system; either with the monomeric compound **12** or the corresponding polymer of **12**.



Reagents and conditions: (i) *n*-BuLi, THF, -78°C

Figure 3.0.6 Formation of highly extended TTF derivatives.

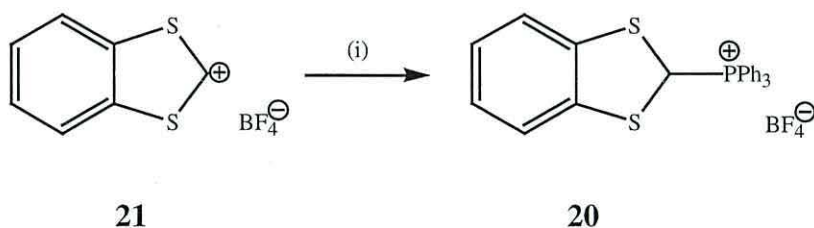
Thus taking a ten-fold excess [15] of the anion generated from phosphonate ester **19**, and reacting at -78°C with compound **12**, it was possible to obtain red crystalline needles of **15** in 41% yield (scheme 3.0.1). This is in line with that reported by Hudhome *et al.*



Reagents and conditions: (i) *n*-BuLi, THF, -78 °C, 15 min; (ii) **12**, THF, -78 °C, 20 min, R.T., 1h.

Scheme 3.0.1 Preparation of **15**.

The reaction was then attempted using standard Wittig conditions in which the ylid intermediate generated from the action of *n*-BuLi on the phosphorane **20** in THF at -78 °C was reacted with **12** (scheme 3.0.2). Unfortunately we were unable to effect the olefination of **12** under these conditions even by varying the reaction temperature and time.



Reagents and conditions: (i) PPh_3 , MeCN, R.T., 24h.

Scheme 3.0.2 Preparation of the phosphorane **20**.

3.3.2 Crystallography.

X-ray crystal structure determination was carried out for **15** (figure 3.0.7, appendix 1) showing the conformation of the diastereomeric structure.

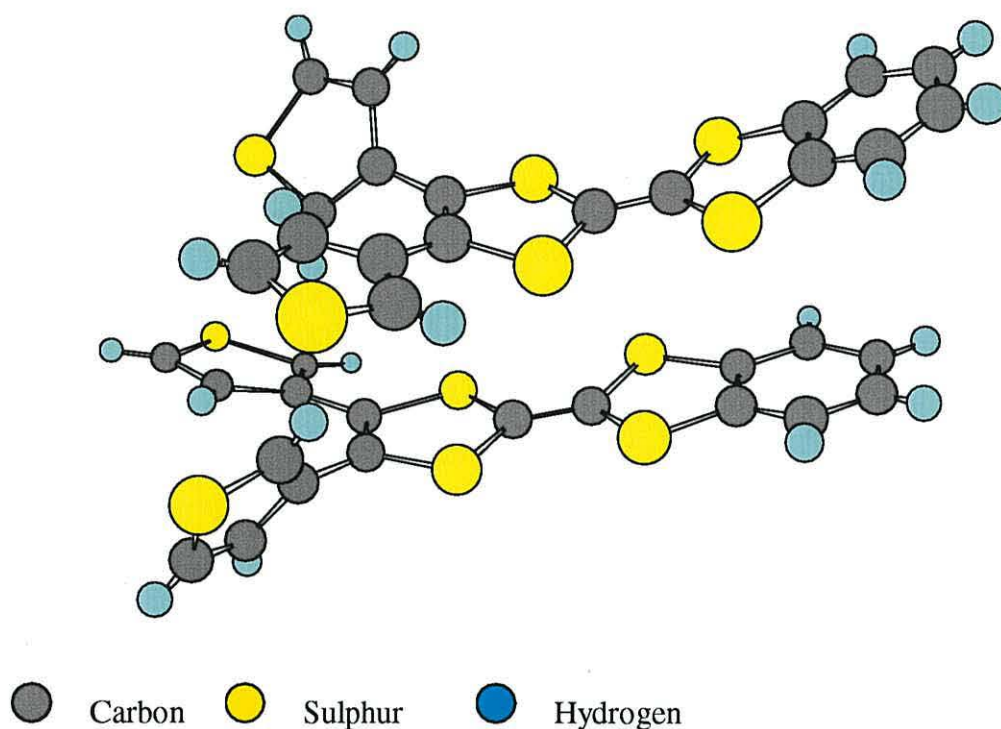


Figure 3.0.7 The conformation of **15**.

3.4.0 The attempted electropolymerisation of 2-(4,5-di-thiophen-3-yl-[1,3]dithiol-2-ylidene)-benzo[1,3]dithiole **15**.

Before continuing with the electrochemical characteristics of **15** it would be prudent to give a brief discussion of the electrochemical properties of TTF.

3.4.1 Tetrathiafulvalene (TTF).

As mentioned in chapter one TTF and its derivatives have been well documented. [18-21] Compounds that possess the TTF moiety exhibit

characteristic redox couples that are best displayed in voltammograms (figure 3.0.8).

The voltammogram of a TTF couple shows the sequence in which the TTF unit is sequentially oxidised from the neutral form to the radical cation (E_{ox}^1) and the dication (E_{ox}^2).

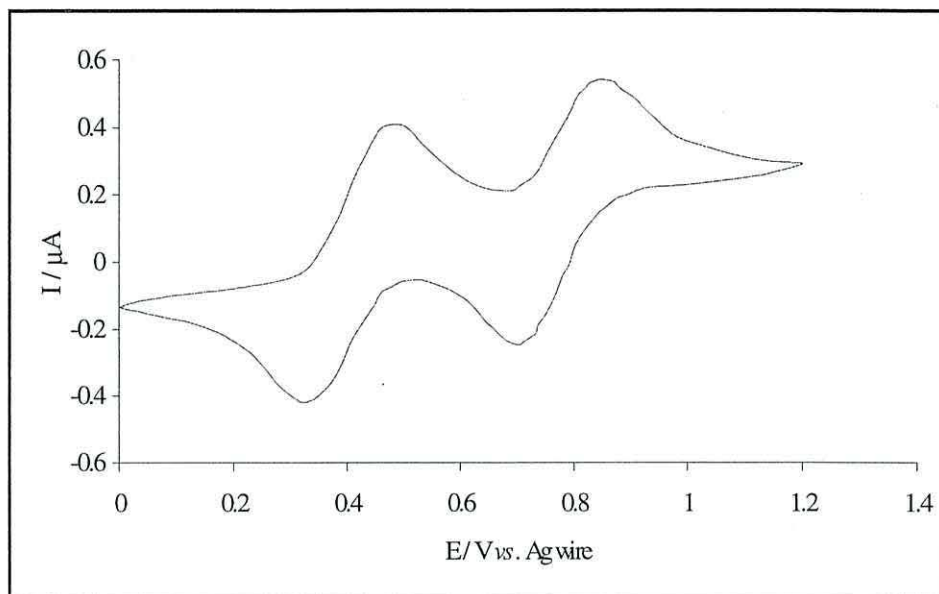


Figure 3.0.8 Typical CV of tetrathiafulvalene (TTF).

By introducing substituents onto the TTF moiety the positions of the redox couples (oxidation peaks) will vary. For example BEDT-TTF shows oxidation potentials at $E_{1/2}^1$ +0.36V and $E_{1/2}^2$ +0.78V [18] as compared to TTF; $E_{1/2}^1$ +0.30V and $E_{1/2}^2$ +0.70V. [20]

By exploiting this concept it is possible that such compounds can be designed allowing the production of tailor made polymers.

3.4.2 The electrochemical properties of **15**.

The solution electropolymerisation was performed using cyclic voltammetry (CV). A 0.05 mol dm⁻³ solution of **15** in a 0.1 mol dm⁻³ solution of TBATFB in MeCN was used.

The CV (figure 3.0.9) obtained showed behaviour typical of TTF derivatives in which the characteristic TTF redox couples appeared at $E_{ox}^1 + 0.68$ V and $E_{ox}^2 + 1.07$ V vs. Ag wire. These values are shifted towards more positive potentials compared to TTF. This shift can be attributed to the electron withdrawing effect of the thiophene moieties. Electropolymerisation studies were carried out but were found to be unsuccessful.

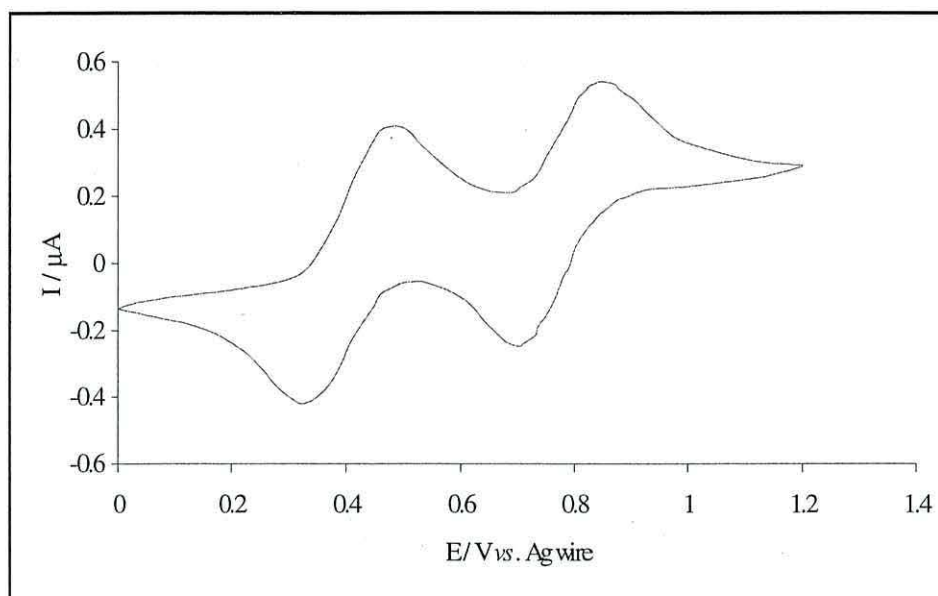


Figure 3.0.9 The CV of compound **15**.

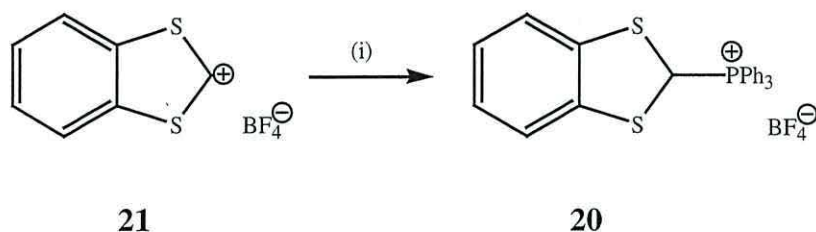
3.5.0 *In situ* modification of polymer **12**.

3.5.1 Modification of the polymerised compound **12**.

The first step in the modification procedure was to polymerise *bis*-4,5-(3-thienyl)-1,3-dithiole-2-one **12**. This was achieved *via* potentiodynamic deposition. Deposition was carried out by cycling, at a sweep rate of 100mVs^{-1} , from -0.3 to $+1.8$ V (vs. Ag wire) in a 0.02 M solution of monomer **12** in 0.1 M TBATFB/ acetonitrile.

Once the polymer was grown, it was necessary to produce the ylid intermediate. This was prepared by reacting, 1,3-benzodithiol-2-ylum

tetrafluoroborate **21** with PPh_3 in MeCN giving **20** in quantitative yield (scheme 3.0.2).



Reagents and conditions: (i) PPh_3 , MeCN, R.T, 24h.

Scheme 3.0.2 Preparation of the phosphorane **20**.

The ylid itself was produced by the drop-wise addition of $n\text{-BuLi}$ to a 25 fold excess (based on the monomer solution containing 0.02 M per 100 cm^3) of **20** dissolved in diethyl ether at 0°C , and stirred for 30 minutes. The accepted literature preparations of ylid intermediates quote THF as reaction solvent. [21] Unfortunately THF was known to dissolve the polymerised compound **12**, so, diethyl ether was utilised.

When deposited, the electrochemical characterisation was carried out in an electrolyte solution (0.1 M TBATFB, MeCN). The CV shows only one oxidation wave at $E_{\text{ox}}^1 + 1.68\text{V}$ (figure 3.1.0) and displays the characteristics of a redox switching polymer. The polymer was removed from solution after equilibrating to 0.0A (0.48 V).

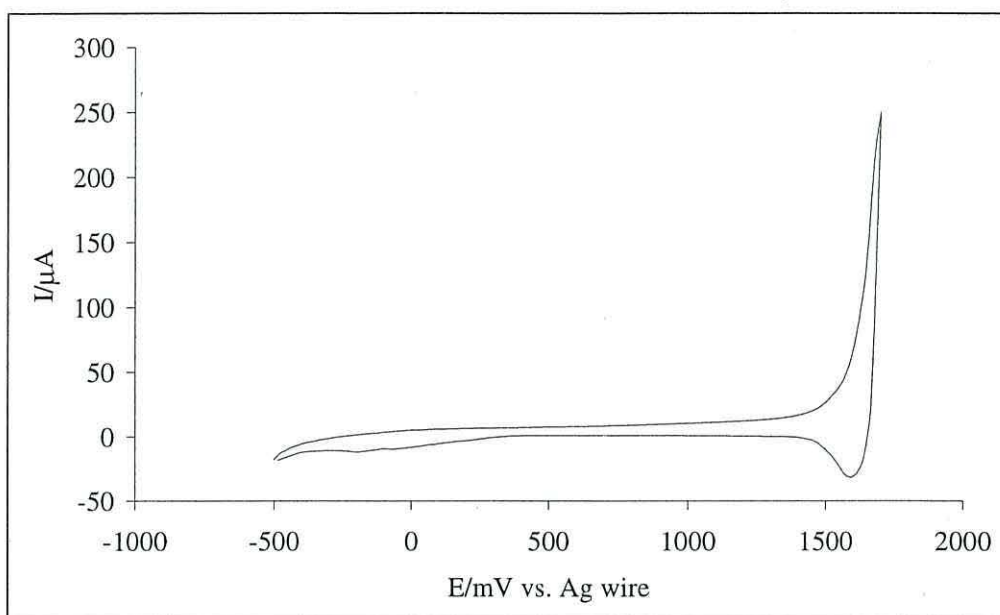


Figure 3.1.0 CV of the polymerised compound **12**.

The electrode with the attached polymer was then introduced (under inert conditions) to the ylid solution and was left overnight allowing the Wittig reaction to proceed as the temperature slowly rose to room temperature.

The now modified polymer was washed with copious amounts of electrolyte solution, removing any traces of unreacted ylid and was characterised electrochemically.

3.5.2 The electrochemical characterisation of the modified polymer.

The voltammogram of the modified polymer shows major changes in comparison to the unmodified polymer (figure 3.1.1), showing differences in both structural and electrochemical characteristics.

Upon cycling from 0.0V on the oxidative sweep, two oxidation waves can be observed at $E_{ox}^1 + 0.88V$ and $E_{ox}^2 + 1.20V$. These are characteristic of the TTF redox couples for the cationic and dicationic states. The reductive sweep shows the associated reduction waves. When cycled to more negative potentials (ca. $-0.7V$), a third oxidation wave can be observed at $E_{ox}^3 + 0.38V$. This has been assigned as the oxidation of the polymer, which would be in agreement that polymer oxidation must occur prior to the dicationic TTF^{2+} state has been achieved.

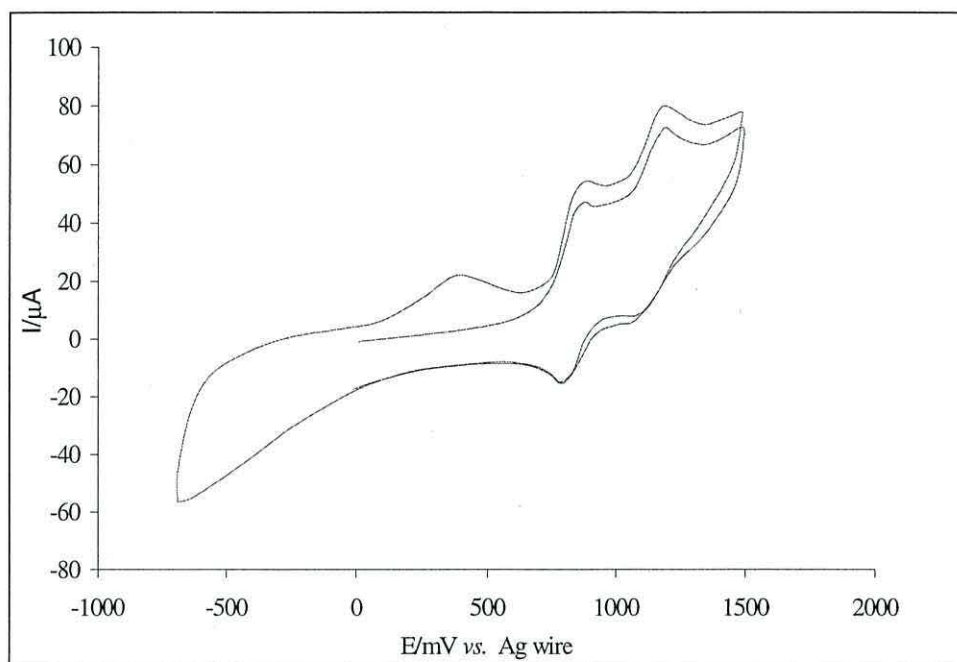


Figure 3.1.1 The voltammogram of the modified polymer.

3.5.3 Modification using the phosphonate **19**.

The modification of the polymer was then tried using the phosphonate ester **19**. It was observed that the action of the anion generated from **19** caused decomposition of the polymer. This may be explained by the potentiodynamic sequence applied to the polymer in which cycling ceases at zero current but at a potential of +0.48V. This would infer that although not in its oxidised state, the polymer is in its neutral form. Thereby there is a possibility that the C=O moieties are weakened, making them more susceptible to the kind of nucleophilic attack the phosphonium salt **20** provides. Another explanation for the lack of success may be due to solvent considerations, in which diethyl ether may not provide the conditions necessary to facilitate the modification that is observed to proceed when THF is used.

This may provide an explanation to why the classical Wittig reaction is successful when used in the modification rather than the synthesis of the TTF derivative **15**.

As mentioned in section 3.1.0 the unmodified and modified polymers were investigated using SNIFTIRS. This would allow the observation of the structural changes occurring within the polymers whilst undergoing redox switching.

3.6.0 Introduction to *in situ* FTIR of conducting polymers.

The use of *in situ* FTIR [23] has allowed an understanding of the structural changes occurring during the redox switching of a conducting polymer. There is general agreement that the switching from the insulating to conducting state of a polymer results in a broad absorbance band around 4000 cm^{-1} that extends to the near IR region (figure 3.1.2).

Figure 3.1.2 Absorbance spectra for a conducting polymer with band-gap in the visible range.

This band has been attributed to the electronic transition between the valence band and the lowest polaronic/ bipolaronic state (chapter one). This

appearance has been reported extensively in the literature for most conducting polymers, for example polypyrrole, [24] polythiophene, [25,26] polyacetylene [27] and poly (3-methylthiophene). [28]

3.6.1 IR of thiophene and related polymers.

The IR characteristics of conducting polymers have been well documented, including detailed studies of polythiophene and thiophene itself. [29-31]

Thiophenes and their derivatives generally absorb between 3100 – 3000 cm^{-1} , attributable to C-H stretching. An additional four bands of differing intensities are found in the region 1555 – 1200 cm^{-1} . The IR bands found in neutral polythiophene (figure 3.1.3) are given in table 3.0.1. [32]

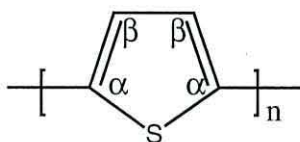


Figure 3.1.3 Carbon assignments in polythiophene.

Bands of neutral polythiophene.	Vibration cm^{-1}
$\text{C}_\beta\text{-H}$ stretch (aromatic)	3100
$\text{C}_\alpha=\text{C}_\beta$ stretch (antisymmetric)	1512
$\text{C}_\alpha=\text{C}_\beta$ stretch (symmetric)	1442
$\text{C}_\beta=\text{C}_\beta$ intra ring vibration (symmetric)	1376
$\text{C}_\beta=\text{C}_\beta$ intra ring vibration (antisymmetric)	1186
$\text{C}_\alpha\text{-H}$ in plane bend	1050
$\text{C}_\alpha\text{-H}$ out of plane bend	785
$\text{C}_\alpha\text{-S-C}_\alpha$ ring deformation	730

Table 3.0.1 IR active bands in neutral polythiophene.

When doped the most important bands observed in conducting polymers occur between $1600 - 1000 \text{ cm}^{-1}$. These are termed Infra Red Active Vibrations (IRAV). [33] In this region C-H in plane vibrational bands and, C=C stretch and ring vibrations are observed, and have been well studied. [24,34,35] When doped, the bands are shifted towards lower energy due to the transition of the polaron state to the bipolaron. This shift is due to the reduction of the aromatic character of the polymer resulting from the formation of the quinoid state. As a result of altering the bond structure, the position of the IR band frequency will also be shifted. These shifts regularly occur during the doping of conducting polymers as the structure is changed. Although such shifts occur, they are not easily observed by conventional spectroscopy performed on electrode surfaces, however, by using Subtractively Normalised Interfacial Fourier Transform Infra-Red Spectroscopy (SNIFTIRS) it is possible to detect these changes.

Another feature evident during the *in situ* redox switching of conducting polymers is the insertion of anions during the doping process. [26,28,36] In general, studies report an increasing signal from the anions during doping (p-doping), however, in SNIFTIRS measurements, this is

represented as an increasing negative band. This is due to the anion being drawn from the bulk solution into the polymer film.

3.6.2 SNIFTIRS spectra of the unmodified polymer 12.

The difference spectra of the unmodified polymer **12** during the oxidation (p-doping) process are given in figures 3.1.4 and 3.1.5, and are summarised in table 3.0.2.

The region around $1600 - 1750\text{ cm}^{-1}$ is particularly informative displaying the effect the doping process has on the strength of the C=O bond. It is of interest as this bond is affected by electronic changes within the polymer. Upon oxidation the dipole moment on the carbonyl carbon atom increases, having the effect of polarising the bond giving $\text{C}^{\delta+}=\text{O}^{\delta-}$, resulting in a stronger bond. This is observed in the oxidation process as the peak at 1636 cm^{-1} representative of the neutral carbonyl group is gradually lost and the peak at 1705 cm^{-1} associated with the oxidised polymer becomes increasingly dominant. [37]

The assignment of the C=O group at 1636 cm^{-1} is in agreement with that found in solution FTIR of the monomer unit, displaying an absorption at 1632 cm^{-1} .

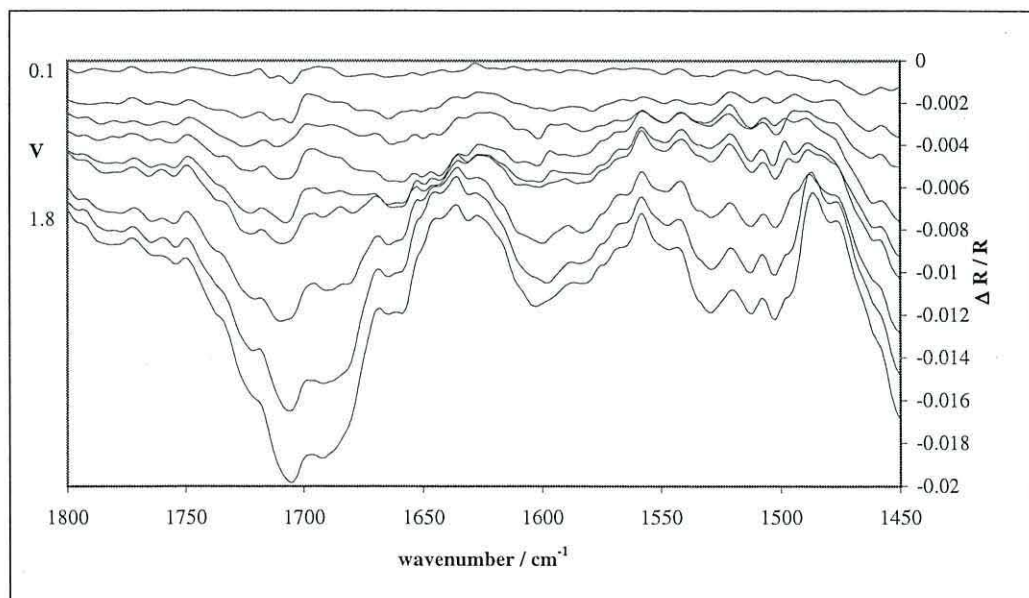


Figure 3.1.4 SNIFTIRS spectra of the unmodified polymer.

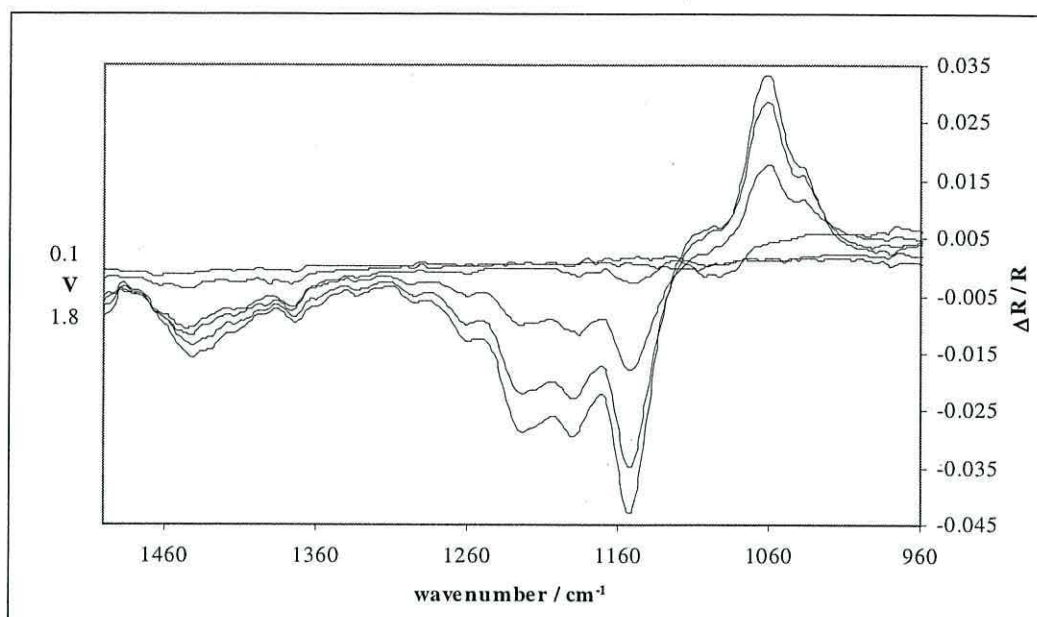


Figure 3.1.5 SNIFTIRS spectra of the unmodified polymer.

Whilst the doping process occurs, further bands become more dominant; the region between $1500 - 1610 \text{ cm}^{-1}$ is of interest. The peak at 1603 cm^{-1} is attributable to the C=C bond of the 1,3-dithiolene unit (figure 3.1.6). [38] The peaks at 1503 and 1533 cm^{-1} appear due to the IR activation of Raman bands assigned to the polymer backbone upon oxidation, showing increased C=C bond strength of quinonoidal type structures. This has been reported in the literature by Cuff and co-workers [39] in which they assign to the switching between aromatic and quinonoid structure of polyisothianaphthalene (figure 3.1.7).

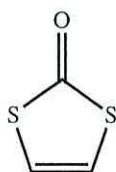


Figure 3.1.6 The 1,3-dithiolene unit.

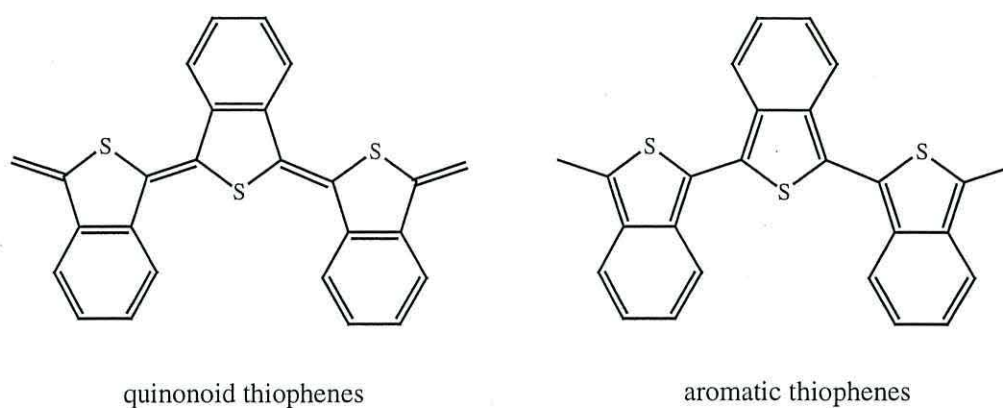


Figure 3.1.7 The quinonoid and aromatic structures of PITN.

An absorbance at 1443 cm^{-1} can be seen to increase upon oxidation, attributable to C-C stretching vibrations in both the polymer backbone and the 1,3 bis-dithiolene unit.

Bands.	Vibrations cm^{-1}
C-C stretching vibration	1446
Activated Raman C=C band	1503
Activated Raman C=C bands	1531
C=C stretch in 1,3-dithiolene unit	1602
C=O neutral polymer	1636
C=O oxidised polymer	1705

Table 3.0.2 Summarised absorbencies of the unmodified polymer.

Further bands characteristic to the polymer backbone at; 1521, 1190 and 1057 cm^{-1} can be observed and are attributable to C=C antisymmetric stretching, antisymmetric intra ring vibrations and C-H in plane mode of vibration. [37] Three further bands located at 1374, 1228 and 1157 cm^{-1} have been reported in the literature for various polymers including polyacetylene, 3-methyl thiophene and PITN, and are attributed to C-H in plane vibrations,

C-CH bends and C-C stretches respectively.

At this point it is not possible to ascribe the polymer structure. However it is possible to state that the polymer does not exhibit absorbancies similar to polythiophene, but more quinoidal in nature. This will be discussed in greater detail in section 3.7.0 and chapters four and five.

3.6.3 SNIFTIRS spectra of the modified polymer.

The bands of interest in the difference spectra of the modified polymer in the neutral and oxidised state are summarised in table 3.0.3 and can be seen in figures 3.1.8 and 3.1.9.

The peaks at 1292, 2969 and 3006 cm^{-1} are representative of the C-C in plane stretching vibration (1292 cm^{-1}), and aromatic C-H stretches of the aromatic 1,3-benzodithiol-2-ylum groups of the now modified polymer and are observed to decrease upon oxidation as the delocalisation reduces in bond strength.

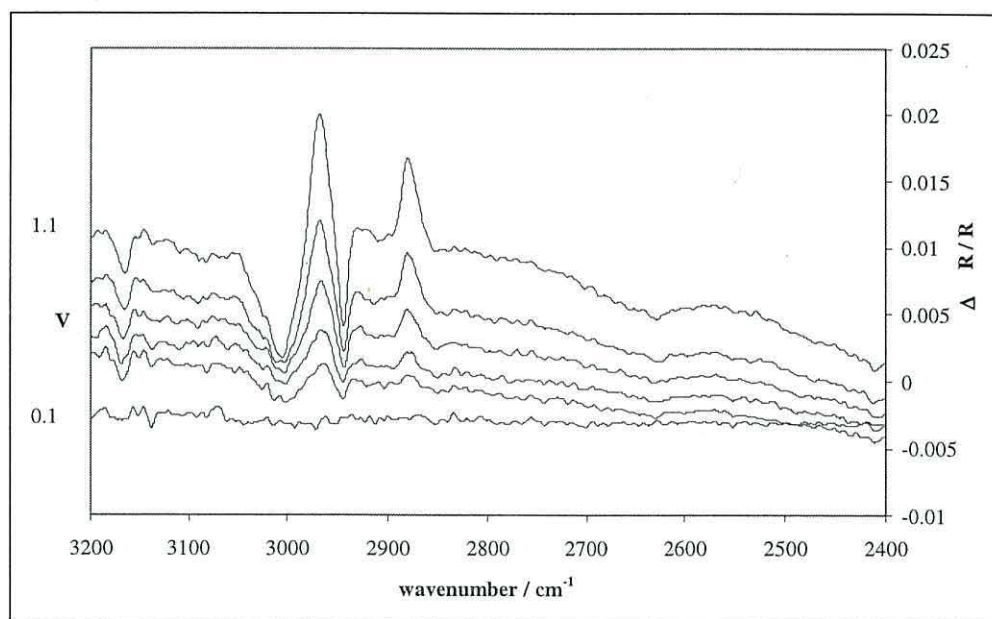


Figure 3.1.8 SNIFTIRS spectra of the modified polymer.

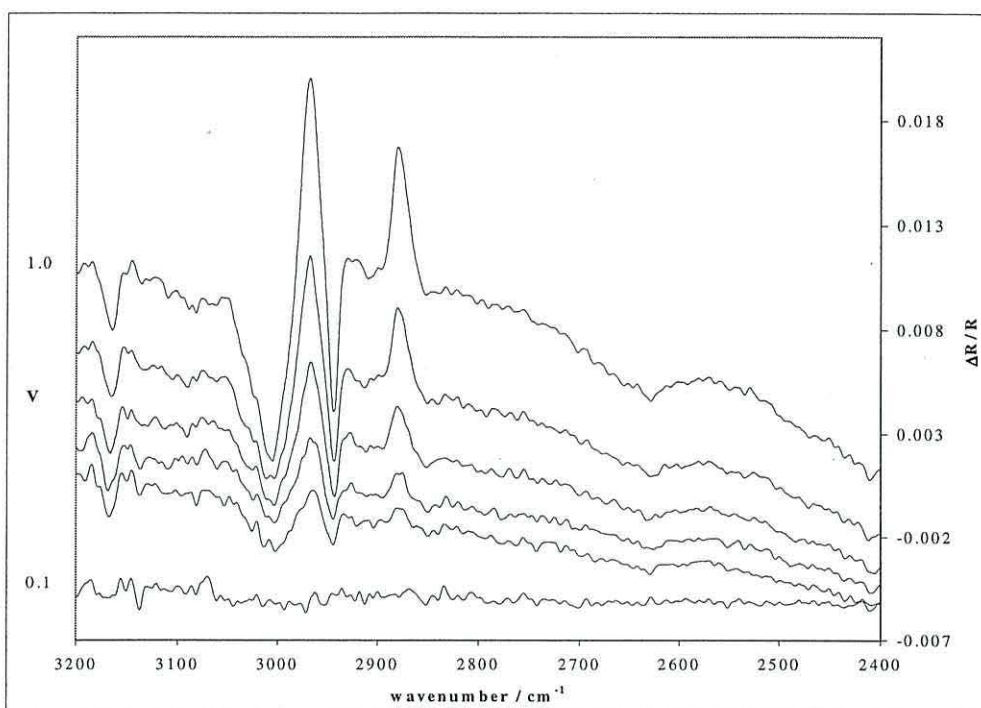


Figure 3.1.9 SNIFTIRS spectra of the modified polymer.

The weak absorbance at 1448 cm^{-1} has been assigned as a C-C stretching vibration inherent to the dithiolene unit, and the decreasing absorbances at 1486 and 1586 cm^{-1} have been assigned as TTF characteristic stretching vibrations for the C=C bonds losing bond strength during the oxidation process. A further peak at 1601 cm^{-1} for the C=C bonds inherent to the 1,3-dithiole groups is also present. [39,41,42]

The peak at 1095 cm^{-1} is indicative of C-S stretching modes. As in the case of the unmodified polymer, peaks at 1530 , 1371 , 1224 , 1142 and 1084 cm^{-1} are characteristic of C=C stretching vibrations in the quinonoidal polymer backbone (1530 cm^{-1}). [39] As observed in section 3.6.2, the latter four bands are attributed to C-H in plane vibrations, C-CH bend, C-C stretch and C-H stretch respectively.

As in the unmodified polymer there is an activation of a Raman band when oxidation occurs, resulting in the absorbance at 1508 cm^{-1} , attributed to C=C stretch of the polymer backbone.

The main bands of interest in the difference spectra of the modified polymer are those at 1371 , 1142 , 1095 and 1658 cm^{-1} . Perhaps the most

important of these bands is that at 1658 cm^{-1} , attributable to the formation of the TTF radical state (and dication) due to the oxidation of the TTF moieties.

As expected certain bands will not be present in the modified spectra. These are the C=O bands found at 1636 and 1705 cm^{-1} . This would infer that a complete surface coverage has taken place. With the disappearance of these two absorbances, there are two new regions. These are for the aromatic ring and for the TTF moiety.

Bands of neutral polythiophene	Vibrations cm^{-1}
C-S Stretching	1095
Aromatic C-C stretching vibration	1291
TTF C=C stretching vibration	1448
TTF C=C stretching vibration	1486
C=C stretching vibration (quinonoid)	1530
TTF C=C stretching vibration	1586
1,3-dithiolene C=C stretch	1600
Aromatic C-H stretch	2969
Aromatic C-H stretch	3006

Table 3.0.3 Summarised absorbencies of the unmodified polymer.

There are two more peaks that must be given mention, these absorb at 1331 and 1369 cm^{-1} and are attributable to C-C and C-H in plane vibrations observed in quinoidal molecules, [39] and will be discussed in more detail in chapter five.

The intensity of the bands in the region attributed to the 1,3-dithiolene units are not as intense and in some cases missing in the spectra of the modified polymer. This is in agreement with the CV data in which the polymer oxidation occurs at a lower potential when compared to that of the

unmodified polymer. This is expected, as the modified polymer is now TTF in character. Thus only bands attributed to this will be seen. This will have an effect on the CVs of both polymers, in that when unmodified, the 1,3-dithiolene unit will exert more influence on the electrochemical properties. When modified the 1,3-dithiolene essentially ceases to exist, thus the polymer back bone and the TTF units will only be observed, effecting the voltammograms. The observed lower oxidation potential of the polymer itself due to the inherent characteristics of TTF compounds.

3.7.0 Conclusions.

To conclude, an *in situ* chemical modification of the polymerised compound **12** has taken place resulting in a polymer in which the TTF moiety is directly bonded to the polymer backbone.

It has been shown through electrochemical and *in situ* FTIR spectroscopy that a complete modification has occurred, also showing that the polymer backbone and TTF moieties are present, but the electrochemical properties of the polymer have changed in comparison to the unmodified polymer.

In the unmodified form, the 1,3-dithiolene unit shows influence on the electrochemistry and the spectroscopy when compared with polythiophene. In addition to this, absorbances at 1503 cm^{-1} and 1531 cm^{-1} are present, and are indicative of quinonoidal type polymer structures. This would infer that the polymer does not consist of repeated units of the compound **12** itself (figure 3.2.0) therefore the polymer is a different structure than first anticipated.

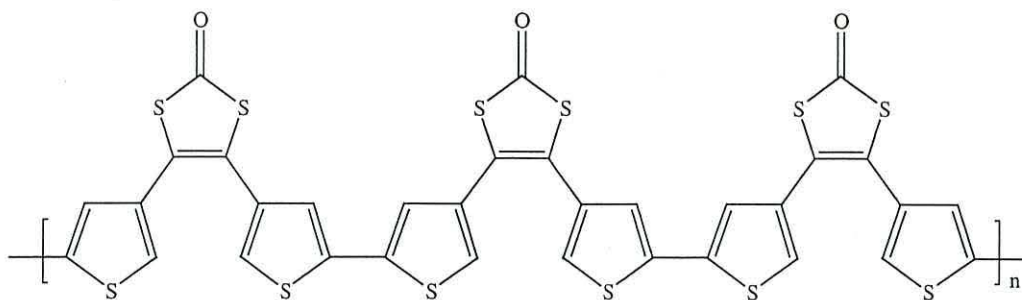
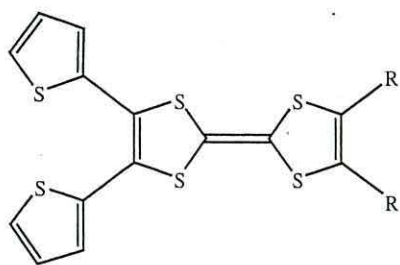


Figure 3.2.0 Repeated unit structure of the unmodified polymer.

To summarise, the modification of the polymer has shown the loss of the C=O group present in the unmodified polymer and exhibits peaks characteristic of a TTF derivative.

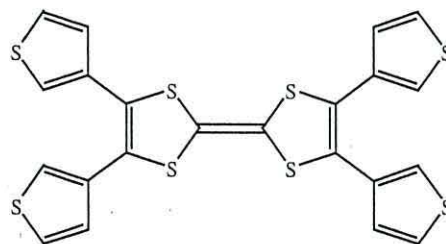
With this in mind, it is apparent that there are some key points to consider; what is the mode of polymerisation of the unmodified and modified polymer, and what is the mechanism of charge transfer within the polymers. It was thus necessary to carry out further investigations, the results of which are discussed in chapters four and five.



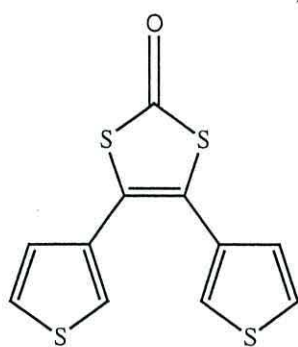
7 : R = 2-thienyl

9 : R = H

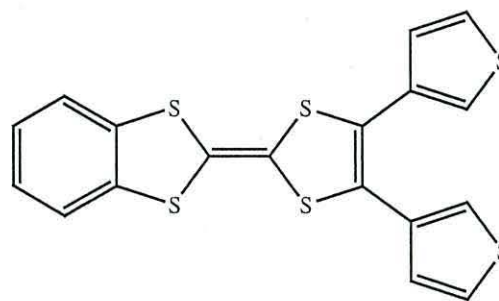
8 : R = -SCH₂CH₂CH



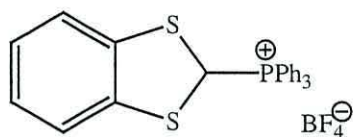
11



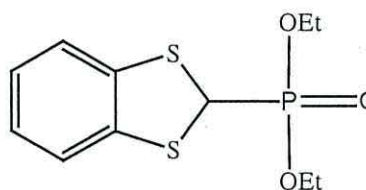
12



15



20



19

3.8.0 References.

- 1) A. Charlton, A. E. Underhill, M. Kalaji, P. J. Murphy, D. E. Hibbs, M. B. Hursthouse and K. M. Malik; *J. Chem. Soc. Chem. Commun.*, (1996) 2423.
- 2) A. Charlton, A. E. Underhill, G. Williams, M. Kalaji, P. J. Murphy, K. M. Abdul Malik and M. B. Hursthouse; *J. Org. Chem.*, **62** (1997) 3098.
- 3) T. Le Gall, M. S. Passos, S. K. Ibrahim, S. Morlat-Therias, C. Sudbrake, S. A. Fairhurst, M. Artlete Quieros and C. J. Pickett; *J. Chem. Soc. Perkin Trans I.*, (1999) 1657.
- 4) L. Pur; *Acta Polym.*, **48** (1997) 116.
- 5) S. J. Higgins, C. L. Jones, S. M. Francis; *Synth. Met.*, **98** (1999) 211.
- 6) A. Deronzier and J. -C. Moutet; *Curr. Top. Electrochem.*, **3** (1994) 159.
- 7) K. S. Ryder, D. G. Morris and J. M. Cooper; *J. Chem. Soc. Chem. Commun.*, (1995) 1471.
- 8) P. Bauerle, M. Hiller, S. Schieb, M. Sokowloski and E. Umbach; *Adv. Mater.*, (1996) 8214.
- 9) C. P. Horwitz, N. Y. Suhu and G. C. Dailey; *J. Electroanal. Chem.*, **324** (1992) 79.
- 10) S. Morlat-Therias, M. S. Passos, S. K. Ibrahim, T. Le Gall, M. A. Quieros and C. J. Pickett; *J. Chem. Soc. Chem. Commun.*, (1998) 1175.
- 11) M. C. Pirrung; *Chem. Rev.*, **97** (1997) 473.
- 12) J. Roncali; *J. Mater. Chem.*, **9** (1999) 1875.
- 13) M. R. Bryce, A. D. Chissel, J. Gopal, P. Kathirgamanathan and D. Parker; *Synth. Met.*, **39** (1991) 397.
- 14) C. Thobie-Gautier, A. Gorgues, M. Jubault and J. Roncali; *Macromolecules.*, **6** (1993) 4094.
- 15) P. J. Skabara, D. M. Roberts, I. M. Serebryakov and C. Pozo-Gonzalo; *J. Chem. Soc. Chem. Commun.*, (2000) 1005.
- 16) P. J. Skabara, I. M. Serebryakov, D. M. Roberts, I. F. Perepichka, S. J. Coles and M. B. Hursthouse; *J. Org. Chem.*, **64** (1999) 6418.
- 17) C. Boulle, O. Desmars, N. Gautier, P. Hudhomme, M. Cariou and A. Gorgues; *J. Chem. Soc. Chem. Commun.*, (1998) 2197.
- 18) M. Iyoda, N. Ueno and M. Oda; *J. Chem. Soc. Chem. Commun.*, (1992) 158.

- 19) M. Adam, A. Bohnene, V. Enkelman and K. Mullen; *Adv. Mater.*, **3** (1991) 600.
- 20) M. Adam and K. Mullen; *Adv. Mater.*, **6** (1994) 439.
- 21) V. Y. Khordorkovsky, J. Y. Becher, C. Wang, A. Ellern, L. Shapiro and J. Bernstein; *Adv. Mater.*, **6** (1994) 656.
- 22) M. S. Passos, M. A. Queiros, T. Le Gall, S. K. Ibrahim and C. J. Pickett; *J. Electroanal. Chem.*, **435** (1997) 189.
- 23) T. R. Britt, B. L. Davies, J. K. Gillie, L. A. Lantz, A. Leugers, R. A. Nyquist, M. L. McKelvry and C. L. Putzig; *Anal. Chem.*, **68** (1996) 1R.
- 24) P. A. Christensen and A. Hamnett; *Electrochimica Acta.*, **36** (1991) 1263.
- 25) B. Rasch and W. Vielstich; *J. Electroanal. Chem.*, **370** (1994) 109.
- 26) P. Novak, B. Rasch and W. Vielstich; *Synth. Met.*, **41** (1991) 2963.
- 27) J. F. Raboult, T. C. Clarke and G. B. Street; *J. Chem. Phys.*, **11** (1979) 71.
- 28) F. Garner, P. Lang, G. Nauer, A. Neckel, H. Neugebauer and G. Tourillon; *J. Phys. Chem.*, **88** (1984) 652.
- 29) J. L. Bredas and R. Silbey (Ed.), *Conjugated polymers*, Kluwer, Amsterdam, Netherlands, (1991).
- 30) T. A. Skotheim (Ed.), *Handbook of conducting polymers*, Marcel Dekker, New York, (1986).
- 31) H. S. Nalwa (Ed.), *Handbook of organic conductive molecules and polymers: Vol. 3. Conductive polymers: Spectroscopy and physical properties*, J. Wiley & Sons Ltd. UK, (1997).
- 32) G. Socrates (2nd Ed.), *Infrared characteristic group frequencies: Tables and charts*, J. Wiley & Sons Ltd. UK, (1994).
- 33) P. A. Christensen, R. Hillman, M. J. Swan and S. J. Higgins; *J. Chem. Soc. Faraday Trans.*, **89** (1993) 821.
- 34) P. A. Christensen, R. Hillman, M. J. Swan and S. J. Higgins; *J. Chem. Soc. Faraday Trans.*, **88** (1992) 595.
- 35) P. A. Christensen, R. Hillman, M. J. Swan and S. J. Higgins; *J. Chem. Soc. Faraday Trans.*, **89** (1993) 921.
- 36) H. Neugebauer, A. Neckel, N. S. Sariciftci and H. Kuzmany; *Synth. Met.*, **29** (1989) 193.
- 37) G. O. Williams; *Ph. D thesis UWB Bangor*, (1999).

- 38) R. Bozio, I. Zanon, A. Girlando and C. Pecile; *J. Chem. Phys.*, **71** (1979) 2282.
- 39) L. Cuff, M. Kertesz, J. Geisselbrecht, J. Kürti and H. Kuzmany; *Synth. Met.*, **55** (1993) 564.
- 40) G. Borch, L. Henriksen, P. H. Nielsen and P. K. Laboe; *Spectrochimica Acta.*, **29** (1972) 1109.
- 41) M. Menghetti, R. Bozio, I. Zanon, C. Pecile, C. Ricotta and M. Zanetti; *J. Chem. Phys.*, **80** (1984) 6210.
- 42) M. E. Kozlov, K. L. Pokhodnia and A. A. Yurchenko; *Spectrochimica Acta.*, **43** (1987) 323.

Chapter Four: An investigation of the polymerisation mode of
bis-4, 5-(3-thienyl)-1,3-dithiole-2-one.

4.1.0 Aims.

Following from the *in situ* modification of the polymerised unit **12** (chapter three), it was decided that a study of the mode of polymerisation was necessary. The aims of this work were to prepare and characterise two new compounds **22** and **23** (figure 4.0.1), the rationale behind this that only **12** would polymerise if the proposed intramolecular cyclisation occurs. The compounds would then be used in electropolymerisation studies to help determine the mode of polymerisation for the unit **12**.

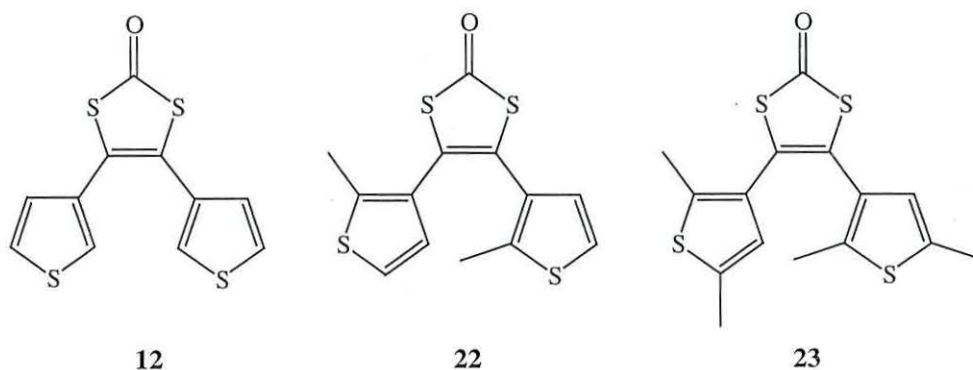


Figure 4.0.1 Target compounds **12**, **22** and **23**.

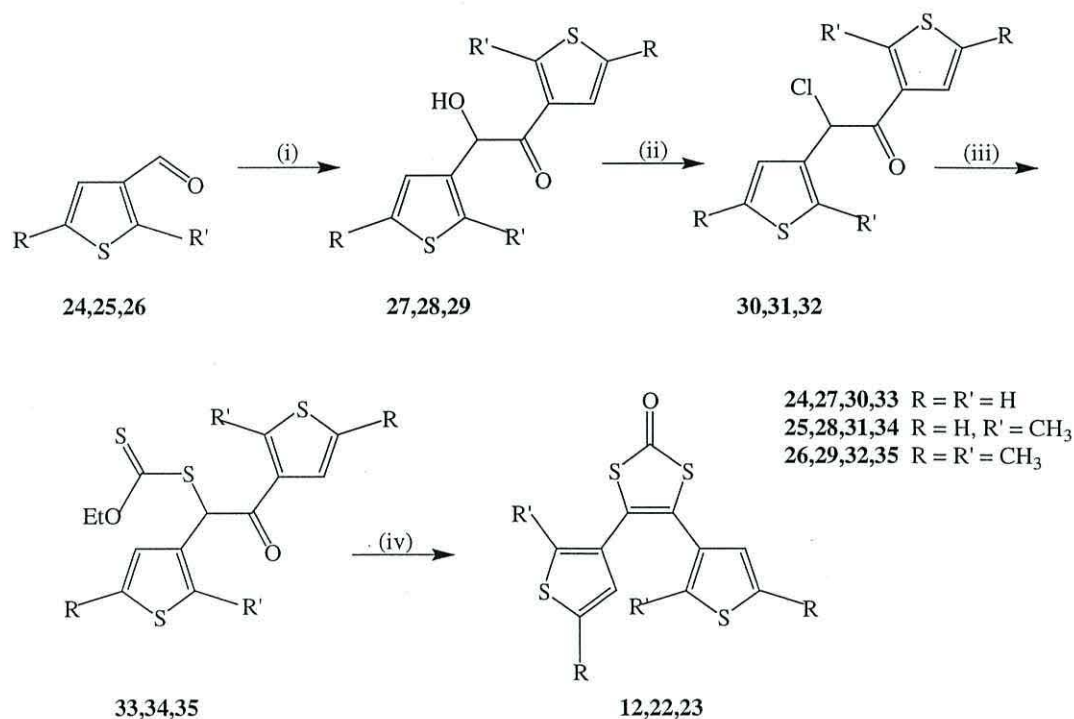
4.2.1 Bis-4, 5-(3-thienyl)-1,3-dithiole-2-one **12.**

Bis-4,5-(3-thienyl)-1,3-dithiole-2-one **12** was first prepared by Charlton *et al* in 1998. [1] This was part of an on-going programme investigating the potential of such compounds as possible precursors for thiophene substituted TTF derivatives for electropolymerisation studies. Previous work had concentrated on 2-thienyl substituted compounds (see chapter two), resulting in an efficient synthesis, though there was little success in respect to the attempted electropolymerisation of their

analogous TTF derivative.[2] The synthesis of the 3-thienyl substituted compounds was carried out in a similar manner to the method reported by Charlton *et al.* [3]

4.2.2 General strategy for the preparation of the *bis*-4, 5-(3-thienyl)-1,3-dithiole-2-ones **12**, **22** and **23**.

The overall synthetic scheme for the preparation of the three compounds is shown in scheme 4.0.1, in which the target compounds are obtained from a thiophene-3-carboxaldehyde in 4 steps.



Reagents and conditions: (i) 3-benzyl-5-(2-hydroxymethyl)-4-methyl-1,3-thiazolium chloride **40** (for conditions see table 4.0.1), NEt₃, ethanol; (ii) PPh₃, CCl₄, CH₂Cl₂, 24h; (iii) KSC(C)OEt, acetone, 1h; (iv) AcOH, R.T., 1h.

Scheme 4.0.1 Preparation of the compounds **12**, **22** and **23**.

The first step in the process is the benzoin condensation of the respective thiophene-3-carboxaldehydes **24**, **25**, **26**, leading to the α -hydroxy-ketones **27**, **28**, **29**. Treatment of the α -hydroxy-ketones with triphenylphosphine in CCl₄ yielded the α -chloro-ketones **30**, **31**, **32**, which due to their unstable nature were

immediately reacted with potassium ethyl xanthate. The xanthates formed (**33**, **34**, **35**) were then cyclised (HBr in acetic acid) resulting in the formation of *bis*-4,5-(3-thienyl)-1,3-dithiole-2-ones **12**, **22** and **23**.

4.3.0 Preparation of aldehydes **24**, **25**, **26**.

Of the starting thiophene-3-carboxaldehydes **24**, **25** and **26**, only thiophene-3-carboxaldehyde **24** was available commercially. Thus syntheses of 2-methyl-thiophene-3-carboxaldehyde **25** and 2,5-dimethyl-thiophene-3-carboxaldehyde **26** were required.

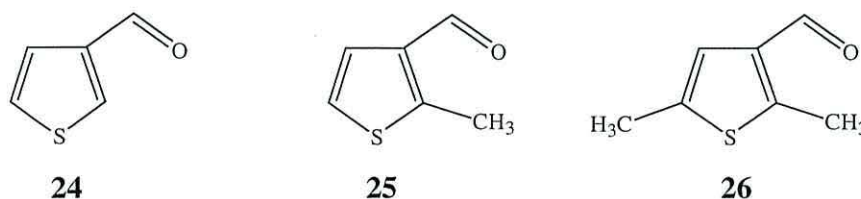


Figure 4.0.2 The two target aldehydes **25**, **26** and aldehyde **24**.

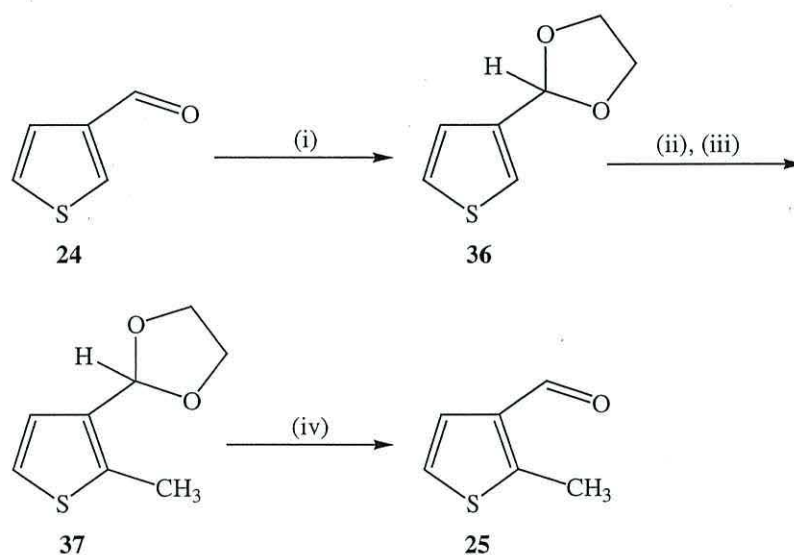
4.3.1 The synthesis of 2-methyl-thiophene-3-carboxaldehyde **25**.

2-Methyl-thiophen-3-carboxaldehyde **25** was prepared in 4 steps from the commercially available 3-thiophene carboxaldehyde **24** as shown in scheme 4.0.2. Prior to the lithiation of the thiophene ring, it was necessary to protect the aldehyde group of the molecule. Acetals are often used as protecting groups for aldehydes and thus **24** was converted to the dioxolane **36** in the manner described by Gronowitz *et al* [4] in 60% yield.

Analysis of the ¹H NMR spectrum showed a multiplet resonance at δ 4.1 – 4.0 ppm for the methylene protons, a singlet resonance at δ 5.9 ppm for the aliphatic acetal proton, and aromatic thiophene resonances at δ 7.4, 7.3 and 7.2 ppm. The lithiation of **36** required a slight excess (1.1 equivalents) of *n*-BuLi to ensure as complete a reaction as possible. This was added over 20 minutes with further

stirring for 30 minutes. Finally freshly distilled methyl iodide was added slowly and stirring continued for a further three hours. [5] After aqueous work-up, **37** was obtained in excellent purity and high yield (95%). The proton NMR data for **37** indicated the presence of a methyl singlet at δ 2.5 ppm that was accompanied by the loss of a signal in the aromatic region of the spectrum.

The hydrolysis of **37** led to aldehyde **25** in a nearly quantitative yield. The loss of the acetal group was confirmed by ^1H NMR spectroscopy with the disappearance of the signal at δ 4.1 – 4.0 ppm, the signal at δ 10.0 ppm was indicative of the aldehyde proton, and together with the presence of a carbonyl stretch 1680 cm^{-1} indicated the formation of aldehyde **25**.



Reagents and conditions: (i) benzene, p-toluene sulphonic acid, reflux, 5h; (ii) THF, n-BuLi, 0°C , 30 min; (iii) MeI, THF, 0°C , 30 min, RT 3h; (iv) c.HCl, H_2O , RT, 2.5 h.

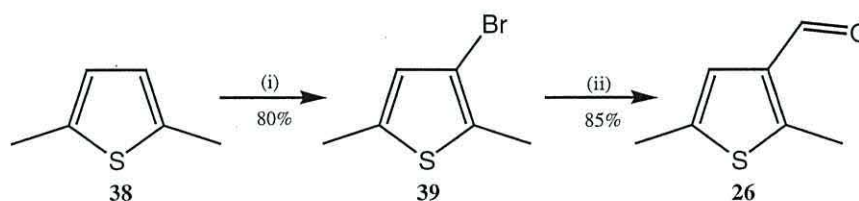
Scheme 4.0.2 Preparation of 2-methyl-thiophene-3-carboxaldehyde **25**

4.3.2 The synthesis of 2,5-dimethyl-thiophene-3-carboxaldehyde **26**.

2,5-Dimethyl-thiophene-3-carboxaldehyde **26** was prepared in two steps from commercially available 2,5-dimethyl-thiophene **38** using a literature method.

[6] The first step of this method involved a bromination using 1.0 equivalents of Br_2 in CHCl_3 at 0°C .

^1H NMR spectroscopy was used to confirm the formation of **39**, with the loss of an aromatic thiophene proton signal being observed. The second step of the synthesis of **26** was the lithiation of **39** by the dropwise addition of 1.1 equivalents of $n\text{-BuLi}$ to a solution of **39** in diethyl ether at -70°C followed by reaction with DMF to give alcohol **26** (scheme 4.0.3) in high yield.



Reagents and conditions: (i) Br_2 , CHCl_3 , 0°C , 5h, dark; (ii) Et_2O , $n\text{-BuLi}$, DMF, -70°C , 30min.

Scheme 4.0.3 Preparation of 2,5-dimethyl-thiophene-3-carboxaldehyde **26**.

^1H NMR spectroscopy confirmed the presence of aldehyde functionality with the presence of a singlet at δ 9.9 ppm, which was accompanied by the presence of a carbonyl stretch at 1672 cm^{-1} in the IR spectrum.

4.3.3 The Benzoin condensation reaction.

The key step in the synthesis of **12**, **22** and **23** is the benzoin condensation. Historically the traditional catalyst in this reaction is hydrogen cyanide, however more recent methodologies have employed thiazolium salts as catalyst. [7-9] The catalyst utilised in this work for the preparation of **30**, **31** and **32** was the commercially available 3-benzyl-5-(2-hydroxyethyl)-4-methylthiazolium chloride **40** (figure 4.0.2).

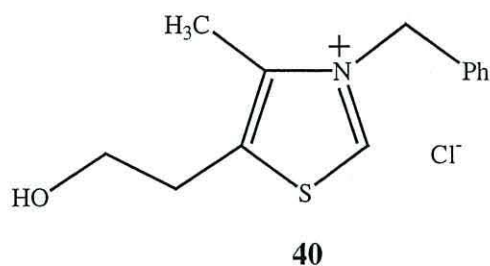


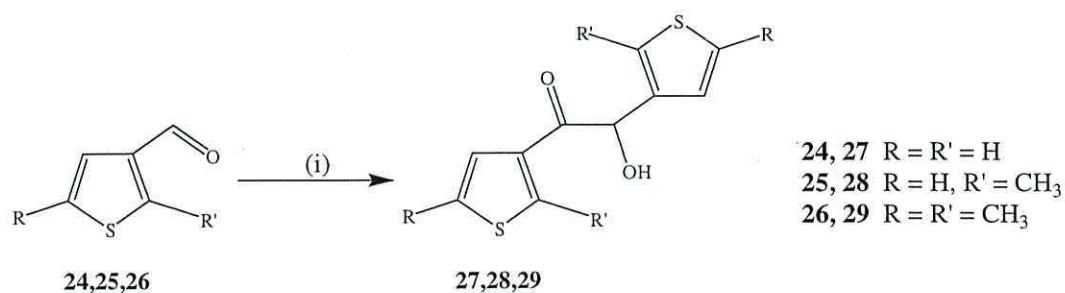
Figure 4.0.2 3-Benzyl-5-(2-hydroxyethyl)-4-methylthiazolium chloride **40**.

The condensation reaction for all three aldehydes (**27**, **28** and **29**) followed a similar procedure and the products **28** and **29** were obtained in their pure forms by column chromatography or recrystallisation.

The success of the benzoin condensation was found to be dependent on 2 factors:

- i) the number of equivalents of the catalyst
- ii) the reflux time.

The optimised conditions for the benzoin condensations are given in table 4.0.1.



Reagents and conditions: (i) **40**, NEt₃, solvent, heat, for other conditions see table 3.0.1.

Scheme 4.0.4 Preparation of **27**, **28** and **29**.

Entry	Aldehyde	Reaction Time (h).	Catalyst Eqv (Mol).	Product	Yield (%).	Solvent
1	24	2.5	0.05	27	66	EtOH
2	25	2.5	0.05	NR	0	EtOH
3	25	2.5	0.10	NR	0	EtOH
4	25	2.5	0.15	NR	0	EtOH
5	25	5.0	0.05	NR	0	EtOH
6	25	5.0	0.10	28	5	EtOH
7	25	5.0	0.15	28	28	EtOH
8	25	5.0	0.15	28	28	EtOH
9	25	5.0	0.15	28	29	EtOH
10	25	24.0	0.15	28	5	EtOH
11	26	2.5	0.15	NR	0	EtOH
12	26	5.0	0.15	NR	0	EtOH
13	26	24.0	0.15	NR	0	EtOH
14	26	24.0	0.30	NR	0	EtOH
15	26	48.0	0.30	NR	0	EtOH
16	26	48.0	0.60	29	13	<i>i</i> -PrOH
17	26	48.0	0.60	29	15	<i>i</i> -PrOH
18	26	48.0	0.60	29	15	<i>i</i> -PrOH

Table 4.0.1 Reaction conditions for the preparation of compounds **24**, **25**, **26**.

It can be seen that aldehyde **24** easily undergoes the condensation reaction with 0.05 equivalents of catalyst and a relatively short reflux time (entry 1). In contrast the benzoin condensation of 2-methyl-thiophene-3-carboxaldehyde **25** was more problematic. As can be seen from table 4.0.1 no appreciable reaction occurs for reflux times under 5 hours (entry 2-5) when using 0.05 – 0.10 equivalents of catalyst. The product **28** was formed only when 0.15 equivalents of catalyst was used and the reaction was heated for 5 hours (entries 7-9). Extending the reflux time to 24 hours led to decomposition of the product (entry 10).

In the case of 2,5-dimethyl-thiophene-3-carboxaldehyde **26**, there is a further increase in the time taken for the reaction to proceed and the amount of catalyst needed. Original attempts using 0.15 – 0.3 equivalents of catalyst and varying the reaction time from 5 – 48 hours, was found to be ineffective (entries 11–15). It was found that switching the solvent from ethanol to the higher boiling *iso*-propanol and increasing the amount of catalyst to 0.6 equivalents was required

to effect the reaction, however yields were consistently poor (entries 16-18). Despite this we were able to obtain quantities of **29** for further studies.

It should be noted that it was not possible to recover any of the aldehydes from the reaction mixtures, decomposition products being obtained.

The ^1H NMR and IR spectral data for **27**, **28** and **29** are detailed in table 4.0.2, and are consistent with the proposed structures.

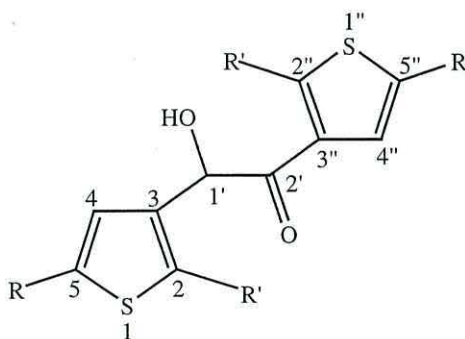


Figure 4.0.3 Nomenclature for compounds **27**, **28** and **29**.

Compound	^1H NMR signal (δ , ppm, J, Hz).									^1H NMR methyl signal	C=O stretch (cm^{-1})
	2	4	5	1'	OH	2''	4''	5''			
27 R = R' = H J = /Hz	7.33* (m)	7.53 (4.9,0.9)	7.33* (m)	5.86 (5.8)	4.38 (5.8)	8.06 (2.8,1.2)	7.01 (4.9,1.2)	7.33* (m)	-		1660
28 R = H, R' = CH ₃ J = /Hz	-	6.86 (5.3)	6.96 (5.3)	5.63 (5.4)	4.44 (5.4)	-	6.63 (5.5)	6.93 (5.5)	2.73, 2.51		1666
29 R = R' = CH ₃ J = /Hz	-	6.67	-	5.53 (5.5)	4.43 (5.5)	-	6.32	-	2.73, 2.51, 2.33, 2.32 (4 x Me)		1659

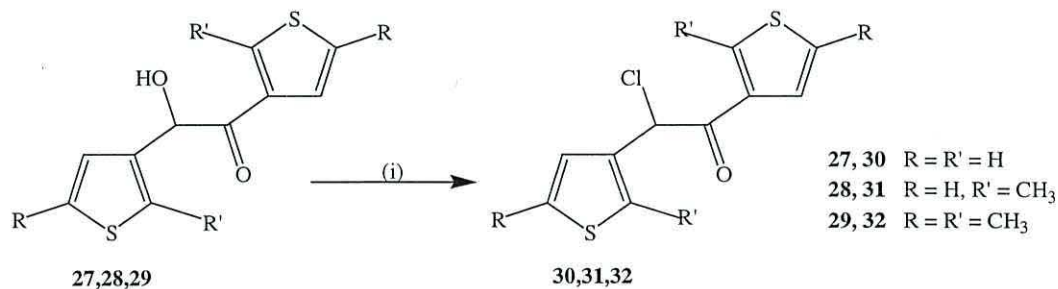
(*Indicates broad multiplet centred at 7.33ppm).

Table 4.0.2. ^1H NMR signals and C=O stretches for compounds **27**, **28** and **29**

The large difference in the reactivity of aldehyde **24** and aldehydes **25** and **26** in the benzoin condensation might be primarily due to the steric effect of the α -methyl group present in **25** and **26**. However it is interesting to note that there is a drop in reactivity when going from aldehyde **25** to **26**, which may reflect a decrease in reactivity of the aldehydes due to the positive inductive effect (+I) of successive attachment of methyl groups to the thiophene nucleus.

4.3.4 Formation of the compounds **12**, **22** and **23** from **27**, **28** and **29**.

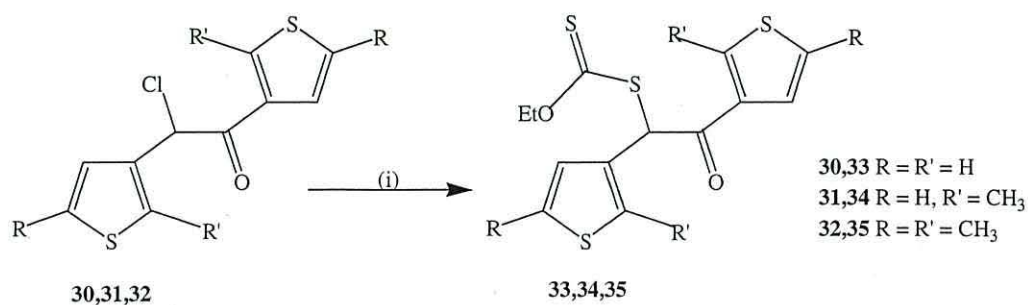
With the α -hydroxyketones **27**, **28** and **29** in hand they were converted into the corresponding α -hydroxychlorides. This was achieved by reaction with triphenylphosphine in CCl_4 and CH_2Cl_2 for 18 hours. After work up **30** was obtained in its crude form in 45% yield. Similarly **31** and **32** are obtained in 80 % and 88 % yield respectively (table 4.0.4).



Reagents and conditions; (i) PPh_3 , CCl_4 , CH_2Cl_2 , R.T., dark, 18h.

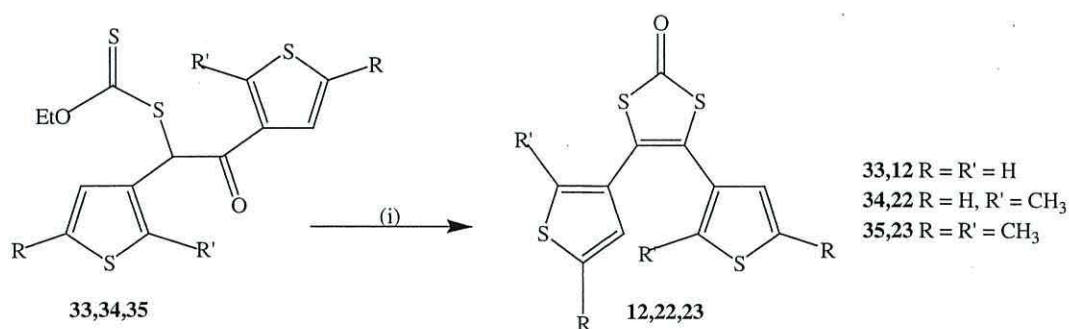
Scheme 4.0.5 Preparation of compounds **30**, **31** and **32**.

Due to the unstable nature of **30**, **31** and **32** they were used immediately in the next step of the synthesis. Thus reaction with potassium ethyl xanthate gave the xanthates **33**, **34** and **35** in high yields (63%, 100% and 76% respectively). These were used immediately in the final step of the synthesis (table 4.0.4).



Reagents and conditions; (i) KSC(S)OEt, acetone, R.T., 15 min.

Scheme 4.0.6 Preparation of the Xanthates **33**, **34** and **35**.



Reagents and conditions; (i) HBr, AcOH, R.T., 30 min.

Scheme 4.0.7 Preparation of the target compounds **22**, **23** and **12**.

Xanthates **33**, **34** and **35** were each stirred vigorously with glacial acetic acid and hydrobromic acid for 30 minutes effecting their cyclisation to the *bis*-4, 5-(3-thienyl)-1,3-dithiole-2-ones **12**, **22** and **23** in good yields; 88%, 50% and 50% respectively.

A combination of ¹H NMR, IR and Mass spectrometry was used to elucidate the structures of the compounds **12**, **22** and **23** (table 4.0.5).

Compound.	¹ H NMR signal (δ, ppm. J, Hz).					IR C=O stretch Cm ⁻¹ .
	2/ 2'	4/ 4'	5/ 5'	C-2 Me	C-5 Me	
12 R = R' = H (J =/ Hz)	6.8 (d, 5.0)	7.2 (m)	7.2 (m)	-	-	1654
22 R = H, R' = CH ₃ (J =/ Hz)	-	6.8 (d, 5.5)	7.0 (d, 5.5)	2.1 (s)	-	1653
23 R = R' = CH ₃ (J =/ Hz)	-	6.4 (s)	-	2.0 (s)	2.3 (s)	1670

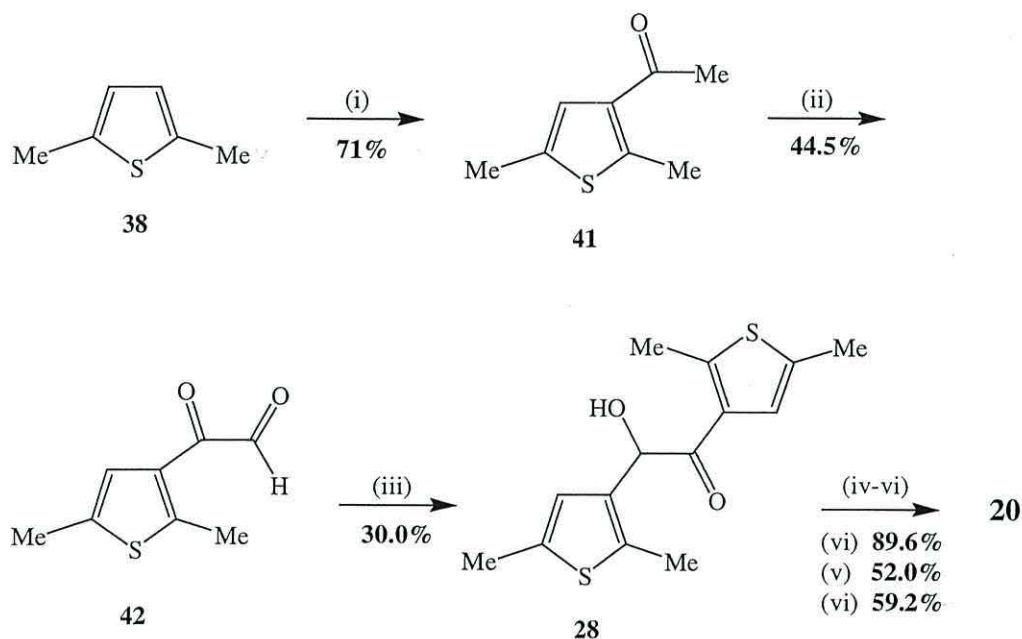
Table 4.0.5 ¹H NMR and C=O stretch data.

Alcohol	Yield (%)	Chloride	Yield (%)	Xanthate	Yield (%)	Bis-dithiolene	Yield (%)	Overall Yield (%)
27	66	30	45	33	63	12	88	17
28	29	31	80	34	100	22	50	12
29	15	32	88	35	76	23	50	5

Table 4.0.4 Summary of yields for the synthesis of compounds **12**, **22**, **23** from the aldehydes **24**, **25**, **26**.

An alternative synthesis of **23** has recently been reported by Irie (scheme 4.0.8) [10] who used the benzoin product **29** as a key intermediate. Acylation of 2,5-dimethylthiophene **26** catalysed with SnCl₄ led to **41** in 71% yield. This was oxidised to α-ketoaldehyde **42** using SeO₂ in 44.5% yield, which was then reacted with further **26** to give our benzoin product **29**. The overall yield for the steps (i)-(iii) in the Irie synthesis was 11%, which when compared to the synthesis reported here yields 10% over three steps (bromination, formylation, benzoin condensation)

shows little difference in yield. The remaining steps in the synthesis were carried out in the same manner as our synthesis, though it can be observed that their respective yields when compared to that in table 4.0.4 are poor.



Reagents and conditions: (i) Ac_2O , SnCl_4 , benzene; (ii) SeO_2 , dioxane; (iii) **24**, SnCl_4 , benzene; (iv) PPh_3 , CCl_4 , CH_2Cl_2 ; (v) KSC(S)OEt , Acetone; (vi) HBr , AcOH .

Scheme 4.0.8 Irie synthesis of compound **23**.

4.3.5 Crystal structures of **12**, **22** and **23**.

For compounds **12**, **22** and **23**, X-ray crystal structure determinations were obtained (figures 4.0.4 a-c, appendix 2). It can be seen in all cases that the thiophene rings adopt a staggered conformation and are thus not coplanar. This is of interest for our photochemical studies discussed in chapter six.

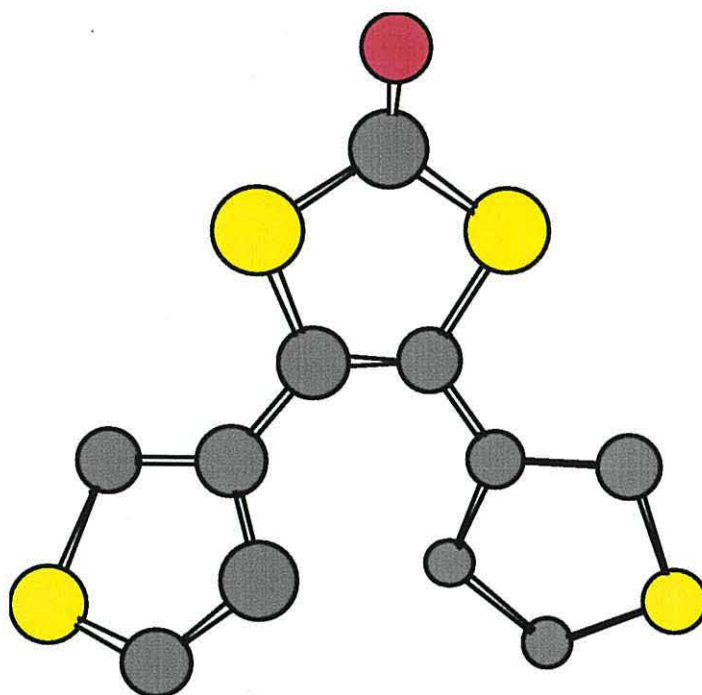


Figure 4.0.4a X-ray crystal structure of **12**.

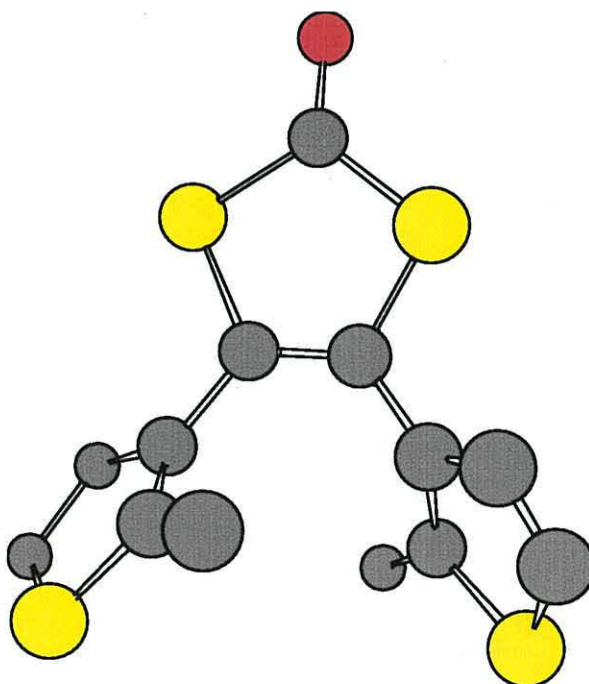


Figure 4.0.4b X-ray crystal structure of **22**.

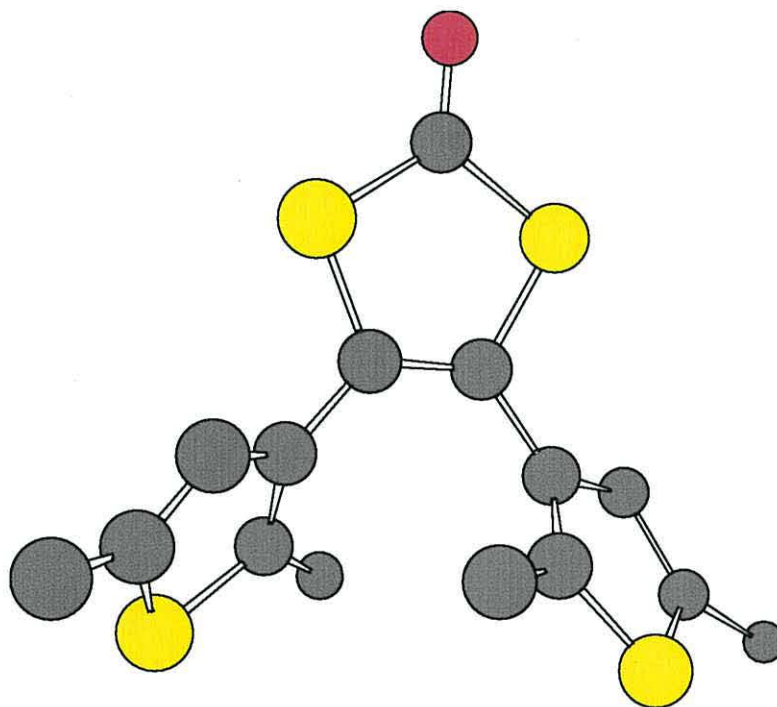


Figure 4.0.4c X-ray crystal structure of **23**.

4.4.0 Electropolymerisation studies.

The electrochemistry of compounds **12**, **22** and **23** was investigated using cyclic voltammetry.

In chapter three it was shown that in order to electropolymerise thiophene substituted TTF derivatives, it would be necessary to produce the cyclised form of the unit **12**. This was not possible, therefore *in situ* modification of the polymer was necessary to attach the TTF moieties.

However, it is important now to know exactly how polymerisation occurs and what sort of polymer is produced prior to the modification. The following section is an investigation of this, whereas in chapter five an investigation of the charge transfer mechanism will be undertaken.

4.4.1 Electrochemical deposition and characterisation of unit **12** by cyclic voltammetry.

The electropolymerisation of **12** has been reported in the literature, [3] in which the polymer was obtained via potentiodynamic deposition. Deposition was carried out by cycling, at a sweep rate of 100 mVs^{-1} , from -0.3 to $+1.8 \text{ V}$ (vs. Ag wire) in a 0.02 M solution of monomer **12** in 0.1 M TBATFB/ acetonitrile. The redox switching of the polymer was subsequently characterised by cyclic voltammetry (CV) in a monomer-free solution of 0.1 M TBATFB/ acetonitrile. The polymer exhibits an oxidation wave at $+1.65 \text{ V}$.

From figure 4.0.5 it can be seen that the cyclic voltammogram resembles that of polydithieno [3,4-b: 3'4'-d] thiophene (pDTT), a well-accepted p- and n-dopable polymer (figure 4.0.6). [11]

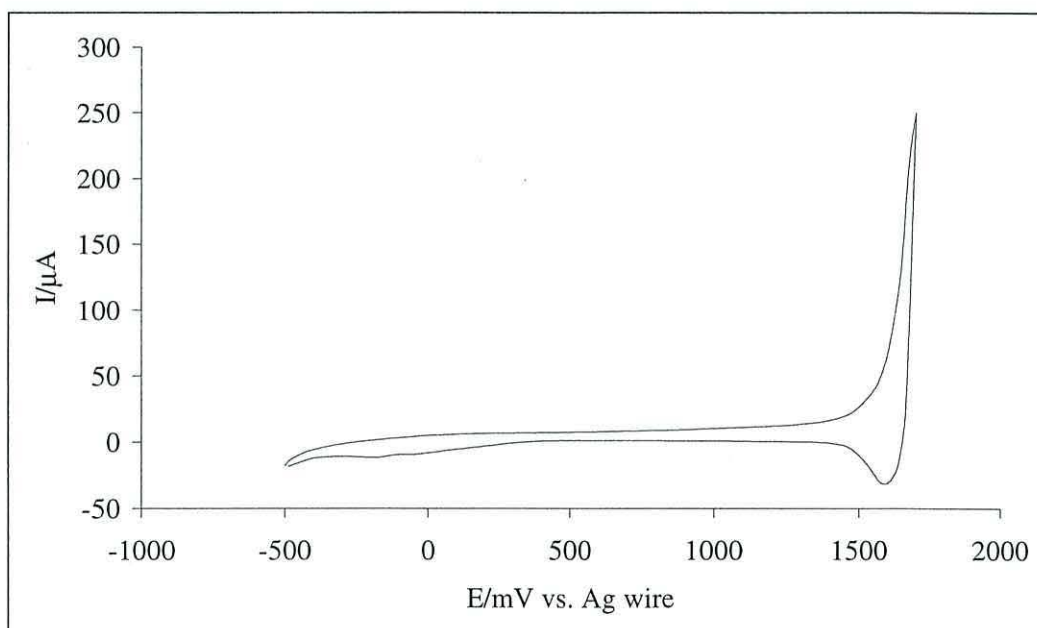


Figure 4.0.5 Cyclic voltammogram of polymerised unit **12**.

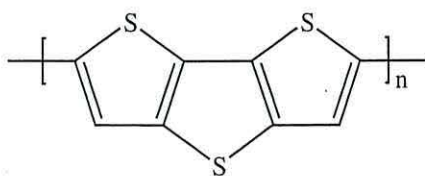


Figure 4.0.6 Polydithieno[3,4-b:3',4'-d] thiophene, pDTT.

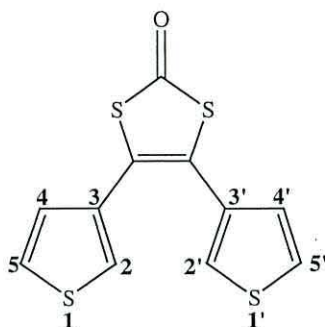


Figure 4.0.7 Compound **12**.

On consideration of the mode of polymerisation of **12** it is possible to speculate that a polymer structure such as **43** (figure 4.0.8) can be formed by linking units of **12** through the 5 and 5' position. Although this seems feasible, it would not be possible for any charge transfer to occur with a polymer of this orientation.

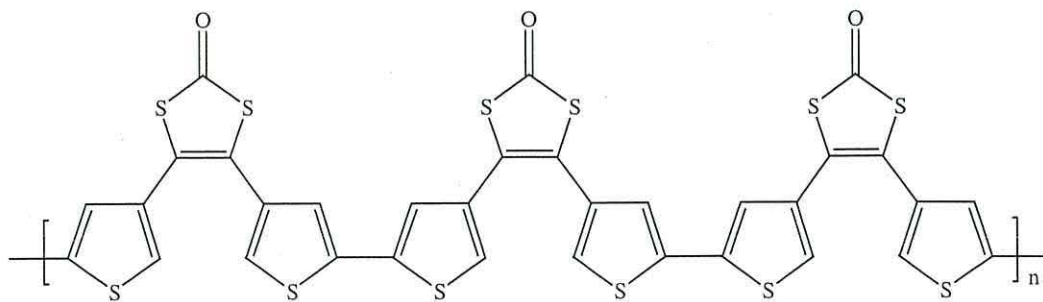


Figure 4.0.8 Polymer structure **43**.

Another possible polymerisation mode is one in which the repeat units are linked *via* the 5 and 5' positions, however an 'intramolecular' cyclisation occurs between the 2 and 2' positions leading to the 'quinoidal' structure **44** (figure 4.0.7, 4.0.9).

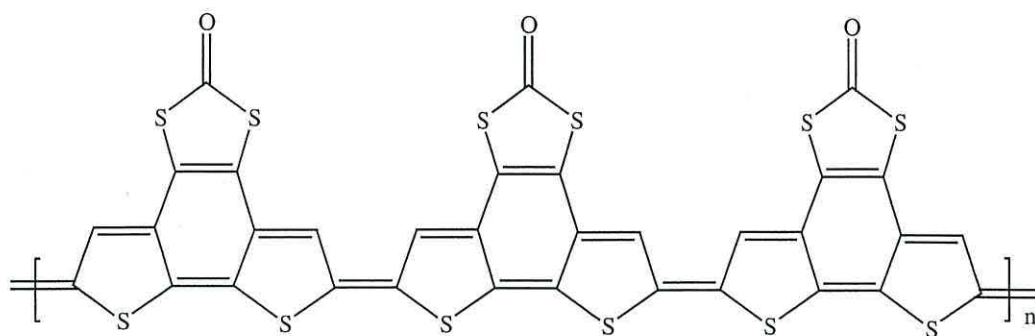


Figure 4.0.9 Polymer structure **44**.

The synthesis of the di- and tetra- methylated units **22** and **23** was directed at testing this hypothesis. It was hoped that by methylating at the 2/2' positions in **22** and at the 2/2' and 5/5' positions in **23** (figure 4.1.0), these sites of polymerisation would be blocked. Methyl functionalities are known to be poor leaving groups under synthetic and electrochemical conditions, thus removing any ability to polymerise if the mode of polymerisation is through the 2 or 5 positions.

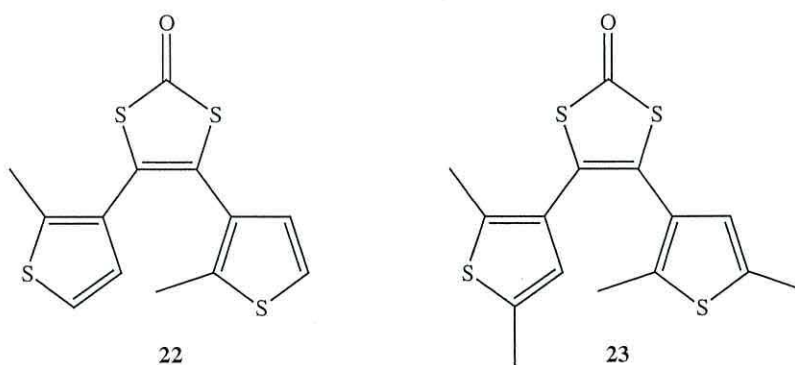


Figure 4.1.0 The methylated compounds **22** and **23**.

4.4.2 Attempted electrochemical deposition and characterisation of unit **22** by cyclic voltammetry.

Compound **22** (0.02 M) was characterised electrochemically in 0.1 M TBATFB in acetonitrile. The cyclic voltammogram is shown in figure 4.1.1. From the CV it can be seen that it resembles that of compound **12**, the unmethylated polymer. There is one oxidation wave at $E_1^{\text{ox}} + 1.56$ V. Attempts to electropolymerise the compound potentiodynamically did not succeed. This was to be expected if the polymerisation mode was *via* an intramolecular cyclisation. The similar shapes of the voltammograms of **12** and **22** are attributed to the radical cations of the monomers essentially being the same, thereby resulting in similar electrochemical properties.

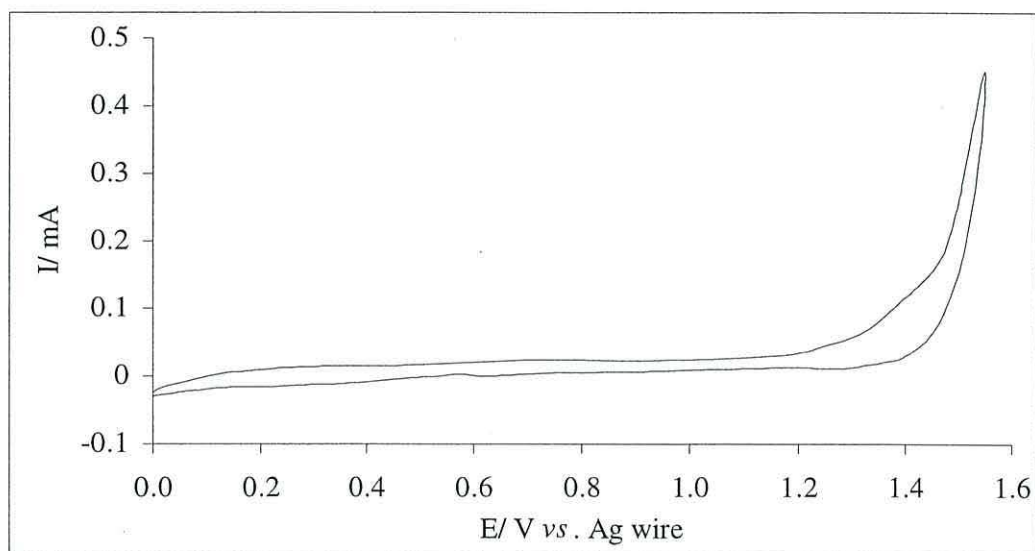


Figure 4.1.1 Cyclic voltammogram of compound **22**.

4.4.3 Attempted electrochemical deposition and characterisation of unit **23** by cyclic voltammetry.

Compound **23** (0.01 M) was similarly characterised electrochemically in

0.1 M TBATFB in acetonitrile. The voltammogram is shown in figure 4.1.2. From the CV it can be seen that there are two oxidation waves at $E_1^{\text{ox}} + 0.86 \text{ V}$ and $E_2^{\text{ox}} + 1.35 \text{ V}$. It is interesting to note that unlike the CV of the monomer **22** and of the polymerised compound **12**, the CV of **23** resembles that of poly bithiophene [12] (figure 4.1.3) rather than the aforementioned compounds or indeed, pDTT (figure 4.0.6, page 16). It should be noted that electropolymerisation attempts were unsuccessful.

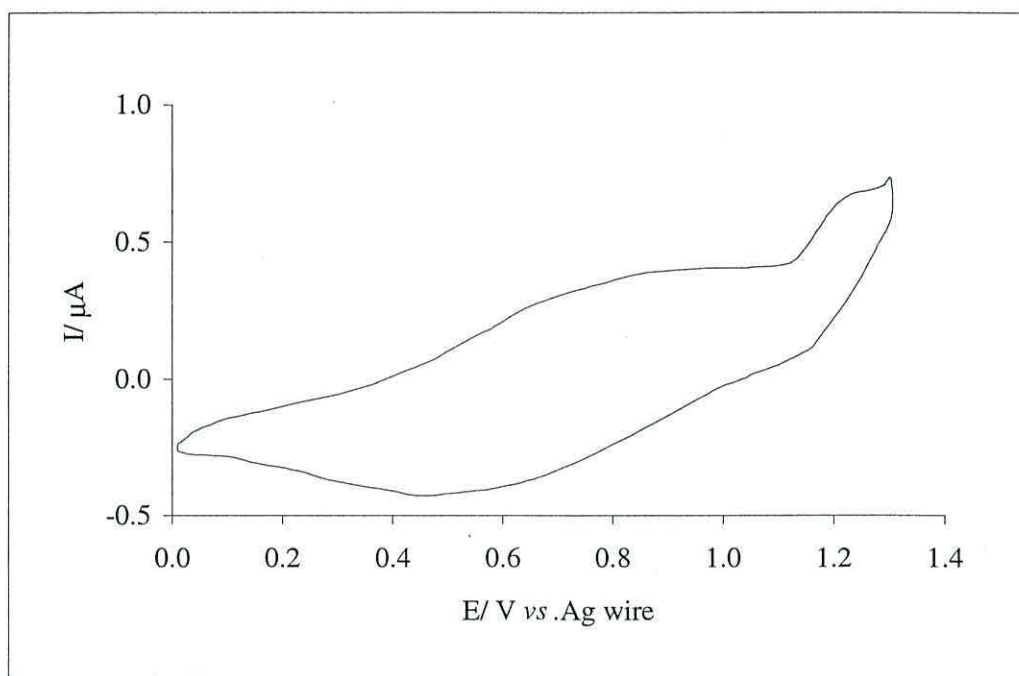


Figure 4.1.2 Cyclic voltammogram of monomer **23**.

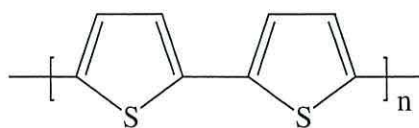


Figure 4.1.3 Polybithiophene.

Attempts were made to electropolymerise the compound potentiodynamically and galvanostatically, however, there was no evidence of

polymerisation on the surface of the working electrode. This was to be expected as the electrochemically stable methyl groups have blocked the preferential polymerisation sites (2/2', 5/5'). Polymerisation through the 3, 3' positions in respect to the thiophene moieties have been reported, however this leads to poor quality polymers. [13] In the case of compound **23**, polymerisation throughout these sites would be unfavourable due to the high levels of steric hindrance, thus rendering compound **23** essentially unpolymerisable.

4.5.0 Conclusions.

The three compounds **12**, **22** and **23** have been synthesised and characterised, their electrochemical properties have been investigated, and attempts at electrochemical polymerisation have been made.

Compound **22** was obtained in 7 steps from 3-thiophene carboxaldehyde and compound **23** in 6 steps from 2,5-dimethyl thiophene. It was found that the units **22** and **23** were not polymerisable by electrochemical methods, this being attributed to the methyl substituents. As previously reported, [3] **12** undergoes electropolymerisation and its mode of polymerisation was investigated. The idea that the polymerised form is quinoidal in nature seems to be in agreement with the data obtained, in that intramolecular cyclisation must occur, for which the 2 and 2' positions must be unsubstituted, as is the case with unit **12**, (if these positions are substituted (compound **22**) then polymerisation cannot occur. It was also true that a substituent at the 5 position effectively blocks polymerisation (compound **23**).

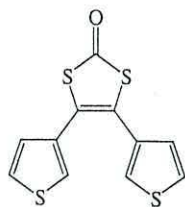
It should also be noted that, as the number of methyl substituents increases the additional increase in inductive effect (+I) causes the oxidation potentials of the compounds to decrease (table 4.0.6) by 90 mV in the case of compound **22** and by 300 mV for **23** (with respect to **12**).

Compound	Oxidation potential (V)
12	+ 1.65 V
22	+ 1.56 V
23	+ 1.35 V

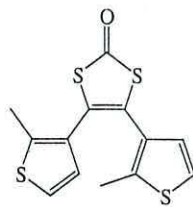
Table 4.0.6 Oxidation potentials of the monomer units.

As was discussed in chapter two, spectrochemical analysis of the polymerised unit **12**, indicated that the polymer showed little, if any, characteristics generally found in polythiophenes. This is in agreement with the similarities to pDTT, and, with the proposed quinoidal structure of the polymer, there would be no reason for the polymer to behave like polythiophene.

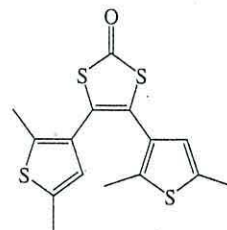
Assuming that intramolecular cyclisation occurred, it was necessary to determine the mechanism of charge-transfer throughout the polymerised compound **12**, which will be discussed in the next chapter, chapter 5.



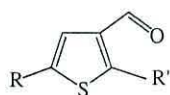
12



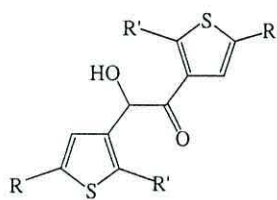
22



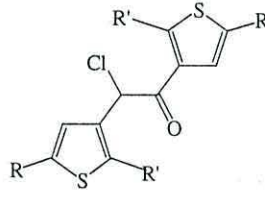
23



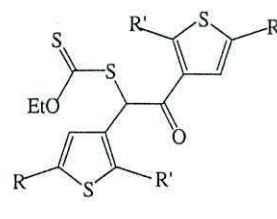
24,25,26



27,28,29

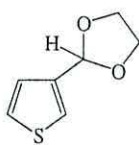


30,31,32

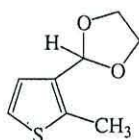


33,34,35

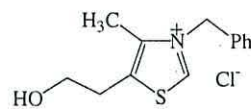
24,27,30,33 R = R' = H
 25,28,31,34 R = H, R' = CH₃
 26,29,32,35 R = R' = CH₃



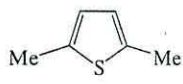
36



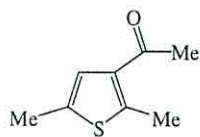
37



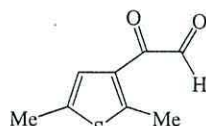
40



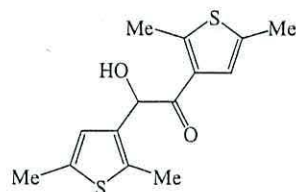
38



41



42



28

4.6.0 References.

- 1) A. Charlton, A. E. Underhill, M. Kalaji, P. J. Murphy, D. E. Hibbs, M. B. Hursthouse and K. M. Malik; *J. Chem. Soc. Chem. Commun.*, (1996) 2423.
- 2) A. Charlton, A. E. Underhill, G. Williams, M. Kalaji, P. J. Murphy and K. M. A. Malik; *J. Org. Chem.*, **62** (1997) 3098.
- 3) A. Charlton, A. E. Underhill, G. Williams, M. Kalaji, P. J. Murphy, S. Salmaso, K. M. A. Malik and M. B. Hursthouse; *Synth. Met.*, **95** (1998) 75.
- 4) S. Gronowitz, B. Gestblom and B. Mathiasson; *Archiv fuer Kemi.*, **20** (1963) 407.
- 5) S. Hibino; *J. Org. Chem.*, **49** (1984) 5006.
- 6) L. N. Lucas, J. V. Esch, R. M. Kellog and B. L. Feringa; *Tet. Lett.*, **40** (1999) 1775.
- 7) S. Inoue, T. Matsumoto and M. Ohishi; *J. Org. Chem.*, **50** (1985) 603.
- 8) J. Castells, F. López-Calahorra and L. Domingo; *J. Org. Chem.*, **53** (1988) 4433.
- 9) C. A. Dvorak and V. H. Rawal; *Tet. Lett.*, **39** (1998) 2925.
- 10) M. Irie, G. Masuda, K. Nakayama, K. Uchida and A. Yoshifumi; *Chem. Lett.*, (1999) 1071.
- 11) C. Arbizzani, M. Catellani, M. Mastragostino and C. Mingazzini; *Electrochimica Acta.*, **40** (1995) 1871.
- 12) P. A. Christensen, A. Hamnett, A. R. Hillman, M. J. Swann and S. J. Higgins; *J. Chem. Soc. Faraday Trans. 1.*, **88** (1992) 595.
- 13) T. A. Skotheim (Ed.), *Handbook of conducting polymers*, Marcel Dekker, New York, (1986).

Chapter Five: An investigation of the charge transfer mechanism and mode of polymerisation in *bis*-4,5-(3-thienyl)-1,3-dithiole-2-one **12.**

5.1.0 Aims.

The aim of the work described in this chapter was to answer the question posed at the end of chapter three; what is the mechanism of charge transfer in the polymerised form of *bis*-4,5-(3-thienyl)-1,3-dithiole-2-one **12**?

This was to be achieved by using the results described in chapter four in which the structure of the polymer was investigated. In this, the structure was given as quinonoidal, in which the monomer units when polymerised undergo an intramolecular cyclisation (figure 5.0.1).

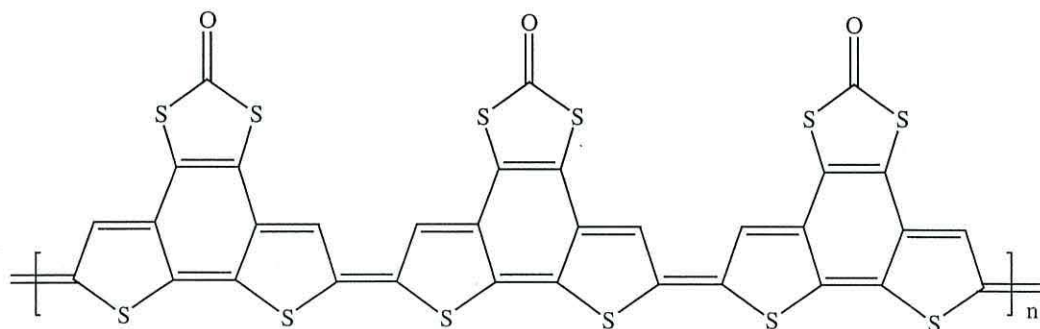


Figure 5.0.1 Proposed polymer structure.

Preliminary SNIFTIRS investigations (chapter 3) provided evidence of such a structure, and gave further evidence to show that the polymer structure is not polythiophenic in nature. To further elucidate the polymer structure and thus the mechanism of charge transfer, the 1,2-dithienylethylenes **45** and **46** (figure 5.0.2) were prepared. The reason for this is that they are likely to polymerise in the same manner as the compound **12**. They are also of interest in that their polymeric properties are expected to show charge delocalisation and structures similar to that of polythiophene and polyacetylene; **46** polymerising as a substituted

polythiophene, and **45** similar to polyacetylene. Using this information it will be possible to propose a mechanism of charge-transfer in these and the polymerised compound **12**, allowing their polymer properties to be elucidated.

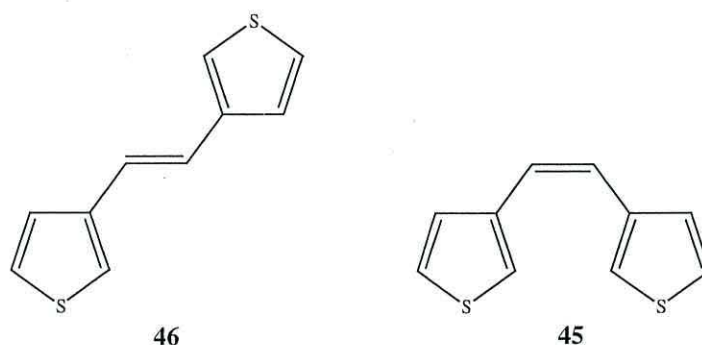


Figure 5.0.2 The 1,2-dithienylethylenes **45** and **46**.

5.2.0 Introduction.

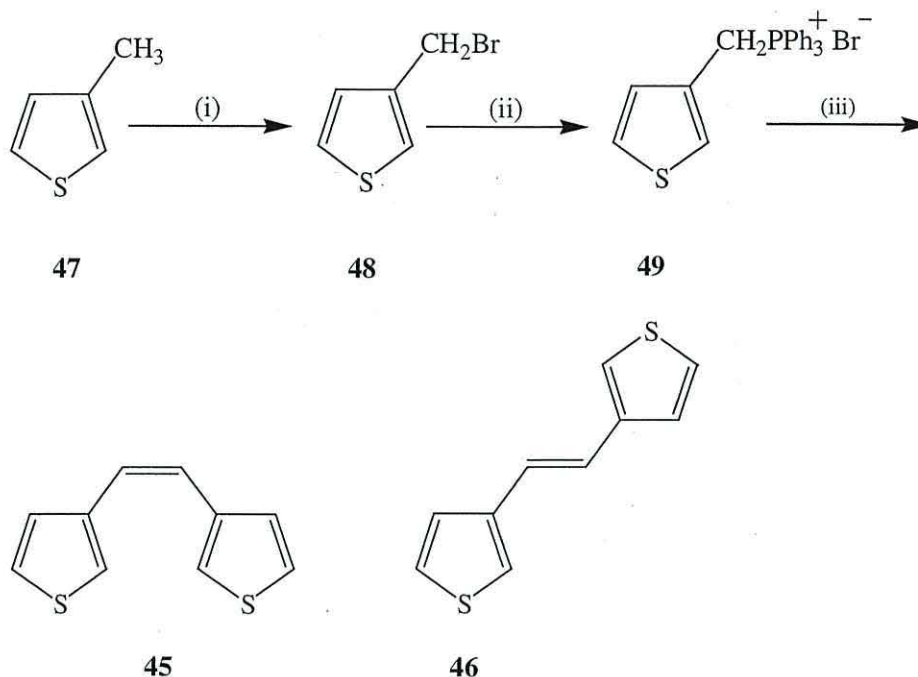
As discussed in chapter one polyacetylene and polythiophene may be doped either chemically or electrochemically. They can be switched between their oxidised and reduced states, and in the case of PT, this is denoted by associated changes in colour. They show improved conduction when doped, for example when exposed to halogen vapours.

Their mechanisms of polymerisation *via* radical cations and electrochemical properties are well understood and documented in the literature. [1,2]

5.3.0 Synthesis of *trans*-1,2-di(3-thienyl)ethylene **46** and *cis*-1,2-di(3-thienyl)ethylene **45**.

The synthesis of the 1,2-dithienylethylenes **45** and **46** is shown in the general scheme 5.0.1. The respective compounds were obtained in three steps from 3-methyl-thiophene **47** [3]. An alternative synthesis forming exclusively **45** by

Cooke and co-workers [4] has been reported in which they coupled 3-thiophene carboxaldehyde **24** using McMurrays' complex.



Reagents and conditions: (i) NBS, 0.9eqv, benzoyl peroxide, CCl_4 , 6h; (ii) PPh_3 , toluene, 3.5h; (iii) **24**, $n\text{-BuLi}$, THF, -78°C , 2.5h.

Scheme 5.0.1 Preparation of the compounds **45** and **46**.

The target compounds **45** and **46** were prepared by bromination of the 3-methyl thiophene **47** under standard conditions [1] leading to the 3-bromomethyl thiophene **48** in 84% yield. This was then reacted with triphenylphosphine in toluene to form the phosphonium salt **49** 84% yield. The final step of the synthesis, the formation of **45** and **46** was accomplished by a Wittig reaction shown in scheme 5.0.1. An ylid was produced by the drop-wise addition of 1.1 equivalents of $n\text{-BuLi}$ to a solution of **49**, into which the aldehyde **24** was added. After aqueous work up, a crude mix of **45** and **46** was yielded that was purified using column chromatography resulting in the isolated compounds **45** and **46**. The *cis*-isomer **45**, was isolated as an oil 41% yield, with a *cis:trans* ratio of 43:57. The more thermodynamically stable isomer of the compound is the *trans* form, and it was

observed that isomerisation of **45** to the *trans* form **46** occurred at room temperature in the absence of light over approximately 24 hours. This phenomena has been previously reported in the literature, and it is known that the *cis*- compound is both thermodynamically and photochemically unstable, undergoing the aforementioned isomerisation. [4]

The *trans* isomer, **46** was isolated as a white crystalline solid in 59% yield. Analysis of the ^1H NMR is in agreement with that reported by Cooke showing resonances at δ 6.9, 7.2 and 7.3 ppm.

By obtaining the X-ray crystal structure (figure 5.0.3, appendix 3) it was possible to elucidate the orientation of the thiophene moieties. It is important to note that *trans*-stilbene compounds similar to **46** have a large planar ring twist ($> 5^\circ$) with respect to the C=C double bond. [5] This is due to steric interactions between the vinyl protons and those protons on the phenyl rings. In the case of **46** the ring twist has been reduced to 3° and it should be noted that the heteroatom is facing away from the double bond. When compared to the 1,2-di-(2-thienyl)-ethylene compound, reported by Cooke, [4] it can be noted that the ring twist is only 1° and the heteroatoms are turned in toward the double bond. Thus there is little interaction between the vinyl protons and the ring protons resulting in a more planar configuration. This when expanded to polymeric terms would produce a polymer that has a more planar chain, resulting in more π -orbital overlap and therefore higher conductivities. [1]

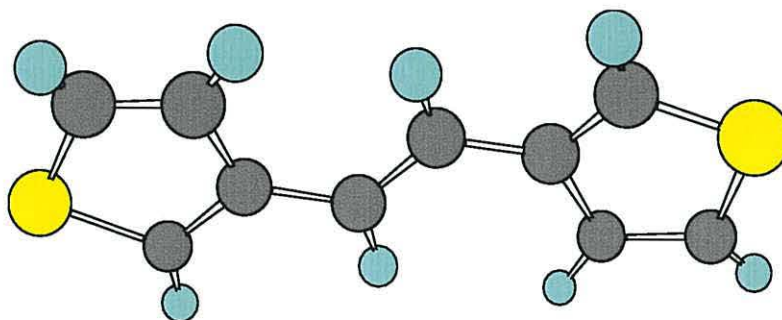


Figure 5.0.3 Crystal structure of *trans*- 1,2-di-(2-thienyl)-ethylene **46**.

5.4.0 Electropolymerisation studies.

As mentioned in 5.0.1, the compounds were prepared so that their mode of polymerisation and charge-transfer mechanisms could be investigated and related to the unit **12** polymer. A solution of 0.02 mol dm^{-3} *cis/trans* 1,2-di-(3-thienyl)-ethylene **45** and **46** in acetonitrile containing 0.01 mol dm^{-3} TBATFB was used for deposition of the polymer onto a Pt disc electrode. In both cases, the electropolymerisation was successful resulting in silvery films attached to the electrode.

5.4.1 The doping and electrochemistry of polyacetylene.

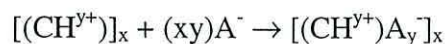
In 1977 it was discovered that polyacetylene could be chemically p-doped with an associated increase in its conductivity through the semi-conducting state to the metallic state. [6,7] Shortly after it was realised that polyacetylene could become a metallic conductor by chemical methodologies, [8] it followed in 1979 that the p- and n-doping of the polyacetylene could be achieved electrochemically, the advantage to the chemical techniques being the reversibility of dopable states. [9]

Polyacetylene may be p-doped with electron donating species such that an increase in conductivity is observed, selected examples of which are given in table 5.0.1. [10]

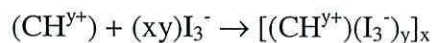
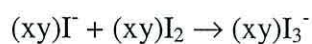
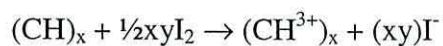
The previous statement although correct in that large increases in conductivity are observed when the material takes up small quantities of chemical species, is incorrect when applied to conducting polymers i.e. p-doping of a conducting polymer refers to the partial oxidation of the polymer;



This may be accomplished chemically or electrochemically [11] and, in order to preserve charge neutrality a counter-anion A^- must be provided:



So, when $(\text{CH})_x$ is p-doped with iodine the reaction can be regarded to occur as follows: [12]



Substance.	Conductivity (S / cm).
<i>Cis</i> - $(\text{CH})_x$	1.7×10^{-9}
<i>Trans</i> - $(\text{CH})_x$	4.4×10^{-5}
<i>p-Doping (oxidation)</i>	
I_2 vapour $[(\text{CH}^{0.07+})(\text{I}_3^-)_{0.07}]_x$	5.5×10^2
AsF_6 vapour $[(\text{CH}^{0.1+})(\text{AsF}_6^-)_{0.1}]_x$	1.2×10^3
HClO_4 (liquid or vapour) $[(\text{CH}\{\text{OH}\}_{0.08})^{0.12+}(\text{ClO}_4^-)_{0.12}]_x$	5×10^1
Electrochemically : $[(\text{CH}^{0.1+})(\text{ClO}_4^-)_{0.1}]_x$	1×10^3

Table 5.0.1 Examples of conductivities in doped conducting polymers.

The electrochemistry of PA is well reported in the literature. [9] Deposited films can be driven repeatedly between the neutral and oxidised states, resulting in *cis-trans*-isomerisation over approximately two oxidation-reduction cycles. [13]

Cis-(CH)_x the more flexible polymer than *trans* (the more thermodynamically stable polymer) shows a well-defined symmetrical oxidation peak ($E_{ox} = +0.8V$ vs. Calomel). The reduction of the oxidised polymer in the reverse sweep shows two peaks ($E_{red} = +0.61V$ and $+0.46V$ vs. Calomel). The combined reduction peaks carrying the same amount of charge found in the oxidation peak. [14]

Trans-(CH)_x shows a large oxidation peak at $E_{ox} = +0.88V$ vs. NaCl calomel though essentially resembles that of the *cis*-polymer. [15]

In both cases it is possible to oxidise further, however, the process is irreversible resulting in a large loss of polymer electroactivity.

In general, upon doping, the *cis* isomer shows higher conductivities than the *trans* isomer, and it is important to note that whether partially (<5%) or heavily doped (>20% -30%) both *cis*- and *trans*-(CH)_x appear to produce the same oxidised structure.

A discussion of the electrochemistry and doping of polythiophene has been given in chapters one and three.

5.4.2 The electropolymerisation of *cis* 1,2-di-(3-thienyl)- ethylene **45**.

As mentioned in section 5.4.0 silvery films of the *cis*-polymer were obtained on Pt working electrodes the cyclic voltammetry of which can be seen in figure 5.0.4.

The polymerised form of **45** shows a well-defined oxidation peak at $E_{ox}^1 +0.85V$ (vs. Ag wire) with two reduction peaks observed on the reverse sweep at $E_{red}^1 +0.75V$ (vs. Ag wire).

It is interesting to note the similarities of the *cis*-polymer **45** to that of polyacetylene (figure 5.0.5). [14] The peak at +0.75V can be assigned as the reductive 'partner' to that found at +0.85V on the oxidative sweep.

As mentioned previously (section 5.4.1) the increase in current at potentials greater than +0.9V, show similarities to the structural reorientation effect observed in *cis/trans*-(CH)_x.

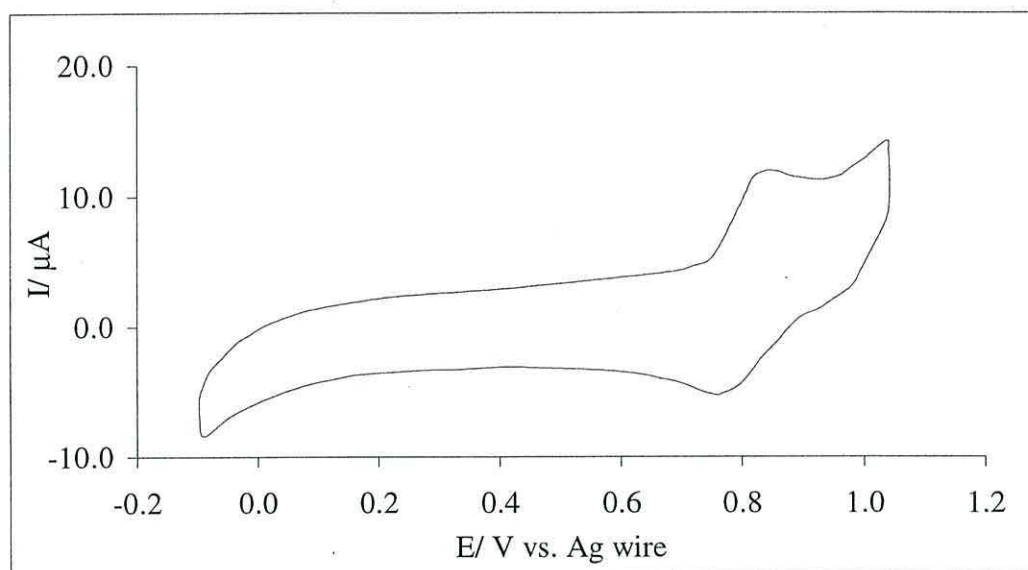


Figure 5.0.4 The cyclic voltammetry of the polymerised **45**.

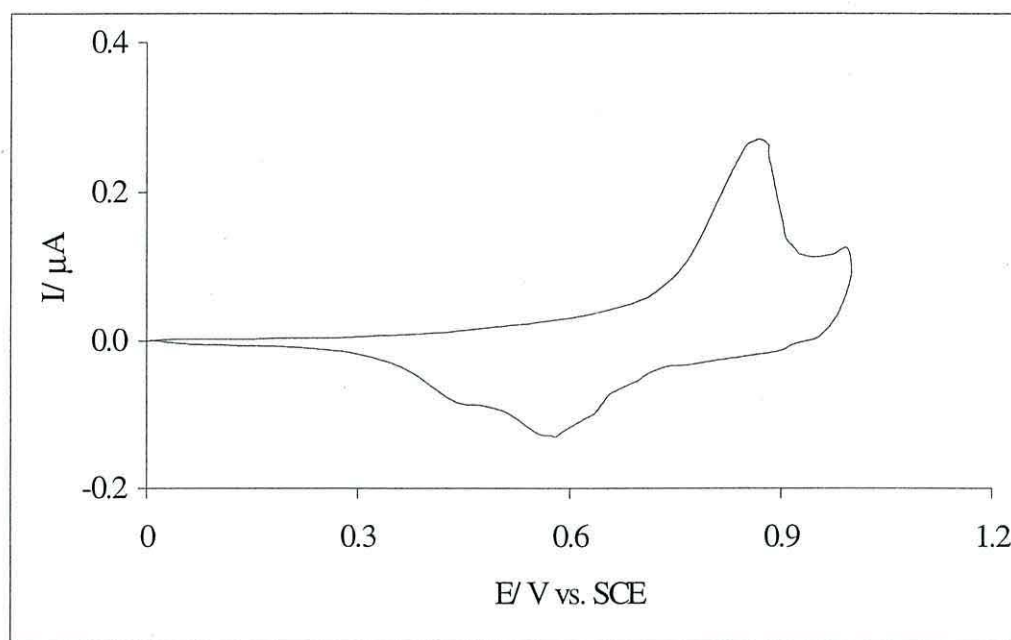


Figure 5.0.5 The cyclic voltammetry of *cis*-(CH)_x (polyacetylene).

5.4.3 The electropolymerisation of *trans* 1,2-di (3-thienyl) ethylene **46**.

Silvery films of the *trans*-polymer were obtained on a Pt working electrode, the cyclic voltammetry of which can be seen in figure 5.0.6.

The polymerised form of *trans* 1,2-di (3-thienyl) ethylene **46** shows a small oxidation peak at $E_{ox}^1 + 0.71V$ (*vs.* Ag wire) and a broad reductive peak at $E_{red}^1 + 0.33V$ (*vs.* Ag wire) on the reverse sweep. In comparison to the polymerised *cis*-**45** there are no similarities. This would infer that two different polymer structures are being produced; *trans*-**46** polymerises in a different manner to that of *cis*-**45**.

By now comparing the *trans*-**46** polymer to that of *trans*-(CH)_x, [14] it can be seen that the two polymers are in no way associated with each other. Thus the charge-transfer mechanism and polymeric properties of *trans*-**46** are unlike the *cis*-**45** polymer and polyacetylene.

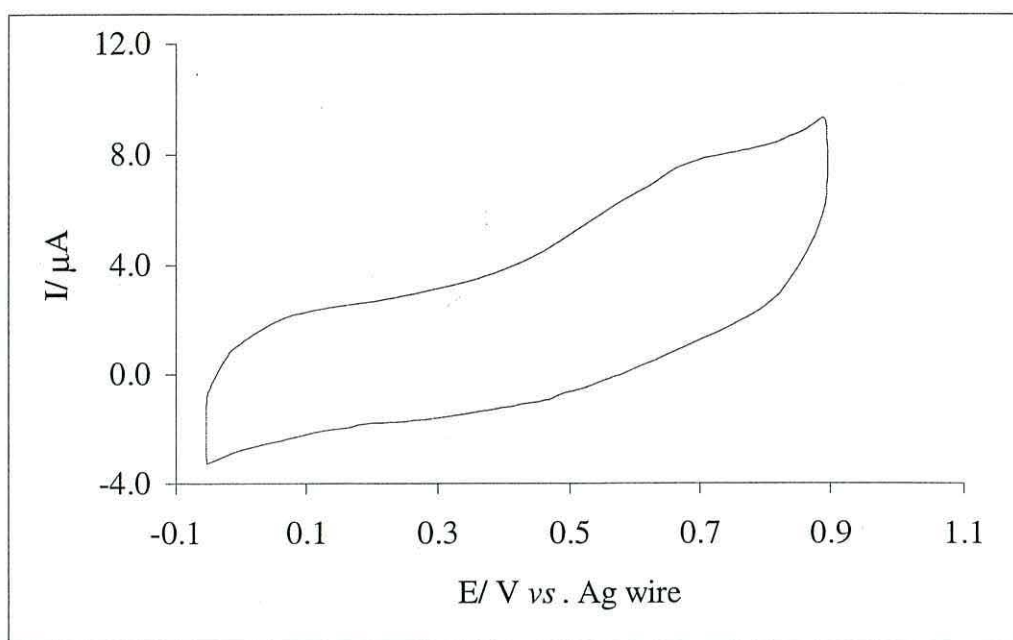


Figure 5.0.6 The cyclic voltammetry of the polymerised *trans*-46.

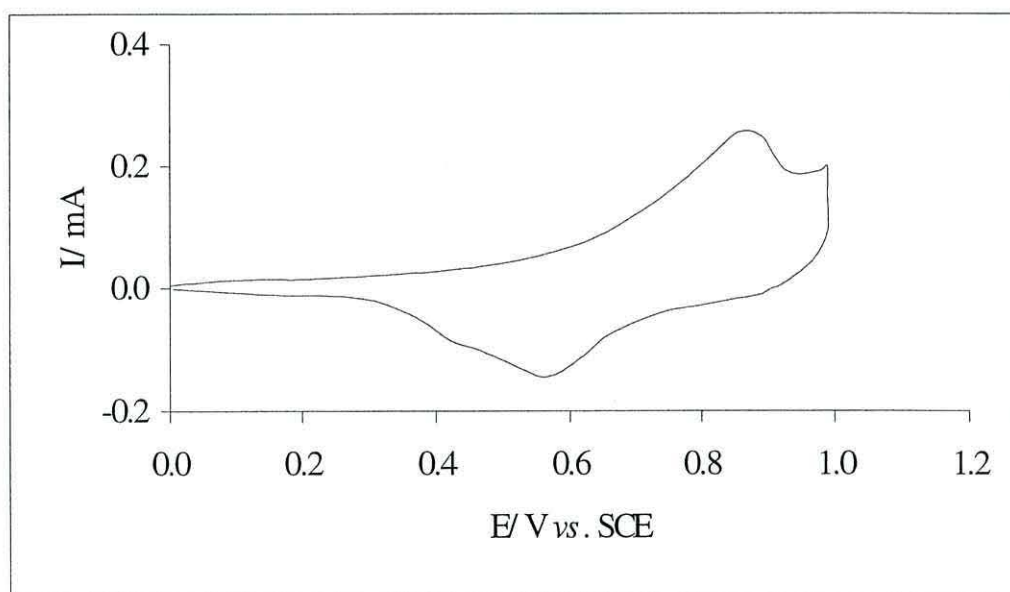


Figure 5.0.7 The cyclic voltammetry of *trans*-(CH)_x (polyacetylene).

5.4.4 The I₂ doping of *cis* 1,2-di-(3-thienyl)-ethylene 45.

When an electrode modified with *cis*-poly 45 is exposed over a period of 5 minutes to iodine vapour, changes are observed in the polymer. The silvery polymer film changes in colour to yellow indicating that chemical doping has occurred. The electrochemistry of the doped sample can be seen on figure 5.0.8, in which there is one oxidation peak at $E_{ox}^1 + 0.83V$ (*vs.* Ag wire) and two reductive peaks at $E_{red}^1 + 0.62V$ and $E_{red}^2 + 0.43V$. In comparison to the undoped sample of *cis*-poly 45, the oxidation peaks are located at the same potentials. This would therefore infer that the doping procedure greatly enhances the oxidative characteristics of the polymer.

Upon reduction two peaks appear at potentials similar to that of *cis*-(CH)_x, and are not similar to those found in the undoped state. By overlaying the doped and undoped CVs it is possible to observe the similarities in the CV shape and oxidation potential of the polymers. However perhaps more interestingly, if the doped CV was compared to that of *cis*-(CH)_x, it can be observed that they are very similar to each other. This would infer that in the doped state, the *cis*-poly 45 has a charge transfer mechanism that is the same/similar as polyacetylene (*cis*-(CH)_x, figure 5.1.0). In which the electrons can move via two routes, both of which result in a polymer with a charge-transfer mechanism similar to polyacetylene.

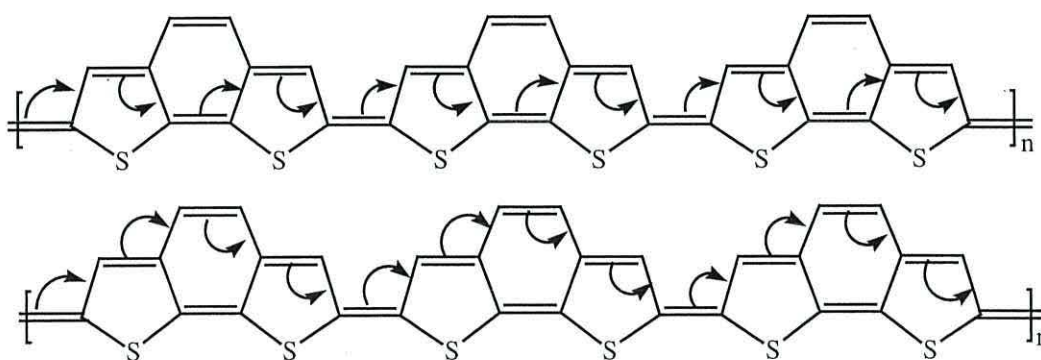


Figure 5.1.0 Proposed structure and charge-transfer mechanism of the doped *cis*-polymer 45.

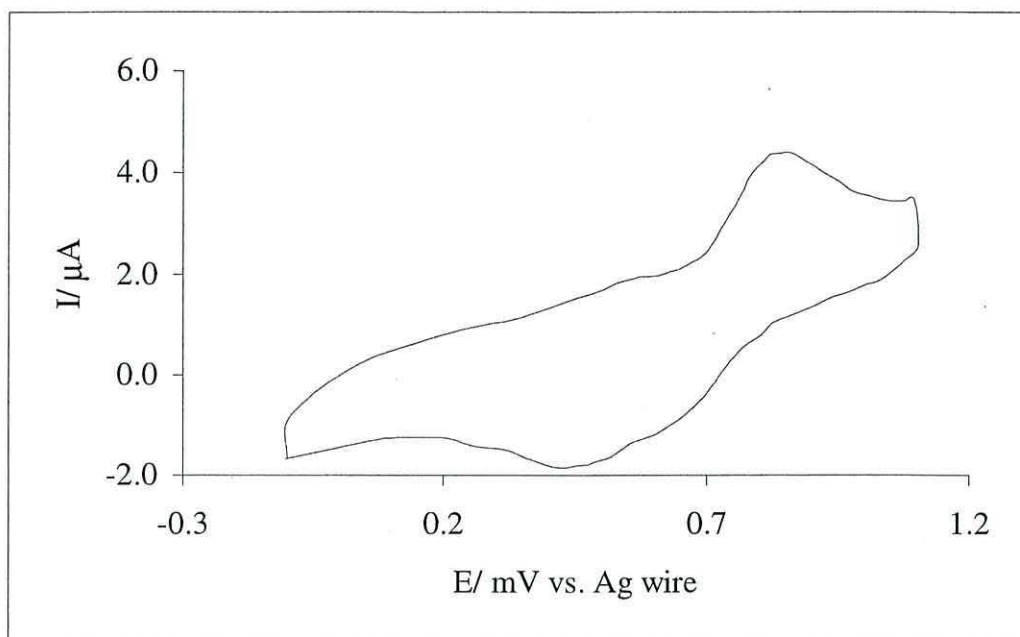


Figure 5.0.8 CV of the I₂ doped *cis*-poly **45**.

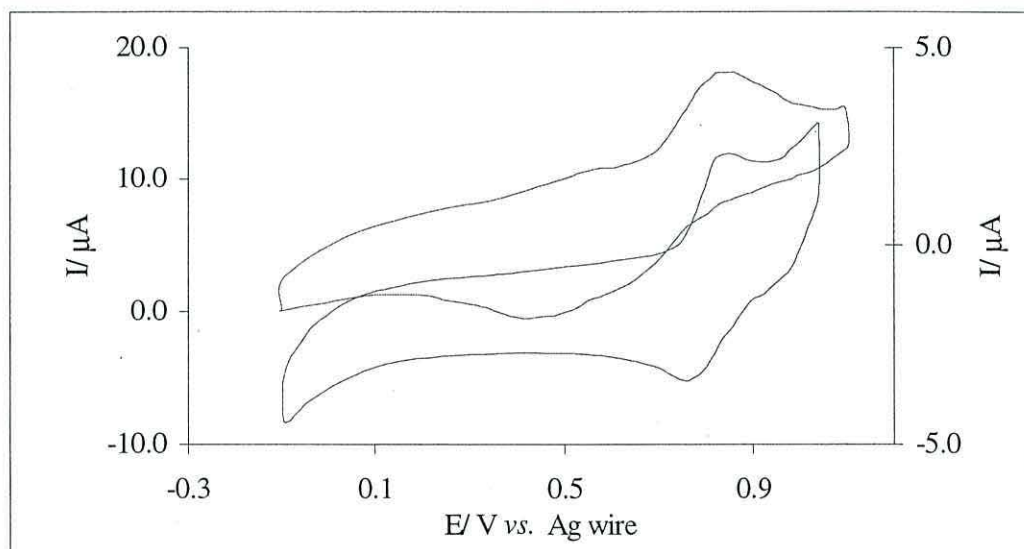


Figure 5.0.9 The overlaid CV of doped and undoped *cis*-poly **45**.

5.4.5 The I₂ doping of *trans* 1,2-di-(3-thienyl)-ethylene 46.

When a sample of polymerised *trans*-46 is exposed to iodine vapour in a manner described in section 5.5.4, changes are observed in the polymer. The polymer itself changes from a silvery white film to a yellow colour indicating that chemical doping has occurred. The electrochemical properties are also dramatically changed.

The voltammogram of the doped sample (figure 5.1.1) shows two clear oxidation peaks at $E_{\text{ox}}^1 +0.51\text{V}$ and $E_{\text{ox}}^2 +0.85\text{V}$ (vs. Ag wire), and two associated reduction peaks at $E_{\text{red}}^1 +0.82\text{V}$ and $E_{\text{red}}^2 +0.52\text{V}$. Though it is not possible at this stage to conclude that a fully reversible redox process is occurring.

The first important point to notice is that the voltammograms of the undoped and doped *trans*-46 are not similar in any way. The oxidation waves occur at different potentials, unlike that observed in the case of *cis*-45, in which the polymer characteristics were enhanced and the charge-transfer mechanism remained unchanged.

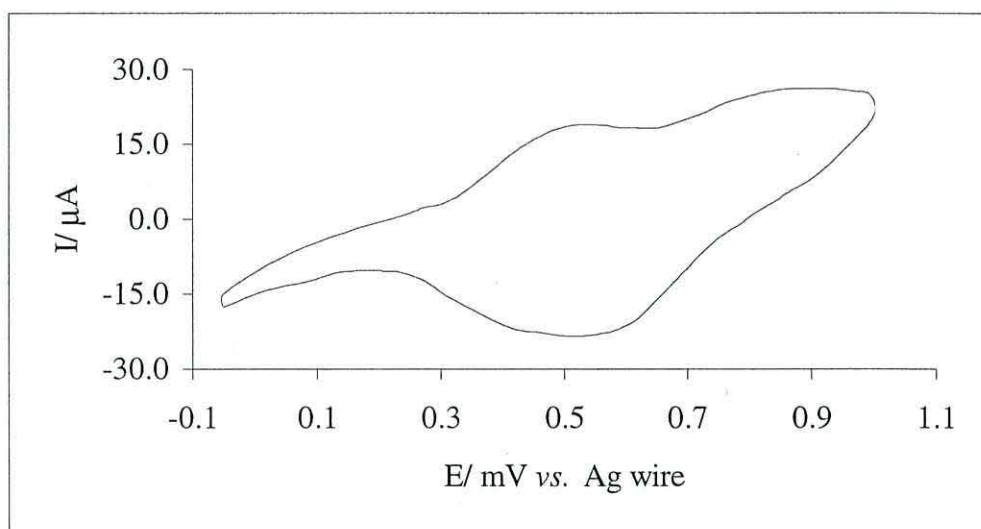


Figure 5.1.1 The CV of Iodine doped *trans*-46.

From this it is possible to draw some conclusions. *Trans-46* when polymerised does not exhibit any characteristics of the polymerised form of *cis-45*. It shows no similarities to that of *cis/trans*-(CH)_x, inferring that the polymer does not behave like polyacetylene. This is also true when in the doped state. When doped and undoped forms of *trans-46* are compared (figure 5.1.2), a large difference in the polymer characteristics is observed. In its undoped form it cannot be compared to any other organic based polymer, it would be assumed that it would polymerise in a way that results in the formation of a polythiophene (figure 5.1.3), however this is not the case.

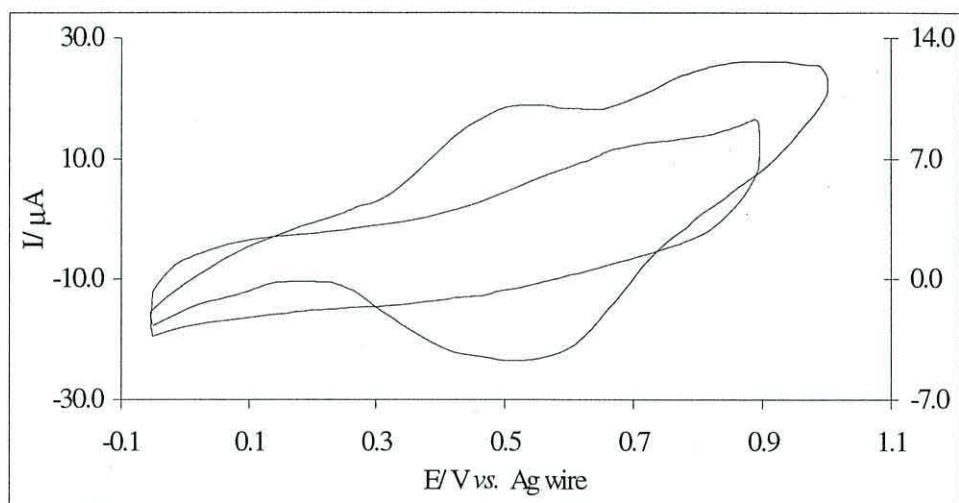


Figure 5.1.2 The CV of doped and undoped polymerised *trans-46*.

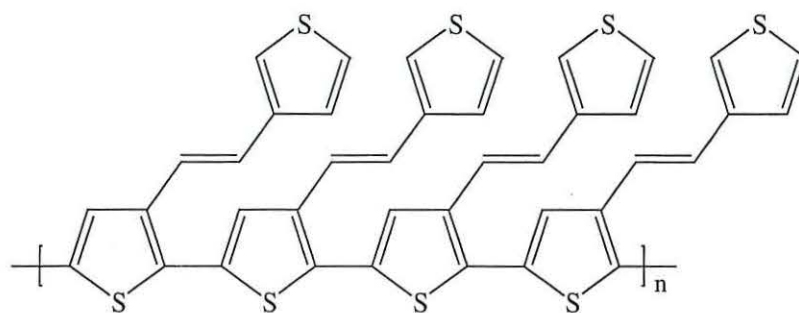


Figure 5.1.3 Proposed polymeric structure of *trans*-**46**.

It is unclear at present what type of structure the polymerised form of *trans*-**46** is and how the charge-transfer mechanism works.

In the doped state however *trans*-**46** displays characteristics similar to that of polythiophene, inferring that unlike the doping of *cis*-**45**, (in which the polymer characteristics are merely enhanced by the presence of dopant (I_3^-)) the chemical doping of *trans*-**46** results in a structural change, changing the characteristics and charge-transfer mechanism of the polymer. This results in the structure given above (figure 5.1.3) in which the moieties are linked in such a way to produce a polythiophene backbone.

5.5.0 A SNIFTIRS investigation of *cis/trans* 1,2-di-(3-thienyl)-ethylene **45** and **46** polymer structure.

With the two polymers in hand SNIFTIRS were run in both undoped and doped states. The SNIFTIRS technique has been previously described in detail in chapter three section 3.6.0. By performing these experiments it will be possible to compare the spectra obtained from the undoped and doped *cis*-**45** polymer, allowing the proposed polymeric structure to be confirmed. If so, it will then be possible to determine whether the proposed polymeric structure and charge-transfer mechanism of the polymerised **12** are similar to those of the polymerised *cis*-**45** as expected.

It may also provide further information to determine the structure of the undoped *trans*-**46** polymer, and confirm that chemical doping does indeed alter the polymer structure to produce a polythiophene.

5.5.1 SNIFTIRS investigation of Poly-*cis* 1,2-di-(3-thienyl)-ethylene **45**.

The difference spectra of the *cis*-polymer is given in figure 5.1.4 and is summarised in table 5.0.2.

The spectra is much simpler than those observed for compound **12** polymer. This is due to the absence of 1,3-dithiolene groups or carbonyl regions.

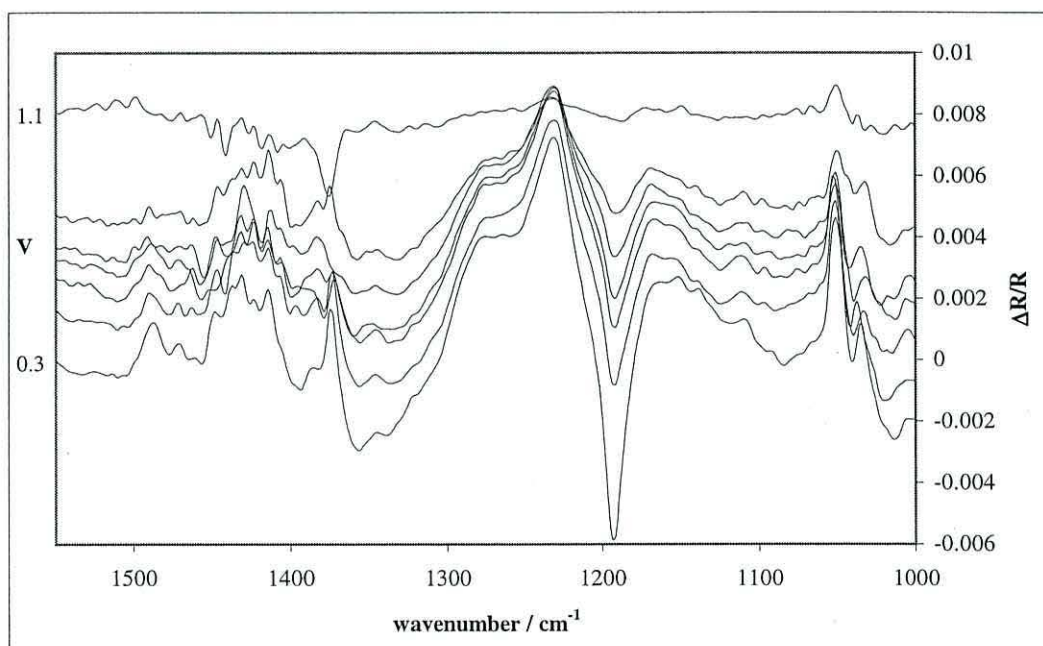


Figure 5.1.4 SNIFTIRS spectra of the *cis*-polymer.

The main region of interest is that between 1550-1100 cm^{-1} . On the onset of oxidation, bands of increasing strength at 1505, 1392, 1190 and 1077 cm^{-1} are seen to increase in absorbance. These are attributable to; an activated Raman C=C band, C-C in plane band, C-H stretching and C-S stretching vibrations respectively. There is also a further region of absorbencies, in which there is a decrease in

absorbance at 1482, 1425, 1374, 1228 and 1157 cm^{-1} . The bands at 1482 and 1157 cm^{-1} are attributable to C-C stretches in moieties similar to 2,5-dimethylene-2,5-dihydrothiophene **50** (figure 5.1.5) reported by Kesper et al. [16]

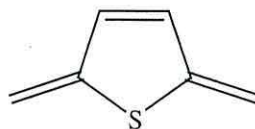


Figure 5.1.5 2,5-dimethylene-2,5-dihydrothiophene **50**.

The peak at 1374 cm^{-1} is an in plane vibration of the polymer backbone, and the peaks at 1425 and 1228 cm^{-1} are for C-CH bends, reported previously in chapter three for the polymer backbone of quinonoidal structures.

Similarities to compound **12** are found in the peaks at 1505, 1190, 1077, 1374, 1228 and 1157 cm^{-1} , with new bands appearing at 1425, 1482 and 1392 cm^{-1} . These bands would infer that the proposed polymer structure (figure 5.1.6) is correct.

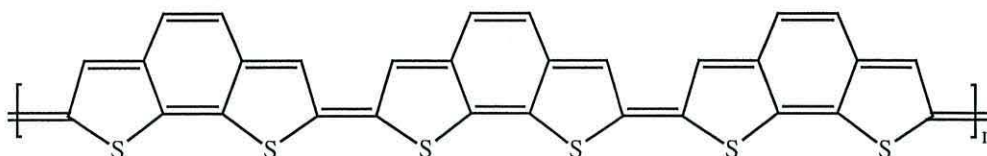


Figure 5.1.6 Proposed polymer structure.

The presence of characteristic bands found in **50**, benzoquinone **51**, and those in the polymerised compound **12** (figures 5.1.5, 5.1.7, 5.1.8), provide further evidence for this. [17]

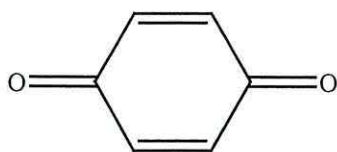


Figure 5.1.7 Benzoquinone **51**.

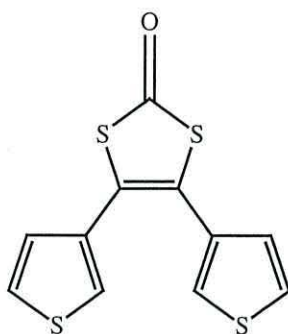


Figure 5.1.8 Compound **12**.

The lack of any characteristic polythiophene absorbances would also provide further evidence to indicate that the mode of polymerisation has to be *via* a non-polythiophene route, inferring that charge transfer must occur via a non-PT route also; the voltammograms previously described provide evidence for this (sections 5.4.2 and 5.4.4).

Bands.	Cm ⁻¹
Activated Raman C=C band	1505
C-C stretch	1482
C-CH bend	1425
C-C in plane band	1392
In plane vibration	1374
C-CH bend	1228
C-H stretching vibration	1190
C-C stretch	1157
C-S stretching vibration	1077

Table 5.0.2 Summarised bands in Poly-*cis* 1,2-di-(3-thienyl)-ethylene **45**.

5.5.2 SNIFTIRS investigation of I₂ doped Poly-*cis* 1,2-di-(3-thienyl)-ethylene **45**.

In the doped state the difference spectra (figure 5.1.9) show no new absorbances of interest, the spectra being less complex than the undoped counterpart, the main peaks are summarised in table 5.0.3.

Bands at 1507, 1449, 1413 and 1374 cm⁻¹ attributable to an activated Raman C=C band, C-C stretch in benzoquinone type structures, C-CH and C-H bends in compounds similar to **51** are present. It should also be noted that these bands are present in the undoped polymer and that of the polymerised compound **12**.

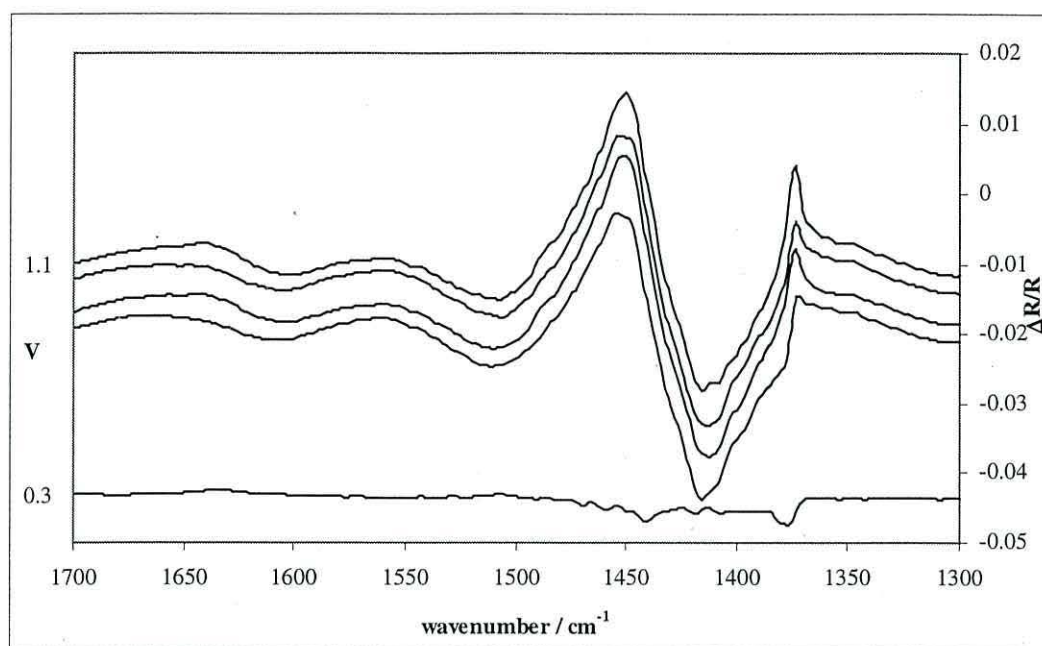


Figure 5.1.9 SNIFTIRS spectra of the iodine doped *cis*-polymer.

Bands.	cm ⁻¹
Activated Raman C=C band	1507
C-C stretch	1449
C-CH bend	1413
C-H bend	1374

Table 5.0.3 Summarised bands for the iodine doped *cis* 1,2-di(3-thienyl)ethylene **45**.

5.5.3 Conclusions for the polymerised *cis* 1,2-di-(3-thienyl)-ethylene **45**.

Cis-45 polymerises to form the quinoidal structure given in figure 5.2.0, and has a charge-transfer mechanism similar to that of polyacetylene. [14] Doping the

polymer acts only to enhance the polymer characteristics, increasing the conductivity of the polymer, but causing no structural reorganisation.

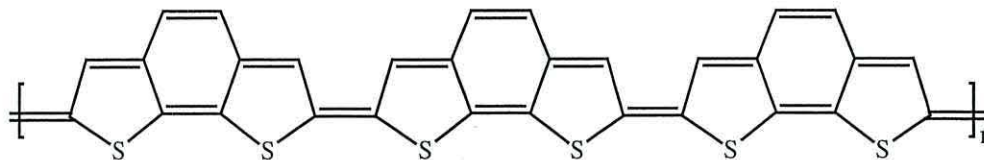


Figure 5.2.0 Polymer structure of *cis* 1,2-di-(3-thienyl)-ethylene **45**.

5.5.4 SNIFTIRS investigation of Poly-*trans* 1,2-di-(3-thienyl)-ethylene **46**.

The difference spectra of the *trans*-polymer are shown in figures 5.2.1 and 5.2.2 and are summarised in table 5.0.4.

The main point to notice about the *trans*-polymer is that as expected, the SNIFTIRS spectra in no way resemble those of the *cis*-polymer, nor that of the polymerised form of **12**. Thus the polymer has a mode of polymerisation and mechanism of charge transfer unique to this compound, which is confirmed by the electrochemical data described in sections 5.4.3 and 5.4.5.

The bands at 3169, 3107, 1412 and 1375 cm^{-1} are characteristic thiophene absorbencies for C-H stretching, C-H stretching, C=C stretching and C=C intra-ring vibrations respectively. Further absorptions at 2970, 2883 and the weak absorbance at 1727 cm^{-1} are attributed to C-H aliphatic stretching (2970 and 2883 cm^{-1}), and C=C stretching respectively. It should be noted that these bands decrease during the oxidation process, attributable to a decrease in bond strength of the ethylene portion of the polymer.

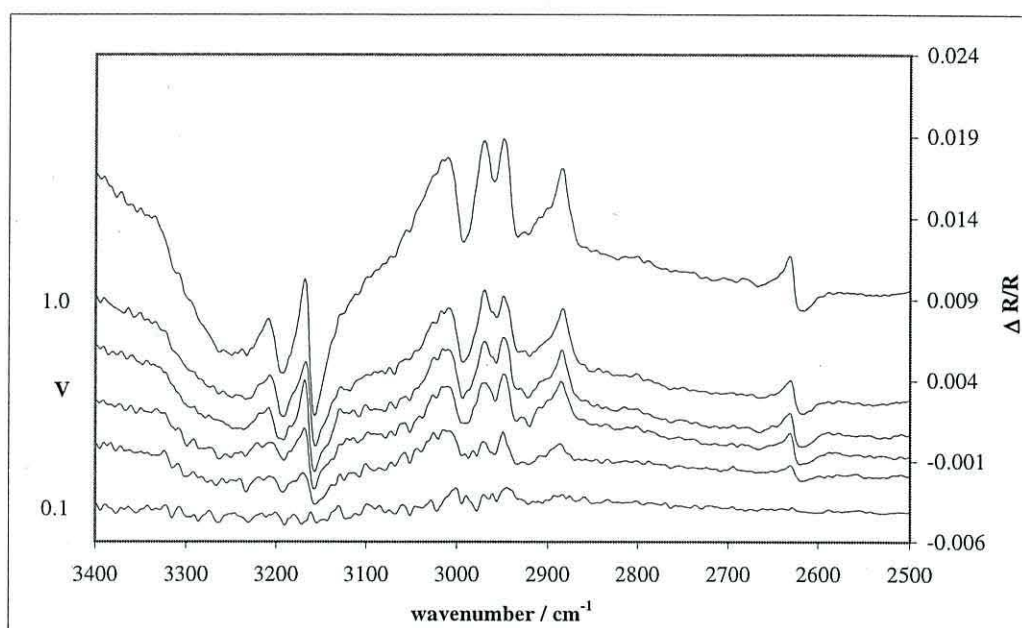


Figure 5.2.1 SNIFTIRS spectra of the *trans*-polymer.

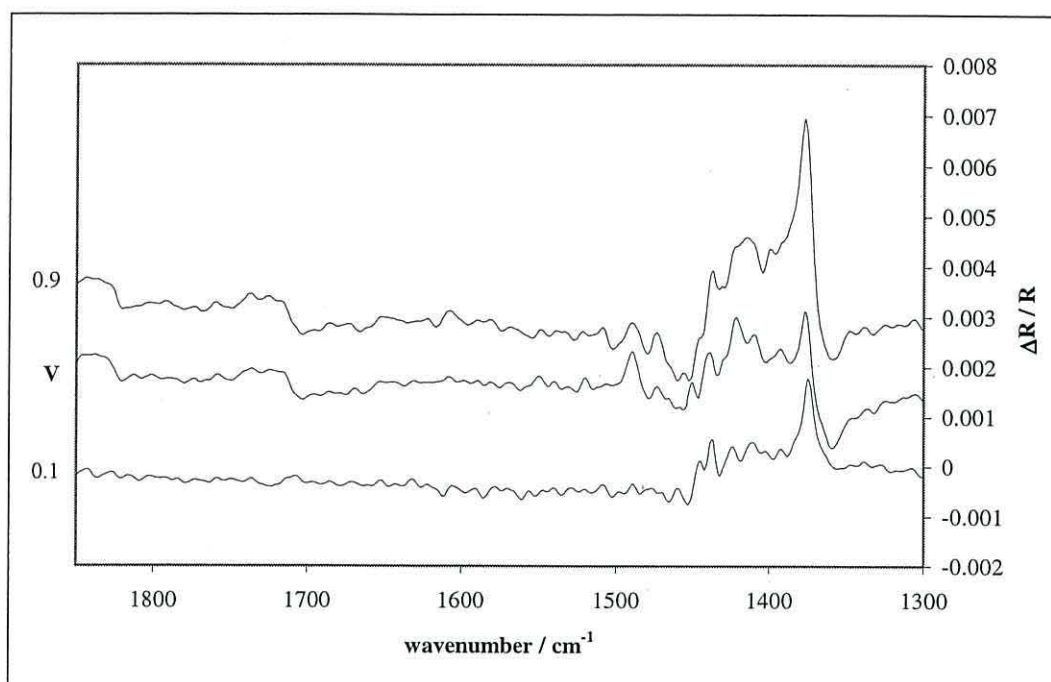


Figure 5.2.2 SNIFTIRS spectra of the *trans*-polymer.

Bands.	Cm^{-1}
C-H aromatic stretch thiophene	3169
C-H stretch thiophene	3107
C-H stretch aliphatic	2970
C-H stretch aliphatic	2883
C=C stretch	1727
C=C stretch thiophene	1412
C=C intra ring vibration thiophene	1375
C-S stretching	900

Table 5.0.4 Summary of bands in the polymerised **46**.

These bands would infer that the polymer is not polythiophene in nature, displaying none of the characteristic absorptions, which is also in agreement with the electrochemical data. Based on this evidence, the polymerised form of *trans*-1,2-di-(3-thienyl)-ethylene **46** is a polymer with no inherent characteristics similar to accepted thiophene based conducting polymers. Indeed the term conducting polymer could not be applied in the case of this. It would seem that 'chains' of **46** consisting of two (or more) monomer functionalities coupled together, are depositing themselves on the electrode surface (figure 5.2.3) in such a way that there is no continuous conducting polymer backbone, the electrochemical characteristics of the whole being observed.

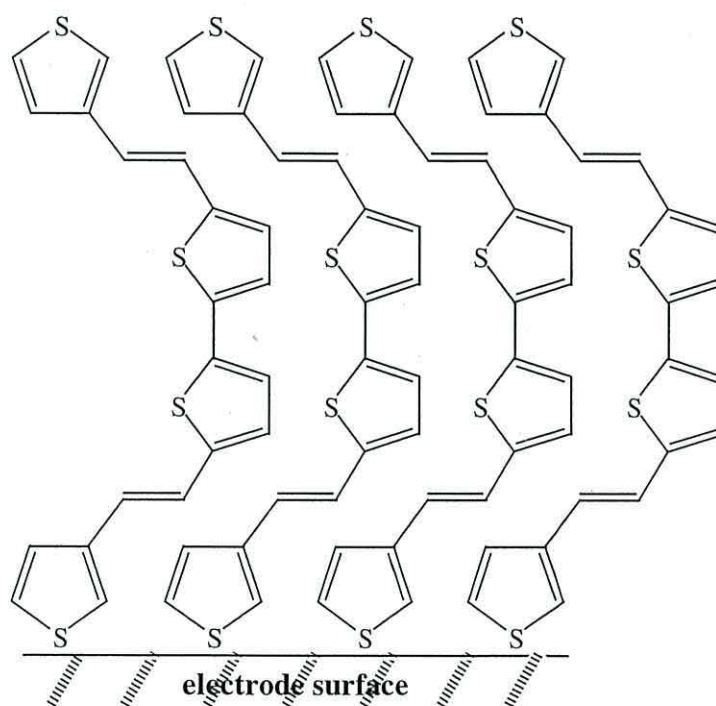


Figure 5.2.3 Proposed structure of the polymerised **46**.

5.5.5 SNIFTIRS investigation of I₂ doped Poly-*trans* 1,2-di-(3-thienyl)-ethylene.

In the doped state the difference spectra are quite different in comparison to the undoped state and can be seen in figure 5.2.4 and are summarised in table 5.0.5.

The first thing to notice is that the spectra are quite different when compared to each other. In the doped state the polymer resembles that of a polythiophene, whereas when undoped, this is not the case.

Several vibrations are apparent during the electrochemical cycle; 3164, 3006 and 2944 cm^{-1} representing characteristic polythiophene C-H stretching vibration, C-H thiophene stretching and C-H aliphatic stretching vibrations respectively. An absorbance at 1505 cm^{-1} is representative of a C=C antisymmetric stretching vibration, with the associated C=C symmetric stretching vibration at 1442 cm^{-1} . Further bands at 1373 and 1035 cm^{-1} are further characteristic absorptions of polythiophenes, the band at 1373 cm^{-1} for C=C symmetric intra ring vibrations and the band at 1035 cm^{-1} is the C-H in plane bend. [1,18] A further band at 1716 cm^{-1} is representative of the C=O stretching vibration in the ethene portion of the polymer.

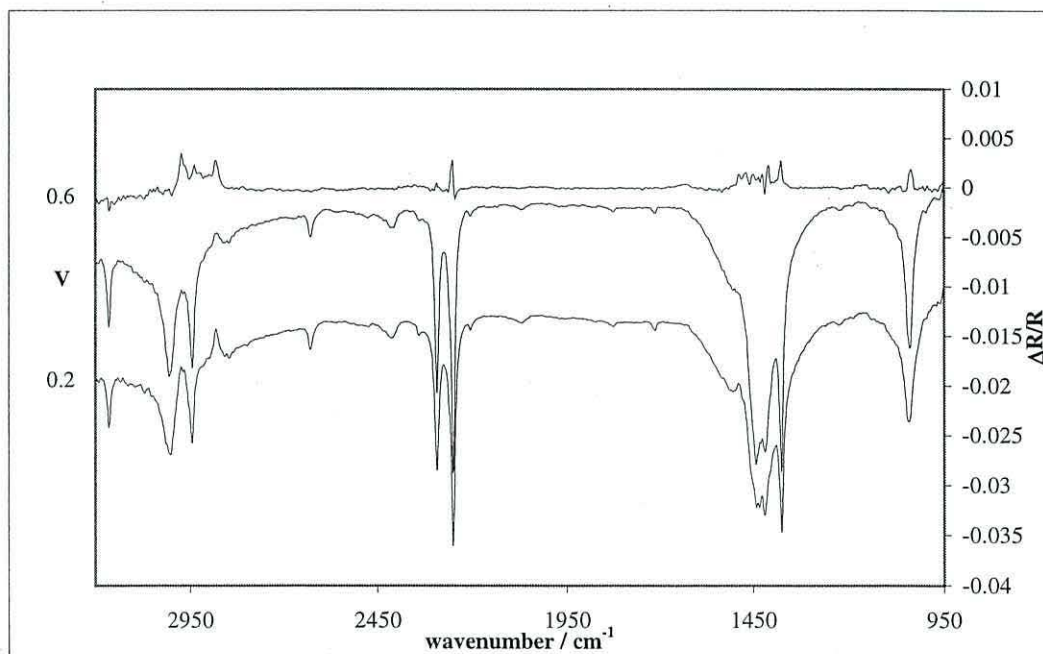


Figure 5.2.4 SNIFTIRS spectra of iodine doped *trans*-polymer.

This would infer that the doping process is causing a structural change in the polymer, resulting in the formation of a polythiophene. The doping is causing the

individual chains of the functionalised monomer units (figure 5.2.3) to form a polymer network by joining the thiophene moieties on the electrode surface, thereby resulting in the formation of a conducting polythiophene backbone (figure 5.2.5).

The proposed structure is in agreement with the electrochemical data, the doped voltammogram resembling polythiophene.

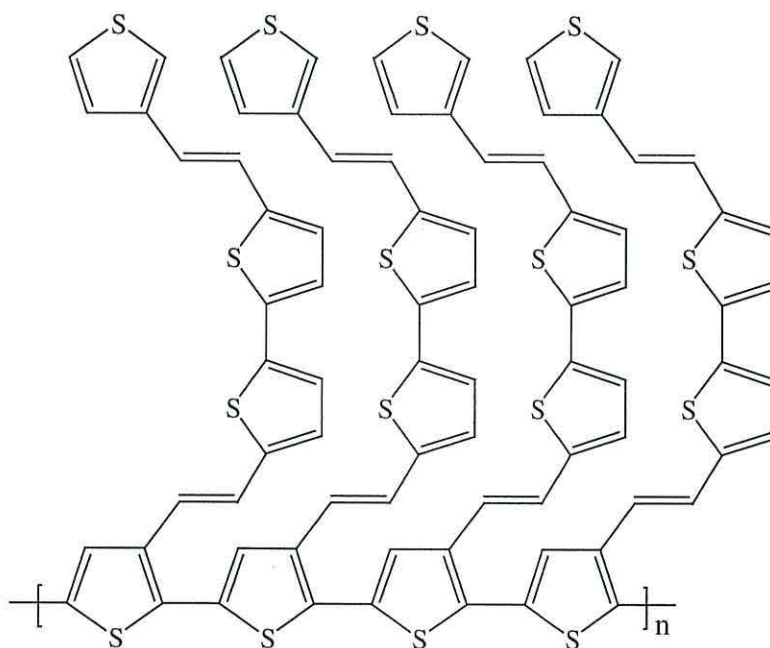


Figure 5.2.5 Proposed structure of the iodine doped polymerised **46**.

Bands.	Vibrations cm ⁻¹
C-H aromatic stretch polythiophene	3164
C-H stretch thiophene	3006
C-H stretch aliphatic	2944
C=C antisymmetric stretch polythiophene	1515
C=C symmetric stretch polythiophene	1442
C=C symmetric intra ring vibration (PT)	1373
C-H in plane bend ring polythiophene	1035
C=C stretch aliphatic	1716
C-S stretching vibration thiophene	910

Table 5.0.5. Summarised bands for the iodine doped *trans*-**46**.

5.5.6 Conclusions for the polymerised *trans* 1,2-di-(3-thienyl)-ethylene.

Trans-**46** polymerises to form the structure given in figure 5.2.3 consisting of chains of coupled monomer units attached to the electrode surface. In this state (undoped) it does not show any properties of a conducting polymer, nor that of a polythiophene. This is displayed in the SNIFTIRS spectra for the oxidation and reductive cycle, also in the voltammetry of the film obtained.

Doping the polymer causes a structural change or reorganisation, in that the thiophene moieties on the electrode surface couple to each other resulting in the formation of a conducting polythiophene backbone (figure 5.2.5). This is also noted in the changes observed in the electrochemical properties of the doped polymer, the voltammograms now resembling a polythiophene. The reason for this is unclear at present, though further studies are in progress to investigate this phenomenon.

5.6.0 Mode of polymerisation and charge-transfer for the polymerised compound 12 (unmodified) and modified polymerised compound 12.

By combining the information obtained from the investigation of compound 45, and comparing to the data found reported in chapters three and four, it is now possible to answer the questions about the mechanism of charge transfer and mode of polymerisation given at the end of chapter three.

5.6.1 Mode of polymerisation and charge-transfer for the unmodified polymer.

With the information obtained about the *cis*-polymer in hand, it is possible to relate this to the unmodified polymer (compound 12). The polymerised form of 12 shows bands present in that of the *cis*-polymer, and further bands relating to the 1,3-dithiolene unit (figure 5.2.6) and the carbonyl functionality.

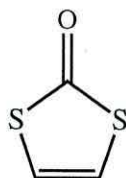


Figure 5.2.6 1,3-dithiolene unit.

The polymer structure is the same as that of the *cis*-polymer though with the 1,3-dithiolene unit forming part of the polymer backbone. Thus the polymerisation process requires the expected intramolecular cyclisation to occur to form the quinoidal structure described in chapter four, shown in figure 5.2.7.

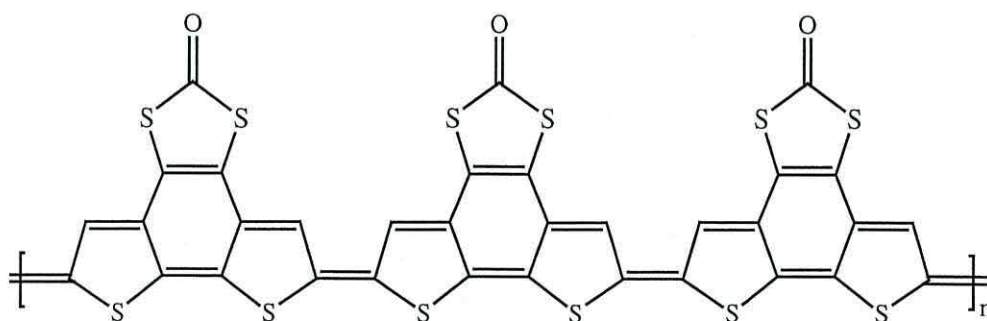


Figure 5.2.7 Structure of the unmodified polymer.

The voltammogram, though not resembling directly that of polyacetylene or *cis*-**45**, has a similar type of charge-transfer mechanism, observed in the similarities between the polymerised compound **12** and that of the polymerised compound **45**. This may also be explained by the effect that the 1,3-dithiolene unit has. It causes the oxidation potential of the 'polymer backbone' to increase due to its inherent electron withdrawing nature. Thus the mechanism of charge-transfer is the same as that in *cis*-**45**.

Further evidence that the 1,3-dithiolene unit imposes a large effect on the electrochemistry was found when attempts to chemically dope the modified polymer were made. It was noticed that doping did not occur effectively preventing any further oxidation.

5.6.2 Mode of polymerisation and charge-transfer for the modified polymer.

When modified, the polymer takes the form of a conducting backbone with a TTF derivative directly attached (figure 5.2.8). The polymer structure is the same as that found in the polymerised compound **12** and the polymerised *cis*-**45**.

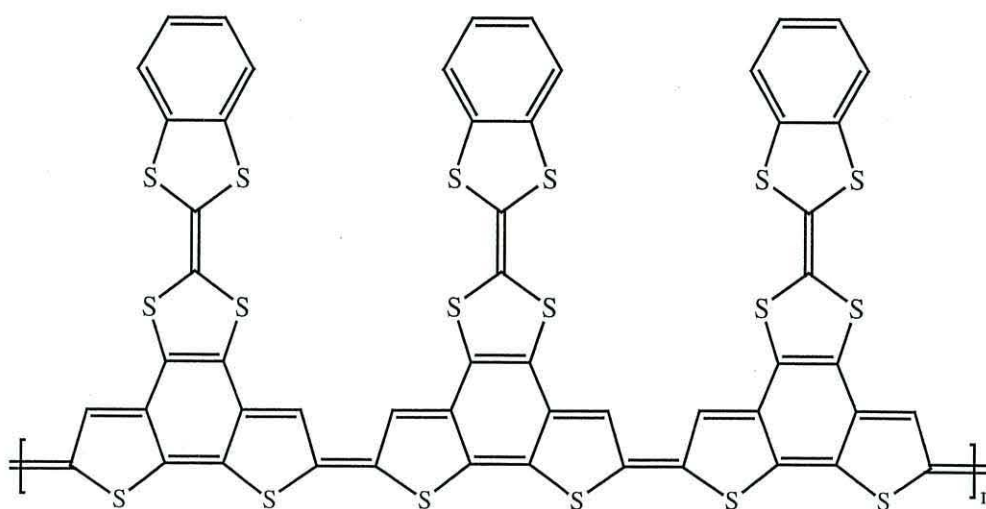


Figure 5.2.8 Structure of the modified polymer.

The mechanism of charge-transfer is the same as that found in **12** and *cis*-**45**, the electrochemistry confirming this type of mechanism in that the voltammogram is similar to that of polyacetylene.

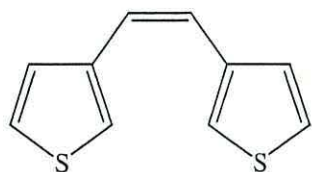
The change in voltammetry from unmodified to modified polymer is expected and is attributable to the TTF moiety. As mentioned in chapter three, when the TTF moieties are oxidised to the TTF^{2+} state, no further oxidation may take place due to the pseudo aromatic nucleus set up within the TTF group, making monomer oxidation occur prior to TTF oxidation.

5.7.0 Conclusions.

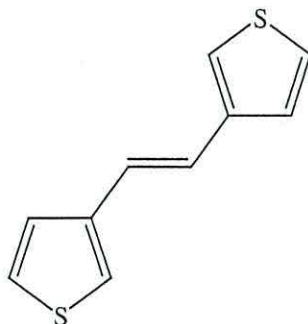
An investigation of the electrochemical and spectroelectrochemical properties of the polymerised compounds **45** and **46** has been performed. It was found that *trans*-1,2-di(3-thienyl)ethylene **46** forms a surface bound polymer consisting of chains of monomer units that upon doping undergoes a structural change resulting in the formation of a polythiophene. Though interesting, this was not the main reason the research was conducted.

The study of **45**, *cis*-1,2-di-(3-thienyl)-ethylene was of importance in that it would show the same mode of polymerisation and mechanism of charge-transfer the polymerised compound **12** undergoes.

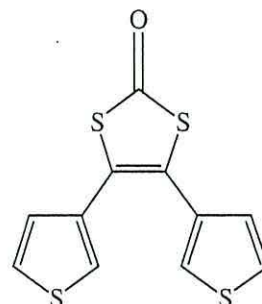
In section 3.7.0, chapter three, a number of points were raised regarding the polymerised form of compound **12**. These were to investigate the mode of polymerisation that **12** undergoes, and to deduce the mechanism of charge-transfer within the polymeric backbone. In the same way the answers obtained could then be used to confirm the modification of **12**. These points have been answered through the work carried out and presented in this chapter and the previous chapter. Briefly it has been shown that **12** polymerises through an intramolecular cyclisation forming a polymer that has a charge-transfer mechanism similar to that of polyacetylene.



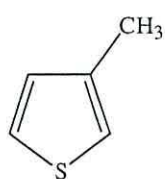
45



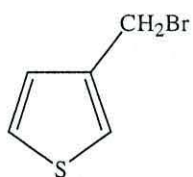
46



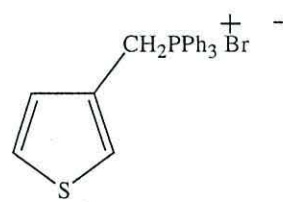
12



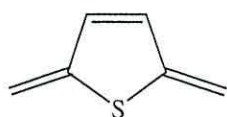
47



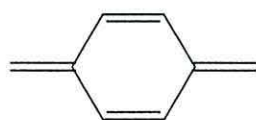
48



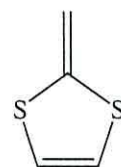
49



50



51



1,3-dithiolene

5.8.0 References.

- 1) T. A. Skotheim (Ed.), *Handbook of conducting polymers, Vol. I*, Marcel Dekker, New York, (1986).
- 2) R. John and G. Wallace; *Polymer international*, **27** (1992) 255.
- 3) J. Lamy, D. Lavit and Ng. Ph. Buu-Hoï; *J. Chem. Soc.*, (1958) 4202.
- 4) A. W. Cooke, K. B. Wagener, G. J. Palenik, A. H. M. Verschuuren, A. E. Koziol and Z.-Y. Zhang; *Polym. Prepr. (Am. Chem. Soc., Div. Polym. Chem.)*, **30** (1989) 330.
- 5) J. A. Bouwstra, A. Schouter and J. Kroon; *Acta. Cryst.*, **C40** (1984) 428.
- 6) H. Shirakawa, E. J. Louis, A. G. MacDiarmid, C. K. Chang and A. J. Heeger; *J. Chem. Soc. Chem. Commun.*, (1977) 578.
- 7) C. K. Chang, C. R. Fincher, Jr, Y. W. Park, A. J. Heeger, H. Shirakawa, E. J. Louis, S. C. Gau and A. G. MacDiarmid; *Phys. Rev. Lett.*, **39** (1977) 1098.
- 8) C. K. Chang, M. A. Druy, S. C. Gau, A. J. Heeger, E. J. Louis, A. G. MacDiarmid, Y. W. Park and H. Shirakawa; *J. Am. Chem. Soc.*, **100** (1978) 1013.
- 9) P. J. Nigrey, A. G. MacDiarmid and A. J. Heeger; *J. Chem. Soc. Chem. Commun.*, (1974) 594.
- 10) A. G. MacDiarmid and A. J. Heeger; *Synth. Met.*, **1** (1979) 101.
- 11) D. MacInnes, Jr, M. A. Druy, P. J. Nigrey, D. P. Nairns, A. G. MacDiarmid and A. J. Heeger; *J. Chem. Soc. Chem. Commun.*, (1981) 317.
- 12) A. G. MacDiarmid and M. Maxfield, R. G. Linford (Ed.), *Electrochemical science and technology of polymers*, Elsevier, London, New York, (1987).
- 13) T. C. Clarke and G. B. Street; *Synth. Met.*, **1** (1980) 119.
- 14) A. F. Diaz and T. C. Clarke; *J. Electroanal. Chem.*, **111** (1980) 115.
- 15) J. F. Raboult, T. C. Clarke and G. B. Street; *J. Chem. Phys.*, **71** (1979) 4614.
- 16) K. Kesper, N. Münzel, A. Schweig and H. Specht; *Tet. Lett.*, **29** (1988) 6239.
- 17) Y. Yamakita and M. Tasumi; *J. Phys. Chem.*, **99** (1995) 8531.
- 18) H. S. Nalwa (Ed.), *Handbook of organic conductive molecules and polymers: Vol. 3. Conductive polymers: Spectroscopy and physical properties*, J. Wiley & Sons Ltd. UK, (1997).

Chapter Six: An investigation of the photochemistry of *bis*-4, 5-(3-thienyl)-1,3-dithiole-2-one.

6.1.0 Aims.

The aim of the work described in this chapter was the photochemical preparation of the compound **13** (figure 6.0.1) in which the thienyl rings are fused at the 2/ 2' positions. The thrust behind this is detailed in chapter seven, in which the preparation of TTF compounds based on **13** would provide access to direct electropolymerisation. This would occur by having the effect of reducing oxidation potentials and providing an alternate 'pathway' for polymerisation to occur. Hence the need for the energetically unfavourable conjugation throughout the pseudo aromatic nucleus that is set up when the dicationic TTF state is achieved has been removed.

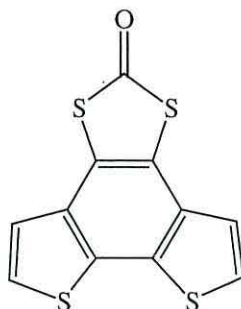
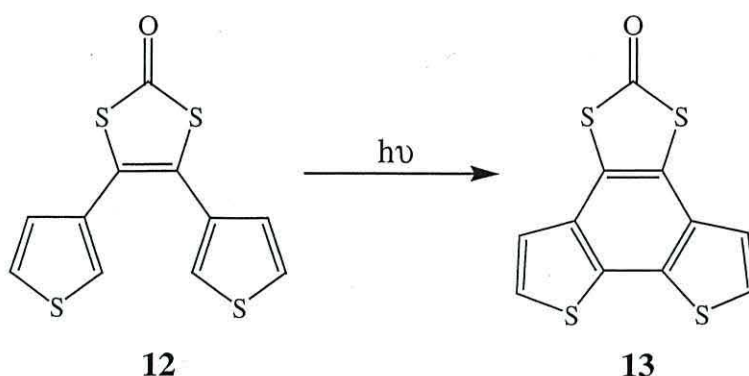


Figure 6.0.1 Compound **13**.

The compound **13** was to be prepared *via* a photochemical cyclisation reaction (scheme 6.0.1). There are many reports of reactions of this type in the literature, [1-9] especially for reactions involving compounds similar to **12** that contain the 1,2-diarylethene unit.



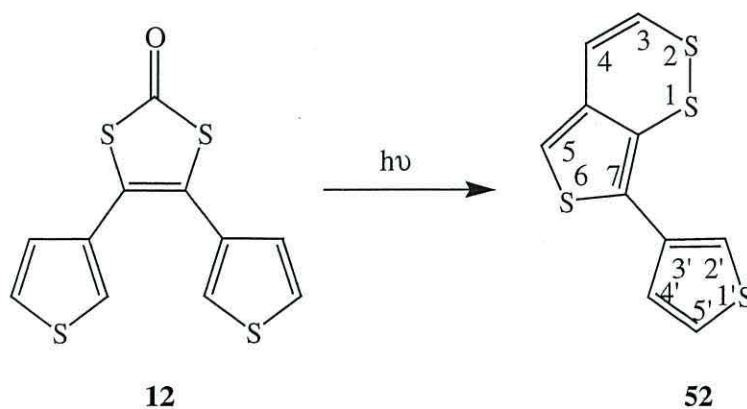
Scheme 6.0.1 The photochemical preparation of **13**.

6.2.0 An investigation of the photochemical properties of bis-4, 5-(3thienyl)-1,3-dithiole-2-one **12**.

Bis-4, 5-(3thienyl)-1,3-dithiole-2-one **12**, discussed in detail in previous chapters is a key precursor in the preparation of TTF compounds, [10, 14] and their respective polymers. The preparation of **13** was to be achieved by irradiating a sample of **12** in benzene with I_2 as initiator. Although **12** underwent a photochemical transformation, the product was not the expected compound **13**. No intramolecular cyclisation was observed to occur.

Following from a report in the literature by Ponticelli *et al.* [15] describing the use of photochemistry in intramolecular cyclisations for compounds similar to that of the compound **12**, we asked if they would perform a more accurate investigation of the photochemical properties of compound **12**.

The cyclisation of **12** was again attempted on a larger scale and at more precise frequencies. When irradiated at $\lambda > 330$ nm [10] it was found that a transformation did indeed take place. However as in this case the desired compound **13** was not achieved. The product obtained was thieno[3,4-c]dithiine **52** (Scheme 6.0.2).



Scheme 6.0.2 Thieno[3,4-c] dithiine **52**.

The structure of **52** was assigned on the basis of spectral evidence. [16] The mass spectrum gave a M^+ ion at $m/z = 254$ indicating a molecular formula of $C_{10}H_6S_4$. This suggested the loss of CO during the photoreaction. A further ion at $m/z = 190$ suggested the possibility of the loss of S_2 (M-64). This was confirmed by neutral loss mass spectrometry, indicating the presence of a -S-S- moiety in the molecule. Analysis of the 1H and ^{13}C NMR spectra (including 600 MHz heterocorrelated 2D experiments) were in agreement with the structure of **52** (table 6.0.1) and it was interesting to note that a nOe effect was observed between the protons at 6.92 and 7.09 ppm (figure 6.0.2).

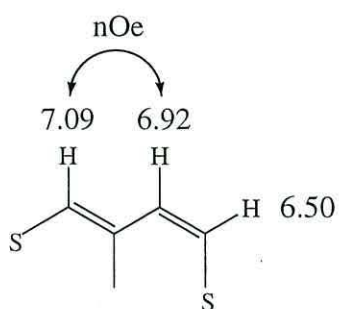


Figure 6.0.2 Arrangement of protons for the nOe effect.

	Position in structure					
	C-3	C-4	C-5	C-2'	C-4'	C-5'
¹ H NMR signal (δ , ppm, J = /Hz)	6.5 (9.5, 0.4)	6.9 (9.5, 0.5)	7.1 (0.5, 0.4)	7.39 (1.8)	7.51 (2.5)	7.41 (2.5, 1.8)
¹³ C NMR signal (δ , ppm)	121.6	127.3	121.8	126.2	127.4	123.5

Table 6.0.1 ¹H and selected ¹³C NMR signals for the compound **52**.

To provide further evidence of the structure, **52** was treated with sodium borohydride. This led to a facile reductive cleavage of the S-S bond, resulting in an intermediate thiol-thioaldehyde **53** that directly cyclised to give the hemi-thioacetal derivative **54** (figure 6.0.3). Its structure was confirmed by X-ray crystallographic analysis (figure 6.0.4).

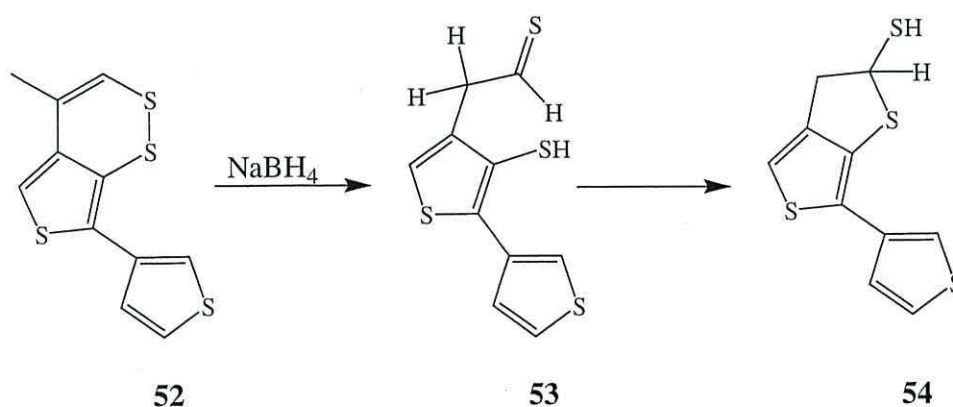


Figure 6.0.3 Reaction of **52** to produce **53** *via* the intermediate **54**.

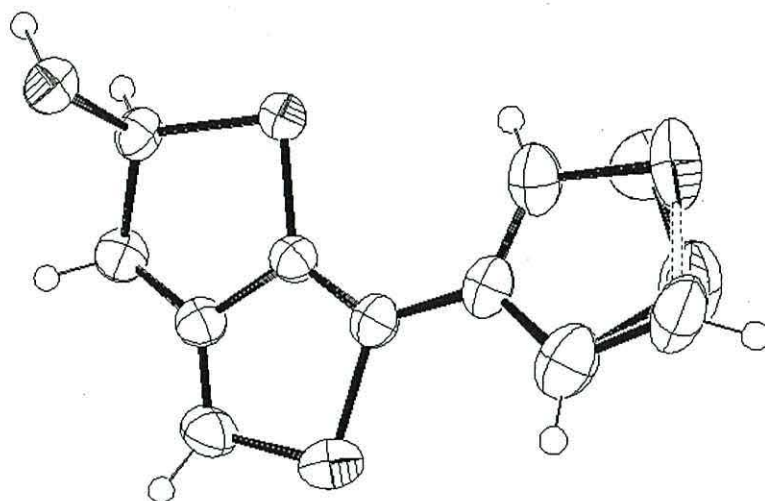
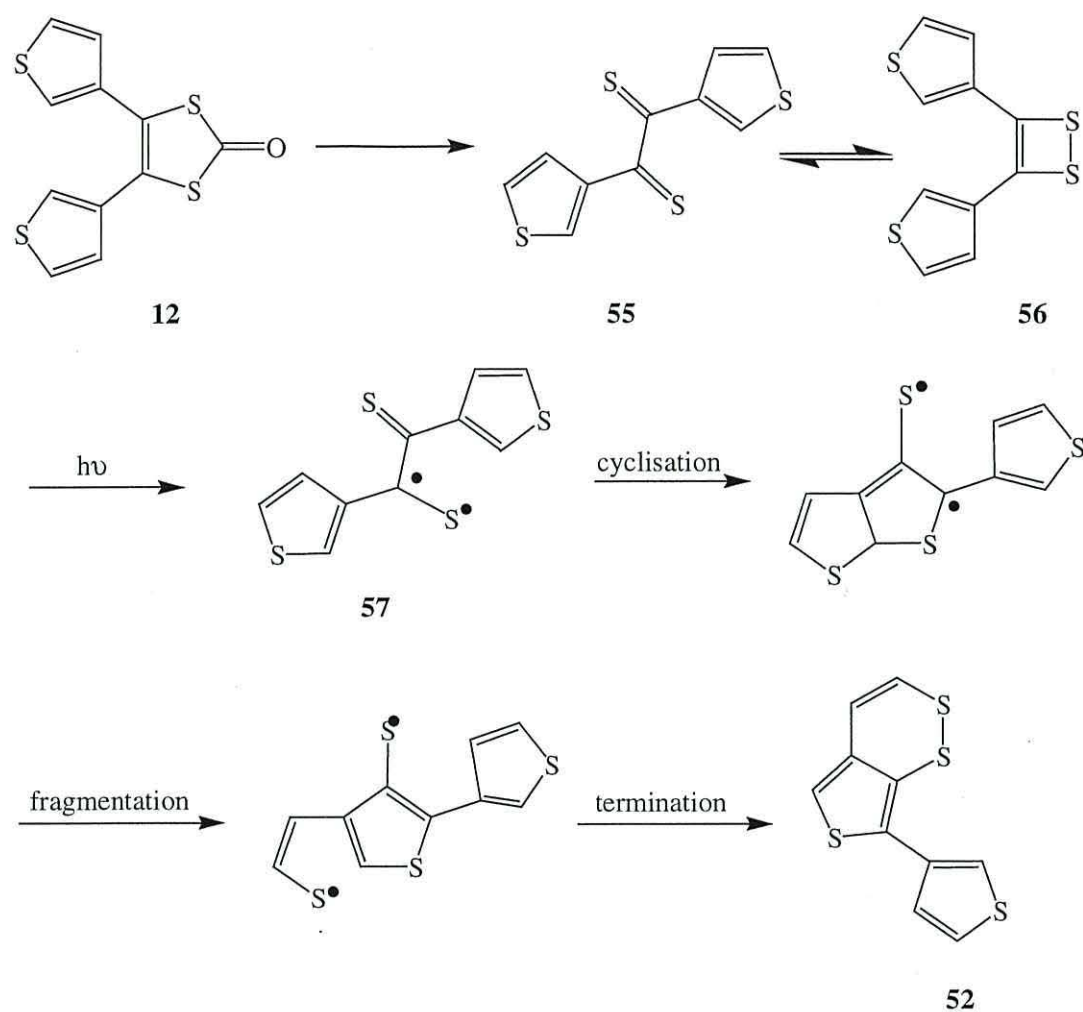


Figure 6.0.4 Ortep drawing of hemi-thioacetal **54** showing the two conformations of the thiophen-3-yl moiety.

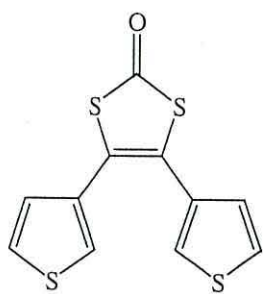
Previous reports on the photoreactivity of diarylvinylene dithiocarbonates [17,18] have reported that the loss of carbon monoxide (observed in the photochemical reaction of **12**) is highly facile. For the case of **12** it would produce the highly reactive dithione **55** and/ or the 1,2-dithiete **56**. The mechanism of the reaction can be visualised as involving the intermediate di-radical **57**, which undergoes cyclisation, ring fragmentation and finally cyclisation to give **52** (scheme 6.0.3).



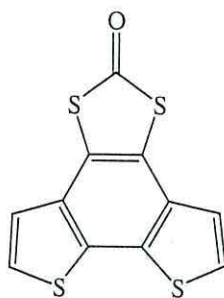
Scheme 6.0.3 Mechanism of formation of compound **52**.

6.4.0 Conclusions.

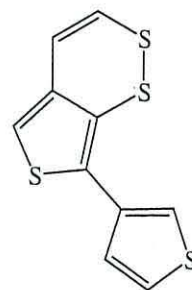
An investigation into the possibility of producing compound **13** *via* a photochemical intramolecular cyclisation has been carried out. Though unsuccessful in the endeavours to effect the transformation of **12** to **13**, a way has been found to produce thieno[3,4-c]dithiine **52**, the first examples of such a type of heterocyclic system.



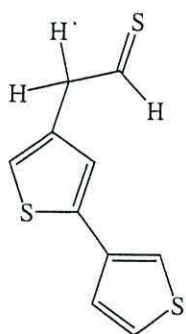
12



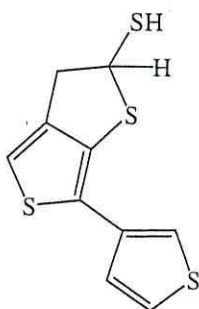
13



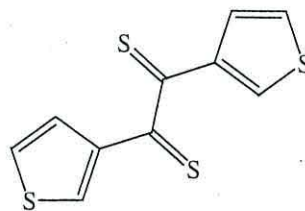
52



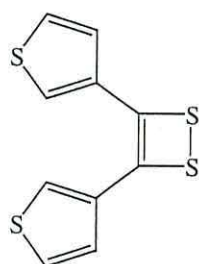
53



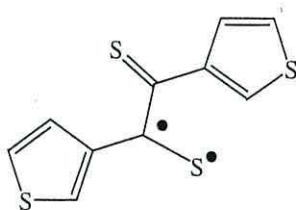
54



55



56



57

6.5.0 References.

- 1) N. L. Lucas, J. V. Esch, M. R. Kellog and B. L. Feringa; *J. Chem. Soc. Chem Commun.*, (1998) 2313.
- 2) M. Irie and M. Mohri; *J. Org. Chem.*, (1998) 8305.
- 3) M. Irie, K. Sakemura, M. Okinaka and K. Uchida; *J. Org. Chem.*, **60** (1995) 8305.
- 4) K. Uchida, Y. Nakayama and M. Irie; *Bull. Chem. Soc. Jpn.*, **63** (1990) 1311.
- 5) L. Dinescu and Z. Y. Wang; *J. Chem. Soc. Chem Commun.*, (1999) 2497.
- 6) C. Denekamp and B. L. Ferringa; *Adv. Mater.*, **10** (1998) 1082.
- 7) J. Ferraris, D. O. Cowan, V. Walatka and J. H. Perlstein; *J. Am. Chem. Soc.*, **95** (1973) 948.
- 8) M. B. Neilstein, N. Thorup and J. Becher; *J. Chem. Soc. Perkin Trans. 1.*, (1998) 1305.
- 9) Y. Nakayama, K. Hayashi and M. Irie; *Bull. Chem. Soc. Jpn.*, **64** (1991) 789.
- 10) S. J. Roberts-Bleming, A. Charlton, M. Kalaji, P. J. Murphy and N. Robertson; *Dalton Trans.* in press.
- 11) S. J. Roberts-Bleming, S. J. Coles, T. Gedbrich, M. B. Hursthouse, M. Kalaji and P. J. Murphy; *J. Mat. Chem.* in press.
- 12) A. Charlton, A. E. Underhill, M. Kalaji, P. J. Murphy, D. E. Hibbs, M. B. Hursthouse and K. M. Malik; *J. Chem. Soc. Chem. Commun.*, (1996) 2423.
- 13) A. Charlton, A. E. Underhill, G. Williams, M. Kalaji, P. J. Murphy, K. M. Abdul Malik and M. B. Hursthouse; *J. Org. Chem.*, **62** (1997) 3098.
- 14) A. Charlton, S. Salmaso, G. O. Williams, M. Kalaji, A. E. Underhill, P. J. Murphy, K. M. A. Malik and M. B. Hursthouse; *Synthetic Metals.*, **92** (1998) 75.
- 15) P. Brooks, D. Donati, A. Pelter and F. Ponticelli; *Synthesis.*, (1999) 1303.
- 16) A. M. Celli, D. Donati, F. Ponticelli, S. J. Roberts-Bleming, M. Kalaji and P. J. Murphy; *Chem. Lett.*, in press, 2001.
- 17) W. Kusters and P. de Mayo; *J. Am. Chem. Soc.*, **96** (1994) 3502.
- 18) K. Hartke, T. Kissel, J. Quante and R. Matusch; *Chem. Ber.*, **113** (1980) 1898.

Chapter Seven: Attempted intramolecular cyclisation of *bis*-4, 5-(3-thienyl)-1,3-dithiole-2-one 12.

7.1.0 Aims.

The aim of the work comprised in this chapter was to synthesise compound **13** (figure 7.0.1) from *bis*-4, 5-(3-thienyl)-1,3-dithiole-2-one **12**. This compound contains one of the proposed bonds (2-4') found in polymerised **12**, providing access for the direct electropolymerisation of the analogous TTF derivatives without having to undergo *in situ* chemical modifications, shedding light on the polymerisation mechanism.

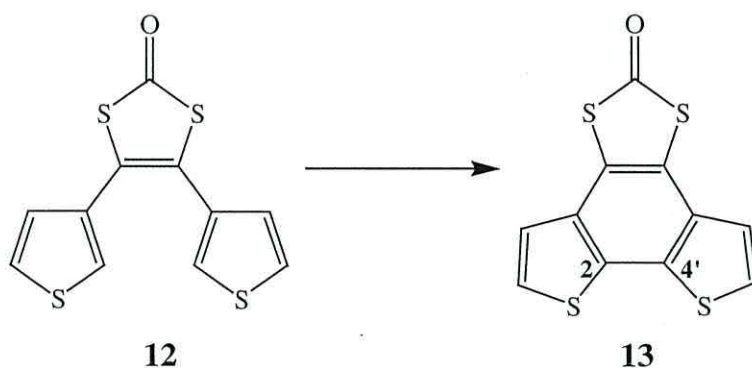


Figure 7.0.1 Preparation of the compound **13** from *bis*-4, 5-(3-thienyl)-1,3-dithiole-2-one **12**.

7.2.0 Introduction.

As mentioned in chapter six, attempts to prepare this compound via photochemical methodologies were unsuccessful – the compound undergoing a transformation to the thieno[3,4-*c*]dithiine **52** (figure 7.0.2). It was thought then that a synthetic approach may provide more success.

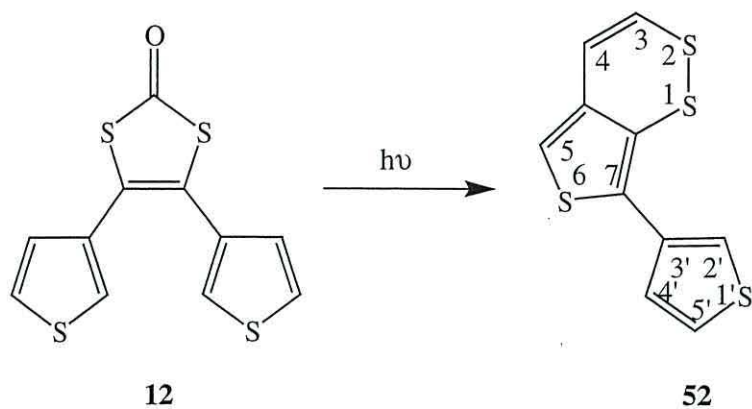


Figure 7.0.2 Photochemical transformation of **12** to thieno[3,4-c]dithiine **52**.

It was proposed that this might be achieved using one of two synthetic methodologies;

- i) An ullman type ring closure
- ii) A palladium catalysed coupling reaction.

In both instances, it was felt that a good starting material would be 4,5-*bis*-(2-bromo-thiophen-3-yl)-[1,3]dithiole-2-one **58**, figure (7.0.3).

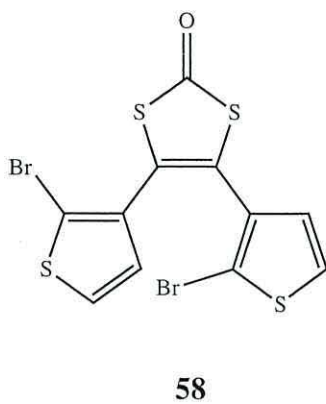
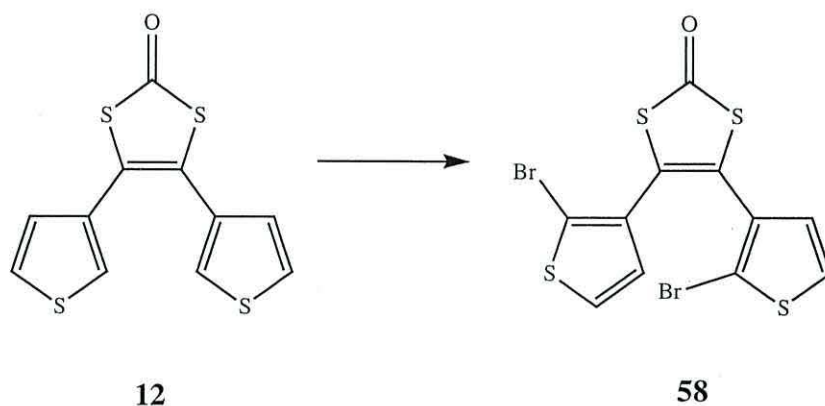


Figure 7.0.3 4,5-*Bis*-(2-bromo-thiophen-3-yl)-[1,3]dithiole-2-one **58**.

7.3.0 Synthetic strategy.

7.3.1 Synthesis of compound 58.

Compound **58** was prepared from the *bis*-4, 5-(3-thienyl)-1,3-dithiole-2-one **12**, (schemes 7.0.1) by two methodologies; bromination using *N*-bromosuccinamide (NBS) or by direct bromination with Br₂.



Scheme 7.0.1 Preparation of **58**.

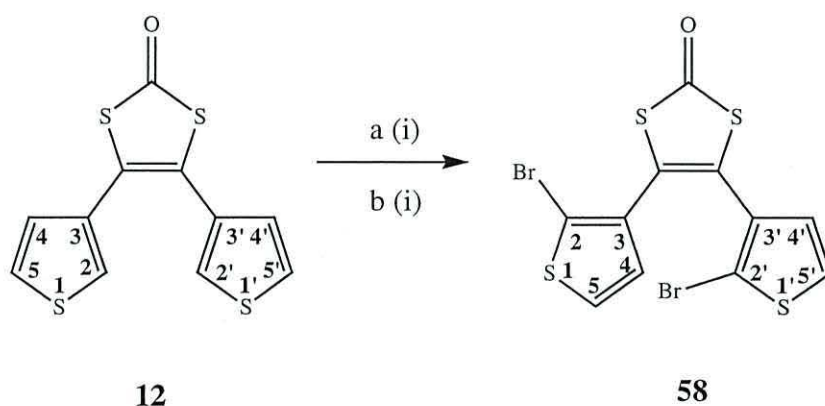
7.3.2 Bromination using *N*-Bromosuccinamide.

The bromination of **12** using NBS was achieved by refluxing in CCl₄ in the dark. The amide residues are then filtered, leaving **58** in crude form that is purified by column chromatography resulting in pure **58** in 90% yield (scheme 7.0.2).

7.3.3 Direct bromination using Br₂.

In this instance **12** was brominated by the drop-wise addition of a solution of Br₂ in CCl₄ to a solution of **12** dissolved in CCl₄ at 0°C for 12 hours (scheme 7.0.2). The pure product **58** that obtained by column chromatography, resulting in **58** in 45% yield.

Confirmation of the success of the reaction was provided using NMR spectrometry. The loss of the two Ar-H protons in the 2/2' positions from the starting material **12**, was confirmed by ^1H NMR analysis. In the starting material, compound **12**, there is a multiplet resonance at δ 7.2 ppm, indicative of four Ar-H protons, when brominated the resonance is now observed as a doublet at δ 7.2 ppm ($J = 5.6$ Hz) confirming the loss of 2 protons at the 2/2' positions. In both the unbrominated and brominated compound, a further doublet resonance is observed at δ 6.7 ppm ($J = 5.6$ Hz), indicative of the protons in the 4/4' positions.



Reagents and Conditions: a (i) NBS, CCl_4 , dark, reflux, 48 h; b (i) Br_2 , CCl_4 , dark, 0°C , 12 h.

Scheme 7.0.2 Reaction conditions for the bromination of **12**.

7.4.0 Attempted intramolecular cyclisation reactions.

With **58** in hand, attempts to perform the ring closure reactions were made. As previously mentioned (section 7.1.0) there were two strategies for this; Ullman ring closure and palladium catalysed coupling.

7.4.1 The Ullman ring Closure reaction.

The Ullman reaction (ring closure) is a “classic” reaction [1] in which aryl halides are coupled to form biaryl compounds by heating with copper. The copper acts to form an aryl radical that reacts with Cu^+ to form an aryl copper(I) species. This further reacts with another aryl halide giving the desired coupling product (figure 7.0.4).

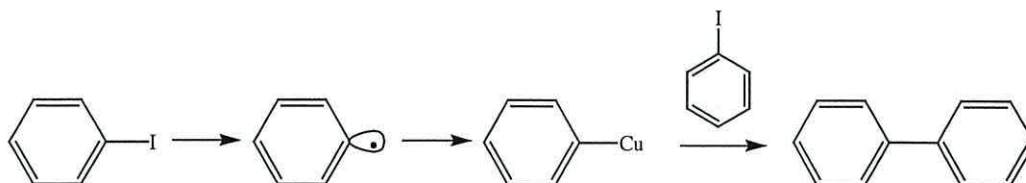
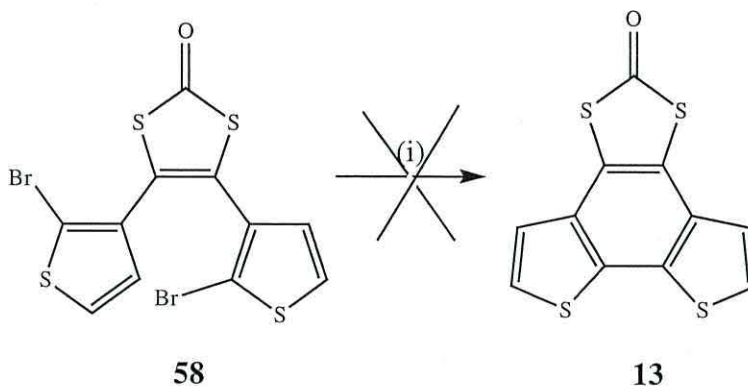


Figure 7.0.4 An example of the Ullman reaction.

In the case of compound **58**, activated copper was added to a solution of **58** in DMF and the mixture was refluxed in the absence of light for 24 hours (scheme 7.0.3). Analysis of the crude product gave no indication of a successful reaction and when purified by column chromatography, it was noted that only the unbrominated compound **12**, *bis*-4, 5-(3-thienyl)-1,3-dithiole-2-one was obtained.



Reagents and Conditions: (i) Cu, DMF, dark, reflux, 24 h.

Scheme 7.0.3 Preparation of compound **13** *via* Ullman ring closure.

The reaction conditions were varied in reflux time only, refluxing for 5, 12 and 48 hours. In each case no meaningful reaction was observed to occur, although

bis-4, 5-(3-thienyl)-1,3-dithiole-2-one **12** was reclaimed in all cases. The lack of reactivity would infer that either, the radical intermediate formed in the first step in the reaction is not strong enough to react with the thiophene-halide, merely terminating itself with protons from the reaction solvent, or, that there is a conformational problem within the thiophene moieties preventing hindering the reaction.

7.4.2 The palladium catalysed coupling reaction.

The Palladium catalysed coupling reaction takes many forms, though for aryl halides the most efficient is that when catalysed with Palladium(0) and tin reagents. [2] Following reports in the literature by Irie and co-workers [3-5], it was thought that such reactions may be suitable for a system such as ours (figure 7.0.5).

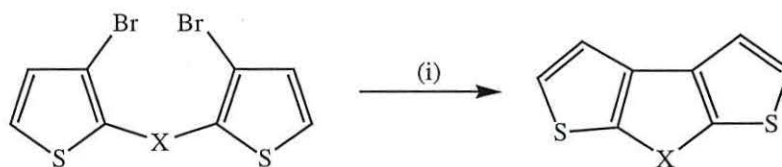
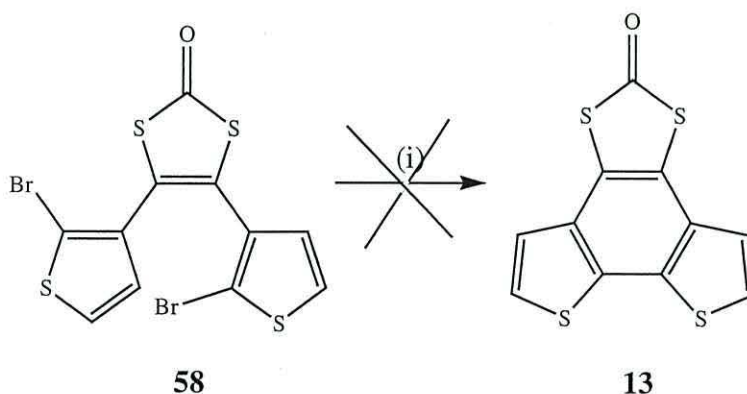


Figure 7.0.5 An example of a Palladium catalysed coupling reaction.

Thus the brominated compound **58** was refluxed in dry dioxane with $\text{Pd}(\text{PPh}_3)_4$, $\text{Me}_3\text{SnSnMe}_3$ and PPh_3 for 12 hours (scheme 7.0.4). After purification by column chromatography, it was found that as in the case of 7.4.1, the reaction was unsuccessful, resulting in the debromination of **58**, forming *bis*-4, 5-(3-thienyl)-1,3-dithiole-2-one **12**. The reason for the lack of success of this reaction is unclear, though again there may be a conformational problem with the thiophene moieties, hindering the reaction.

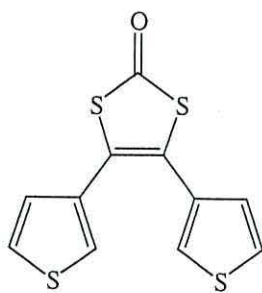


Reagents and Conditions: (i) $\text{Pd}(\text{PPh}_3)_4$, $\text{Me}_3\text{SnSnMe}_3$, PPh_3 , dioxane, reflux, 12 h.

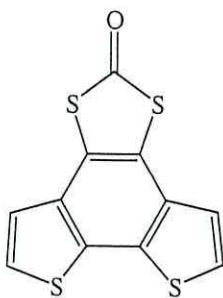
Scheme 7.0.4 Preparation of compound **13** via Ullman ring closure.

7.5.0 Conclusions.

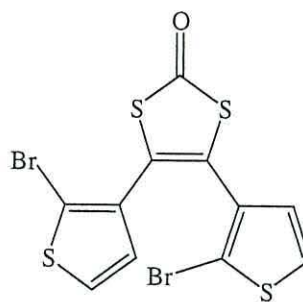
In conclusion, attempts were made to synthesis the compound **13** 4,5-*Bis*-(2-bromo-thiophen-3-yl)-[1,3]dithiole-2-one, using Ullman chemistry and Palladium catalysed coupling reactions. In both cases they were found to unsuccessful in the lack of formation of compound **13**, resulting instead in the debromination of the starting material **58** forming *bis*-4, 5-(3-thienyl)-1,3-dithiole-2-one **12**.



12



13



58

7.6.0 References.

- 1) P. E. Fanta, *Chem. Rev.*, **64** (1964) 613.
- 2) M. Kosugi, Y. Shimizu and T. Migita; *Chem. Lett.*, (1977) 1423.
- 3) K. Uchida, Y. Nakayama and M. Irie; *Bull. Chem. Soc. Jpn.*, **63** (1990) 1311.
- 4) M. Irie and K. Uchida; *Bull. Chem. Soc. Jpn.*, **71** (1998) 985.
- 5) L. Dinescu and Z. Y. Wang; *J. Chem. Soc. Chem. Commun.*, (1999) 2497.

Chapter Eight: Conclusions and further work.

In this study the suitability of the use of *bis*-4, 5-(3-thienyl)-1,3-dithiole-2-one **12** as a precursor for intramolecular cyclisation was examined. It was found not to undergo a synthetic or photochemical transformation to the desired compound **13**, forming the thieno[3,4-c]dithiine **52**, when photo irradiated.

An investigation of the polymer structure of **12** was carried out using cyclic voltammetry and SNIFTIRS investigations, showing that a polyacetylenic structure is obtained, the characteristic of which are only displayed when chemically modified, the 1,3-dithiole unit imposing to a great extent, much character on the unmodified polymer.

The mode of polymerisation for this polymer was obtained by the electrochemical studies of the compounds **12**, **22**, **23** in which methyl groups were used as polymerisation site blocks. The results for which indicated that for polymerisation to occur, intra molecular cyclisations within the respective repeat units must occur.

The mechanism of charge transfer in the polymerised form of **12** was studied, showing that the charge-transfer mechanism is similar to that of polyacetylene. To prove this, the compounds **45** and **46** were prepared and their electrochemical and spectroelectrochemical studies were carried out. It was found that the polymerised form of *cis*- **45** undergoes electropolymerisation to produce a polyacetylene-based polymer, which upon chemical doping shows enhanced polyacetylinic characteristics. *Trans*- **46** when electropolymerised, does not show polythiophene or polyacetylinic character but when doped chemically, shows the characteristics of a polythiophene derivative.

The *in situ* chemical modifications of the polymerised compound **12** showed that it is possible to obtain polymers in which the TTF moiety is directly bonded to the polymer back bone. This was confirmed by electrochemical and spectroelectrochemical methodologies. A full modification is observed to occur.

Thus allowing access to polymers once thought unobtainable *via* direct methodologies, and should be subjected to further development in the future.

There is obviously considerable scope for the continuation of this research.

Further research in the use of *in situ* modifications would be of interest, investigating the possibility of attaching alkyl or unsubstituted moieties providing access to other TTF derivatives. For example attaching an unsubstituted 1,3-dithiolene unit or functionalising compound **12** to form the phosphorane allowing the formation of the originally required polymerised thiophene- TTFs (figure 8.0.1).

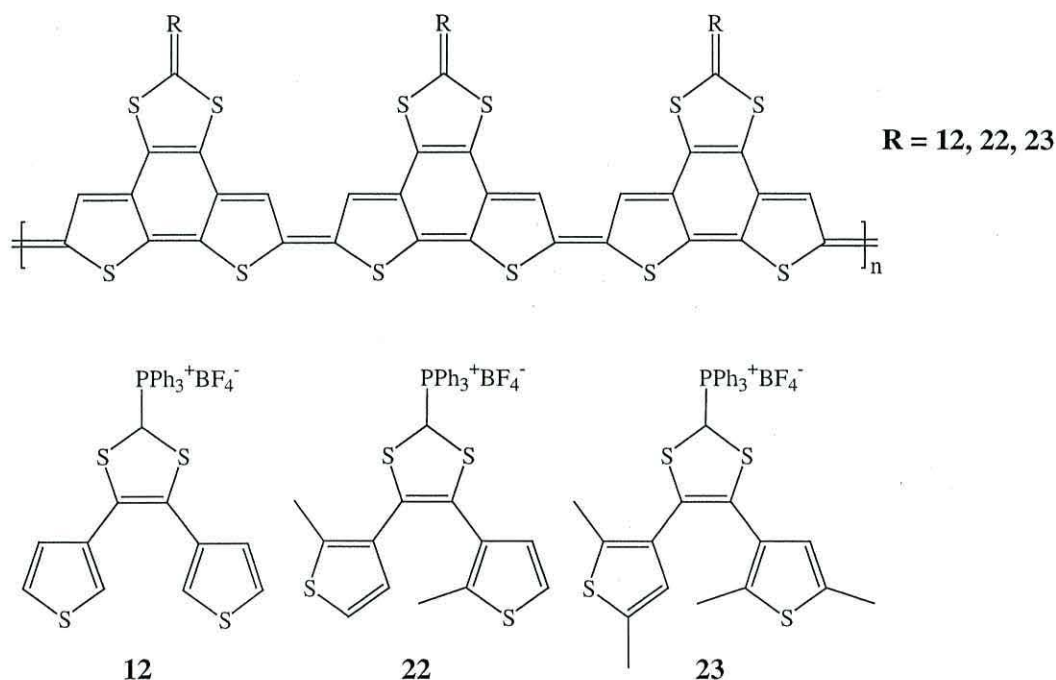


Figure 8.0.1.

The incorporation of metals into the modified polymer, for example Nickel, to make the DMIT compounds would be an interesting possibility, providing access to a second axis of conduction in the polymeric matrix (figure 8.0.2).

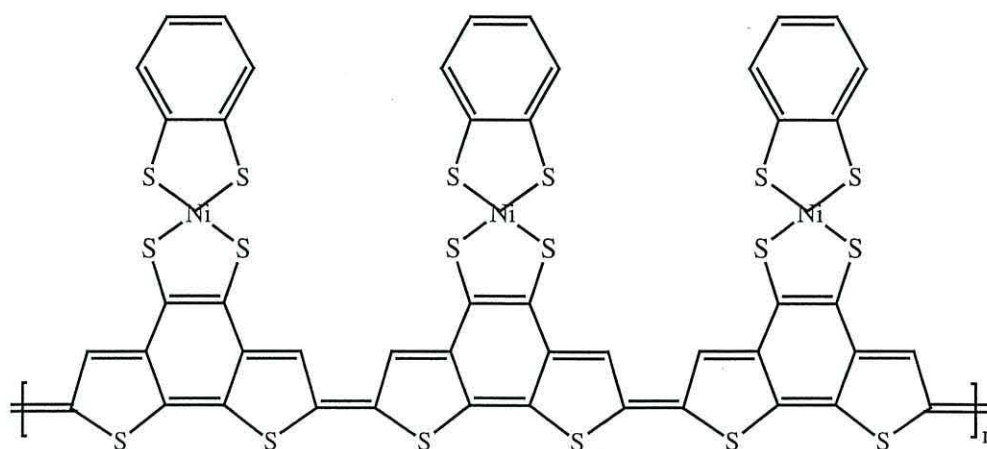


Figure 8.0.2.

It would also be interesting to compare the electrochemistry of the cyclised compound **36**, as it would be expected that the polymer structure would be the same as that of the polymerised compound **5**. Providing further evidence for the determination of the mode of polymerisation and charge-transfer properties of the compound **5**. The synthesis of this compound however will have to be approached from a different perspective to that previously given in chapter four, in that the lower 'half' of the molecule i.e. the cyclised ring structure (figure 8.0.3) would initially be prepared and functionalised to form the 1,3-dithiolene unit. Similar types of reaction are available in the literature, making this a definite possibility.

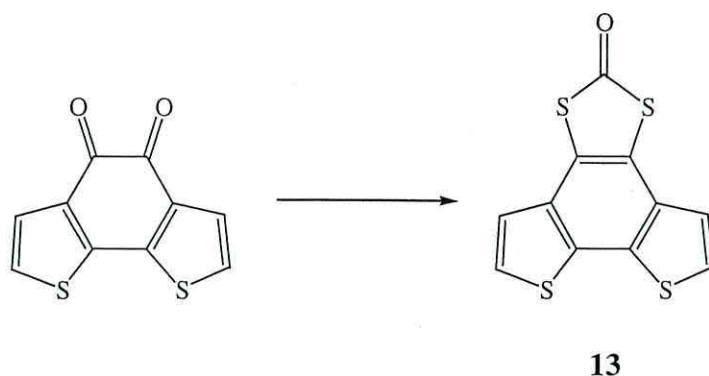


Figure 8.0.3.

If this is true, and succeeds, the original aims of this project could then be exploited by preparing the desired polymers (TTF and DMIT) by direct electropolymerisation and *in situ* chemical modification.

It would also be interesting to investigate more photochemical transformations of units based on that of the compound **5**. For example, that of a mixed compound in which the thiophene moieties are attached in the 2-thienyl and 3-thienyl positions respectively (figure 8.0.4) **59**. This may have an effect on the type of reaction occurring.

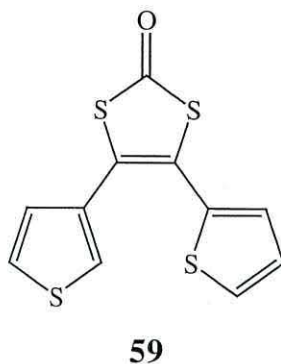


Figure 8.0.4 4-(2-thienyl), 5-(3-thienyl)-1,3-dithiole-2-one **59**.

Chapter Nine: Experimental.

9.1.0 General experimental for the synthesis procedures.

9.1.1 Chemicals and Solvents.

Chemicals were obtained from the Aldrich chemicals company Ltd, Lancaster or Avocado and were used without further purification. Solvents were dried using the standard conditions detailed in the literature. [1]

9.1.2 Chromatography.

Thin layer chromatography (TLC) was performed on glass plates coated with Kieselgel 60 F254 (Art. 5554, Merck). Compounds were seen using ultraviolet light and/or staining with phosphomolybdic acid (PMA) in ethanol, and 2,4 DNPH in ethanol. The column chromatography was performed using Merck 7736 silica gel (size 40-63 μ m) with the eluting solvent specified in each case.

9.1.3 Spectroscopy.

Proton NMR spectra were recorded in CDCl_3 unless stated otherwise, and run on a Bruker AC250 spectrometer at 250MHz unless otherwise stated. Carbon-13 NMR were recorded in CDCl_3 unless otherwise stated, and run on a Bruker AC250 spectrometer at 62.5MHz unless otherwise stated and are all decoupled. J values are given in Hz, chemical shifts are reported as δ values (ppm) in relation to tetramethylsilane as internal standard. Infra-red spectra were recorded as thin films on a Perkin-Elmer 1600 FT-IR spectrometer with absorption frequencies reported in wavenumbers ν , and recorded at a resolution of 4 cm^{-1} . Elemental analyses were obtained using a Carlo-Erba model 1106 CHN analyser. Electron impact (EI) and chemical ionisation (CI) were recorded on a VG Masslab Model 12/253

spectrometer and on a VG Analytical ZAB-E spectrometer at the EPSRC Mass Spectrometry Service Centre at Swansea. Mass measurements are reported in daltons.

9.2.0 General experimental for the electrochemical procedures.

Electropolymerisation and voltammetric studies were carried out in a three electrode cell shown in figure 9.0.1. The working electrode was a polished platinum disc. A silver wire was used as a pseudo reference electrode and the counter electrode consisted of a platinum mesh. All solvents were distilled under nitrogen and stored over activated molecular sieves to remove traces of water. Prior to use all electrolyte solutions were degassed with argon for ten minutes.

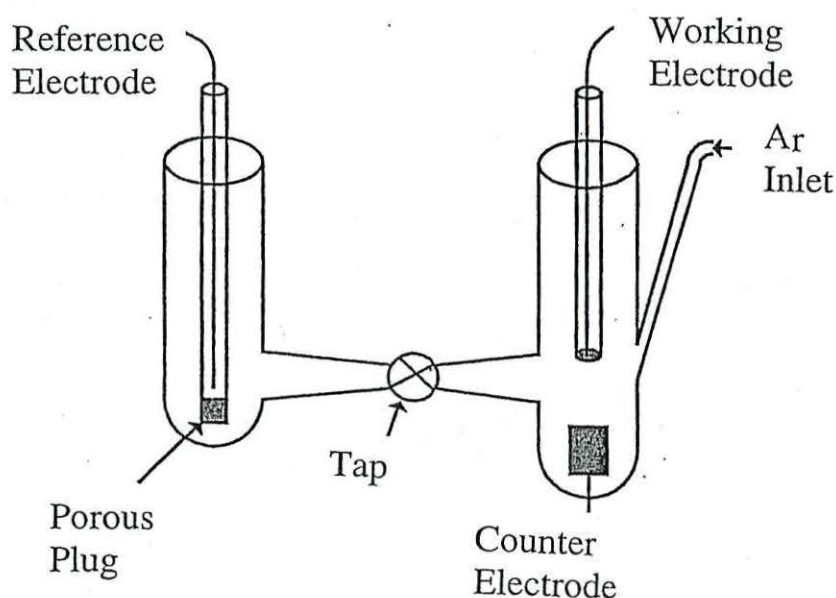


Figure 9.0.1 Electrochemical cell.

For galvanostatic deposition the same cell set-up was used, though the desired current was applied between the working and secondary electrode only. After deposition the films were rinsed with a monomer free solution of TBATFB in acetonitrile, then characterised by voltammetry in a fresh monomer-free solution (0.1 M TBATFB in acetonitrile). All measurements were carried out using a

potentiostat (HI-TEK DT2101) and a waveform generator (HI-TEK PPR1). The output was recorded using an X-Y recorder.

9.2.1 *In Situ* FT-IR studies.

Subtractively normalised interfacial Fourier transform infra-red spectroscopy (SNIFTIRS) was performed using a fully evacuated Bruker IFS 113v spectrometer. The computer-controlled spectrometer (under Opus 2.0 software) employed a Si-carbide source, which has a range of $6000 - 100 \text{ cm}^{-1}$, and a mercury-cadmium-telluride detector cooled with liquid nitrogen and a Ge/KBr beam splitter. The instrument was set-up to allow external reflection by focusing the *p* polarised IR beam onto the working electrode. The purposely designed *in situ* FTIR cell (figure 9.0.2) incorporating working, counter, and reference electrodes allowed the electrode to be positioned flush against the IR transparent silicon window. By mounting the electrode in this way a thin layer of electrolyte (*ca.* $1 - 10 \text{ }\mu\text{m}$) is trapped between the electrode and the silicon window, thus minimising the loss of signal by electrolyte absorption. In order to align the electrode surface parallel with the silicon window a joint using “heat shrink” tubing was made at the end of the electrode. To allow good reflection, the platinum disc-working electrode (0.79 cm^2) was polished using successively fine grades of alumina (down to $0.5 \text{ }\mu\text{m}$).

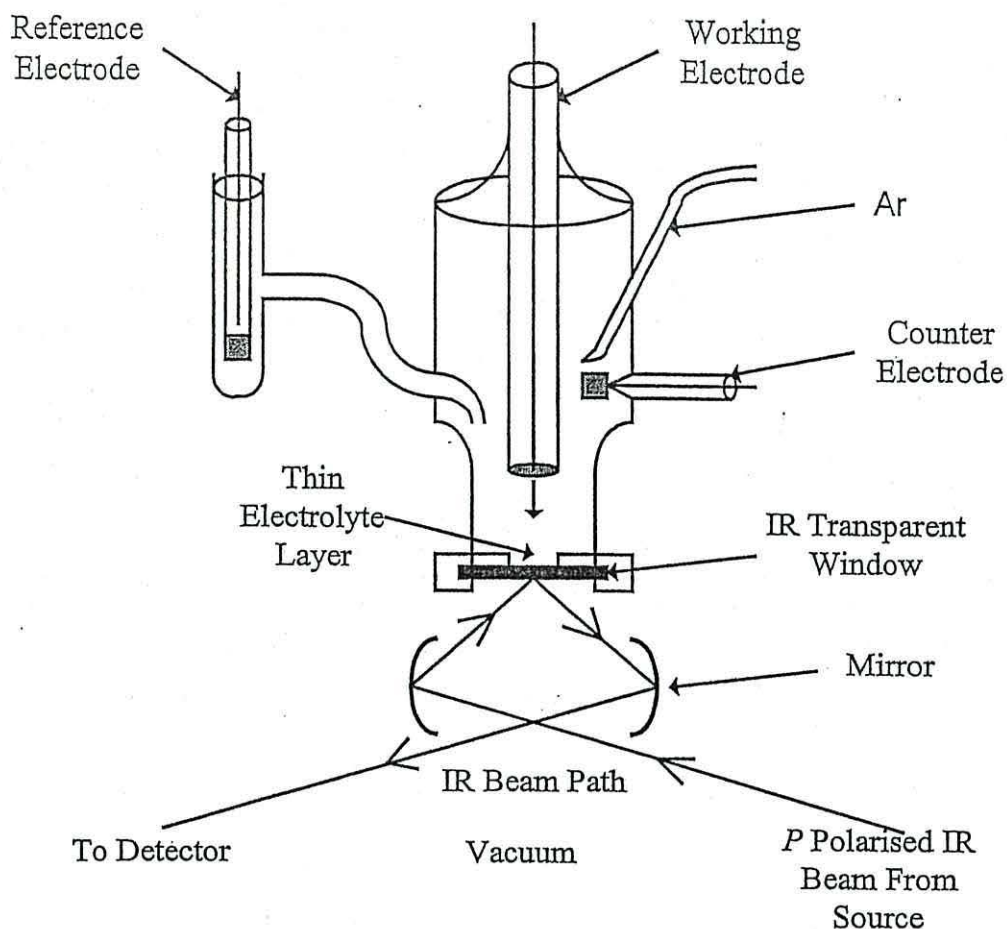


Figure 9.0.2 SNIPTIRS cell.

The potential bias was applied to the working electrode using a potentiostat, the electrode was then allowed to stabilise at this potential for one minute before collecting the IR data. For each polymer the potential was stepped in either 0.05 or 0.1 V increments, exploring both oxidised and reduced regions. At each potential a hundred interferograms were collected, the final spectrum being the average value. In order to interpret the results the information was represented as normalised difference spectra.

The normalisation is described by the equation below:

$$\frac{E_x - E_1}{E_1} = \frac{\Delta R}{R}$$

The 'normalised spectra' (the differences between the spectra, E_1 , at individual potentials and the reference spectrum, E_2) at individual potentials are then placed together to give a cumulative spectrum.

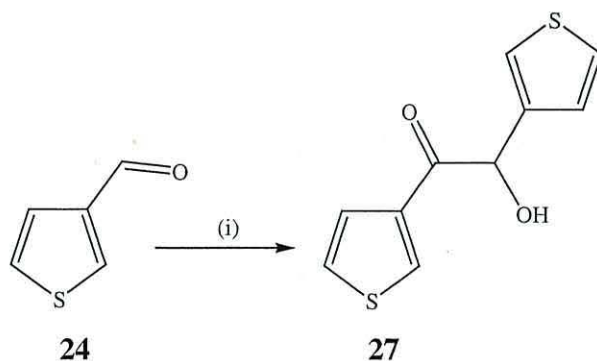
The resulting difference spectrum ($\Delta R/R$) gives information on the change in spectral absorbance of the polymer over the chosen potential range. In such spectrum positive bands represent a decrease in spectral absorbance, and negative band represent an increase in spectral absorbance.

9.3.0 Miscellaneous.

All glassware used for synthetic purposes was oven-dried (250°C). Glassware used for electrochemical procedures was left in a H_2SO_4/HNO_3 (1:1 mix) bath for an hour and rinsed with ultra pure water (Elegastat UHQ). The glassware was then steamed for 10 min and dried in an oven (60°C). All experiments were conducted under blanket coverage of Argon unless stated otherwise. *n*-Butyllithium was titrated against diphenylacetic acid in THF or diethyl ether immediately before use. All yields given along with number of moles refer to the pure isolated compound. The term *in vacuo* refers to the use of a Büchi rotary evaporator at water pump pressure and/or rotary vacuum pump pressure. The electrolyte tetrabutylammonium tetrafluoroborate (TBATFB) was dried in a vacuum oven at 60°C.

9.4.1 Synthetic Experimentals.

9.4.2 Preparation of 3,3'-theonin 27. [2]



3-Thiophene carboxaldehyde (25 g, 223 mmol) was dissolved in absolute ethanol (67.5 ml) and triethylamine (9.3 ml, 70.3 mmol), and 3-benzyl-5-(2-hydroxy ethyl) 4-methyl-1,3-thiazolium chloride (1.2 g, 4.5 mmol) were added. The reaction was heated at 120 °C (oil bath) for 2.5 hours, then cooled, diluted with water (750 ml) and extracted with dichloromethane (3 x 100 ml). The combined organic fractions were washed with sodium bicarbonate (3 x 100 ml), dried (magnesium sulfate) and evaporated *in vacuo* to give a pale brown solid. The solid was recrystallised from chloroform, producing white crystals.

Yield: 13.1 g, 58.5 mmol, 52.5%.

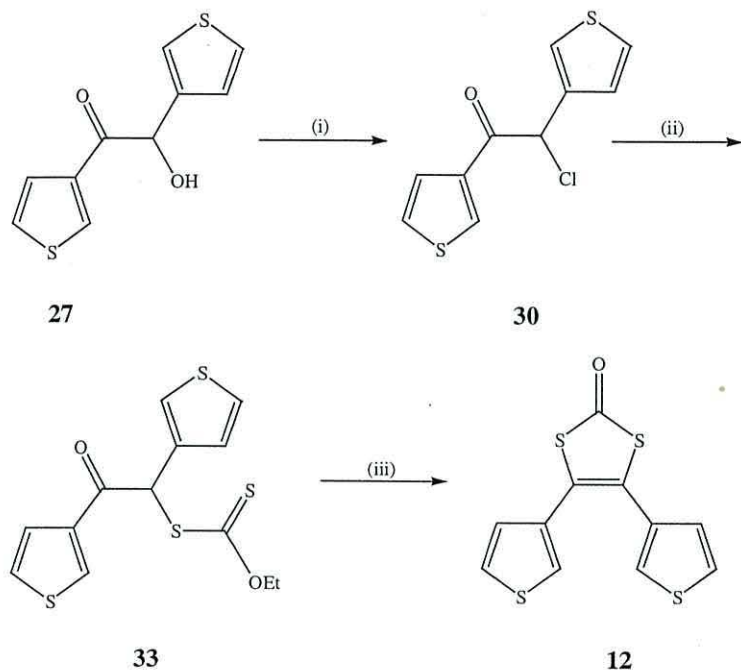
M. Pt: 108°C.

¹H NMR: δ 4.38 (d, 1H, J = 5.8 Hz, OH), δ 5.86 (d, 1H, J = 5.8 Hz, CH), δ 7.01 (d.d, 1H, J = 1.2, 4.9 Hz, C-H), δ 7.33 (m, 3H, C-H), δ 7.53 (d.d, 1H, J = 0.9, 4.9 Hz, C-H), δ 8.06 (d.d, 1H, J = 1.2, 2.8 Hz, C-H).

¹³C NMR: δ 192.4 (C), δ 139.9 (C), δ 139.9 (C), δ 134.3 (CH), δ 127.3 (CH), δ 128.1 (CH), δ 126.6 (CH), δ 126.3 (CH), δ 72.9 (CH).

IR (cm⁻¹): ν: 3428 (O-H), 3097 (C-H), 3018 (C-H), 1667 (C=O).

9.4.3 Preparation of *Bis*-4, 5-(3-thienyl)-1,3-dithiole-2-one **12**. [2]



3,3'-theonin **27** (5.4 g, 24.1 mmol) was dissolved in dichloromethane (25 ml) and added to triphenylphosphine (12.7 g, 48.5 mmol) in tetrachloromethane (50 ml). The reaction mixture was stirred in the dark for 18 hours, then diluted with ether (100 ml) which caused the precipitation of a yellow solid. The solution was decanted with filtration through a silica pad and the precipitate redissolved in dichloromethane (20 ml) and precipitated again by the addition of diethyl ether (100 ml) and petroleum ether (50ml). The supernatant layer was decanted and filtered as before and the process was repeated twice more.

After evaporation, the product was then purified by column chromatography using 30: 70 (1000 ml) diethyl ether: petrol (collecting pots containing R_f 0.2) as eluent producing a white solid of sufficient purity to be used immediately in the next step.

Yield: 5.3g, 21.9 mmol, 91%.

2-chloro-1,2-di-thiophen-3-yl-ethanone **30** (5.3 g, 21.9 mmol) was dissolved in dried acetone (5 ml) and added to a solution of potassium ethyl xantate (13.9 g, 86.8 mmol) in acetone (100 ml). The reaction mixture was stirred for 15 minutes and then diluted with diethyl ether (200 ml). The resultant solution was filtered through a silica pad and washed with dried diethyl ether with solvents evaporated *in vacuo* producing a cream coloured solid. The compound was sufficiently pure enough to be used in the next step of the reaction without further purification.

Yield: 4.5 g, 13.7 mmol, 63%.

Dithiocarbonic acid *O*-ethylester *S*- (2-oxo-1,2-di-thiophen-3-yl-ethyl) ester **33** (4.5 g, 13.8 mmol) was dissolved in glacial acetic acid (15 ml) and 45 % hydrobromic in acetic acid (15 ml) was then added. The mixture was stirred vigorously for 15 minutes, where upon dichloromethane (50 ml) and water (200 ml) were added. The resultant solution was separated and the aqueous phase extracted with dichloromethane (3 x 25 ml). The combined organic fractions were washed with saturated sodium bicarbonate (3 x 25 ml) and dried (magnesium sulfate), evaporated *in vacuo* to give a cream coloured oil. The oil was purified by column chromatography using diethyl ether: petroleum ether (3:97, 10:90, 30:70, collecting pots containing R_f 0.25). Recrystallisation was performed with hexane and diethyl ether producing cream needles.

Yield: 3.4 g, 12.1 mmol, 88%.

M.Pt: 102⁰C.

¹H NMR: δ 6.8 (d, 2H, J = 5.0Hz, 2x C-H), δ 7.2 (m, 4H, 2x C-H).

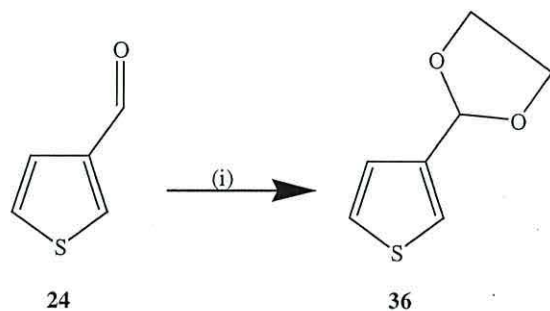
¹³C NMR: δ 189.9 (C), δ 131.7 (C), δ 127.8 (CH), 126.42 (CH), 125.9 (CH), 123.4 (C).

IR (cm⁻¹): v: 3111 (C-H), 1659 (C=O), 1629 (C=C).

Mass Spec: C₁₁H₆OS₄ [M⁺] requires: 281.9302
Found: 281.9302

Crystal Data: See Appendix 2.

9.4.4 Preparation of 3-acetal thiophene 36. [3]



To a stirred solution of **24** (56.0 g, 0.5 mol) in benzene (50 ml), ethylene glycol (40.0 g, 0.7 mol) and a catalytic amount of *p*-toluene sulphonic acid (ca. 20 mg) were added. The mixture was refluxed under a Dean-Stark head for 5 hours, with monitoring by tlc. On completion of the reaction (starting material Rf 0.1, product Rf 0.15, 10:90 diethyl ether: petrol), the crude mixture was washed with NaHCO₃ (100 ml), water (50 ml), and extracted with dichloromethane (3 x 50 ml). The combined organic fractions were dried (MgSO₄) and solvents removed *In vacuo*, and the product was purified by vacuum distillation (120⁰C/10 mmHg).

Yield: 46.9 g, 0.3 mol, 60%.

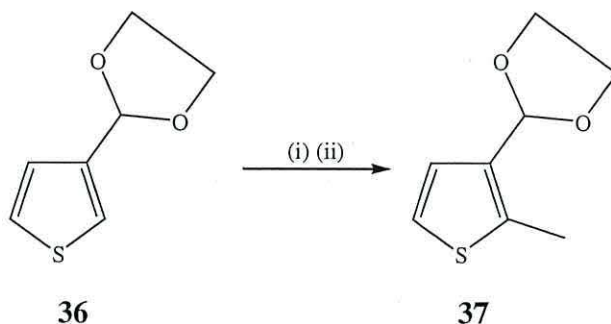
B. Pt: literature 120⁰C/10mmHg
found 160⁰C/14mmHg

¹H NMR: δ 7.4 (d, 1H, J = 5.7 Hz, C-H), δ 7.2 (m, 1H, C-H), δ 7.1 (d, 1H, J = 5.5 Hz, C-H), δ 4.1 (m, 2H), δ 4.0 (m, 2H).

¹³C NMR: δ 130.7 (C), δ 126.8 (C-H), δ 125.1 (C-H), δ 122.0 (C-H) δ 102.4 (O-CH₂), δ 101.5 (O-C-O).

IR (cm⁻¹): ν: 2945 (C-H), 1374 (C-C), 1132 (C-O)

9.4.5 Preparation of 2-methyl-3-acetal thiophene **36**. [4]



To a cooled (-78°C) solution of **36** (15.6 g, 100 mmol) in THF (75 ml), *n*-BuLi (0.11 mol, 44 ml) was added drop-wise over 10 min and then stirred for 30 minutes. Freshly distilled MeI (17.0 g, 0.1 mol) in THF (10 ml) was then added and the reaction was then slowly warmed to RT and stirring continued for 3 hours. The reaction was then quenched with water (50 ml) and extracted with diethyl ether (3x100 ml). The combined organic fractions were washed with brine (100 ml), dried (Na_2SO_4) and the solvents removed *In vacuo* producing a clear liquid that was used without further purification.

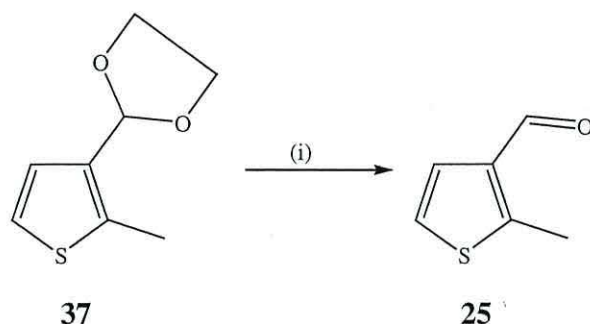
Yield: 16.1 g, 94.5 mmol, 95%.

^1H NMR: δ 7.1 (s, 2H, C-H), δ 5.8 (s, 1H, CH), δ 4.1 (m, 4H, $2\times\text{CH}_2$), δ 2.5 (s, 3H, CH_3).

^{13}C NMR: δ 130.1 (C), δ 127.4 (C-H), δ 124.0 (C), δ 121.0 (C-H), δ 103.0 (O- CH_2) δ 12.6 (CH_3).

IR (cm^{-1}): ν : 2947 (C-H), 1378 (C-C), 1125 (C-O)

9.4.6 Preparation of 2-methyl-3-thiophene carboxaldehyde **25**.



2-methyl-3-acetal thiophene **37** (35.1 g, 206 mmol) was vigorously stirred in H₂O (60 ml) and c.HCl (30 ml) for 2.5 hours. The reaction was diluted with diethyl ether: petrol (20:80) (100 ml) and H₂O (100 ml). The crude product was separated and then extracted with diethyl ether (3 x 50 ml), and the organic fractions were dried over MgSO₄ and solvents were removed *in vacuo*. The residues were extracted with diethyl ether (100 ml) and solvents were removed *in vacuo* producing a brown liquid. The compound was obtained in a pure enough state (¹H NMR) that required no further purification.

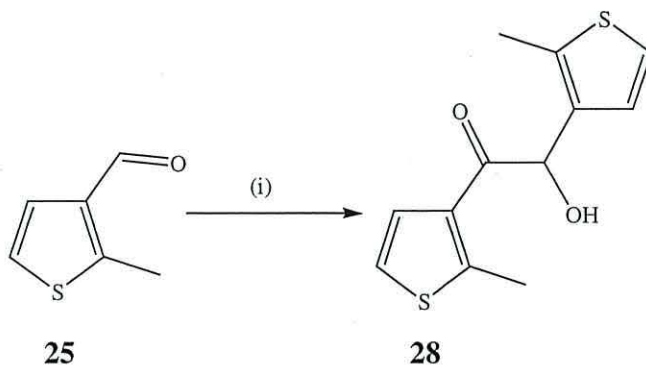
Yield: 28.2 g, 223.8 mol, 100 %.

¹H NMR: δ 9.4 (s, 1H, CHO), δ 7.2 (d, 1H, C-H, J = 5.6 Hz), δ 6.9 (d, 1H, C-H, J = 5.6 Hz), δ 2.7 (s, 3H, CH₃).

¹³C NMR: δ 184.9 (CHO), δ 184.6 (C), δ 125.3 (C-H), δ 122.7 (C-H), δ 122.7 (C-H).

IR (cm⁻¹): ν: 2838 (C-H), 1674 (C=O), 1386 (C-C), 1521 (C=C), 910 (C-S).

9.4.7 Preparation of 2-hydroxy-1,2-bis-(2-methyl-thiophen-3-yl)-ethanone **28**.



To a solution of **25** (8.3 g, 65.9 mmol) in absolute ethanol (200 ml), triethylamine (2.0 g, 20 mmol) and 3-benyl-5-(2-hydroxyethyl)-4-methylthiazolium chloride (3.6 g, 10 mmol) was added and the mixture was allowed to reflux for 5 hours. The reaction was quenched with H₂O (200 ml) and organic fractions were extracted with dichloromethane (3 x 100 ml). The combined organic fractions were washed with brine (75 ml), and dried (MgSO₄). The crude mixture was then purified using column chromatography 10:90 (1000 ml), 20:80 (750 ml) diethyl ether: petrol, collecting pots with R_f : 0.68 (20:80 diethyl ether : petrol).

Yield: 2.3 g, 9.1 mmol, 28%.

M. Pt: 83-86⁰C.

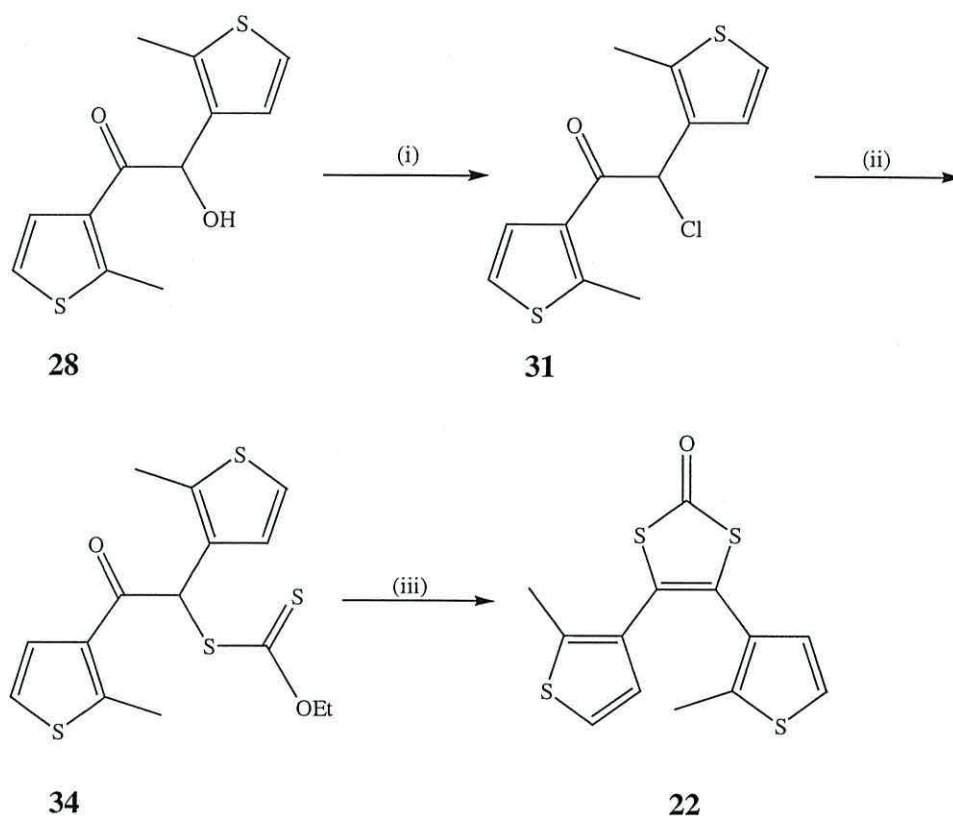
¹H NMR: δ 2.73 (s, 3H, CH₃), δ 2.51 (s, 3H, CH₃), δ 4.44 (d, 1H, J = 5.4 Hz, OH), δ 5.63 (d, 1H, J = 5.4 Hz, CH), δ 6.63 (d, 1H, J = 5.4 Hz, C-H), δ 6.86 (d, 1H, J = 5.3 Hz, C-H), δ 6.93 (d, 1H, J = 5.5 Hz, C-H), δ 6.96 (d, 1H, J = 5.3 Hz, C-H).

¹³C NMR: δ 194.3 (C=O), δ 152.4 (C), δ 137.7 (C), δ 134.8 (C), δ 131.8 (C) δ 127.4 (C-H), δ 126.7 (C-H), δ 122.7 (C-H), δ 121.8 (C-H), δ 71.1 (C-OH), δ 16.3 (CH₃), δ 13.1 (CH₃).

IR (cm⁻¹): ν: 2921 (C-H), 1666 (C=O), 1508 (C=C), 1375 (C-H), 1270 (C-C).

Mass Spec: C₁₂H₁₆S₂NO₂ [M+NH₄] requires: 270.0622
found: 270.0620

9.4.11 Preparation of 4,5-Bis-(2-methyl-thiophen-3-yl)-[1,3]dithiol-2-one 22.



To a solution of **28** (2.2 g, 8.73 mmol) dissolved in dichloromethane (10 ml), triphenylphosphine (4.6 g, 17.5 mmol) dissolved in carbon tetrachloride (30 ml) was added and the mixture stirred in the dark for 18 hours. The reaction was then poured onto a column (150 g Silica) loaded with carbon tetrachloride and eluted with 50:50 diethyl ether: petrol. The pots containing R_f: 0.45 (20:80 diethyl ether: petrol) were collected and solvents were removed *in vacuo* producing a creamy yellow solid. The product was sufficiently pure enough to be used in the next step of the reaction without further purification.

Yield: 1.9 g, 7.0 mmol, 80%.

To a solution of **31** (1.9 g, 7.0 mmol) in acetone (80 ml) potassium ethyl xanthate (1.11 g, 7.0 mmol) was added and the reaction was stirred for 15 minutes.

Diethyl ether (200 ml) was added and the reaction filtered through a silica pad. The solvents were then removed *In vacuo*, producing an off-white solid that was used without further purification.

Yield: 2.5 g, 7.0 mmol, 100%.

Dithiocarbonic acid *S*-[1,2-*bis*-(2-methyl-thiophen-3-yl)-2-oxo-ethyl] ester *O*-ethyl ester **34** (2.5 g, 7.0 mmol) was dissolved in glacial acetic acid (15 ml) and 45 % hydrobromic in acetic acid (15 ml) was then added. The mixture was stirred vigorously for 15 minutes, where upon dichloromethane (50 ml) and water (200 ml) were added. The resultant solution was separated and the aqueous phase extracted with dichloromethane (3 x 25 ml). The combined organic fractions were washed with saturated sodium bicarbonate (3 x 25 ml) and dried (magnesium sulfate), evaporated *in vacuo* to give a cream coloured oil. The oil was purified by column chromatography using diethyl ether: petroleum ether (3:97, 10:90, 30:70). Recrystallisation was performed with hexane and diethyl ether producing cream coloured needles.

Yield: 1.1 g, 3.54 mmol, 50%.

M.Pt: 131 – 135⁰C.

¹H NMR: δ 7.0 (d, 1H, J = 5.1 Hz, C-H), δ 6.8 (d, 1H, J = 5.5 Hz, C-H),
δ 2.1 (s, 6H).

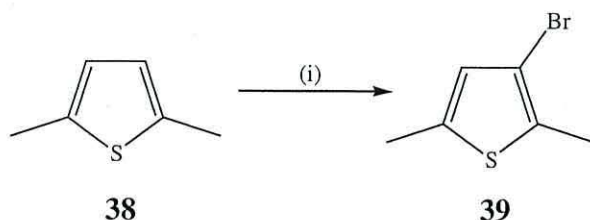
¹³C NMR: δ 191.1 (C=O) δ 142.6 (C), δ 128.4 (2x C-H), δ 128.1 (C),
δ 126.1 (C), δ 124.9 (C), δ 122.6 (2x C-H), δ 13.9 (2x CH₃).

IR (cm⁻¹): ν: 2920 (C-H), 1653 (C=O), 1545 (C=C), 1377 (C-H), 1200 (C-C).

Mass Spec: C₁₃H₁₄S₄NO₂ [M+NH₄] required: 327.9958
obtained: 327.9957

Crystal data: See Appendix 2.

9.4.9

Preparation of 3-bromo-2,5-dimethyl thiophene **39**. [5]

A solution of 2,5-dimethylthiophene **38** (5.0 g, 44.6 mmol) in CCl_3 (10 ml) was stirred at 0°C in the dark. Bromine liquid (7.2 g, 44.6 mmol) dissolved in CHCl_3 (15 ml) was then added and the reaction was allowed to stir for 5 hours. The reaction was quenched with water (50 ml) and extracted with diethyl ether (3x 50 ml). The combined organic fractions were washed with NaHCO_3 (sat, 2 x 50 ml) and dried (MgSO_4). The solvents were removed *in vacuo*, to give pure **39** as an oil that required no further purification.

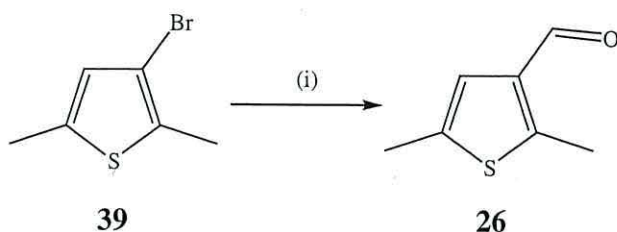
Yield: 7.5 g, 39.3 mmol, 88%

^1H NMR: δ 6.6 (s, 1H, C-H), δ 2.4 (s, 6H, 2x CH_3).

^{13}C NMR: δ 135.0 (C), δ 139.2 (C), δ 127.5 (CH), δ 107.4 (C), δ 13.8 (CH_3), δ 6.7 (CH_3).

IR (cm^{-1}): ν : 2918 (C-H), 1527, 1438 (C=C).

9.4.10 Preparation of 2,5 dimethyl, 3-thiophene carboxaldehyde 26.



To a cooled (-70°C) solution of **39** (7.5 g, 3.93 mmol) in diethyl ether (50 ml) at -70°C , *n*-BuLi (1.1eqv, 0.04 mol) was added dropwise and the reaction stirred for 15 minutes. DMF (5.71 g, 0.08 mol) in diethyl ether (15 ml) was then added drop-wise, and the reaction was stirred at -70°C for a further 30 minutes. The reaction was then quenched with 2M HCl (50 ml) and extracted with diethyl ether (3x 50 ml). The combined organic fractions were dried (MgSO_4) and solvents were removed *in vacuo*. The product was obtained in a sufficiently pure form requiring no further purification.

Yield: 4.2 g, 30 mmol, 76%

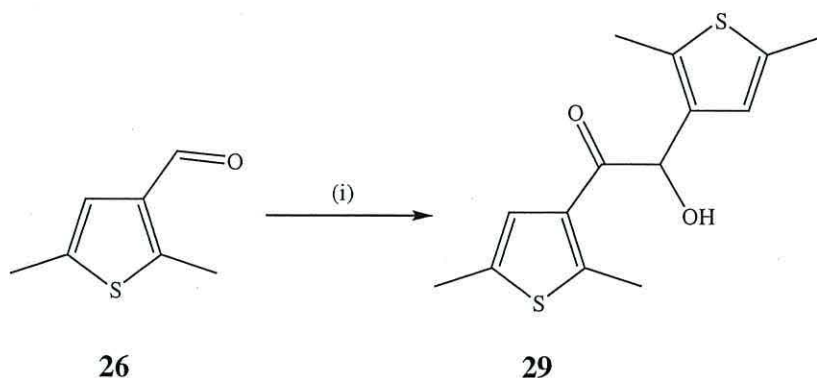
^1H NMR: δ 9.9 (s, 1H, CHO), δ 6.9 (s, 1H, C-H), δ 2.7 (s, 3H, CH_3),
 δ 2.4 (s, 3H, CH_3).

^{13}C NMR: δ 184.3 (CHO), δ 150.5 (C-CHO), δ 141.8 (C-H), δ 137.1 (C), δ 136.6 (C) δ 14.9 (CH_3) δ 13.3 (CH_3).

IR (cm^{-1}): ν : 2922, 2958 (C-H), 1672 (C=O), 1554 (C=C), 1377 (C-H).

Mass Spec: $\text{C}_7\text{H}_9\text{SO}$ [$\text{M}+\text{H}$] requires: 141.0375
found: 141.0375

9.4.11 Preparation of 1,2-Bis-(2,5-dimethyl-thiophen-3-yl) 2-hydroxyethyl-ethanone 29.



To a solution of **26** (4.9 g, 35 mmol) in isopropanol (9.4 ml) triethylamine (1.1 g, 11.0 mmol) and 3-benzyl-5-(2-hydroxyethyl)-4-methyl-1,3-thiazolium chloride (5.8 g, 21.0 mmol) was added. The reaction mixture was refluxed for 48 hours and then quenched with water (150 ml) and extracted with DCM (3x 30 ml). The combined organic residues were washed with NaHCO₃ (30 ml) and dried (MgSO₄). The solvents were removed *in vacuo* producing a brown solid that was purified by column chromatography using diethyl ether: petrol (30:70) as eluent, collecting pots containing R_f 0.15 (20:80).

Yield: 0.76 g, 2.7 mmol, 15.5%.

M. Pt: 144-146⁰C.

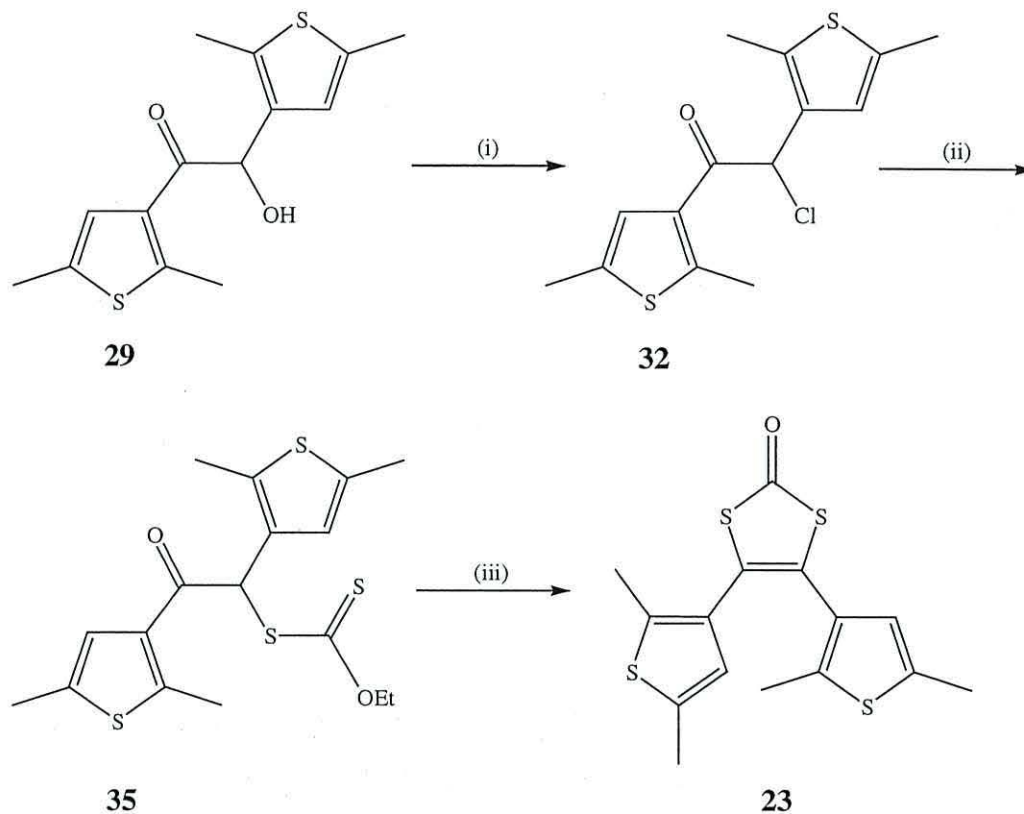
¹H NMR: δ 6.67 (s, 1H, C-H), δ 6.32 (s, 1H, C-H), δ 5.53 (d, 1H, J = 5.5 Hz) δ 4.43 (d, 1H, J = 5.5 Hz), δ 2.73 (s, 3H, CH₃), δ 2.51 (s, 3H, CH₃) δ 2.33 (s, 3H, CH₃), δ 2.32 (s, 3H, CH₃).

¹³C NMR: δ 194.2 (CHO), δ 150.7 (C, C-CHO), δ 136.9 (C), δ 135.6 (C), δ 135.1 (C) δ 134.4 (C), δ 131.6 (C), δ 124.9 (C-H), δ 124.2 (C-H), δ 70.9 (OH), δ 16.3 (CH₃), δ 15.1 (CH₃), δ 15.0 (CH₃), δ 13.0 (CH₃).

IR (cm⁻¹): ν: 3097 (OH), 2918 (C-H), 1659 (C=O), 1550 (C=C), 1377 (C-H), 1244 (C-C).

Mass Spec: C₁₄H₁₇S₂O₂ [M+H] requires: 280.0595
found: 280.0592

9.4.12 Preparation of 4,5-Bis-(2,5-dimethyl-thiophen-3-yl)-[1,3]dithiole-2-one 23.



To a solution of **29** (2.2 g, 7.86 mmol) in dichloromethane (30 ml), a solution of triphenylphosphine (4.6 g, 17.5 mmol) in CCl_4 (10 ml) was added and the reaction mixture was stirred in the dark for 18 hours. The crude reaction mixture was poured onto a silica column (150 g) loaded in CCl_4 , and the product was eluted 50:50 diethyl ether:petrol producing a yellow solid that was used immediately in the next step of the reaction.

Yield: 1.9 g, 6.37 mmol, 81 %.

To a solution of **32** (0.6 g, 2.01 mmol) in dried acetone (50 ml) a solution of potassium ethyl xanthate (0.5 g, 1.1 mmol) in acetone (20 ml) was added and the mixture stirred for 30 minutes. This was then diluted with diethyl ether (80 ml),

filtered through a silica pad and washed with an excess of diethyl ether. Solvents were evaporated *in vacuo* producing a cream coloured solid that was used immediately in the next step of the reaction.

Yield: 0.6 g, 1.56 mmol, 78 %.

Dithiocarbonic acid *S*-[1,2 *bis*-(2,5-dimethyl-thiophen-3-yl)-2-oxo-ethyl] ester *O*-ethyl ester **35** (0.6 g, 1.56 mmol) was dissolved in glacial acetic acid (5 ml) and hydrobromic acid (5 ml, 45% w/v) was then added and the mixture stirred vigorously for 15 minutes. Water (50 ml) and DCM (50 ml) were then added and the reaction extracted with DCM (3 x 25 ml) and the combined organic fractions were washed with NaHCO₃ (3x 20 ml) and dried (MgSO₄). Solvents were removed *in vacuo*, and the pure product was obtained by column chromatography eluting with diethyl ether / petrol (3: 97 (500 ml), 10: 90 (1000 ml)).

Yield: 0.3 g, 0.89 mmol, 57%.

M. Pt: 295-298⁰C.

¹H NMR: δ 6.4 (s, 2H, C-H), δ 2.3 (s, 6H, 2x CH₃), δ 2.0 (s, 6H, 2x CH₃).

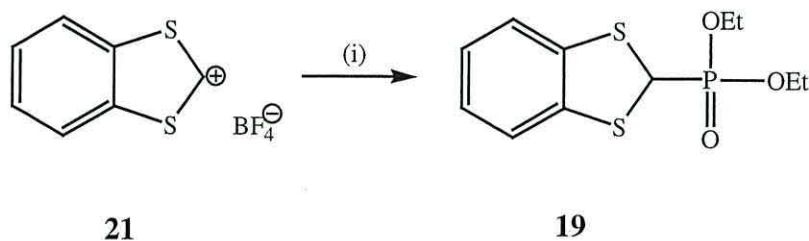
¹³C NMR: δ 191.4 (C=O), δ 136.6 (C), δ 136.3 (C), δ 132.6 (2x C), δ 128.6 (2x C) δ 127.6 (C-H), δ 126.5 (C-H), δ 124.8 (2x C), δ 32.2 (CH₃), δ 29.6 (CH₃), δ 29.3 (CH₃), δ 21.9 (CH₃).

IR (cm⁻¹): ν: 2920 (C-H), 1670 (C=O), 1545 (C=C), 1377 (C-H), 1200 (C-C).

Mass Spec: C₁₅H₁₃S₄O [M+H] requires: 337.9928
found: 337.9913

Crystal data: See Appendix 2.

9.4.13

Preparation of Benzo [1,3] dithiol-2-yl-phosphonic acid diethyl ester **19**.

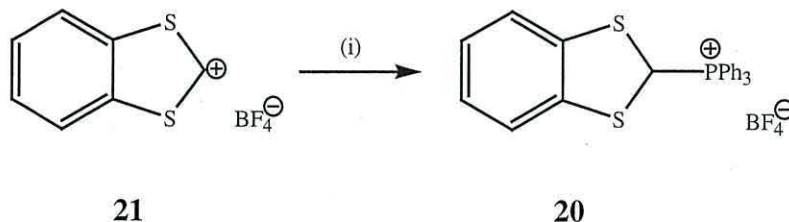
Triethylphosphite (0.7 g, 4.2 mmol) and sodium iodide (0.6 g, 4.2 mmol) were added to a solution of **21** (1.0 g, 4.2 mmol) in cooled (0°C) anhydrous acetonitrile (30 ml) and the reaction stirred for 1 hour. The solvents were then removed *in vacuo*, water (100 ml) was added and the reaction extracted using dichloromethane (3 x 50 ml) and the combined organic fractions were dried (MgSO_4) and solvents removed producing a dark red solid that was purified by recrystallisation with acetonitrile.

Yield: 1.2g, 4.2 mmol, 100 %.

M.Pt: 220°C

^1H NMR: δ 7.2 (d.d, 2H, $J = 5.7$ Hz, 2x C-H), δ 7.0 (d.d, 2H, $J = 5.8$ Hz, 2x CH), δ 4.8 (d, 1H, $J = 5.0$ Hz, C-H), δ 4.3 (m, 4H, 2x CH_2), δ 1.3 (t, 6H, 2x CH_3).

9.4.14 Preparation of benzo[1,3]dithiol-2-yl-triphenyl-phosphonium tetrafluoroborate 20.



Triphenylphosphine (0.55g, 21 mmol) was added to a solution of 1,3-benzodithiol-2-ylum tetrafluoroborate **21** (0.5g, 2.1 mmol) in acetonitrile (15 ml) and stirred for 24 hours under nitrogen. Solvents were evaporated *in vacuo* producing an off-red solid that required no further purification.

Yield: 1.03 g, 2.06 mmol, 98 %.

M.Pt: 294-296⁰C.

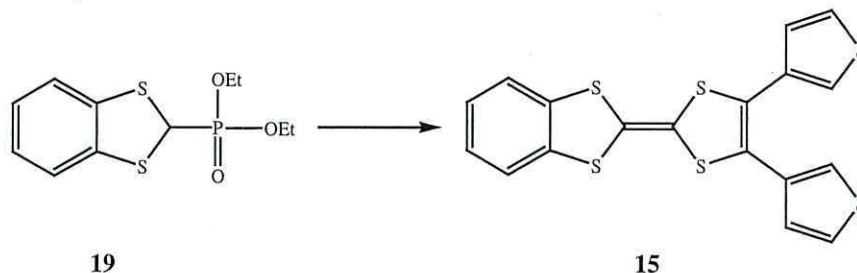
¹H NMR: δ 7.8 (m, 15H, PPh₃), δ 7.6 (m, 4H, 4 x CH), δ 3.1 (s, 1H, C-H).

¹³C NMR: δ 135.5 (C-H), δ 134.1 (CH), δ 130.0 (PPh₃), δ 126.7 (PPh₃), δ 122.1 (PPh₃), δ 116.7 (C), δ 115.3 (C), δ 48.8 (C-H).

IR (CM⁻¹): ν: 3052 (C-H), 1439 (C=C), 1173 (C-H), 1050 (BF₄⁻), 993 (C-S).

Mass Spec: [C₂₅H₂₀S₂P]⁺ requires: 415.0744
found: 415.0737

9.4.15 Preparation of 2-(4,5-di-thiophen-3-yl-[1,3] dithiol-2-ylidene)-benzo[1,3]dithiole 15.



A solution of **28** (1.0 g, 3.45 mmol) dissolved in THF (15 ml) was stirred at -78°C and *n*-BuLi (1.38 ml, 3.45 mmol) was added and the reaction mixture was stirred for 15 minutes. To the stirred mixture **5** (0.2 g, 0.71 mmol) in THF (10 ml) was added over 5 minutes and the reaction was then stirred for a further 20 minutes at -78°C . The mixture was then warmed to room temperature and stirred for a further hour. At this point the solvent was removed *in vacuo*, and dichloromethane (50 ml) and HCl (50 ml) were added successively. After separation the reaction was extracted with further dichloromethane (3 x 50ml), and the combined organic extracts were then washed with H_2O (25 ml) and dried (MgSO_4). Solvents were then removed and the crude product purified by column chromatography, eluting with (0:100, 5:95, 10:90 diethyl ether: petrol), the pots containing R_f : 0.64 (5:95 diethyl ether: petrol) being combined.

Yield: 0.15 g, 0.36 mmol, 51%.

M.Pt: $101 - 104^{\circ}\text{C}$.

^1H NMR: δ 7.3 (m, 4H, 4x C-H), δ 7.1 (d.d, 4H, $J = 5.8$ Hz, 4x C-H), δ 2.1 (d.d, 2H, $J = 4.4$ Hz, 2x C-H).

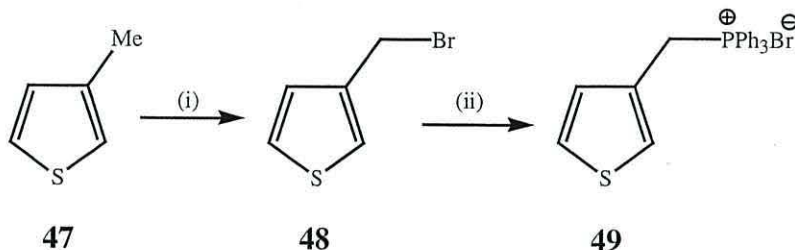
IR (cm^{-1}): ν : 1657 (C=C), 3111 (C-H), 3098 (C-H), 2047 (C-H).

Mass Spec: $[\text{M}^+]$ Calculated: 417.9107

Found: 417.9109

Crystal data: See Appendix 1.

9.4.16 Preparation of triphenyl-thiophen-3-yl methyl-phosphonium;bromide 49. [6]



To a solution of **47** (25.0 g, 255 mmol) in CCl_4 (70 ml), *n*-bromosuccinamide (40.6 g, 230 mmol) and benzoyl peroxide (0.1 g) were added. The mixture was stirred vigorously and heated for 1 hour, after which, a further amount of benzoyl peroxide (0.1 g) was added and reflux continued for a further 5 hours. The reaction was then cooled in an ice bath precipitating the succinamide which was then filtered and the precipitate washed with CCl_4 (30 ml). The product **48** was purified by distillation under vacuum (2 mmHg, 70-100°C), and was used immediately in the next step of the reaction without further purification.

Yield: 36.5 g, 206 mmol, 81 %.

To a solution of **48** (36.5 g, 206 mmol) in toluene (200 ml), PPh_3 (59.5 g, 200 mol) was added and the reaction mixture was stirred for 3.5 hours in which **49** was observed to precipitate out of solution. The reaction mixture was filtered and the product **49** washed with toluene (2x 100 ml) and petrol (200 ml) yielding a white solid.

Yield: 75.9 g, 173 mmol, 84 %.

M.Pt: literature 298°C
found 294-296°C

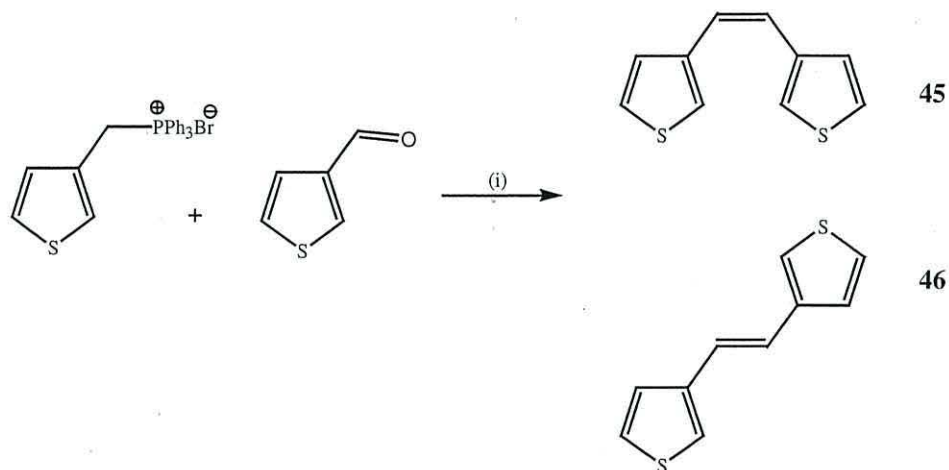
^1H NMR: δ 7.7 (m, 15H, C-H PPh_3), δ 7.2 (m, 2H, C-H), δ 6.7 (d, 1H, $J = 5.4$ Hz, C-H), δ 2.3 (s, 2H, CH_2).

¹³C NMR: δ 135.3 (C-H), δ 133.4 (C-H), δ 130.2 (C-H), δ 128.6 (C-H, PPh₃), δ 127.2 (C-H, PPh₃), δ 127.1 (C-H, PPh₃), δ 125.6 (C, PPh₃), δ 118.0 (C, PPh₃), δ 26.1 (C-H).

IR (cm⁻¹): v: 3056 (C-H), 2392 (C-H), 1584 (C=C), 1462 (C=C), 1157 (C-C), 1109 (C-C).

Mass Spec: $[\text{C}_{24}\text{H}_{20}\text{S}]^- [\text{M}-\text{Br}]^+$ Calculated: 359.1023
Found: 359.1018

9.4.17 Preparation of *cis*-1,2-dithienylethylene **45 and *trans*-1,2-dithienylethylene **46**. [7]**



To a cooled (0°C) stirred solution of **49** (1.20 g, 2.73 mmol) in THF (10 ml), *n*-BuLi (1.17 ml, 2.5 mmol) was added and the reaction stirred for 30 minutes. The reaction was then cooled to -78°C and **24** (0.3 g, 2.68 mmol) was added dropwise. The reaction mixture was stirred for 2 hours at -78°C and allowed to warm to R.T slowly. The reaction was quenched by the addition of H₂O, (50 ml), and was extracted with diethyl ether (3x 50 ml). The combined organic fractions were then washed with HCl (50 ml), NaHCO₃ (50 ml) and dried (MgSO₄). Solvents were removed *in vacuo*, and the crude products were purified by column chromatography using 5:95, 10:90 diethyl ether: petrol as eluent. Pots containing R_f: 0.15 were combined producing a clear oil **45** and pots combining R_f: 0.1 were combined producing a white crystalline solid **46**. The *cis*: *trans* ratio was 43:57, with *cis* undergoing isomerisation to *trans* in ca. 2 days.

***CIS* **45**.**

Yield: 0.2 g, 1.04 mmol, 39%.

¹H NMR: δ 7.2 (m, 4H, 4 x C-H), δ 7.0 (d.d, 2H, J = 5.0 Hz, 2 x C-H), δ 6.5 (s, 2H, 2 x C-H).

¹³C NMR: δ 140.0 (2x (C)), δ 126.1 (2x (C-H)) δ 124.8 (2x (C-H)), δ 122.9 (2x (C-H)), δ 121.9 (2x (CH₂)).

IR (cm⁻¹): ν: 2922 (C-H), 1427 (C=C), 1348 (C-H), 1263 (C-C).

Mass Spec: C₁₁H₈S₂ [M+H] requires: 193.0145
 found: 193.0143

TRANS 46

Yield: 0.26 g, 1.35 mmol, 51%.

M. Pt: 192⁰C.

¹H NMR: δ 7.3 (d, 4H, J = 5.4 Hz, 4 x C-H), δ 7.2 (t, 2H, J = 4 Hz, 2 x C-H), δ 6.9 (s, 2H, 2 x C-H).

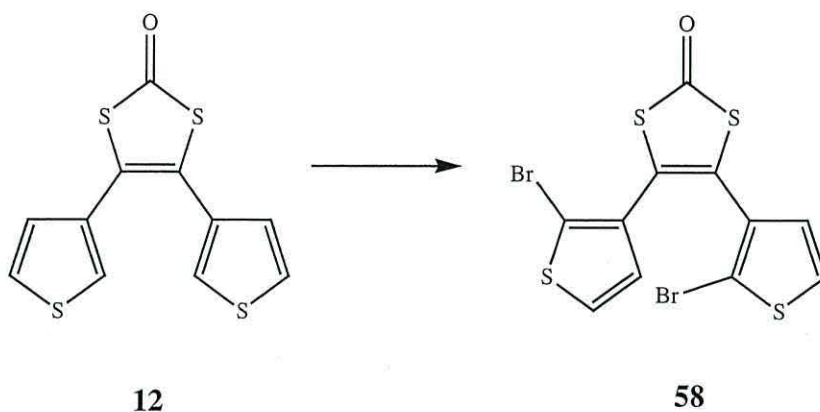
¹³C NMR: δ 140.0 (2x (C)), δ 126.1 (2x (C-H)) δ 124.7 (2x (C-H)), δ 122.9 (2x (C-H)), δ 121.8 (2x (CH₂)).

IR (cm⁻¹): ν: 2922 (C-H), 1427 (C=C), 1348 (C-H), 1263 (C-C).

Mass Spec: C₁₁H₈S₂ [M+H] requires: 193.0145
 found: 193.0146

Crystal data: See Appendix 3.

9.4.18 Preparation of 4,5-Bis-(2-bromo-thiophen-3-yl)-[1,3]dithiole-2-one **58**.



Bis-4,5-(3-thienyl)-1,3-dithiole-2-one **12** (0.5 g, 1.77 mmol) and N-Bromosuccinamide (0.6 g, 3.54 mmol) was dissolved in CCl_4 (30 ml) and refluxed for 30 hours in the dark. The resultant solution was filtered and washed with CCl_4 (20 ml) and dichloromethane (5 ml). The solvents were removed *in vacuo* producing a pale cream solid. The crude product was purified by column chromatography using diethyl ether: petrol (3:97 (500 ml), 5:95 (500 ml), 10:90 (500 ml) collecting pots containing R_f 0.2 (diethyl ether: petrol, 10:90) giving the title compound as a pale cream solid.

Yield: 0.22 g, 0.50 mmol, 28 %.

M. Pt: 281°C .

^1H NMR: δ 6.7 (d, 2H, $J = 5.6$ Hz, C-H), δ 7.2 (d, 2H, $J = 5.7$ Hz, C-H).

^{13}C NMR: δ 128.8 (C=O), δ 126.7 (), δ 77.5 (), δ 77.0 (), δ 76.5 (), δ 20.3 ().

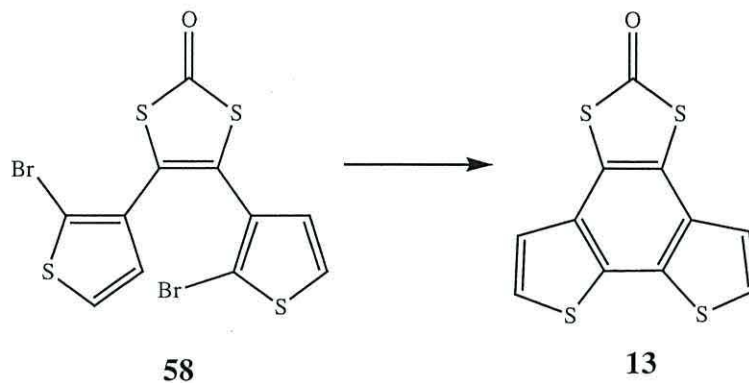
IR (cm^{-1}): ν : 2923 (C-H), 1624.8 (C=O), 1461.8 (C-C), 1376.4 (thiophene)

GC-MS: m/z 440 (M^+)

MS (CI): m/z 458 (18% $[\text{M}+\text{NH}_4]^+$), 440 (100% $[\text{M}]^+$) daltons.

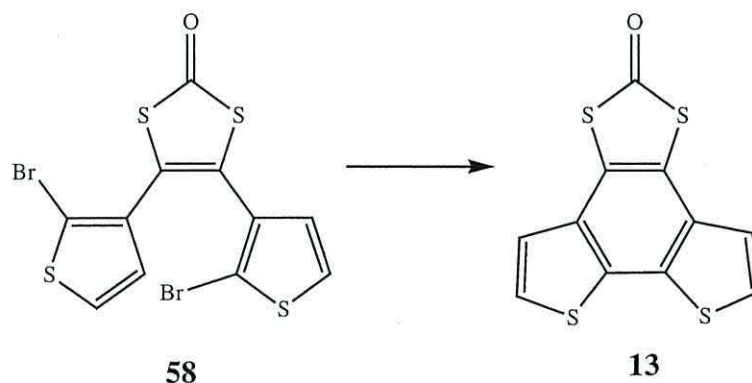
9.4.19

Attempted intramolecular cyclisation of 4,5-Bis-(2-bromo-thiophen-3-yl)-[1,3]dithiole-2-one **58**. [8]



Activated copper (0.65 g, 100 mmol) was added to a solution of **58** (1.0 g, 10 mmol) in DMF (25 ml) and the mixture was refluxed (160⁰C) in the dark for 24 hours. The cooled reaction mixture was then filtered over celite and washed with excess ethyl acetate, LiBr (100 ml) and dried over MgSO₄. The solvents were then removed *in vacuo* and purified by column chromatography (50:50 ethyl acetate: petrol). ¹H NMR analysis indicated that compound **12** was obtained, reaction unsuccessful.

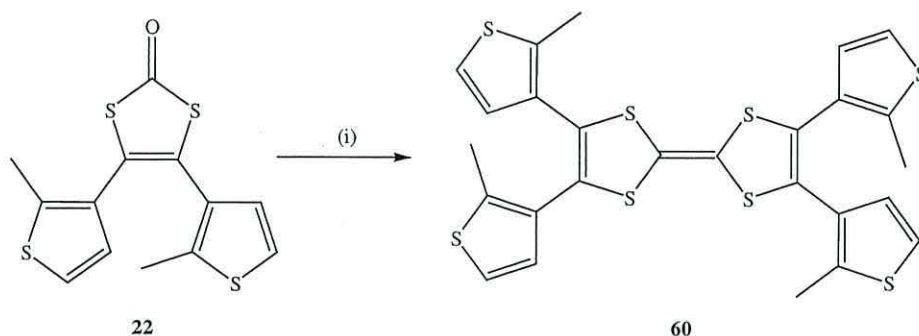
9.4.20 Attempted intramolecular cyclisation of 4,5-Bis-(2-bromo-thiophen-3-yl)-[1,3]dithiole-2-one **58. [9,10]**



4,5-Bis-(2-bromo-thiophen-3-yl)-[1,3]dithiole-2-one **58** (0.5 g, 5 mmol), $\text{Pd(PPh}_3)_4$ (0.25 g, 0.23 mmol) $\text{Me}_3\text{SnSnMe}_3$ (0.3 g, 1.0 mmol) and PPh_3 (0.14 g, 0.56 mmol) was dissolved in dioxane and refluxed at 160°C for 18 hours. The cooled reaction mixture was then diluted with CH_2Cl_2 (30 ml), washed with H_2O (3 x 50 ml), washed with a solution of NaF (200 ml, 0.1M) and extracted with CH_2Cl_2 (3 x 30 ml). The mixture was then dried over MgSO_4 and solvents removed *in vacuo*, and purified using column chromatography 5:95 (500 ml), 10:90 (500 ml), 20 (1000 ml), ^1H NMR analysis indicating that compound **12** was obtained, reaction unsuccessful.

9.5.0 Miscellaneous reactions.

9.5.1 Preparation of 4,4',5,5'-Tetrakis 2,2',5,5'methyl (3-thienyl) tetrathiafulvalene **60**.



A solution of **22** (0.5 g, 1.61 mmol) in triethylphosphite (10 ml) was refluxed for 3 hours. The product was obtained by column chromatography using 0:100, 20:80 diethyl ether : petrol as eluent. The pots containing R_f : 0.53 were collected (20:80 diethyl ether : petrol), resulting in an orange crystalline solid.

Yield: 0.2 g, 0.34 mmol, 42 %.

M. Pt: 588⁰C.

¹H NMR: 6.9 (d, 4H, $J = 5.4$ Hz, 4x C-H), 6.7 (d, 4H, $J = 5.2$ Hz, 4x C-H), 2.1 (s, 12H, 4x CH₃)

¹³C NMR: δ 142.6 (C), δ 128.4 (C-H), δ 128.1 (C),
 δ 126.1 (C), δ 124.9 (C), δ 122.6 (C-H), δ 13.9 (CH₃).

IR (cm⁻¹): ν : 2924 (C-H), 1463 (C=C), 1376 (C-C).

Mass Spec: C₂₆H₂₀S₈ [M⁺] requires: 587.9331
 found: 587.9323

Crystal Data: See Appendix 4.

9.6.0 Electrochemical experimental.

All monomers for electropolymerisation were in a pure state; prior to use their purity was confirmed by NMR, MS, IR and X-ray Crystallography. All electropolymerisation studies were carried out using the same experimental set-up given in section x.1.x and were performed on solutions of the monomers (0.02 mol) dissolved in an electrolyte solution containing TBATFB (0.1 mol). The solvents were acetonitrile and dichloromethane. All potentials are quoted *versus* silver wire.

9.6.1 Modification of polymer.

A platinum working electrode with a freshly deposited polymer of the unit (5) (potentiostatic growth, cycle 1 hour -0.3 V to $+1.8$ V, cycling stopped at 0.0 A, $+0.483$ V) was added to a 25 fold excess (ref) of the intermediate ylid, produced by the reaction of **16** (0.25 g, 0.5 mmol) dissolved in diethyl ether (10 ml) at 0°C with *n*-BuLi (0.5 mmol, 0.23 ml). The electrode in the reaction mixture was left in an inert atmosphere over night, and washed copiously with electrolyte solution, to remove any traces of unreacted ylid.

9.7.0 References.

- 1) M. Casey, J. Leonard, B. Lygo and G. Procter, (Ed.), *Advanced practical organic chemistry*, Blackie Ltd. (1990).
- 2) A. Charlton, M. Kalaji, P. J. Murphy, S. Salmasso, A. E. Underhill, G. Williams, M. B. Hursthouse and K. M. A. Malik; *Synth. Met.*, **95** (1998) 75.
- 3) S. Gronowitz, B. Gestblom and B. Mathiasson; *Archiv fuer Kemi.*, **20** (1963) 407.
- 4) S. Hibino; *J. Org. Chem.*, **49** (1984) 5006.
- 5) L. N. Lucas, J. V. Esch, R. M. Kellog and B. L. Feringa; *Tet. Lett.*, **40** (1999) 1775.
- 6) A. V. Samet, A. M. Shestopalov and V. N. Nesterov; *Synthesis.*, (1997) 622.
- 7) K. Ishikawa, K-Ya. Akiba and N. Inamoto; *Tet. Lett.*, (1976) 3695.
- 8) J. Lamy, D. Lavit and Ng. Ph. Buu-Hoi; *J. Chem. Soc.*, (1958) 4202.
- 9) A. W. Cooke, K. B. Wagener, G. J. Palenik, A. H. M. Verschuuren, A. E. Koziol and Z.-Y. Zhang; *Polym. Prepr. (Am. Chem. Soc., Div. Polym. Chem.)*, **30** (1989) 330.
- 10) P. E. Fanta; *Chem. Rev.*, **64** (1964) 613.
- 11) K. Uchida, Y. Nakayama and M. Irie; *Bull. Chem. Soc. Jpn.*, **63** (1990) 1311.
- 12) M. Irie and K. Uchida; *Bull. Chem. Soc. Jpn.*, **71** (1998) 985.
- 13) A. Charlton, A. E. Underhill, G. Williams, M. Kalaji, P. J. Murphy and K. M. A. Malik; *J. Org. Chem.*, **62** (1997) 3098.

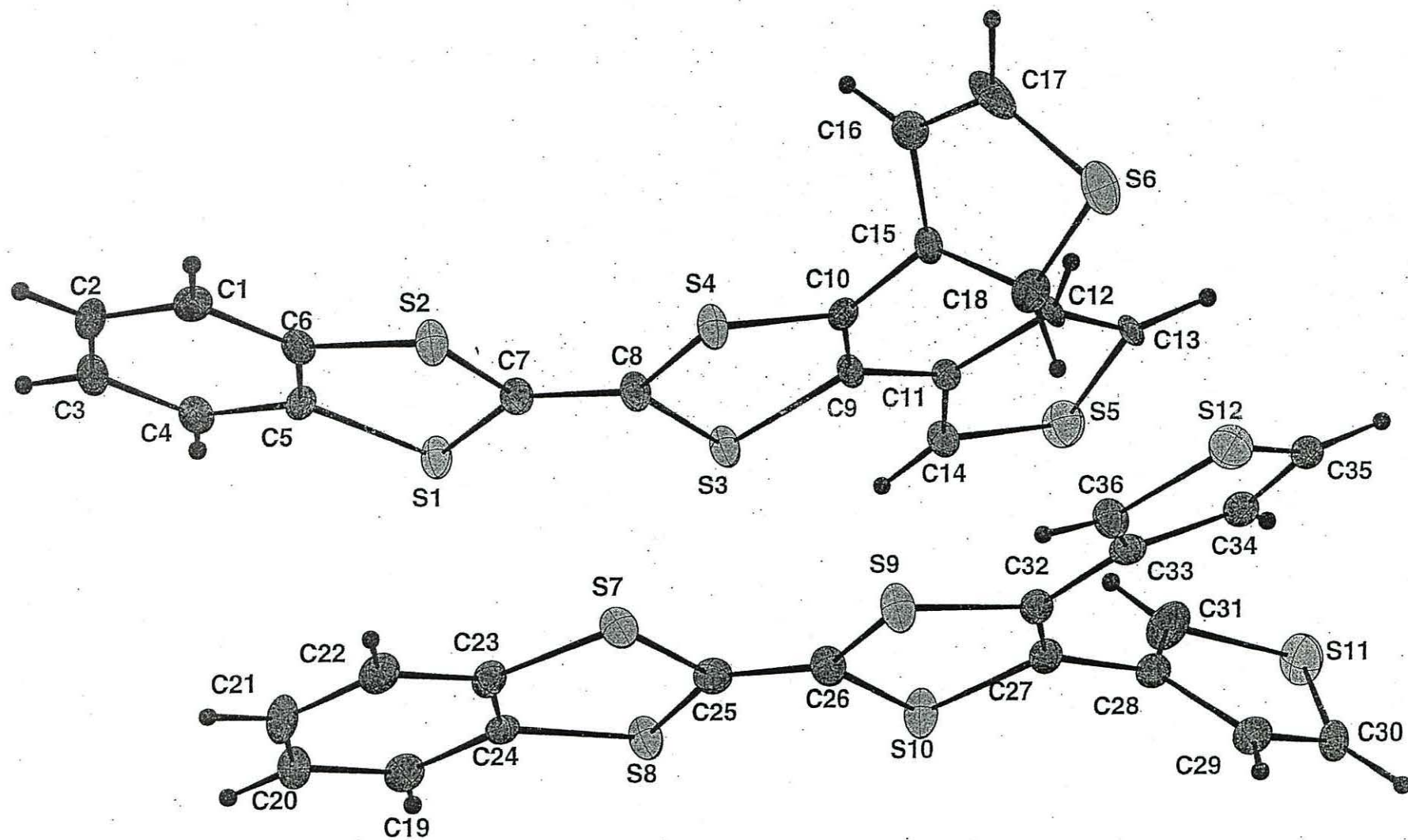
Table 1. Crystal data and structure refinement for 99src029.

Identification code	99src029
Empirical formula	C ₃₆ H ₂₀ S ₁₂
Formula weight	837.24
Temperature	150(2) K
Wavelength	0.71073 Å
Crystal system	Triclinic
Space group	P-1
Unit cell dimensions	a = 9.300(2) Å alpha = 80.75(3) deg. b = 12.701(3) Å beta = 85.77(3) deg. c = 16.235(3) Å gamma = 68.59(3) deg
Volume	1761.9(7) Å ³
Z	2
Density (calculated)	1.578 Mg/m ³
Absorption coefficient	0.773 mm ⁻¹
F(000)	856
Crystal size	0.25 x 0.25 x 0.05 mm
Theta range for data collection	2.35 to 26.34 deg.
Index ranges	-11 ≤ h ≤ 11, -15 ≤ k ≤ 15, -20 ≤ l ≤ 20
Reflections collected	28940
Independent reflections	7068 [R(int) = 0.0985]
Refinement method	Full-matrix least-squares on F ²
Data / restraints / parameters	7068 / 0 / 443
Goodness-of-fit on F ²	0.918
Final R indices [I > 2sigma(I)]	R1 = 0.0532, wR2 = 0.1247
R indices (all data)	R1 = 0.1137, wR2 = 0.1517
Largest diff. peak and hole	0.861 and -0.660 e.Å ⁻³

Table 3. Bond lengths [Å] and angles [deg] for 99src029.

S(1)-C(7)	1.755(4)	S(1)-C(5)	1.755(4)
S(2)-C(7)	1.752(4)	S(2)-C(6)	1.757(4)
S(3)-C(8)	1.752(4)	S(3)-C(9)	1.771(4)
S(4)-C(8)	1.749(4)	S(4)-C(10)	1.762(4)
S(5)-C(13)	1.683(4)	S(5)-C(14)	1.689(4)
S(6)-S(6')	1.516(8)	S(6)-C(17)	1.65(3)
S(6)-C(18)	1.710(5)	C(17')-S(6')	1.81(3)
S(7)-C(25)	1.748(4)	S(7)-C(23)	1.756(4)
S(8)-C(24)	1.749(4)	S(8)-C(25)	1.755(4)
S(9)-C(26)	1.757(4)	S(9)-C(32)	1.769(4)
S(10)-C(27)	1.752(4)	S(10)-C(26)	1.752(4)
S(11)-S(11')	1.618(12)	S(11)-C(30)	1.70(3)
S(11)-C(31)	1.692(6)	C(30')-S(11')	1.81(4)
S(12)-C(36)	1.707(4)	S(12)-C(35)	1.711(4)
C(1)-C(6)	1.379(5)	C(1)-C(2)	1.388(6)
C(2)-C(3)	1.386(6)	C(3)-C(4)	1.379(5)
C(4)-C(5)	1.389(6)	C(5)-C(6)	1.408(5)
C(7)-C(8)	1.349(5)	C(9)-C(10)	1.353(5)
C(9)-C(11)	1.462(5)	C(10)-C(15)	1.470(5)
C(11)-C(14)	1.375(5)	C(11)-C(12)	1.426(5)
C(12)-C(13)	1.458(5)	C(15)-C(18)	1.391(5)
C(15)-C(16)	1.399(5)	C(16)-C(17)	1.297(16)
C(19)-C(24)	1.381(6)	C(19)-C(20)	1.390(6)
C(20)-C(21)	1.381(6)	C(21)-C(22)	1.389(6)
C(22)-C(23)	1.377(6)	C(23)-C(24)	1.405(6)
C(25)-C(26)	1.356(6)	C(27)-C(32)	1.349(5)
C(27)-C(28)	1.473(6)	C(28)-C(31)	1.381(6)
C(28)-C(29)	1.399(5)	C(29)-C(30)	1.330(18)
C(32)-C(33)	1.476(6)	C(33)-C(36)	1.373(6)
C(33)-C(34)	1.425(6)	C(34)-C(35)	1.392(6)
C(7)-S(1)-C(5)	94.89(19)	C(7)-S(2)-C(6)	95.25(19)
C(8)-S(3)-C(9)	95.87(19)	C(8)-S(4)-C(10)	95.34(19)
C(13)-S(5)-C(14)	94.8(2)	S(6')-S(6)-C(17)	13.6(7)
S(6')-S(6)-C(18)	103.3(3)	C(17)-S(6)-C(18)	89.7(6)
C(25)-S(7)-C(23)	95.6(2)	C(24)-S(8)-C(25)	95.7(2)
C(26)-S(9)-C(32)	95.8(2)	C(27)-S(10)-C(26)	95.9(2)
S(11')-S(11)-C(30)	111.3(8)	S(11')-S(11)-C(31)	101.1(4)
C(30)-S(11)-C(31)	90.2(6)	C(36)-S(12)-C(35)	92.7(2)
C(6)-C(1)-C(2)	119.7(4)	C(3)-C(2)-C(1)	120.5(4)
C(4)-C(3)-C(2)	120.1(4)	C(3)-C(4)-C(5)	120.3(4)
C(4)-C(5)-C(6)	119.3(4)	C(4)-C(5)-S(1)	123.9(3)
C(6)-C(5)-S(1)	116.8(3)	C(1)-C(6)-C(5)	120.2(4)
C(1)-C(6)-S(2)	123.9(3)	C(5)-C(6)-S(2)	115.9(3)
C(8)-C(7)-S(2)	121.6(3)	C(8)-C(7)-S(1)	122.9(3)
S(2)-C(7)-S(1)	115.5(2)	C(7)-C(8)-S(3)	124.4(3)
C(7)-C(8)-S(4)	122.3(3)	S(3)-C(8)-S(4)	113.3(2)
C(10)-C(9)-C(11)	129.3(4)	C(10)-C(9)-S(3)	115.5(3)
C(11)-C(9)-S(3)	115.1(3)	C(9)-C(10)-C(15)	131.1(4)
C(9)-C(10)-S(4)	117.3(3)	C(15)-C(10)-S(4)	111.6(3)
C(14)-C(11)-C(12)	109.7(4)	C(14)-C(11)-C(9)	123.3(4)
C(12)-C(11)-C(9)	127.0(4)	C(11)-C(12)-C(13)	114.0(3)
C(12)-C(13)-S(5)	107.8(3)	C(11)-C(14)-S(5)	113.6(3)
C(18)-C(15)-C(16)	111.5(4)	C(18)-C(15)-C(10)	125.1(4)
C(16)-C(15)-C(10)	123.0(3)	C(17)-C(16)-C(15)	110.9(13)
C(16)-C(17)-S(6)	117.1(17)	S(6)-S(6')-C(17')	12.0(8)
C(15)-C(18)-S(6)	110.6(3)	C(24)-C(19)-C(20)	119.7(4)
C(21)-C(20)-C(19)	119.9(4)	C(20)-C(21)-C(22)	120.9(4)
C(23)-C(22)-C(21)	119.4(4)	C(22)-C(23)-C(24)	120.1(4)
C(22)-C(23)-S(7)	123.6(3)	C(24)-C(23)-S(7)	116.3(3)

C(19)-C(24)-C(23)	120.1(4)	C(19)-C(24)-S(8)	123.3(3)
C(23)-C(24)-S(8)	116.5(3)	C(26)-C(25)-S(7)	122.6(3)
C(26)-C(25)-S(8)	121.7(3)	S(7)-C(25)-S(8)	115.7(2)
C(25)-C(26)-S(10)	122.9(3)	C(25)-C(26)-S(9)	123.2(3)
S(10)-C(26)-S(9)	113.8(2)	C(32)-C(27)-C(28)	127.5(4)
C(32)-C(27)-S(10)	117.6(3)	C(28)-C(27)-S(10)	114.9(3)
C(31)-C(28)-C(29)	110.9(4)	C(31)-C(28)-C(27)	123.7(4)
C(29)-C(28)-C(27)	125.3(4)	C(30)-C(29)-C(28)	112.6(12)
C(29)-C(30)-S(11)	113.4(15)	S(11)-S(11')-C(30')	12.3(12)
C(28)-C(31)-S(11)	112.6(3)	C(27)-C(32)-C(33)	128.4(4)
C(27)-C(32)-S(9)	116.1(3)	C(33)-C(32)-S(9)	115.4(3)
C(36)-C(33)-C(34)	110.7(4)	C(36)-C(33)-C(32)	122.8(4)
C(34)-C(33)-C(32)	126.2(4)	C(35)-C(34)-C(33)	113.8(4)
C(34)-C(35)-S(12)	110.0(3)	C(33)-C(36)-S(12)	112.7(3)



Appendix 2.



Table 1. Crystal data and structure refinement.

Identification code	99src490	
Empirical formula	C ₁₁ H ₆ OS ₄	
Formula weight	282.40	
Temperature	150(2) K	
Wavelength	0.71073 Å	
Crystal system	Monoclinic	
Space group	P2 ₁ /c	
Unit cell dimensions	$a = 9.3195(4)$ Å	$\alpha = 90^\circ$
	$b = 15.3964(11)$ Å	$\beta = 96.040(3)^\circ$
	$c = 7.920(3)$ Å	$\gamma = 90^\circ$
Volume	1130.1(4) Å ³	
Z	4	
Density (calculated)	1.660 Mg / m ³	
Absorption coefficient	0.811 mm ⁻¹	
<i>F</i> (000)	576	
Crystal	Prism; colourless	
Crystal size	0.20 × 0.10 × 0.10 mm ³	
θ range for data collection	2.20 – 25.98°	
Index ranges	–11 ≤ <i>h</i> ≤ 11, –18 ≤ <i>k</i> ≤ 18, –8 ≤ <i>l</i> ≤ 9	
Reflections collected	6137	
Independent reflections	2194 [<i>R</i> _{int} = 0.0425]	
Completeness to $\theta = 25.98^\circ$	98.7 %	
Max. and min. transmission	0.9233 and 0.8547	
Refinement method	Full-matrix least-squares on <i>F</i> ²	
Data / restraints / parameters	2194 / 0 / 164	
Goodness-of-fit on <i>F</i> ²	0.975	
Final <i>R</i> indices [<i>F</i> ² > 2σ(<i>F</i> ²)]	<i>R</i> 1 = 0.0393, <i>wR</i> 2 = 0.0893	
<i>R</i> indices (all data)	<i>R</i> 1 = 0.0597, <i>wR</i> 2 = 0.0960	
Extinction coefficient	0.0035(10)	
Largest diff. peak and hole	0.389 and –0.352 e Å ⁻³	

Diffractometer: *Enraf Nonius KappaCCD* area detector (ϕ scans and ω scans to fill *Ewald* sphere). **Data collection and cell refinement:** *Denzo* (Z. Otwinowski & W. Minor, *Methods in Enzymology* (1997) Vol. 276: *Macromolecular Crystallography*, part A, pp. 307–326; C. W. Carter, Jr. & R. M. Sweet, Eds., Academic Press). **Absorption correction:** *SORTAV* (R. H. Blessing, *Acta Cryst. A* 51 (1995) 33–37; R. H. Blessing, *J. Appl. Cryst.* 30 (1997) 421–426). **Program used to solve structure:** *SHELXS97* (G. M. Sheldrick, *Acta Cryst.* (1990) A46 467–473). **Program used to refine structure:** *SHELXL97* (G. M. Sheldrick (1997), University of Göttingen, Germany).

Further information: <http://www.soton.ac.uk/~xservice/strat.htm>

Special details:

Table 2. Atomic coordinates [$\times 10^4$], equivalent isotropic displacement parameters [$\text{\AA}^2 \times 10^3$] and site occupancy factors. U_{eq} is defined as one third of the trace of the orthogonalized U^{ij} tensor.

Atom	<i>x</i>	<i>y</i>	<i>z</i>	U_{eq}	<i>S.o.f.</i>
S1	5886(1)	7692(1)	1012(1)	26(1)	1
S2	8520(1)	6719(1)	2073(1)	26(1)	1
S3	6317(1)	10801(1)	1584(1)	32(1)	1
S4	12823(1)	8280(1)	3567(1)	34(1)	1
O1	6044(2)	5979(1)	976(2)	35(1)	1
C1	6680(3)	6654(2)	1288(3)	26(1)	1
C2	7433(3)	8303(2)	1654(3)	21(1)	1
C3	8652(3)	7853(2)	2137(3)	19(1)	1
C4	6218(3)	9732(2)	2108(3)	24(1)	1
C5	7273(3)	9247(2)	1463(3)	21(1)	1
C6	8164(3)	9768(2)	518(3)	27(1)	1
C7	7756(3)	10650(2)	476(3)	21(1)	1
C8	11341(3)	7737(2)	2661(3)	27(1)	1
C9	10091(3)	8199(2)	2752(3)	22(1)	1
C10	10377(3)	9015(2)	3571(3)	25(1)	1
C11	11806(3)	9143(2)	4074(3)	29(1)	1

Table 3. Bond lengths [Å] and angles [°].

S1-C2	1.752(3)
S1-C1	1.766(3)
S2-C3	1.750(3)
S2-C1	1.764(3)
S3-C7	1.694(3)
S3-C4	1.702(3)
S4-C11	1.705(3)
S4-C8	1.707(3)
O1-C1	1.208(3)
C2-C3	1.351(3)
C2-C5	1.467(4)
C3-C9	1.477(3)
C4-C5	1.375(4)
C4-H4	0.89(3)
C5-C6	1.423(4)
C6-C7	1.410(4)
C6-H6	1.01(4)
C7-H7	0.9500
C8-C9	1.374(4)
C8-H8	0.95(3)
C9-C10	1.426(4)
C10-C11	1.363(4)
C10-H10	0.90(3)
C11-H11	0.9500
C2-S1-C1	97.37(13)
C3-S2-C1	97.49(12)
C7-S3-C4	93.46(13)
C11-S4-C8	92.01(14)
O1-C1-S2	124.0(2)
O1-C1-S1	124.2(2)
S2-C1-S1	111.77(15)
C3-C2-C5	127.6(2)
C3-C2-S1	116.7(2)
C5-C2-S1	115.46(18)
C2-C3-C9	128.0(2)
C2-C3-S2	116.66(19)
C9-C3-S2	115.34(18)
C5-C4-S3	112.0(2)
C5-C4-H4	124.4(19)
S3-C4-H4	123.5(19)
C4-C5-C6	111.6(2)
C4-C5-C2	124.7(2)
C6-C5-C2	123.7(2)
C7-C6-C5	112.6(2)
C7-C6-H6	122(2)
C5-C6-H6	125(2)
C6-C7-S3	110.21(19)
C6-C7-H7	124.9
S3-C7-H7	124.9
C9-C8-S4	112.2(2)
C9-C8-H8	126.5(17)
S4-C8-H8	120.9(18)
C8-C9-C10	111.2(2)
C8-C9-C3	122.8(2)
C10-C9-C3	126.0(2)
C11-C10-C9	113.0(3)
C11-C10-H10	121.2(18)
C9-C10-H10	125.8(18)

C10-C11-S4	111.7(2)
C10-C11-H11	124.2
S4-C11-H11	124.2

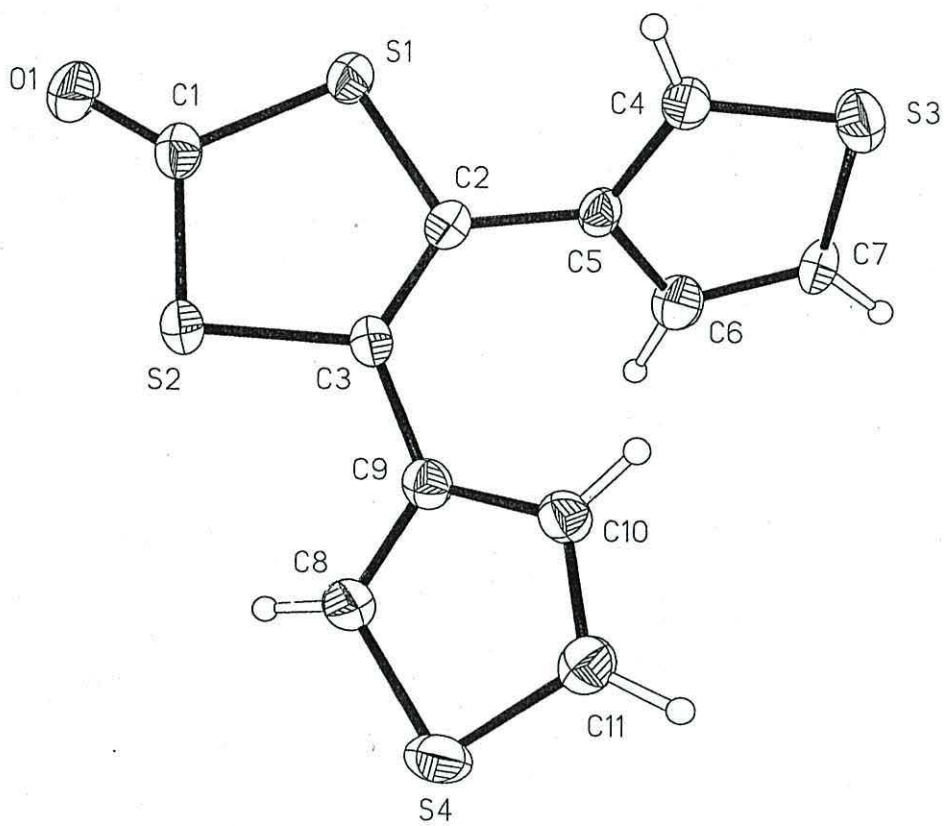
Symmetry transformations used to generate equivalent atoms:

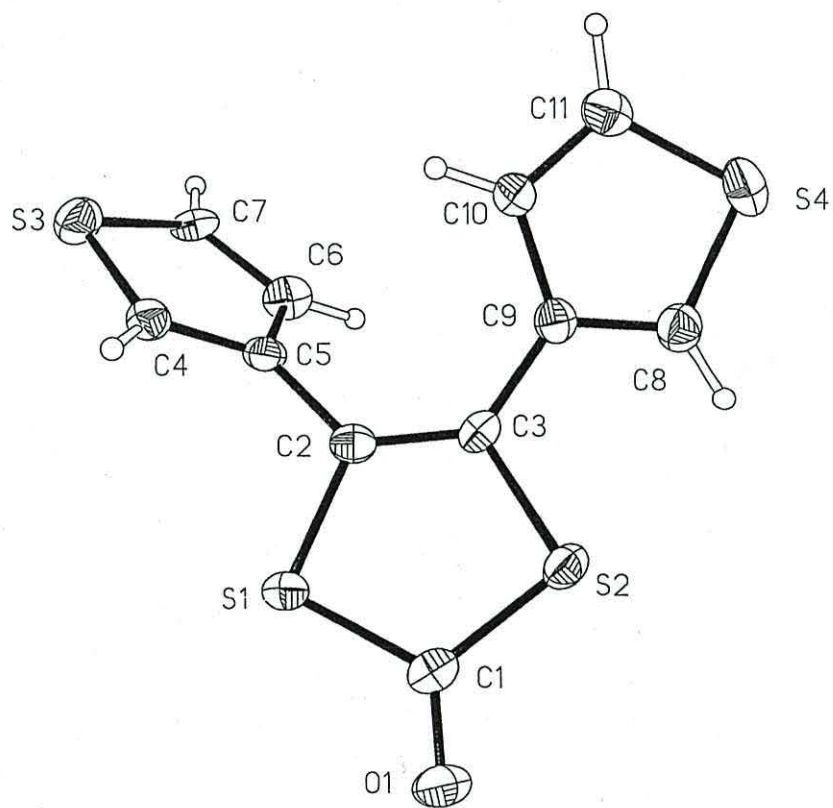
Table 4. Anisotropic displacement parameters [$\text{\AA}^2 \times 10^3$]. The anisotropic displacement factor exponent takes the form: $-2\pi^2[h^2 a^{*2} U^{11} + \dots + 2 h k a^* b^* U^{12}]$.

Atom	U^{11}	U^{22}	U^{33}	U^{23}	U^{13}	U^{12}
S1	24(1)	20(1)	34(1)	-2(1)	-2(1)	-3(1)
S2	29(1)	17(1)	32(1)	1(1)	4(1)	2(1)
S3	37(1)	23(1)	34(1)	0(1)	-2(1)	5(1)
S4	22(1)	41(1)	40(1)	9(1)	-1(1)	3(1)
O1	36(1)	23(1)	45(1)	-8(1)	4(1)	-6(1)
C1	32(2)	20(2)	26(1)	-1(1)	6(1)	-1(1)
C2	23(1)	20(1)	21(1)	0(1)	3(1)	-3(1)
C3	25(1)	16(1)	18(1)	1(1)	6(1)	2(1)
C4	24(1)	20(1)	27(1)	1(1)	-1(1)	-1(1)
C5	22(1)	18(1)	23(1)	-1(1)	-4(1)	-2(1)
C6	32(2)	26(2)	24(1)	1(1)	3(1)	-2(1)
C7	32(1)	15(1)	16(1)	-1(1)	3(1)	-6(1)
C8	26(2)	24(2)	32(1)	3(1)	2(1)	1(1)
C9	24(1)	23(1)	21(1)	3(1)	1(1)	1(1)
C10	25(2)	25(2)	25(1)	-3(1)	-1(1)	2(1)
C11	31(2)	28(2)	26(1)	4(1)	0(1)	-3(1)

Table 5. Hydrogen coordinates [$\times 10^4$] and isotropic displacement parameters [$\text{\AA}^2 \times 10^3$].

Atom	<i>x</i>	<i>y</i>	<i>z</i>	U_{eq}	<i>S.o.f.</i>
H4	5550(30)	9516(19)	2710(40)	38(8)	1
H6	8900(40)	9530(20)	-220(40)	67(11)	1
H7	8222	11096	-92	32(8)	1
H8	11440(30)	7210(20)	2060(40)	34(8)	1
H10	9720(30)	9424(19)	3730(30)	26(7)	1
H11	12187	9650	4637	50(9)	1





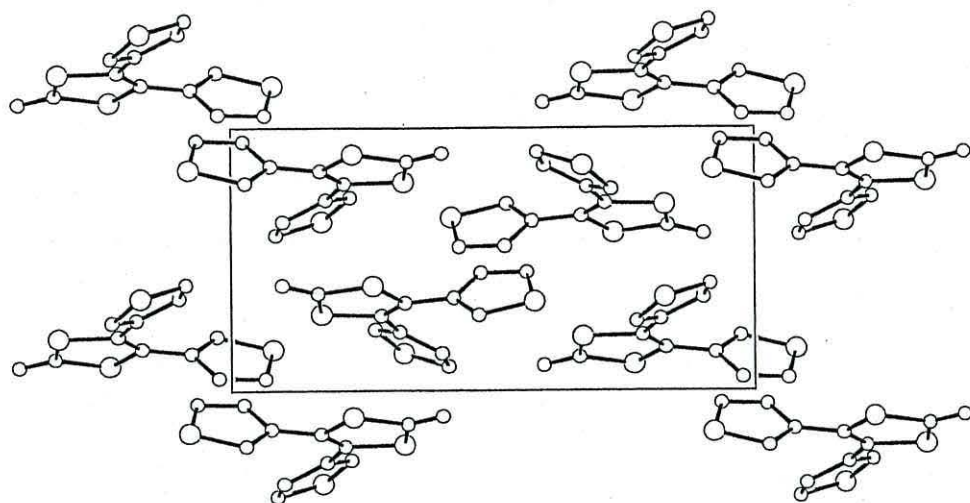




Table 1. Crystal data and structure refinement.

Identification code	00src186	
Empirical formula	C ₁₃ H ₁₀ OS ₄	
Formula weight	310.45	
Temperature	150(2) K	
Wavelength	0.71073 Å	
Crystal system	Orthorhombic	
Space group	<i>Pbcn</i>	
Unit cell dimensions	<i>a</i> = 14.5002(3) Å	$\alpha = 90^\circ$
	<i>b</i> = 13.4816(3) Å	$\beta = 90^\circ$
	<i>c</i> = 7.00910(10) Å	$\gamma = 90^\circ$
Volume	1370.18(5) Å ³	
Z	4	
Density (calculated)	1.505 Mg / m ³	
Absorption coefficient	0.676 mm ⁻¹	
<i>F</i> (000)	640	
Crystal	Block; colourless	
Crystal size	0.20 × 0.20 × 0.15 mm ³	
θ range for data collection	3.02 – 25.99°	
Index ranges	–15 ≤ <i>h</i> ≤ 17, –16 ≤ <i>k</i> ≤ 15, –8 ≤ <i>l</i> ≤ 8	
Reflections collected	5309	
Independent reflections	1343 [<i>R</i> _{int} = 0.0298]	
Completeness to $\theta = 25.99^\circ$	99.3 %	
Max. and min. transmission	0.9054 and 0.8766	
Refinement method	Full-matrix least-squares on <i>F</i> ²	
Data / restraints / parameters	1343 / 0 / 93	
Goodness-of-fit on <i>F</i> ²	1.081	
Final <i>R</i> indices [<i>F</i> ² > 2σ(<i>F</i> ²)]	<i>R</i> 1 = 0.0380, <i>wR</i> 2 = 0.1020	
<i>R</i> indices (all data)	<i>R</i> 1 = 0.0426, <i>wR</i> 2 = 0.1049	
Extinction coefficient	0.0000(19)	
Largest diff. peak and hole	0.672 and –0.600 e Å ⁻³	

Diffractometer: *Enraf Nonius KappaCCD* area detector (ϕ scans and ω scans to fill *Ewald* sphere). **Data collection and cell refinement:** *Denzo* (Z. Otwinowski & W. Minor, *Methods in Enzymology* (1997) Vol. 276: *Macromolecular Crystallography*, part A, pp. 307–326; C. W. Carter, Jr. & R. M. Sweet, Eds., Academic Press). **Absorption correction:** *SORTAV* (R. H. Blessing, *Acta Cryst. A* 51 (1995) 33–37; R. H. Blessing, *J. Appl. Cryst.* 30 (1997) 421–426 **Program used to solve structure:** *DIRDIF-96* (P. T. Beurskens, G. Beurskens, W. P. Bosman, R. de Gelder, S. Garcia-Granda, R. O. Gould, R. Israël & J. M. M. Smits (1996). Crystallography Laboratory, University of Nijmegen, The Netherlands. **Program used to refine structure:** *SHELXL97* (G. M. Sheldrick (1997), University of Göttingen, Germany).

Further information: <http://www.soton.ac.uk/~xservice/strat.htm>

Special details:

Table 2. Atomic coordinates [$\times 10^4$], equivalent isotropic displacement parameters [$\text{\AA}^2 \times 10^3$] and site occupancy factors. U_{eq} is defined as one third of the trace of the orthogonalized U^{ij} tensor.

Atom	<i>x</i>	<i>y</i>	<i>z</i>	U_{eq}	<i>S.o.f.</i>
S1	991(1)	566(1)	2117(1)	29(1)	1
S2	1918(1)	4213(1)	2888(1)	33(1)	1
O1	0	-1068(2)	2500	48(1)	1
C1	586(2)	3455(2)	5353(3)	36(1)	1
C2	1109(1)	3339(2)	3530(3)	25(1)	1
C3	1075(1)	2588(2)	2217(3)	23(1)	1
C4	2226(2)	3557(2)	893(4)	40(1)	1
C5	1730(2)	2721(2)	705(3)	35(1)	1
C6	458(2)	1725(1)	2340(3)	22(1)	1
C10	0	-172(2)	2500	32(1)	1

Table 3. Bond lengths [Å] and angles [°].

S1-C6	1.751(2)
S1-C10	1.7688(18)
S2-C4	1.714(3)
S2-C2	1.722(2)
O1-C10	1.207(4)
C1-C2	1.494(3)
C2-C3	1.369(3)
C3-C5	1.434(3)
C3-C6	1.470(3)
C4-C5	1.344(3)
C6-C6 ⁱ	1.347(4)
C10-S1 ⁱ	1.7688(18)
C6-S1-C10	97.45(11)
C4-S2-C2	92.15(11)
C3-C2-C1	129.32(18)
C3-C2-S2	110.79(15)
C1-C2-S2	119.85(16)
C2-C3-C5	112.36(19)
C2-C3-C6	124.59(18)
C5-C3-C6	123.03(19)
C5-C4-S2	111.92(17)
C4-C5-C3	112.8(2)
C6 ⁱ -C6-C3	127.58(11)
C6 ⁱ -C6-S1	116.78(7)
C3-C6-S1	115.62(15)
O1-C10-S1	124.24(8)
O1-C10-S1 ⁱ	124.24(8)
S1-C10-S1 ⁱ	111.53(17)

Symmetry transformations used to generate equivalent atoms:

(i) $-x, y, -z+1/2$

Table 4. Anisotropic displacement parameters [$\text{\AA}^2 \times 10^3$]. The anisotropic displacement factor exponent takes the form: $-2\pi^2[h^2 a^{*2} U^{11} + \dots + 2 h k a^* b^* U^{12}]$.

Atom	U^{11}	U^{22}	U^{33}	U^{23}	U^{13}	U^{12}
S1	35(1)	21(1)	31(1)	-2(1)	-9(1)	8(1)
S2	27(1)	24(1)	48(1)	7(1)	5(1)	-5(1)
O1	74(2)	17(1)	54(2)	0	-28(1)	0
C1	43(1)	35(1)	30(1)	-10(1)	5(1)	-16(1)
C2	22(1)	23(1)	29(1)	4(1)	2(1)	-3(1)
C3	21(1)	22(1)	25(1)	4(1)	2(1)	4(1)
C4	35(1)	36(1)	50(1)	11(1)	21(1)	3(1)
C5	36(1)	32(1)	38(1)	3(1)	14(1)	9(1)
C6	29(1)	18(1)	18(1)	-1(1)	-2(1)	5(1)
C10	47(2)	20(2)	29(2)	0	-17(1)	0

Table 5. Hydrogen coordinates [$\times 10^4$] and isotropic displacement parameters [$\text{\AA}^2 \times 10^3$].

Atom	<i>x</i>	<i>y</i>	<i>z</i>	U_{eq}	<i>S.o.f.</i>
H1A	766	4077	5974	50(20)	0.45(7)
H1B	724	2896	6200	80(30)	0.45(7)
H1C	-77	3468	5080	80(30)	0.45(7)
H1D	176	2884	5528	24(15)	0.55(7)
H1E	218	4065	5302	70(20)	0.55(7)
H1F	1019	3493	6422	42(17)	0.55(7)
H4	2692	3760	24	47(7)	1
H5	1805	2267	-320	38(7)	1

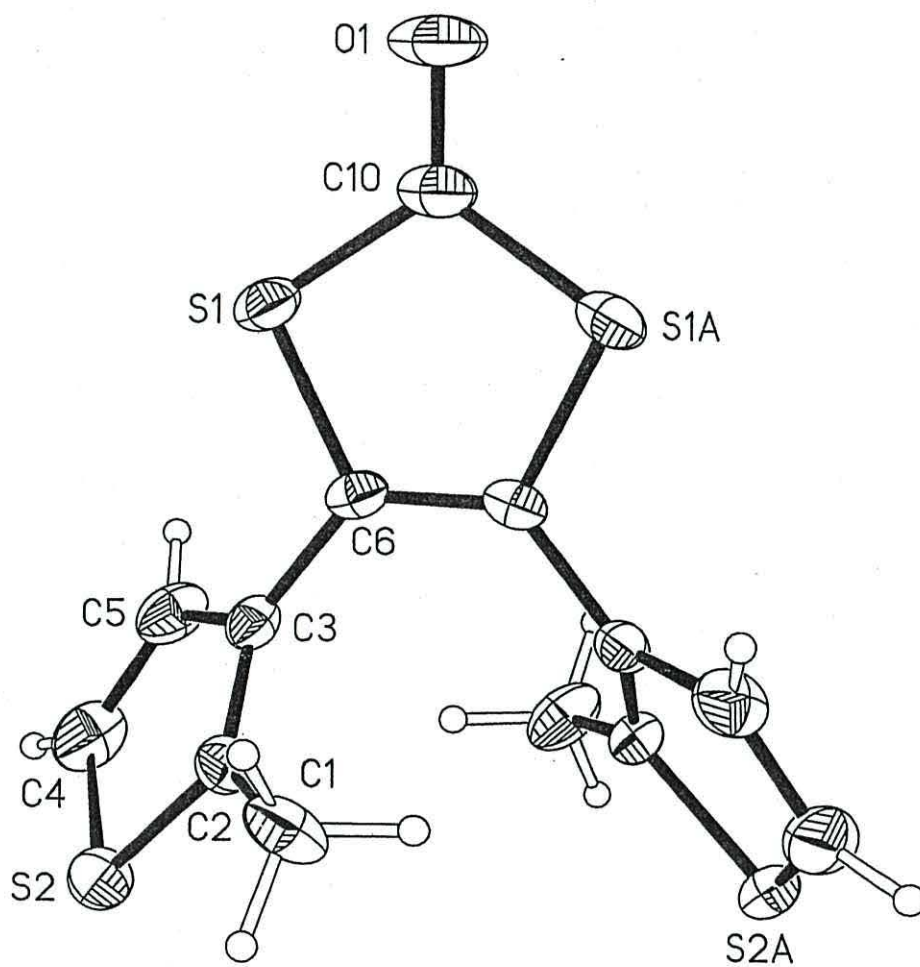




Table 1. Crystal data and structure refinement.

Identification code	99SRC296
Empirical formula	C ₁₅ H ₁₄ OS ₄
Formula weight	338.50
Temperature	150(2) K
Wavelength	0.71073 Å
Crystal system	Monoclinic
Space group	C2/c
Unit cell dimensions	$a = 15.2123(4)$ Å $b = 14.4906(3)$ Å $c = 9.0328(2)$ Å $\beta = 125.8601(13)^\circ$
Volume	1613.72(6) Å ³
Z	4
Density (calculated)	1.393 Mg / m ³
Absorption coefficient	0.580 mm ⁻¹
$F(000)$	704
Crystal	Colourless block
Crystal size	0.30 × 0.30 × 0.20 mm ³
θ range for data collection	3.30 – 25.03°
Index ranges	–18 ≤ h ≤ 18, –16 ≤ k ≤ 17, –10 ≤ l ≤ 10
Reflections collected	9039
Independent reflections	1433 [$R_{int} = 0.0356$]
Completeness to $\theta = 25.03^\circ$	96.0 %
Absorption correction	Empirical, SORTAV
Max. and min. transmission	0.8927 and 0.8451
Refinement method	Full-matrix least-squares on F^2
Data / restraints / parameters	1433 / 0 / 121
Goodness-of-fit on F^2	1.051
Final R indices [$F^2 > 2\sigma(F^2)$]	$RI = 0.0289$, $wR2 = 0.0731$
R indices (all data)	$RI = 0.0314$, $wR2 = 0.0749$
Extinction coefficient	0.0059(8)
Largest diff. peak and hole	0.251 and –0.247 e Å ⁻³

Diffractometer: *Enraf Nonius KappaCCD* area detector (ϕ scans and ω scans to fill *Ewald* sphere). **Data collection and cell refinement:** *Denzo* (Z. Otwinowski & W. Minor, *Methods in Enzymology* (1997) Vol. 276: *Macromolecular Crystallography*, part A, pp. 307–326; C. W. Carter, Jr. & R. M. Sweet, Eds., Academic Press). **Absorption correction:** *SORTAV* (R. H. Blessing, *Acta Cryst. A* 51 (1995) 33–37; R. H. Blessing, *J. Appl. Cryst.* 30 (1997) 421–426). **Program used to solve structure:** *SHELXS97* (G. M. Sheldrick, *Acta Cryst.* (1990) A46 467–473). **Program used to refine structure:** *SHELXL97* (G. M. Sheldrick (1997), University of Göttingen, Germany).

Further information: <http://www.soton.ac.uk/~xservic/strat.htm>

Special details: Hydrogen atoms were located from the difference map and freely refined.

Table 2. Atomic coordinates [$\times 10^4$], equivalent isotropic displacement parameters [$\text{\AA}^2 \times 10^3$] and site occupancy factors. U_{eq} is defined as one third of the trace of the orthogonalized U^{ij} tensor.

Atom	x	y	z	U_{eq}	S.o.f.
S2	756(1)	643(1)	9485(1)	26(1)	1
S1	1940(1)	4002(1)	11183(1)	34(1)	1
O1	0	-873(1)	7500	34(1)	1
C4	897(1)	2518(1)	9654(2)	22(1)	1
C7	365(1)	1727(1)	8417(2)	21(1)	1
C6	1434(2)	3419(1)	7812(3)	31(1)	1
C3	1009(2)	2593(1)	11338(2)	27(1)	1
C8	0	-36(2)	7500	26(1)	1
C5	1368(1)	3239(1)	9374(2)	24(1)	1
C2	1547(2)	3357(1)	12313(3)	32(1)	1
C1	1796(3)	3672(2)	14104(3)	50(1)	1

Table 3. Bond lengths [\AA] and angles [$^\circ$].

S2-C7	1.7552(16)	C4-C7	1.469(2)
S2-C8	1.7569(14)	C7-C7 ⁱ	1.350(3)
S1-C5	1.7272(17)	C6-C5	1.495(2)
S1-C2	1.7281(18)	C3-C2	1.351(3)
O1-C8	1.213(3)	C8-S2 ⁱ	1.7569(14)
C4-C5	1.371(2)	C2-C1	1.500(3)
C4-C3	1.433(2)		
C7-S2-C8	97.57(9)	O1-C8-S2	124.02(7)
C5-S1-C2	93.23(8)	O1-C8-S2 ⁱ	124.02(7)
C5-C4-C3	112.85(15)	S2-C8-S2 ⁱ	111.97(13)
C5-C4-C7	124.70(15)	C4-C5-C6	129.65(16)
C3-C4-C7	122.41(15)	C4-C5-S1	109.94(13)
C7 ⁱ -C7-C4	128.59(9)	C6-C5-S1	120.41(13)
C7 ⁱ -C7-S2	116.40(6)	C3-C2-C1	128.75(18)
C4-C7-S2	115.00(12)	C3-C2-S1	110.16(14)
C2-C3-C4	113.82(16)	C1-C2-S1	121.09(15)

Symmetry transformations used to generate equivalent atoms:

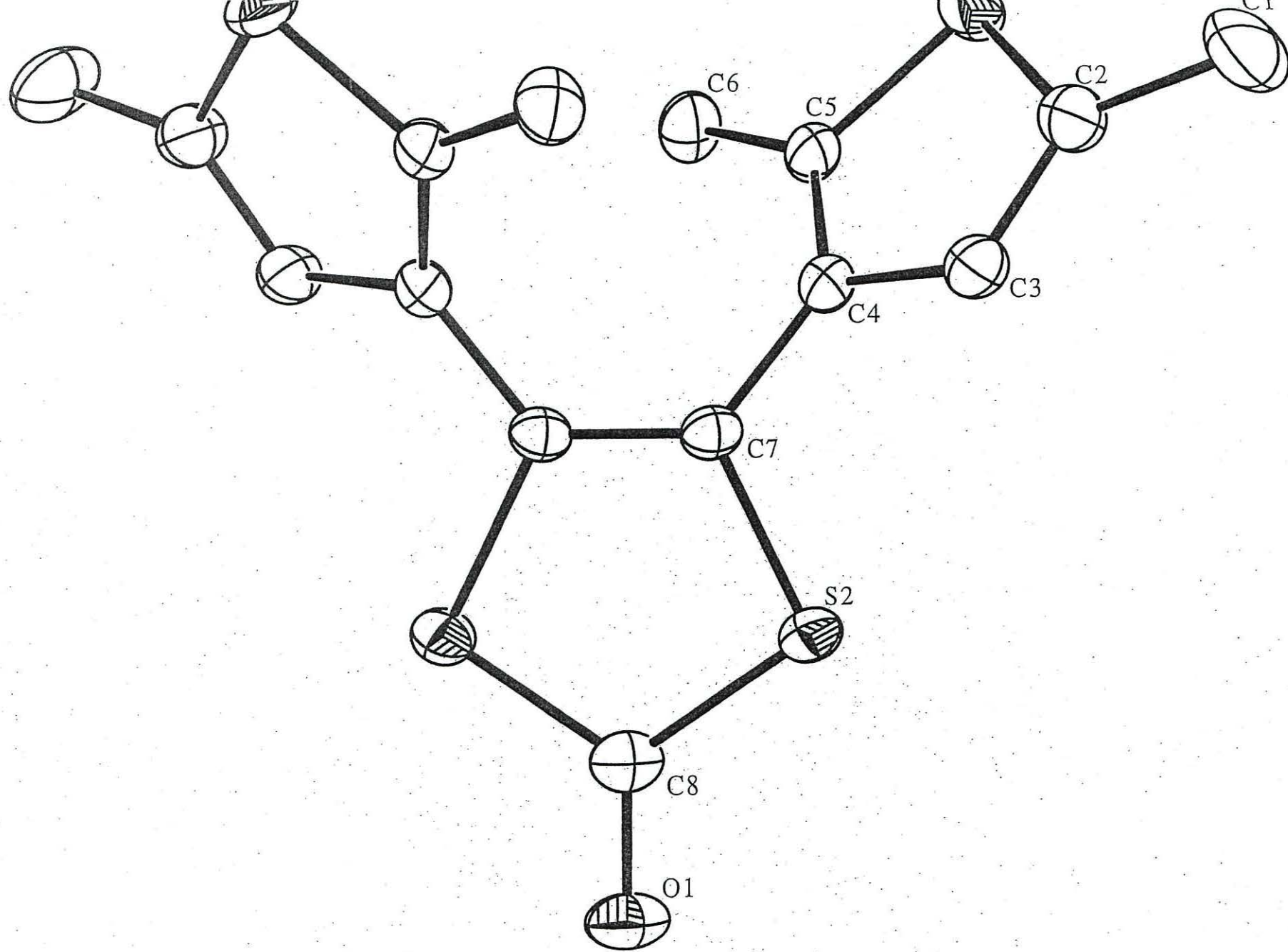
(i) $-x, y, -z+3/2$

Table 4. Anisotropic displacement parameters [$\text{\AA}^2 \times 10^3$]. The anisotropic displacement factor exponent takes the form: $-2\pi^2 [h^2 a^{*2} U^{11} + \dots + 2 h k a^* b^* U^{12}]$.

Atom	U^{11}	U^{22}	U^{33}	U^{23}	U^{13}	U^{12}
S2	33(1)	20(1)	26(1)	3(1)	18(1)	-2(1)
S1	46(1)	24(1)	29(1)	-3(1)	20(1)	-12(1)
O1	55(1)	19(1)	44(1)	0	37(1)	0
C4	24(1)	21(1)	20(1)	2(1)	12(1)	0(1)
C7	24(1)	19(1)	24(1)	2(1)	16(1)	-1(1)
C6	31(1)	35(1)	27(1)	4(1)	17(1)	-7(1)
C3	36(1)	24(1)	24(1)	2(1)	20(1)	-3(1)
C8	35(1)	23(1)	34(1)	0	28(1)	0
C5	26(1)	23(1)	21(1)	2(1)	12(1)	-2(1)
C2	46(1)	26(1)	27(1)	-1(1)	23(1)	-4(1)
C1	79(2)	41(1)	36(1)	-12(1)	37(1)	-14(1)

Table 5. Hydrogen coordinates [$\times 10^4$] and isotropic displacement parameters [$\text{\AA}^2 \times 10^3$].

Atom	x	y	z	U_{eq}	$S.o.f.$
H3	730(16)	2145(15)	11730(30)	33(5)	1
H6B	810(20)	3735(17)	6810(30)	50(6)	1
H6A	1464(18)	2830(17)	7310(30)	45(6)	1
H6C	2069(19)	3763(16)	8170(30)	43(6)	1
H1A	1610(20)	3220(20)	14580(40)	63(8)	1
H1B	2560(30)	3810(30)	14990(60)	105(12)	1
H1C	1330(20)	4180(20)	13940(40)	71(9)	1



Appendix 3.



Table 1. Crystal data and structure refinement.

Identification code	00SRC180
Empirical formula	C ₁₀ H ₈ S ₂
Formula weight	96.14
Temperature	150(2) K
Wavelength	0.71073 Å
Crystal system	Orthorhombic
Space group	<i>Pnaa</i>
Unit cell dimensions	$a = 5.6592(4)$ Å $b = 7.4172(6)$ Å $c = 21.2420(17)$ Å
Volume	891.64(12) Å ³
Z	4
Density (calculated)	1.432 Mg / m ³
Absorption coefficient	0.531 mm ⁻¹
<i>F</i> (000)	400
Crystal	Colourless plate
Crystal size	0.25 × 0.20 × 0.02 mm ³
θ range for data collection	3.84 – 25.03°
Index ranges	–5 ≤ <i>h</i> ≤ 6, –7 ≤ <i>k</i> ≤ 8, –24 ≤ <i>l</i> ≤ 25
Reflections collected	2665
Independent reflections	776 [<i>R</i> _{int} = 0.0411]
Completeness to $\theta = 25.03^\circ$	98.4 %
Absorption correction	Empirical
Max. and min. transmission	0.9895 and 0.8787
Refinement method	Full-matrix least-squares on <i>F</i> ²
Data / restraints / parameters	776 / 0 / 72
Goodness-of-fit on <i>F</i> ²	1.054
Final <i>R</i> indices [<i>F</i> ² > 2σ(<i>F</i> ²)]	<i>R</i> 1 = 0.0423, <i>wR</i> 2 = 0.1153
<i>R</i> indices (all data)	<i>R</i> 1 = 0.0580, <i>wR</i> 2 = 0.1240
Extinction coefficient	0.005(5)
Largest diff. peak and hole	0.458 and –0.353 e Å ⁻³

Diffractometer: *Enraf Nonius KappaCCD* area detector (ϕ scans and ω scans to fill *Ewald* sphere). **Data collection and cell refinement:** *Denzo* (Z. Otwinowski & W. Minor, *Methods in Enzymology* (1997) Vol. 276: *Macromolecular Crystallography*, part A, pp. 307–326; C. W. Carter, Jr. & R. M. Sweet, Eds., Academic Press). **Absorption correction:** *SORTAV* (R. H. Blessing, *Acta Cryst. A* 51 (1995) 33–37; R. H. Blessing, *J. Appl. Cryst.* 30 (1997) 421–426). **Program used to solve structure:** *SHELXS97* (G. M. Sheldrick, *Acta Cryst.* (1990) A46 467–473). **Program used to refine structure:** *SHELXL97* (G. M. Sheldrick (1997), University of Göttingen, Germany).

Further information: <http://www.soton.ac.uk/~xservice/strat.htm>

Special details: All hydrogen atoms were located from the difference map and fully refined.

Table 2. Atomic coordinates [$\times 10^4$], equivalent isotropic displacement parameters [$\text{\AA}^2 \times 10^3$] and site occupancy factors. U_{eq} is defined as one third of the trace of the orthogonalized U^{ij} tensor.

Atom	<i>x</i>	<i>y</i>	<i>z</i>	U_{eq}	<i>S.o.f.</i>
C1	4460(4)	5720(3)	3574(1)	25(1)	1
C2	3773(4)	5145(3)	4157(1)	24(1)	1
C3	1520(4)	4250(4)	4128(1)	28(1)	1
C4	624(4)	4159(3)	3528(1)	24(1)	1
C5	5210(5)	5371(4)	4719(1)	29(1)	1
S1	2482(1)	5148(1)	2998(1)	29(1)	1

Table 3. Bond lengths [\AA] and angles [$^\circ$].

C1–C2	1.366(3)	C3–C4	1.374(4)
C1–S1	1.711(2)	C4–S1	1.706(2)
C2–C3	1.438(4)	C5–C5 ⁱ	1.337(5)
C2–C5	1.455(4)		
C2–C1–S1	112.6(2)	C4–C3–C2	112.9(2)
C1–C2–C3	111.0(2)	C3–C4–S1	111.30(19)
C1–C2–C5	123.3(2)	C5 ⁱ –C5–C2	126.0(3)
C3–C2–C5	125.7(2)	C4–S1–C1	92.21(14)

Symmetry transformations used to generate equivalent atoms:

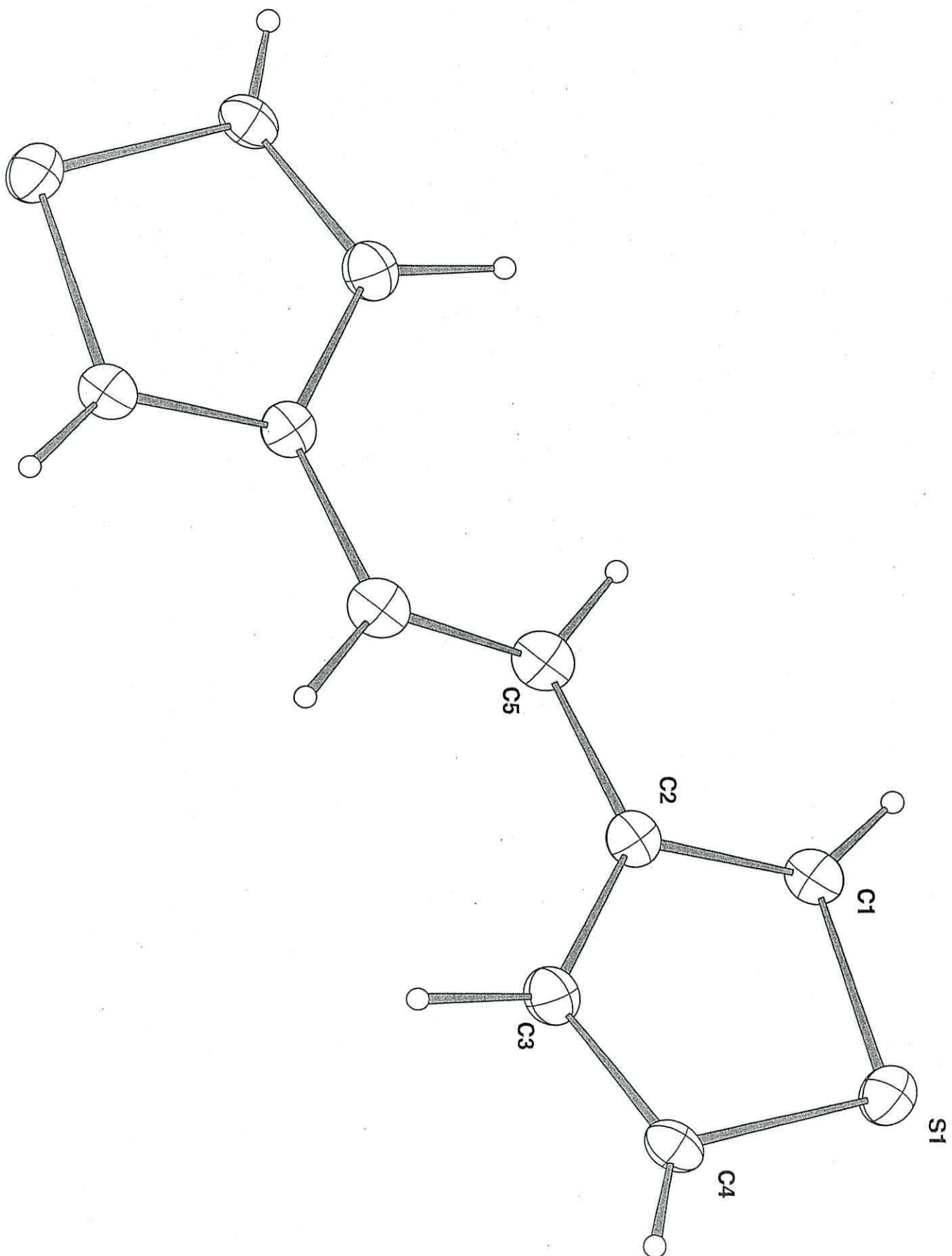
(i) $-x+1, -y+1, -z+1$

Table 4. Anisotropic displacement parameters [$\text{\AA}^2 \times 10^3$]. The anisotropic displacement factor exponent takes the form: $-2\pi^2 [h^2 a^{*2} U^{11} + \dots + 2 h k a^* b^* U^{12}]$.

Atom	U^{11}	U^{22}	U^{33}	U^{23}	U^{13}	U^{12}
C1	24(1)	20(1)	31(1)	2(1)	1(1)	0(1)
C2	25(1)	19(1)	27(1)	−2(1)	2(1)	1(1)
C3	27(1)	26(1)	29(2)	1(1)	3(1)	−2(1)
C4	19(1)	20(1)	33(2)	−2(1)	1(1)	−1(1)
C5	29(2)	22(2)	35(2)	−2(1)	1(1)	−1(1)
S1	32(1)	30(1)	25(1)	2(1)	−1(1)	1(1)

Table 5. Hydrogen coordinates [$\times 10^4$] and isotropic displacement parameters [$\text{\AA}^2 \times 10^3$].

Atom	<i>x</i>	<i>y</i>	<i>z</i>	U_{eq}	<i>S.o.f.</i>
H1	5760(40)	6340(30)	3474(11)	25(7)	1
H3	660(50)	3790(40)	4513(12)	42(8)	1
H4	−600(40)	3770(40)	3419(11)	28(8)	1
H5	6670(50)	6090(40)	4660(13)	52(8)	1



Appendix 4.



Table 1. Crystal data and structure refinement.

Identification code	00src209	
Empirical formula	C ₂₆ H ₂₀ S ₈	
Formula weight	588.90	
Temperature	150(2) K	
Wavelength	0.71073 Å	
Crystal system	Monoclinic	
Space group	C2/c	
Unit cell dimensions	$a = 27.083(2)$ Å	$\alpha = 90^\circ$
	$b = 10.09110(10)$ Å	$\beta = 110.212(3)^\circ$
	$c = 20.304(2)$ Å	$\gamma = 90^\circ$
Volume	$5207.5(6)$ Å ³	
Z	8	
Density (calculated)	1.502 Mg / m ³	
Absorption coefficient	0.702 mm ⁻¹	
$F(000)$	2432	
Crystal	Platelet; colourless	
Crystal size	$0.12 \times 0.02 \times 0.01$ mm ³	
θ range for data collection	$3.04 - 23.48^\circ$	
Index ranges	$-29 \leq h \leq 25, -8 \leq k \leq 11, -21 \leq l \leq 22$	
Reflections collected	11126	
Independent reflections	3519 [$R_{int} = 0.1172$]	
Completeness to $\theta = 23.48^\circ$	91.4 %	
Max. and min. transmission	0.9965 and 0.9205	
Refinement method	Full-matrix least-squares on F^2	
Data / restraints / parameters	3519 / 0 / 325	
Goodness-of-fit on F^2	1.073	
Final R indices [$F^2 > 2\sigma(F^2)$]	$R1 = 0.0709, wR2 = 0.1212$	
R indices (all data)	$R1 = 0.1452, wR2 = 0.1354$	
Largest diff. peak and hole	0.462 and -0.357 e Å ⁻³	

Diffractometer: *Enraf Nonius KappaCCD* area detector (ϕ scans and ω scans to fill *Ewald* sphere). **Data collection and cell refinement:** *Denzo* (Z. Otwinowski & W. Minor, *Methods in Enzymology* (1997) Vol. 276: *Macromolecular Crystallography*, part A, pp. 307–326; C. W. Carter, Jr. & R. M. Sweet, Eds., Academic Press). **Absorption correction:** *SORTAV* (R. H. Blessing, *Acta Cryst. A* 51 (1995) 33–37; R. H. Blessing, *J. Appl. Cryst.* 30 (1997) 421–426). **Program used to solve structure:** *SHELXS97* (G. M. Sheldrick, *Acta Cryst.* (1990) A46 467–473). **Program used to refine structure:** *SHELXL97* (G. M. Sheldrick (1997), University of Göttingen, Germany).

Further information: <http://www.soton.ac.uk/~xservice/strat.htm>

Special details:

R value is somewhat high due to extremely small crystal size (very thin platelets)

Table 2. Atomic coordinates [$\times 10^4$], equivalent isotropic displacement parameters [$\text{\AA}^2 \times 10^3$] and site occupancy factors. U_{eq} is defined as one third of the trace of the orthogonalized U^{ij} tensor.

Atom	<i>x</i>	<i>y</i>	<i>z</i>	U_{eq}	<i>S.o.f.</i>
S1	3060(1)	6710(2)	4913(1)	42(1)	1
S2	3727(1)	4355(2)	5346(1)	44(1)	1
S3	4246(1)	10670(2)	5831(1)	52(1)	1
S4	5608(1)	6273(2)	6084(1)	57(1)	1
C1	3113(3)	4988(6)	4825(3)	39(2)	1
C2	3735(3)	6987(6)	5289(3)	38(2)	1
C3	4043(3)	5907(6)	5481(3)	40(2)	1
C4	4177(3)	9013(6)	5965(3)	44(2)	1
C5	3893(3)	8383(6)	5357(3)	40(2)	1
C6	3743(3)	9289(6)	4782(3)	44(2)	1
C7	3906(3)	10531(7)	4957(3)	49(2)	1
C8	4393(4)	8431(7)	6690(3)	60(2)	1
C9	4963(3)	6467(6)	5536(3)	43(2)	1
C10	4625(3)	5905(5)	5810(3)	38(2)	1
C11	4896(3)	5296(6)	6479(4)	50(2)	1
C12	5414(4)	5437(6)	6685(4)	60(2)	1
C13	4840(3)	7164(7)	4839(3)	56(2)	1
S1'	2115(1)	4949(2)	3895(1)	45(1)	1
S2'	2764(1)	2554(1)	4261(1)	44(1)	1
S3'	640(1)	4480(2)	1671(1)	55(1)	1
S4'	1892(1)	-812(2)	2332(1)	53(1)	1
C1'	2726(3)	4264(6)	4382(3)	42(2)	1
C2'	1891(3)	3564(6)	3332(3)	41(2)	1
C3'	2196(3)	2471(6)	3510(3)	42(2)	1
C4'	1275(3)	4665(6)	2254(3)	43(2)	1
C5'	1381(3)	3719(6)	2757(3)	40(2)	1
C6'	935(3)	2866(6)	2663(4)	53(2)	1
C7'	519(3)	3204(6)	2095(3)	52(2)	1
C8'	1630(4)	5663(7)	2118(4)	66(2)	1
C9'	1937(3)	875(6)	2470(4)	50(2)	1
C10'	2099(3)	1138(6)	3174(3)	41(2)	1
C11'	2193(3)	-39(6)	3594(4)	50(2)	1
C12'	2079(3)	-1156(7)	3211(4)	61(2)	1
C13'	1809(4)	1796(7)	1861(3)	57(2)	1

Table 3. Bond lengths [\AA] and angles [$^\circ$].

S1-C2	1.743(7)
S1-C1	1.757(6)
S2-C1	1.754(7)
S2-C3	1.761(7)
S3-C7	1.700(7)
S3-C4	1.715(6)
S4-C12	1.709(7)
S4-C9	1.727(7)
C1-C1'	1.338(8)
C2-C3	1.346(8)
C2-C5	1.465(8)
C3-C10	1.483(9)
C4-C5	1.365(8)
C4-C8	1.503(8)
C5-C6	1.428(8)
C6-C7	1.335(8)
C6-H6	0.9500
C7-H7	0.9500
C8-H8A	0.9800
C8-H8B	0.9800
C8-H8C	0.9800
C9-C10	1.351(9)
C9-C13	1.510(8)
C10-C11	1.440(9)
C11-C12	1.324(9)
C11-H11	0.9500
C12-H12	0.9500
C13-H13A	0.9800
C13-H13B	0.9800
C13-H13C	0.9800
S1'-C1'	1.751(7)
S1'-C2'	1.774(6)
S2'-C1'	1.750(6)
S2'-C3'	1.753(7)
S3'-C7'	1.645(7)
S3'-C4'	1.727(7)
S4'-C12'	1.715(7)
S4'-C9'	1.723(6)
C2'-C3'	1.350(8)
C2'-C5'	1.477(9)
C3'-C10'	1.490(8)
C4'-C5'	1.355(8)
C4'-C8'	1.483(9)
C5'-C6'	1.440(9)
C6'-C7'	1.349(9)
C6'-H6'	0.9500
C7'-H7'	0.9500
C8'-H8'1	0.9800
C8'-H8'2	0.9800
C8'-H8'3	0.9800
C9'-C10'	1.368(8)
C9'-C13'	1.489(8)
C10'-C11'	1.432(8)
C11'-C12'	1.343(8)
C11'-H11'	0.9500
C12'-H12'	0.9500
C13'-H13D	0.9800
C13'-H13E	0.9800
C13'-H13F	0.9800

C2-S1-C1	95.3(3)
C1-S2-C3	94.5(3)
C7-S3-C4	92.1(3)
C12-S4-C9	91.4(4)
C1'-C1-S2	124.4(5)
C1'-C1-S1	122.4(5)
S2-C1-S1	113.2(4)
C3-C2-C5	128.3(7)
C3-C2-S1	116.7(5)
C5-C2-S1	115.0(5)
C2-C3-C10	126.0(6)
C2-C3-S2	117.1(6)
C10-C3-S2	116.9(4)
C5-C4-C8	127.7(6)
C5-C4-S3	111.6(5)
C8-C4-S3	120.6(5)
C4-C5-C6	110.7(5)
C4-C5-C2	126.1(6)
C6-C5-C2	123.2(6)
C7-C6-C5	114.2(6)
C7-C6-H6	122.9
C5-C6-H6	122.9
C6-C7-S3	111.4(5)
C6-C7-H7	124.3
S3-C7-H7	124.3
C4-C8-H8A	109.5
C4-C8-H8B	109.5
H8A-C8-H8B	109.5
C4-C8-H8C	109.5
H8A-C8-H8C	109.5
H8B-C8-H8C	109.5
C10-C9-C13	128.2(7)
C10-C9-S4	111.5(5)
C13-C9-S4	120.3(6)
C9-C10-C11	111.7(7)
C9-C10-C3	125.5(6)
C11-C10-C3	122.8(7)
C12-C11-C10	113.1(7)
C12-C11-H11	123.5
C10-C11-H11	123.5
C11-C12-S4	112.4(6)
C11-C12-H12	123.8
S4-C12-H12	123.8
C9-C13-H13A	109.5
C9-C13-H13B	109.5
H13A-C13-H13B	109.5
C9-C13-H13C	109.5
H13A-C13-H13C	109.5
H13B-C13-H13C	109.5
C1'-S1'-C2'	95.7(3)
C1'-S2'-C3'	95.4(3)
C7'-S3'-C4'	93.3(4)
C12'-S4'-C9'	92.9(3)
C1-C1'-S2'	124.3(6)
C1-C1'-S1'	122.1(5)
S2'-C1'-S1'	113.5(4)
C3'-C2'-C5'	128.1(6)
C3'-C2'-S1'	115.4(5)
C5'-C2'-S1'	116.3(5)
C2'-C3'-C10'	128.3(6)

C2'-C3'-S2'	117.8(5)
C10'-C3'-S2'	113.9(5)
C5'-C4'-C8'	129.5(7)
C5'-C4'-S3'	110.0(5)
C8'-C4'-S3'	120.1(5)
C4'-C5'-C6'	111.8(7)
C4'-C5'-C2'	124.6(7)
C6'-C5'-C2'	123.6(6)
C7'-C6'-C5'	112.1(7)
C7'-C6'-H6'	123.9
C5'-C6'-H6'	123.9
C6'-C7'-S3'	112.7(6)
C6'-C7'-H7'	123.6
S3'-C7'-H7'	123.6
C4'-C8'-H8'1	109.5
C4'-C8'-H8'2	109.5
H8'1-C8'-H8'2	109.5
C4'-C8'-H8'3	109.5
H8'1-C8'-H8'3	109.5
H8'2-C8'-H8'3	109.5
C10'-C9'-C13'	130.1(6)
C10'-C9'-S4'	110.0(5)
C13'-C9'-S4'	119.9(5)
C9'-C10'-C11'	112.8(6)
C9'-C10'-C3'	126.6(5)
C11'-C10'-C3'	120.6(6)
C12'-C11'-C10'	113.2(7)
C12'-C11'-H11'	123.4
C10'-C11'-H11'	123.4
C11'-C12'-S4'	111.0(5)
C11'-C12'-H12'	124.5
S4'-C12'-H12'	124.5
C9'-C13'-H13D	109.5
C9'-C13'-H13E	109.5
H13D-C13'-H13E	109.5
C9'-C13'-H13F	109.5
H13D-C13'-H13F	109.5
H13E-C13'-H13F	109.5

Symmetry transformations used to generate equivalent atoms:

Table 4. Anisotropic displacement parameters [$\text{\AA}^2 \times 10^3$]. The anisotropic displacement factor exponent takes the form: $-2\pi^2 [h^2 a^{*2} U^{11} + \dots + 2 h k a^* b^* U^{12}]$.

Atom	U^{11}	U^{22}	U^{33}	U^{23}	U^{13}	U^{12}
S1	43(2)	47(1)	34(1)	-3(1)	10(1)	3(1)
S2	47(2)	47(1)	35(1)	0(1)	9(1)	3(1)
S3	56(2)	49(1)	45(1)	-8(1)	10(1)	-3(1)
S4	46(2)	73(1)	47(1)	6(1)	11(1)	3(1)
C1	34(5)	56(4)	25(4)	-5(3)	9(4)	-7(4)
C2	47(6)	44(4)	23(4)	2(3)	14(4)	16(4)
C3	51(6)	46(4)	24(4)	-4(3)	14(4)	8(4)
C4	47(6)	56(4)	25(4)	-10(3)	8(4)	2(4)
C5	40(5)	42(4)	37(5)	-5(4)	10(4)	-2(3)
C6	54(6)	36(4)	39(4)	-1(3)	12(4)	9(4)
C7	47(6)	59(5)	36(4)	15(4)	9(4)	13(4)
C8	87(7)	65(5)	24(4)	-13(4)	11(4)	3(5)
C9	44(6)	45(4)	40(5)	-5(3)	16(4)	1(4)
C10	38(6)	46(4)	22(4)	-4(3)	1(4)	-1(4)
C11	45(7)	67(5)	41(5)	10(4)	17(5)	-7(4)
C12	58(8)	80(5)	33(5)	9(4)	6(5)	-4(5)
C13	58(7)	68(5)	43(5)	12(4)	20(4)	13(5)
S1'	45(2)	44(1)	38(1)	-6(1)	5(1)	1(1)
S2'	52(2)	44(1)	32(1)	1(1)	9(1)	4(1)
S3'	52(2)	66(1)	40(1)	-6(1)	6(1)	3(1)
S4'	61(2)	51(1)	44(1)	-8(1)	12(1)	2(1)
C1'	58(6)	47(4)	21(4)	6(3)	15(4)	2(4)
C2'	52(6)	47(4)	22(4)	11(3)	11(4)	5(4)
C3'	49(6)	50(4)	23(4)	6(3)	9(4)	-11(4)
C4'	52(6)	35(4)	39(4)	-6(3)	13(4)	5(4)
C5'	57(6)	36(4)	29(4)	-3(3)	17(4)	6(4)
C6'	60(7)	60(5)	43(5)	-10(4)	24(5)	-8(4)
C7'	30(6)	80(5)	35(5)	-20(4)	-3(4)	-13(4)
C8'	82(8)	51(4)	55(5)	8(5)	11(5)	-8(5)
C9'	50(6)	65(5)	39(5)	-6(4)	20(4)	3(4)
C10'	45(6)	43(4)	43(5)	-3(4)	24(4)	3(3)
C11'	62(6)	42(4)	45(5)	-3(4)	18(4)	-4(4)
C12'	82(8)	42(5)	68(6)	1(4)	38(5)	-4(4)
C13'	93(8)	56(4)	31(5)	4(4)	33(4)	3(5)

Table 5. Hydrogen coordinates [$\times 10^4$] and isotropic displacement parameters [$\text{\AA}^2 \times 10^3$].

Atom	<i>x</i>	<i>y</i>	<i>z</i>	<i>U</i> _{eq}	<i>S.o.f.</i>
H6	3544	9031	4316	53	1
H7	3840	11245	4633	3(12)	1
H8A	4574	9123	7025	100(30)	1
H8B	4642	7722	6698	140(40)	1
H8C	4104	8068	6821	260(70)	1
H11	4722	4840	6745	21(15)	1
H12	5650	5110	7117	70(20)	1
H13A	5168	7459	4783	280(80)	1
H13B	4615	7932	4823	110(30)	1
H13C	4656	6551	4458	120(30)	1
H6'	935	2148	2966	64	1
H7'	191	2753	1955	34(17)	1
H8'1	1431	6208	1714	100(30)	1
H8'2	1917	5211	2019	260(80)	1
H8'3	1776	6230	2532	200(50)	1
H11'	2322	-30	4092	70(20)	1
H12'	2101	-2022	3403	34(17)	1
H13D	1701	1284	1424	130(30)	1
H13E	2121	2325	1896	140(40)	1
H13F	1522	2386	1863	180(50)	1

